The Importance of Surface Treatment of Aluminium Surface in the Context of Cost-Effective Fibre Reinforced Polymer/Metal Joint Structural Frameworks

Ardeshir Saniee

A thesis submitted in fulfilment of the requirement for the degree of Doctor of Philosophy in Mechanical Engineering, Auckland University of Technology, 2023

Supervisors:

Dr Marcel Schaefer

Prof Zhan Chen

Faculty of Design & Creatives Technologies, Department of Mechanical Engineering

Auckland University of Technology (AUT), Auckland, New Zealand

June 2023

ABSTRACT

The joining of dissimilar materials, including metals and carbon fibre reinforced polymers (CFRPs), has emerged as a critical area of research in various advanced industries, including aerospace, automotive, electronics, and construction. This is driven by the growing demand for lightweight structures, improved performance, and enhanced functionality. The combination of aluminium and CFRP offers a unique opportunity for achieving lightweight and high-strength structures. Among the various joining techniques, adhesive bonding had garnered significant attention due to its unique advantages which can enables the formation of durable and resilient joints between aluminium and CFRP, providing good load transfer, fatigue resistance, and overall joint integrity. However, the full realisation of this potential is hindered by certain limitations and dependencies associated with adhesive bonding, specifically related to surface treatment and the challenges posed by the aluminium surface. Surface treatment plays a crucial role in enhancing the adhesion strength and durability of bonded joints. Yet, the effectiveness of surface treatments in achieving optimal bonding performance is still a subject of ongoing research. Additionally, the high level of dependency on surface characteristics, such as surface roughness and chemistry, further complicates the adhesive bonding process. In the case of aluminium and CFRP bonding, the aluminium surface presents particular challenges due to its oxide layer and modified chemical composition. These factors require careful consideration and specialised surface preparation techniques to ensure successful adhesive bonding. Addressing the limitations and dependencies of adhesive bonding for surface treatment, particularly in aluminium and CFRP bonding, is crucial to fully exploit the potential of adhesive bonding and realise its benefits in creating durable and high-performance structures. In light of these limitation and significance of surface treatment for aluminium surfaces in adhesive bonding, this study aims to provide further insights and advancement in this field. By delving into the intricate details of surface treatment techniques, including mechanical abrasion, chemical etching, and surface modification methods such as deposition of coupling agents, a comprehensive understanding of their impact on the adhesion performance both initial and exposed of the adhesively aluminium adhesively bonded joints can be gained. As a result, to investigate the influence of different set of surface treatments, both individually and in combination to each other, on the adhesion performance of the adhesively bonded joints different approaches, analytical and experimental, were conducted. For this

purpose, sandpapering with mesh sizes of 240, 120 and 80, etching in diluted NaOH solution and deposition of silane, dipodal silane and zirconate were selected as the mechanical, chemical and modification methods of surface treatment, respectively, Initially, the influence of abovementioned surface treatment on different surface characteristics of the aluminium alloy, such as surface roughness parameters as well as total surface free energy and its polar and dispersive components, were investigated. Then the single lap joint and Boeing wedge test were conducted to investigate the influence of the selected surface treatment on initial and exposed performance of the adhesively bonded joints, respectively.

A total of 80 treated specimens were fabricated to investigate the influence of selected surface treatment on five different surface roughness parameters, surface free energy and its polar and dispersive components and elemental composition. The polished condition of aluminium surface was selected as a benchmark in this study. The result form this study shows that etching aluminium alloy in NaOH solution can significantly alter the surface roughness parameters such as S_a and S_q of the polished aluminium surface, which was misjudged in the literature due to the lack of systematic comparison. In addition to this it was argued that the rough surface texture developed by sandpapering can enhance the effectiveness of NaOH treatment and depositing the coupling agents. First, it provides a larger surface area for NaOH treatment to react with the aluminium surface. Secondly, it can facilitate mechanical interlocking, which can favour higher adhesion between adhesive and adherend in the case of adhesive bonding.

On the other hand, a total of 180 aluminium-to-aluminium bonded specimens were fabricated to study the influence of the investigated surface treatment and identify the correlation between different surface parameters and initial and exposed performance of the adhesively bonded joints. The results reveal that the NaOH treatment can significantly enhance the ultimate shear strength of adhesively bonded joints. This enhancement can be accurately predicted by the combination of surface roughness parameters S_a and S_q, as a direct relationship was observed. Furthermore, it was found that surface roughening of the aluminium alloy can indirectly affect the inital adhesion performance of the bonded joint. Specifically, roughening the aluminium surface can increase the reaction zone for NaOH treatment, thereby leading to an increase in the shear strength of the bonded joint. It was also found that the surface roughening of aluminium surface prior to NaOH treatment and coupling agent application can enhance initial adhesion performance compared to polished specimens, as observed in this study. The most significant improvement, with a 22.33% increase of ultimate shear strength, was achieved by roughening the

aluminium surface with #120 grit prior to NaOH treatment, followed by zirconate deposition. This finding highlights the importance of surface preparation in achieving optimal adhesion performance in aluminium-to-aluminium bonding. Furthermore, in order to achieve the best exposed performance of the PUR adhesively bonded joint, it was found that the optimal surface roughness should be in the range of 2-2.5μm, which can be achieved through a combination of sandpapering prior to NaOH treatment and dipodal silane. It has been observed that having a high fracture toughness in dry conditions does not necessarily ensure better exposed performance of the PUR adhesively bonded joint. The fracture toughness of the PUR adhesively bonded joint decreased to 30% of its original value within the first three days of exposure time when only surface roughness was altered through manual sandpapering and NaOH treatment. This phenomenon was also observed when coupling agents were used. The study revealed that silane and dipodal silane coupling agents had better exposed performance in chamber environmental conditions compared to a zirconate coupling agent, despite having lower initial fracture toughness values.

Keywords

Adhesive bonding; Combination of surface treatment; Correlation of surface characteristics and adhesion performance; Mechanical Abrasion; Etching; Coupling agent; Initial strength; Durability

ACKNOWLEDGMENTS

I wish to express my profound gratitude to my esteemed supervisor, Dr. Marcel Schaefer, for his invaluable mentorship, guidance, and unwavering support throughout the course of my doctoral studies. In addition to providing invaluable feedback and scholarly insights on my research, Dr. Schaefer exhibited exceptional understanding and sensitivity to my personal circumstances, which greatly impacted my progress. His compassionate and empathetic approach, coupled with his unwavering dedication to my success, played an instrumental role in helping me to surmount the challenges that faced during this arduous journey. He was not only an exceptional mentor but also a caring friend who provided me with invaluable insights and advice. He always stood by me, providing unwavering support and encouragement even during the most challenging times. His immense faith in my abilities motivated me to work harder and achieve my academic goals. I feel deeply privileged and fortunate to have had Dr. Marcel Schaefer as my mentor and I am profoundly grateful for his unwavering encouragement, mentorship, and friendship.

I would also like to extend my sincere appreciation to my second supervisor, Professor Zhan Chen, for his continuous support and valuable insight. He was always approachable and ready to help whenever I had any questions or concerns. In addition to this, I would like to express my appreciation to Mark Masterton and Ross Jamieson, the senior technicians in the mechanical department, for their assistance and support with laboratory experiments. Their guidance and expertise were crucial in helping me to conduct my experiments efficiently and effectively. Also, I should make a huge shout out to Anna Matich, our librarian here at AUT. She may often be behind the scenes, but her contributions are invaluable. I want to thank her for her remarkable efforts and acknowledge her vital role in supporting the academic success of countless PhD students.

Lastly, I want to use this chance to thanks my family, my lovely great family, which no matter what, they were on my side and I believe that they will always do the same. I can write a chapter about how grateful I am about each single member of my family but considering the limits that I have here, I should just summarise it into a huge THANK YOU. Besides that, I would like to express my deep longing for my county, Iran, and my hometown, Neyshaboor. Although I am grateful for the opportunities that studying abroad has afforded me, I miss the familiar sights, sounds, and smells of my childhood and the warmth of my family and friends. To conclude, I want to share a poem by Omar Khayyam that speaks to the joys and companionship and simple pleasures of life:

“The moving finger writes; and, having writ,

Moves on: nor all thy piety nor Wit

Shall lure it back to cancel half a Line

TABLE OF CONTENTS

LIST OF FIGURES

LIST OF TABLES

LIST OF SYMBOLS AND ABBREVIATIONS

CFRP	carbon fibre reinforced polymer
a	crack length
ANOVA	analysis of variance
MANOVA	Multivariate analysis of variance
PUR	Polyurethane reactive adhesive
OWRK	Owen, Wendt, Rabel, Kaelble method
γ	surface energy
d	dispersive
p	polar
EDX	energy dispersive x-ray spectroscopy
θ	contact angle
SFE	Surface free energy
SEM	Scanning electron microscopy
E	Young modulus
G_I	Fracture Toughness
h	Thickness of substrate
w	Opening displacement
ASTM	American Standard Testing Method
Λ	Wilks' Lambda

CHAPTER 1

Introduction

1.1 Overview

The use of adhesive bonding to join dissimilar materials has been a prevalent practice for over 50 years, and it continues to find application in diverse industries, including aerospace, automotive, and marine sectors. This technique represents a highly promising alternative to mechanical fastening for assembling structures. Its versatility enables the joining of different materials, such as metals and composites, to leverage the benefits of both worlds in a single assembly. Adhesive bonding presents several benefits over conventional bonding methods, such as improving the corrosion resistance of a structure's framework (Barnes & Pashby, 2000) and increasing the feasibility of producing lightweight structures at a lower cost (Marques et al., 2021). However, to obtain these advantages, joint design requires careful attention. Despite these benefits, some industries still hesitate to adopt adhesive bonding as the primary joining method for structural applications due to limited knowledge regarding joint performance over the structure's entire lifetime. Aluminium, a lightweight metal with excellent formability and high strength-to-weight ratio, is a popular choice for adherends when combined with various fiber-reinforced polymers (FRPs). As a result, aluminium and FRPs are widely utilised to develop lightweight structures for advanced industrial applications.

The performance of adhesively bonded joints of metal-to-composite can be influenced by various factors, such as the joint configuration and surface treatments of adherends. However, the evidence to date shows that surface treatments can play a significant role in strengthening and improving the bonded joints' performance, especially when the joints' durability is the primary concern. Therefore, further investigation into the characterisation of different surface treatments is essential, depending on their nature, whether mechanical, chemical or a combination of both. Considering different studies in

this area, the correlation between adhesion performance and surface roughness is not fully understood due to its complex nature. The optimal surface finish varies from one adhesive to another and depends upon the adherend characteristics (Sykes, 1982). Therefore, surface treatment of metallic materials such as aluminium, have been the subject of numerous research studies to enhance the adhesion between adhesive and adherend (Critchlow & Brewis, 1996). Most of the previous studies considered surface roughness as a design parameter to influence the initial performance of the adhesively bonded joint. However, little data is available on the influence of surface roughness on the exposed adhesion performance of the bonded joints. Thus, further research in this area is needed to improve understanding of this critical factor. In general, the aluminium's surface is more problematic than the composite surface in the case of the presence of water, either in the form of humidity or liquid (Pramanik et al., 2017). As a result, it is essential to investigate different surface treatments affecting the initial and exposed performance of the metal-to-composite bonded joints by considering greater attention to the metallic substrate surface.

1.2 Problem statement and gap

Despite the extensive body of research on enhancing the initial and exposed performance of adhesively bonded joints involving dissimilar materials through various mechanical and chemical surface treatments, accurate prediction of the performance of such joints remains elusive. Further investigations are therefore imperative to gain deeper insights into the underlying mechanisms and optimise the effectiveness of different surface treatment techniques.

Considerable research efforts have been dedicated to exploring the impact of individual surface treatments on the surface properties of the treated substrate and the ensuing initial and exposed performance of adhesively bonded joints in dissimilar material configurations. Nevertheless, utilising a single surface treatment method for structural adhesive bonding applications may not yield optimal results. Additional investigations are warranted to examine the effectiveness of synergistically employing various surface treatment methodologies to enhance the performance of adhesive joints, encompassing both initial and exposed durability aspects. The term "performance" in the context of adhesive bonding pertains to the ability of the bonded joint to fulfil or surpass the desired functional requirements and expectations throughout its intended service life. It encompasses various dimensions, including the strength and durability of the bond, resistance to environmental factors such as humidity and temperature, exposed stability, fatigue resistance, and any specific performance criteria relevant to the application or

industry. In this study, the term "initial" specifically denotes the initial strength of the adhesively bonded joint under ambient conditions, while "exposed" generally pertains to the durability of the adhesively bonded joint within the specified environmental conditions considered in this investigation.

Most of the available surface treatments, as found in the literature, have been evaluated for their efficacy based on only one or, at most, two surface characteristics. However, it should be noted that a surface resulting from machining consists of numerous length scales exhibiting superimposed roughness (Gadelmawla et al., 2002). These surfaces are typically characterised by three distinct types of parameters, namely amplitude parameters, spacing parameters, and hybrid parameters. Therefore, relying solely on a single parameter for assessing surface quality is inadequate and may not provide sufficient information for designing structurally efficient bonds. This study aimed to contribute to a better understanding of the effect of different surface characteristics, such as surface roughness, wettability, and composition, in a set of well-known surface treatments using destructive and non-destructive methods. However, due to the complex nature of the adhesion performance and the interplay of multiple factors, further research is necessary to investigate the influence of different mechanical and chemical surface treatments on the bonded joints' adhesion performance. To this end, employing three-dimensional surface analysing methods, such as a 3D profilometer, would be useful for providing a more comprehensive characterisation of the surface topography and its impact on adhesion performance.

1.3 Objectives

Considering the identified gap in the literature, the objectives of this study are to:

- Assess the influence of simple surface treatments, both mechanically and chemically, on the aluminium substrate's surface finish alternation, utilising a new set of surface roughness parameters.
- Assess the influence of combinations of different surface treatments in comparison to sole treatments, either mechanical or chemical.
- Assess the influence of different surface parameters, such as surface roughness and surface wettability of the treated surface, on predicting the performance of the adhesively bonded joints.
- Assess the influence of different surface parameters, such as roughness and surface wettability of the treated surface, on predicting the exposed performance of the adhesively bonded joints.

1.4 Thesis organisation

This thesis contains six chapters in total, as follows:

Chapter 1 provides an introduction to the use of adhesively bonded joints as a promising alternative to traditional mechanical fastening techniques for joints of both similar and dissimilar materials. The chapter emphasises on the significance of investigating the impact of various surface treatments on metallic substrates, particularly aluminium, with regards to the initial and exposed performance of adhesively bonded joints. The chapter also highlights the research problem and gaps that currently exist in this field. The objective of this study is then presented, followed by an overview of the organisation of the thesis.

Chapter 2 presents a fundamental background about well-accepted adhesion theories to date. Then the factors such as geometry configurations of the bonded joints, surface treatment of the substrate and the importance of the materials selection of the adherend and adhesive are discussed. Different surface analysing and destructive testing methods, such as single lap-joint and wedge tests, were reviewed, in consideration of the relevant standards. Furthermore, the critical role of surface treatments of an aluminium surface is explained, and a state-of-the-art review on the most recently developed surface treatment for this type of metal is assessed to identify topics for further research.

Chapter 3 proposes a set of different treatments to alter the surface of the aluminium alloy as a selected substrate for this study. The influence of a different set of treatments on the surface characteristic parameters is measured using different standard surface analysing methods such as contact angle analysing, 3D surfaces profilometer and energy-dispersive X-ray (EDX). Statistical analysis is performed to show the level of confidence in the measured values. The specific changes regarding the different surface treatment's nature are identified and discussed.

Chapter 4 presents the initial performance of the adhesively bonded joints treated with the studied surface treatments of the previous chapter. The correlation between the surface parameters and the initial strength of the single lap joints is identified based on the results found in Chapter 3. Also, the same statistical method is applied to identify the confidence level in developed results.

Chapter 5 presents the exposed performance of the adhesively bonded joints according to the well-known testing method for examining the durability of the adhesive bond. The correlation between the surface parameters and initial strength is further expanded to the exposed durability of the metal-to-metal bonded joints. Additionally,

statistical analysis is undertaken to confirm the confidence level in the result found in this chapter.

Chapter 6 provides a complete summary of the previous chapters to lead the study into the main conclusions. In addition to that, further studies are recommended for future research.

CHAPTER 2

Literature Review

2.1 Overview

In this chapter, the relevant literature and state-of-the-art technologies are reviewed to understand the fundamentals in adhesion science by introducing a brief historical perspective. Then, the most important and relevant adhesion mechanisms in this field are addressed. The Challenges were further investigated in defining good adhesion based on the existing mechanisms. Also, we look at the bonding of dissimilar materials, specifically metals and composites, by employing adhesive bonding as a selected joining method. Additionally, the known adhesion mechanism's dependency on different factors, such as surface characteristics of the materials and environmental factors are reviewed. Based on the review and discussion, this study has identified potential gaps in the existing literature that could be addressed in this study. It is concluded that there is a need to perform further systematic/parametric research to investigate the influence of combined surface treatments on both the initial and exposed performance of the adhesively bonded joints. Furthermore, further research is warranted to validate the correlation between specific surface parameters and the adhesive strength of the bonded joints.

2.2 Introduction

Lighter structures utilising multi-materials have been in high demand in the last few decades, thus introducing a high emergence for joining dissimilar materials(Groche et al., 2014). Advancements in material science and the expanding use of additive manufacturing processes have the potential to reduce the necessity for joining and the quantity of joint components in a final product. (Zhang et al., 2004). Despite the potential benefits of a "joint-free" concept resulting from recent developments in material properties and additive manufacturing processes, the complex functions required of advanced products and their production processes render this concept impractical in many cases. Therefore, understanding different joining technologies and the underlying

mechanism in each of these methods is a key issue in effective manufacturing. In essence, the combination of different materials will necessitate a systematic approach to material selection due to the introduction of new interactions, which may require the implementation of a new manufacturing system. (Sakundarini et al., 2013). A recent prominent example is the Boeing 787 Dreamliner, which utilised composite materials as the primary material in the airframe structure, in addition to other metallic materials such as steel, titanium, and aluminium. However, joining dissimilar materials presents unique challenges due to their distinct properties, such as differences in mechanical, chemical, and thermal characteristics. This difference can directly influence the integrity of the joints during the service life of the assembly. Therefore, issues like different thermal expansion, galvanic corrosion, etc., should be addressed with good care.

Within the spectrum of diverse joining methods, adhesive bonding occupies an unequivocal and pivotal position in the realm of advanced manufacturing applications (Baldan, 2012). The fundamentals of adhesive bonding have been based on several complex theoretical adhesion mechanisms. This section provides a critical evaluation of a state-of-the-art review of previous studies pertaining to the recent advancements in comprehending the impact of various parameters - including surface roughness and surface wettability - on the initial and exposed performance of dissimilar bonded joints. Different surface treatments of a mechanical and chemical nature, such as sandpapering, grit and sandblasting, etching in alkaline or acidic solutions, etc., are considered. An analysis of recent studies in this field is conducted to identify potential gaps that may require further investigation. Subsequently, this review examines studies that investigate the effects of surface treatments such as sandpapering, sodium hydroxide treatments, and the application of various coupling agents on surface characteristics and adhesion performance, as these treatments have a substantial influence. Following a comprehensive evaluation, recommendations for further research are proposed.

2.3 Adhesion

2.3.1 Brief history of adhesion science

The term adhesion is extracted from the Latin words for to stick (ad=to, hesion= stick) (Viswanadham, 2000). For over a thousand years, the adhesion phenomenon has attracted much attention among our ancestors. A great example from the evidence in the archaeological record is the glue-like adhesives made and used by Pleistocene ancestors in southern Africa as early as the Middle Stone Age. Ultimately, nature can be a fascinating, inspiring resource for most adhesion definitions. For instance, the Greek philosopher Aristotle remarked on the ability of the gecko to stick to vertical surfaces. It can also refer to the challenge first presented by Sir Isaac Newton, who mentioned: "There are therefore agents in nature able to make the particles of bodies stick together by powerful attractions. And it is the business of experimental philosophy to find them out." (Allen, 1993).

As Newton mentioned, the adhesion phenomenon can be subdivided into two different considerations. He focuses on the bonding agents used to hold the components together, while the other type investigates the various forces required to separate the bonded components. These concerns are usually cited as *fundamental* and *practical* adhesion (Da Silva et al., 2018).

The main concern with fundamental adhesion is the existing forces to hold the different components of an adhesive bond on the molecular scale. Consequently, the magnitude of mechanical force applied to break an adhesive bond is the primary concern of practical adhesion. Despite Newton's excitement about the challenges around the adhesion phenomenon, it was not until 1922 that McBain introduced the theory of fundamental adhesion with his co-workers (Allen, 1993). Since then, there have been several endeavours to advance a singular description or theory that would cover all aspects of adhesion. Many of the publications from that period, and even some contemporary literature, may reflect this methodology. Accordingly, it is appropriate to carefully review established theories concerning adhesion phenomena on an individual basis.

2.3.2 Adhesion mechanisms/theories

Despite the existing lack of universal theory, a significant amount of information is available in the literature on different theories associated with adhesion. In general, the complex nature of adhesion can be summarised into four primary and well-accepted theories (Figure 1). Most of the studies in the literature agreed with the difficulties in addressing adhesion performance based on a single theory. Realistically, a combination of

two or more adhesion mechanisms might be ideal for defining adhesion performance. This can be mainly due to the multi-disciplinary nature of the adhesion topic, which includes fracture analysis, surface chemistry, physics, and rheology. All the theories considered the interface of adherend and adhesive as the most critical zone of investigation due to the interatomic and intermolecular interaction in this area. This will strengthen the dependency of the adhesion performance to the surface characteristics of the adherend. The core section of these changes occurs in the interfaces' surrounding areas (Mittal & Pizzi, 1999). Despite the extensive body of research conducted in this domain, a notable deficiency persists in the foundational comprehension and insights into adhesion mechanisms. This observation is drawn from the most recent literature available (Cavezza et al., 2020; Croll, 2020; Issa & Luyt, 2019), some essential adhesion models and mechanisms have been covered in the following section with further details. As a result, adhesion sat off as a separate scientific subject. Despite considerable progress in narrowing the gap between theory and practice, adhesion remains an area where technology and empiricism continue to outpace scientific understanding (Adams, 2005). The subsequent section will comprehensively examine all aforementioned theories, providing pertinent details, and assess their current level of contribution towards enhancing adhesion.

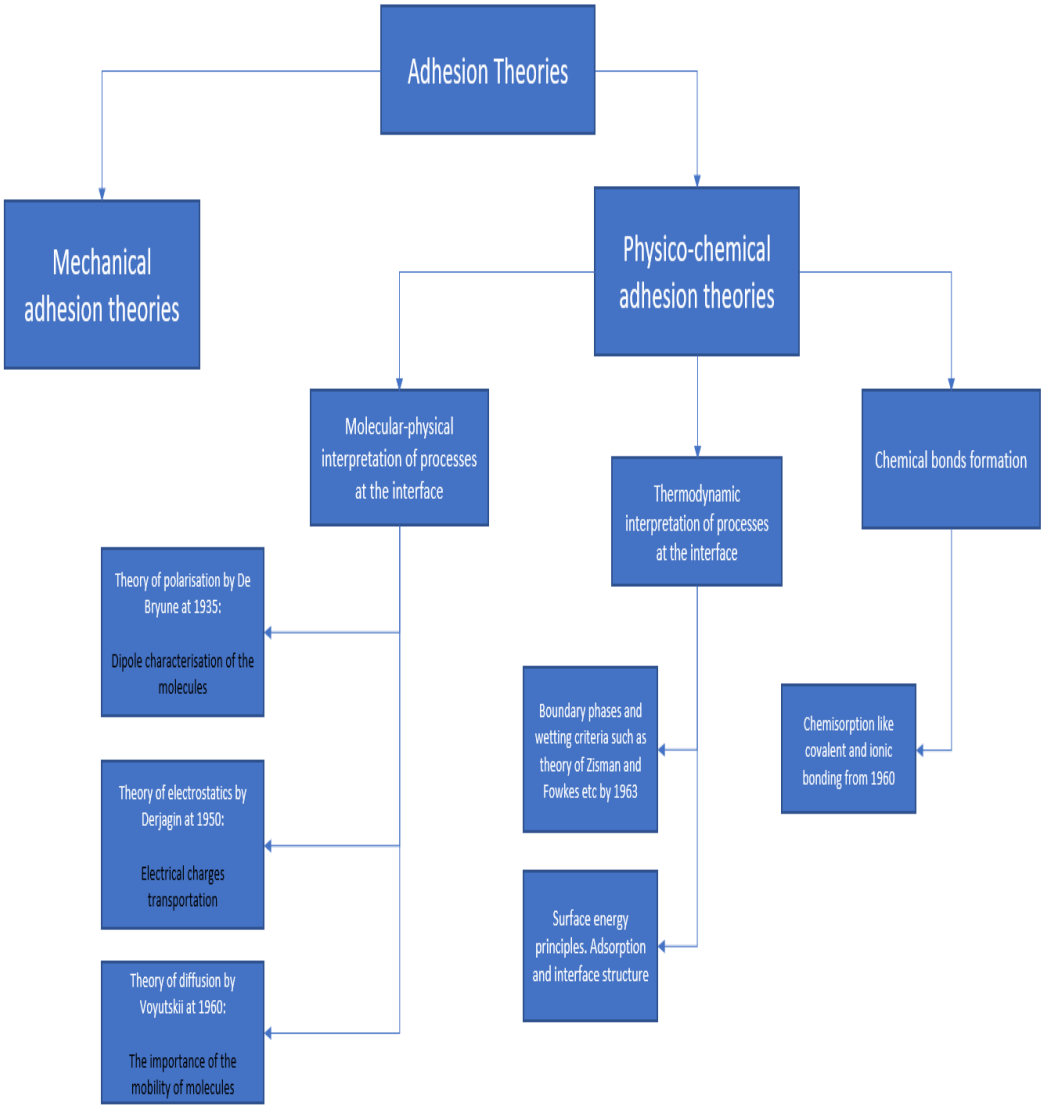

Figure 1: The overview of different adhesion theories

2.3.2.1 Mechanical interlocking theory

McBain first introduced it in 1925; the mechanical theory of adhesion is founded on the extent of interlocking between the adhesive and the irregularities or pores of the adherent on a macroscopic scale (Figure 2). In other words, the mechanical theory posits that the adhesion between two substrates occurs due to the polymeric adhesive's mechanical interlocking into the cavities of the substrates. According to this theory, the rougher surface can introduce more interlocking points, thereby increasing adhesion, especially when applying a liquid adhesive. The study conducted by Gude et al. (Gude et al., 2012) aimed to investigate the relationship between the mechanical properties of the bonded joint and the thermodynamic surface characteristics of the roughened surface. The empirical results stated that the dominant adhesion mechanism that influenced mode-I fracture was mechanical interlocking.

By contrast, a rougher surface did not influence the shear strength. The current debate in the literature about mechanical theory concerns the importance of interlocking in describing surface adhesion (van Dam et al., 2020). On one side of the concurrence, it is believed that a higher degree of roughness produces a surface with more irregularities, thereby improving the adhesion performance. Conversely, it is believed that a rougher surface ideally increases the surface area providing more molecular sites for intermolecular interactions.

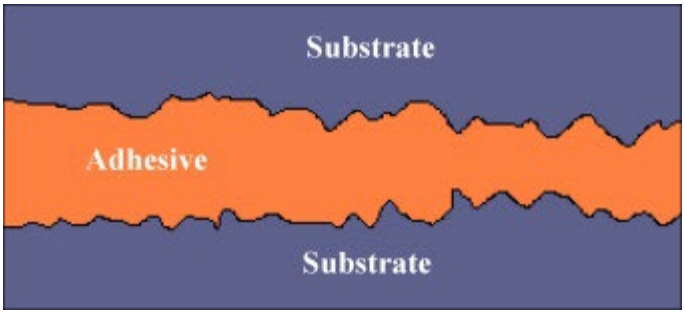

Figure 2:Illustration of mechanical interlocking between surfaces of adherents and adhesive (Awaja et al., 2009)

The mechanical interlocking theory, which is one of the earliest proposed adhesion theories, has been subject to debate due to the observation of strong bonding that can occur between smooth surfaces without any surface irregularities. As a result, this theory is not universally accepted in the field of adhesion (Ebnesajjad & Ebnesajjad, 2013). Instead, in the study by Osouli-Bostanabad et al. (Osouli-Bostanabad et al., 2017), the polished substrate performed well enough to develop high-level adhesion strength. Due to the deficiency of molecular consideration, mechanical interlocking theory can only be used for preliminary investigation of adhesion mechanisms.

2.3.2.2 Diffusion theory

The theory of molecular diffusion at the adhesive-substrate interface was originally proposed by Voyutskii. It postulates that adhesion occurs due to the migration of molecules across the interface between the adhesive and the substrate (Ungureanu et al., 2016). Later, Fourche (Baldan, 2012) illustrated the different diffusion phases (Figure 3). According to this theory, when two polymeric materials are under constant pressure and in contact, they tend to diffuse together in compliance with Fick's first law of diffusion (Banea & da Silva, 2009). Wake (Wake, 1982) postulated that the thermodynamic compatibility of the bonded materials is a crucial determinant in the diffusion theory. It is notable that the diffusion theory is considered invalid for the majority of fibre-reinforced polymer (FRP)-based and metallic materials, as stated by several researchers. Therefore,

it is generally regarded as relevant primarily to autohesion polymer bonding (Baldan, 2004).

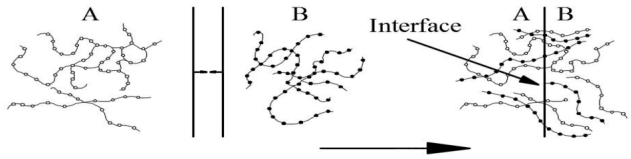

Figure 3:Diffusion theory of adhesion (a) interdiffusion of adhesive and (b) substrate molecules (Baldan, 2012)

2.3.2.3 Adsorption theory

According to this theory, the adhesive and substrates are in intimate contact due to the inter-atomic and molecular interaction at the interface. Interfacial forces are formed due to various primary and secondary bonds, which include covalent interactions, hydrogen bonding, van der Waals' forces, and electrostatic interactions. These forces arise from the interaction between atoms or molecules at the interface, resulting in the formation of an adhesion zone. These intermolecular forces can influence the thermodynamic characteristics of the adherend and adhesive by modifying surface free energy and surface tension, respectively. It is widely acknowledged that the initial stage in the formation of a bond between an adhesive and adherend occurs at the liquid-solid interface. Thereby adhesion quality can be highly affected by the surface's wetting characteristics (Pramanik et al., 2017). This theory proposes that when the surface energy of the substrate is higher than that of the adhesive, there is a greater propensity for adhesion interaction, leading to improved bonding properties. Consequently, numerous researchers have directed their efforts towards investigating factors that enhance bonding strength by augmenting the surface energy of substrates (Butt et al., 2008; Yang et al., 2019). Further comprehensive coverage of this topic will be provided in subsequent sections of this chapter.

2.3.2.4 Electrostatic theory

The electrostatic theory was first introduced by a group of scientists from the Soviet Union with the leadership of Deryagin in the 1950s (Ungureanu et al., 2016). According to this theory, the interface can be considered as an electrical condenser with two different charges distributed over both sides of the substrate (Figure 4). This physical model was used to illustrate the three-dimensional region consisting of a double layer of electricity at the interface of the polymer-solid interface.

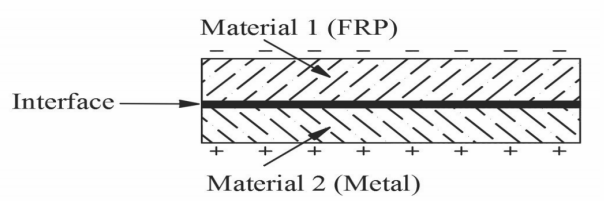

Figure 4:Electrical double layer at the polymer-metal interface (Ungureanu et al., 2016)

As stated in this theory, there are always some free charges at the interface, even under complete dielectrics. Therefore, there will be a chance for the difference in electrochemical potentials across the interface between two different materials when they get close. Then, the double electric layer will be developed due to the free electron and ionic charge movement over the interface. According to this theory, the work of adhesion can be characterised as the amount of work necessary to separate a condenser plate, with the rate of separation and gas pressure of the working environment being the primary factors influencing the adhesion (Baldan, 2012).

This theory gained attention during the 1950s to late 60s, when it found itself next to other already accepted theories, such as mechanical interlocking and chemical theories. However, the electrostatic theory has faced criticism from scholars who have cited instances where the presence of filler charge resulted in the absence of the electrostatic phenomenon. As a result, by the late 1970s, Deryagin was willing to acknowledge the perspectives of his opponents and ultimately made the following statement in his most recent publication: “An adhesive bond is always caused by either the forces of chemical bonding or by so-called van der Waals forces” (Baldan, 2012). The abovementioned conserves were enough to make this theory a rare condition for defining the adhesion phenomenon.

2.3.2.5 Chemical or intermolecular bonding theory

Chemical bonding theory is the most accepted one among other established theories for defining the adhesion performance between adherend and adhesive surfaces. Significant parallels can be observed between the theories of chemical bonding and thermodynamics, as previously discussed in relation to the diverse chemical bonds present at the interface. These similarities primarily arise from the shared metric scale of interest between these two theories. The compatibility between chemical groups on the adhesive surface and corresponding chemical groups on the adherend surface plays a crucial role in facilitating the formation of chemical bonds between the substrate and adhesive. The strength of these chemical bonds can also be influenced by factors like the number and type of bonds that form on the interface (Mittal & Pizzi, 1999).

Chemical bonds can generally be categorised into four types: Van der Waals forces, acid-base interactions, hydrogen, and covalent bonding. The term Van der Waals forces can be classified into three types: Debye, Keesom and London interactions. London interaction arises from electron-cloudy motions unrelated to dipole interactions (Pletincx et al., 2019). This model of interactions (i.e. Van der Waals) is known to be the weakest force that generally participates in adhesive bonding. An acid-base reaction, as can be recalled from its name, is a chemical reaction between an acid and a base molecule.

Also, hydrogen bonding can arise due to the interaction between a hydrogen atom and an electronegative solid atom. Although hydrogen bonds promote weak bond strength, physical adsorption can lead to strong initial adhesion interactions. To improve the exposed stability of the chemical bond, covalent and ionic bonds show a promising aspect in this regard. A relevant study conducted by Mohseni et al. (Mohseni et al., 2006) proposes that a stronger interface interaction can be achieved by promoting the formation of covalent bonds at the adherend-adhesive interface. Therefore, strong chemical bonds across the interface can be considered an essential factor in improving the adhesion performance between substrate and adhesive. The overview of the different characteristics of the abovementioned chemical bonds are given in Table 1.

Table 1: Overview of different chemical bonds in terms of their bond energy and length (Pletincx et al., 2019)

Bond type	Bond energy (kJ mol^{-1})	Equilibrium length (nm)
Primary, chemical		
Ionic	600–1000	0.2–0.4
Covalent	60–800	0.1–0.3
Metallic	100–350	0.2–0.6
Acid–base interactions		
Conventional Brø nsted	<1000	
Lewis	<80	
Secondary, physical		
Hydrogen	50	0.3
Van der Waals		
London dispersion	1–40	<1
Keesom orientation	2–8	0.4
Debye induction	<2	0.4

It is noteworthy to mention that in the past four decades, chemical theory has made significant contributions to defining adhesion performance, thanks to the development of surface analysis technologies and the application of specific methodologies (Pletincx et al., 2019). Based on the understanding derived from various adhesion theories, the following section focuses on exploring the essential theoretical and practical aspects of adhesive bonding.

2.4 Adhesive bonding

According to historical evidence, adhesive bonding appears to be among the few first joining methods that had been employed to form a structural framework. Researchers have long been concerned with improving the performance of adhesively bonded joints in both the initial and exposed. In this section, a comprehensive review of the crucial factors affecting the adhesively bonded joints' performance is provided. These factors include the bonding process, surface preparation techniques, geometrical factors, properties of the adherend and adhesive materials, as well as the various failure modes encountered. The review presents the latest findings and insights in each of these areas to provide an up-to-date understanding of the most significant parameters influencing adhesive bonding performance. The latest advancements in materials, methods, and techniques have overcome some of the limitations associated with adhesive bonding. However, determining the optimal combination of driving factors that can enhance the performance of adhesively bonded joints is yet to be addressed.

2.4.1 Historical introduction of metal and composite bonding

Carbon fibre-reinforced polymer (CFRP) is deemed as a crucial material for lightweight structural frameworks which provides support, stability, shape and retrofit to the existing structures, particularly in the aviation and automotive industries, owing to its high strength-to-weight ratio. In practical applications, the use of CFRP often requires it to be combined with metal frames. Thus, there is a need to comprehend the challenges involved in manufacturing, machining, and joining CFRP with metal materials in a hybrid design. Hybrid design is a technique that involves the joining of dissimilar materials possessing distinct and desirable material characteristics, such as design flexibility and increased strength. These unique functional properties of hybrid design offer an opportunity to maximize the performance of the overall joint system.

One of the effective ways to construct composite/metal structures is to use a laminate formation, in which the lightweight characteristics can be achieved, as well as the high bending rigidity of the structure. To name some examples, composite panel manufacturing in commercial aircraft is well dominated by a sandwich stack-up formation. Similarly, CFRP joints with aluminium, titanium and itself are among the most used material formations in engine and wing panels of aircrafts like Airbus A380 or Boeing Dreamliner (Castanie et al., 2020). However, from the manufacturing perspective, stack-ups as a selected joining method between metal and composite, introduce high manufacturing costs and high labour intensiveness due to the numerous steps undertaken from the initial stage all the way to completion (Groche et al., 2014).

Alternatively, more straightforward steps are required for conventional mechanical fastening to join metals and composites together. In this method, adequate joining strength can be achieved using bolts and rivets, thereby can be applied to various engineering applications. However, conventional mechanical fastening introduces additional weight, and its lack of sealing can be problematic for specific applications. Moreover, the drilling process can have a considerable impact on the mechanical properties of CFRP, as it can cause damage to the fibre structure and elevate stress concentrations at the hole's cross-section. Rather than relying on conventional mechanical fastening methods, adhesive bonding presents itself as a viable alternative for joining dissimilar materials. Adhesive bonding is a widely utilised process in the aviation, automotive, and building industries, wherein two components, or adherents, are bound together using a suitable binder, or adhesive. The process of adhesive bonding enables the joining of dissimilar materials, and is therefore commonly employed to bond materials with distinct physical and chemical properties (Belingardi et al., 2015; Grant et al., 2009). Adhesive bonding is a crucial process that not only seals the joints but also mitigates the possibility of galvanic corrosion between CFRP and aluminium alloy (Wu et al., 2021). Its high diversity in joining almost any pair of materials makes it a suitable method for bonding materials that are hard to bond via other traditional methods, such as mechanical fastening and welding. Adhesive bonding can facilitate access to lightweighted structures with respect to other assembly methods, owing to the small addition of weight that the adhesive itself adds to the overall structural framework. Additionally, the structural weakening due to the bolt holes, which can introduce a high-stress concentration zone, will be eliminated (Rudawska, 2012). Like any other joining method, adhesive bonding contributes to numerous challenges and limitations that require special care, such as selecting proper adhesives and high sensitivity to selected surface treatments. Despite the advantages of adhesive bonding, limitations such as reduced load-carrying capacity, lower fatigue life, and reduced durability have prevented significant improvement in joining strength compared to conventional mechanical fastening methods. By such means, adhesive bonding is still not fully trusted in many industrial sectors, where more established conventional joining methods are preferred. To overcome this concern, clear insight into the different factors which can improve the performance of the adhesively bonded joints is required.

The subsequent sections delineate the crucial parameters that impact the performance of adhesively bonded joints. These parameters are classified into two categories: design-dependent factors, including joint configuration and surface treatment, and environmental-dependent factors, encompassing humidity and elevated temperature levels.

2.4.2 Bonding procedure

The bonding procedure is thought to be one of the important aspects to consider while manufacturing an adhesively bonded joint. The bonding process can influence different mechanical properties of the adhesively bonded joints, such as bond strength and failure mode (Arenas et al., 2013; Mohan et al., 2014; Park et al., 2010). The bonding procedures can be categorised into three distinct methods: co-curing, co-bonding, and secondary bonding (Da Silva et al., 2011). A schematic diagram of each of them can be seen in Figure 5.

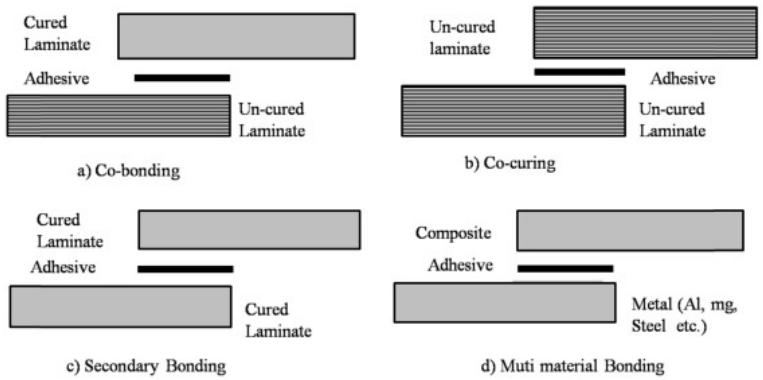

Figure 5: Layout of the most common bonding procedure between composite materials (Budhe et al., 2017)

Co-bonding and co-curing have some similarities in appearance; however, they differ in terms of the curing process. In co-bonding, one adherend is entirely cured with the adhesive, whereas in co-curing, both substrates are cured simultaneously with the adhesive. In contrast, in secondary bonding, the adhesive is placed between two previously cured substrates. In multi-material bonding, the adhesive is applied between metallic and composite materials instead of two composites. In recent years, there has been considerable interest in enhancing the strength, weight, and durability of structures by integrating traditional metals with composite materials (Banea, 2019; Reddy et al., 2019). This approach combines the excellent formability and high strength of metallic materials with the superior lightweight and structural efficiency of composite materials. The strength of the bonded joints using a different multi-material bonding method were evaluated by several studies (Arenas et al., 2013; Rudawska, 2010), and the improvement in the performance of the bonded structure was reported. As a result, developing a lighter structure could be enabled by a smart combination of different materials. However, as discussed in the following sections, other parameters can influence the multi-materials bonded joints' performance.

2.4.3 Performance of the adhesively bonded joint

The performance of adhesively bonded joints between metal and composite materials can be influenced by various parameters, including those related to design and environmental factors. Therefore, during the design stage of such joints, all these parameters need to be considered carefully to ensure their feasibility performance. Several studies have emphasised the importance of taking these parameters into account to achieve optimal performance of metal-composite adhesively bonded joints (Banea, 2019; Banea et al., 2018; Budhe et al., 2017).

2.4.3.1 Design dependent factors

2.4.3.1.1 Geometrical factor/joint configuration

Geometrical factors play a crucial role in determining the performance of adhesively bonded joints in metal-composite substrate systems. Factors such as bondline thickness, joint configuration, and overlap length can significantly affect the strength and durability of the joint. Recent research has shown increasing interest in investigating the impact of adhesive thickness on bonded joints using both analytical models (Arenas et al., 2010; Liao et al., 2013) and experimental methods (Anyfantis & Tsouvalis, 2013; Davies et al., 2009). It has been reported that the strength of the adhesively bonded joints can develop an inverse relationship with the thickness of the bondline (Anyfantis & Tsouvalis, 2013). The correlation between the adhesive thickness and joint performance has been attributed to the rise in defects such as microcracks and voids at the interface in thicker bondlines. However, in the study by Liao et al. (Liao et al., 2013), higher fracture energy was recorded in a ductile adhesive for thinner adhesive bondlines.

Additionally, the numerical results supported the statement that higher adhesive thickness can lead to higher ductility behaviour on the adhesive. Despite recent studies on the effect of bondline thickness, no generalised tendency is proposed between bondline thickness and strength of the bonded joints. The different responses of bonded joints to variations in adhesive thickness can be attributed to various factors, including the type of loading, adherend and adhesive characteristics, physical properties, and joint geometry, among others (Banea et al., 2015; Budhe et al., 2017). These factors can have an impact on the properties of the bonded joints. the optimisation of adhesive thickness requires careful consideration of adhesive properties, geometrical parameters, and various types of loading.

Another crucial geometric aspect is to consider the essential factors when designing the joint layout, which can mitigate issues associated with premature failure of the bonded joint. Such issues include local stress concentration and high interfacial and

peel stresses (Banea & da Silva, 2009). The most common joint configurations that have been investigated in the literature are given in Figure 6. The single lap joint, thanks to its effectivity and simplicity, is used to identify the most crucial behaviour of the adhesively bonded joints with numerous of researchers.

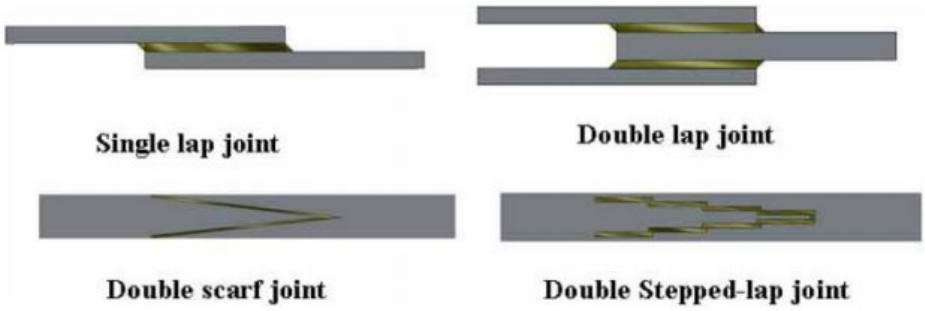

Figure 6: Most common joint configurations for adhesively bonded joints (Budhe et al., 2017)

Another factor that can influence the performance of adhesively bonded joints is the length of the bondline. Studies have shown that the initial performance of the bonded joint can be improved up to a certain limit by increasing the length of the bondline (Anyfantis & Tsouvalis, 2013). However, the same as the other geometrical parameters, the scale of improvement is strongly depends on the type of loading (Jen & Ko, 2010), adherend material (Reis et al., 2011) and adhesive material (Li et al., 2015). For instance, in the study by Neto et al. (Neto et al., 2012), the correlation between failure load and overlap length was studied concerning two different adhesive types. It was reported that the failure load increased to a certain value for brittle adhesive and then remained constant by increasing the overlap length. On the other hand, the ductile adhesive shows different characteristics where failure load had a proportional correlation with overlap length.

Practical experience in the operation of adhesive structures consistently reveals that the majority of failures in the constituent elements are linked to the damage or outright destruction of the adhesive layer. This vulnerability is inherently attributed to the comparatively low strength of the adhesive material itself and the compromised contact zone between the adhesive and the connected surfaces. Concurrently, the thickness of the adhesive layer, which serves as the conduit for force transmission between connected parts, stands out as a critical structural parameter. This parameter significantly influences the overall strength and longevity of the joint (Kostin et al., 2021). The notable impact of adhesive layer thickness on the overall strength of the joint is primarily attributed to the uneven distribution of the stress-strain state along both the

length of the bonding section and the thickness of the adhesive layer. This unevenness results in stress concentration at the edges and boundaries of the joint. Consequently, there is an increased significance placed on experimental and theoretical investigations into the stress-strain state and strength of the adhesive intermediate layer. Such inquiries particularly focus on its geometric parameters, with thickness being a key determinant. In the study by Kostin et al. (Kostin et al., 2021) The outcomes derived from tensile tests conducted on slender adhesive joints (where the thickness, h, is less than the reference thickness, h0) consistently align with the predictions of fracture mechanics. These results affirm the observed trend of strength augmentation in thin joints up to thicknesses approximating 0.2 to 0.3 mm. Within this thickness range, factors such as the influence of the connected elements (substrates) and the blunting of microcracks, attributed to the constrained deformations, exert a discernible impact.

The model predicts that the apex of strength values aligns with the adhesive thickness corresponding to the size of the cracking zone. However, experimental determination of strength characteristics precisely at this point proves challenging in practical applications, as achieving an adhesive layer thickness with an accuracy of 0.01 mm is arduous. Nonetheless, in the context of designing adhesive joints, there exists a favourable prospect for calculating the optimal adhesive layer thickness. This calculation can be accomplished by leveraging the strength and crack resistance characteristics of the adhesive through fracture mechanics methodologies.

2.4.3.1.2 Adhesive and adherend material parameters factor

The demand for new adhesive materials with advanced properties is high in almost all industries. However, selecting the most effective adhesive for a specific application can be a complex task, as it depends on several factors, including the type of adherend material, expected environmental exposure conditions, and cost. Although various adhesive materials are currently available in the market, the development of new adhesive materials with advanced properties continues to meet the demands of limited applications.

While adhesive bonding is a widely used joining technique in industry, there are concerns about its environmental impact, particularly in terms of the recyclability, reusability, and recovery of bonded parts. To address the concerns regarding the environmental impact of adhesives, a range of green adhesives have been developed with the aim of minimising or overcoming these issues (Zain et al., 2014). The development of a new type of advanced adhesive that allows for bonding and de-bonding represents an exciting opportunity for advancements in this field and holds significant promise for

future potential (S. Wang et al., 2019). Also, adhesives that exhibit greater toughness, higher ductility, and better impact resistance than conventional epoxy adhesives have emerged. These types of adhesives are explicitly relevant to the automotive industry (Da Silva et al., 2011). Some studies involve improving the toughness of the bonded joints without termination in initial strength by adding polyurethane to the epoxy adhesive (Imanaka et al., 2009; Monteiro et al., 2015; Saldanha et al., 2013). To date, there are key concerns appertaining to the environmental issues, as synthetic adhesives like epoxies can be categorised as toxic in nature, non-renewable, with debonding difficulties etc. (McDevitt & Grigsby, 2014). To combat these concerns, a thermoplastic adhesive, such as hot melt adhesive (HMA) provides a better alternative for ease of application, reusability, and environmentally friendly features. Therefore, significant attention has been given to the development of adhesively bonded joints in recent years. During this time, a variety of thermoplastic adhesive materials have been developed, including water-based adhesives (dos Santos et al., 2016) and strengthen hot melt adhesives (Sun et al., 2022).

Nevertheless, most of these adhesives are used mainly for the bonding between composite and wood and not adhesive bonding between metals and CFRP(Sun et al., 2022; S. Wang et al., 2019). The need for further evaluation of the actual adhesion performance of thermoplastic adhesive, specifically reactive polyurethane hot melt adhesive (PUR), in bonding metal/CFRP materials arises from the distinctive challenges and requirements associated with this specific bonding combination. The dissimilar surface properties, thermal expansion coefficients, and mechanical behaviors of metals and CFRP materials contribute to the complexity of achieving effective adhesion. Moreover, the bonding of metals and CFRP entails joining materials with contrasting characteristics, such as disparate thermal conductivities and coefficients of thermal expansion. Therefore, a comprehensive assessment of the performance of thermoplastic adhesive, particularly PUR, in establishing strong and durable bonds between these dissimilar materials becomes imperative. Through extensive evaluations, researchers and industry practitioners can gain valuable insights into the adhesion performance of PUR adhesive in metal/CFRP bonding applications, thereby identifying any potential limitations and areas that warrant further improvement.

The escalating concerns related to water and land pollution, coupled with the potential depletion of raw materials and the enduring resilience of plastics to various physical and chemical influences, underscore the heightened significance of recycling, recovery, and environmentally sustainable disposal methods for synthetic polymers. Within this context, polyurethanes (PU) emerge as a versatile family of synthetic

polymers, exhibiting a wide range of applications. This class of polymers is derived from the condensation reaction involving polyisocyanates and polyalcohols. The imperative to address the environmental impact of synthetic polymers, particularly polyurethanes, emphasizes the growing need for efficient and eco-friendly strategies in their management and disposal (Kemona & Piotrowska, 2020)

The selection of adherend materials is a critical factor that requires special attention, as different materials exhibit distinct behaviours that can impact the overall performance of the bonded joints. A significant distinction in the strength of the bonded joints was reported, in the case of different adherend materials, under the same testing conditions (Ozel et al., 2014). One of the most interesting topics is related to dissimilar material selection of adherend which can introduce unique challenges. This is due to the complexity involved in simultaneously studying the two different interfaces' behaviour. In this case, further investigation needs to be undertaken to ensure good compatibility between the adhesive and adherend materials in both mechanical and chemical perspectives. It has been suggested that an in-depth comprehension of the fracture analysis of bonded joints can be advantageous for achieving fully optimised adhesive bonding with different adherend materials (Budhe et al., 2017).

2.4.3.1.3 Surface treatment

In the process of adhesively bonding joints, the surface treatment of the adherend is perhaps the most crucial step that determines the quality of the joint (Park et al., 2018). The chosen surface treatment can have a significant impact on the surface texture and chemistry of the treated substrates, which in turn affects the initial adhesion performance and durability of the adhesively bonded joints (Budhe et al., 2017). The alterations made to surface properties can be achieved through mechanical, chemical, or a combination of both methods. An effective treatment can form a contaminant-free surface, able to roughen it on a macro- and microscopic scale and able to form a fresh, stable oxide layer in the case of metallic materials. Furthermore, it can also enhance the surface free energy and change the chemical composition or introduce a new functional group on the top layer of the substrate's surface that ensures effective modification (Galvez et al., 2019; Guo et al., 2019; Martínez-Landeros et al., 2019; Narbon et al., 2019; Osouli-Bostanabad et al., 2017; Tao et al., 2019; van Dam et al., 2020; Zhu et al., 2016). Hence, the creation of controlled surface characteristics is the primary objective to produce consistent adhesively bonded joints, which remains a significant challenge in selecting an appropriate surface treatment.

The selection of an appropriate surface treatment is dependent on several parameters, including but not limited to cost-effectiveness, safety and environmental

concerns, efficiency, stability of the treated surface, compatibility with the chosen adhesive, as well as the speed, simplicity, and ease of integration into the manufacturing process. In this favour, a wide range of surface treatment methods are available such as mechanical, chemical, thermal or plasma treatment (Budhe et al., 2017). Mechanical (physical) modifications increase the roughness of the treated surface to form an interlocking phenomenon with adhesive and enlarge the surface area, as shown in Figure 7(a). These are in line with the ideal requirements to promote sufficient adhesion according to the mechanical interlocking theory. Generally, appropriate surface treatment can be an effective step for a substrate with a neutral charge to create dipoles on the treated substrate surface, improving surface energy and wettability. Therefore, chemical modifications can be employed to improve the ability of the treated surface to form strong chemical bonds by providing different functional groups (e.g., hydroxides and silanes) which can be compatible with the various adhesives (Figure 7b). As a result, a number of studies have been carried out to investigate the influence of different surface treatments, including solvent degreasing (Leena et al., 2016), mechanical abrasion and peel-ply (Yang et al., 2019), chemical etching (Saleema et al., 2012), plasma treatment (Rhee et al., 2003) to enhance the surface characteristics, and consequently improve the strength and durability of the adhesively bonded joint. In practice, mechanical and chemical contributions to improve adhesion performance are interrelated, however, it has not been identified in most of the previous studies.

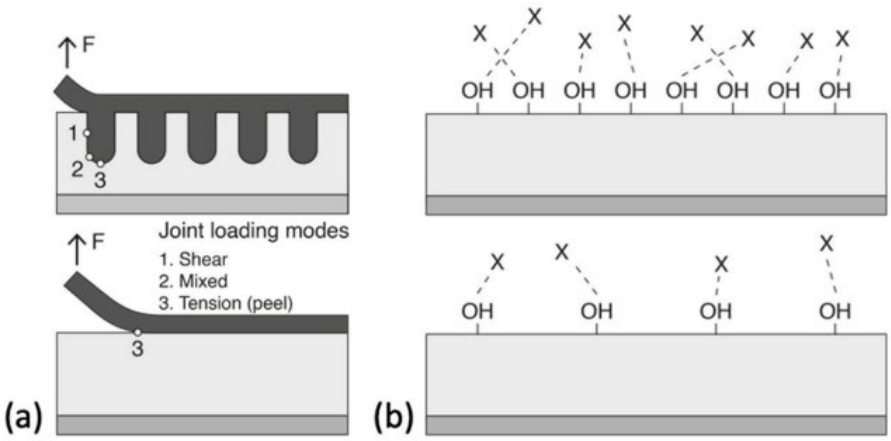

Figure 7: Schematic sketch of the (a) Mechanical advantages provided by surface treatments that increase the surface roughness and bonding are and (b) Higher density of the hydroxyl density on interfacial zone (represented by X) (Abrahami et al., 2017)

There are various techniques that can be employed to achieve the above-mentioned modifications, and the selection of a suitable method is dependent on the properties of the adhesive, adherend, and the requirements of the intended application. In light of this, surface treatments can be categorised into three distinct groups as outlined below:

1. Surface cleaning and degreasing, which removes any contaminants,
2. Surface pre-treatment, which can be either mechanical, chemical, or a combination,
3. Surface post-treatment, which contains the application of coupling agents.

Considering the crucial role of surface treatments in determining the performance of adhesively bonded joints, the ensuing sections will expound on the latest advancements in various surface treatment processes.

2.4.3.1.3.1. Surface cleaning and degreasing processes

The presence of any external contaminants, such as dust and oil, at the interface, can cause premature adhesive failure in the adhesively bonded joint. Therefore, removing any external contaminants should be considered an essential step for any surface treatment procedure at a very early stage of surface treatments. The literature provides various studies investigating different degreasing methods on different types of materials (Marques et al., 2020; Osouli-Bostanabad et al., 2017). In this manner, it has been reported that degreasing the organic materials (i.e., aluminium alloys) is essential for removing the old oxide layer to a certain level without damaging the bulk material and developing a fresher oxide layer with higher surface energy (Zain et al., 2014). However, the high surface energy of the oxide layer over the surface of the metallic materials can introduce unique advantages and disadvantages, which will be discussed in the following sections. In general, the surface treatments should be considered to control some of the surface characters in favour of good adhesion performance.

Various techniques have been reported in literature for removing the weak surface layer by means of degreasing with different solutions tailored for specific adherends (Osouli-Bostanabad et al., 2017). Immersing the specimen in a pure solvent, such as hydrocarbons, is one approach to degreasing. The contaminants on the substrate surface are dissolved and removed using a condensing agent after condensation occurs (Baldan, 2004). The main drawback of using the vapour degreasing method is its level of toxicity at liquid and gas phases, which requires a highly ventilated working environment. An excellent alternative method is to scrub the surface joint in a solution of detergent mixed with water. As an example, metallic substrates can undergo immersion or spraying with alkaline degreasing agents, followed by rinsing with hot water and subsequent drying through methods such as hot air, steam, or ambient air. Moreover, ultrasonic cleaning utilising acetone exhibits favourable surface finish results for small-sized components (Paz et al., 2016).

It can be inferred that the careful selection of degreasing agents can greatly impact the efficiency of the degreasing step in the surface treatment process. The solvent should

be selected by considering its compatibility with the substrate to avoid any material degradation. For instance, chlorinated hydrocarbon-based degreasing agents can produce stress corrosion, which can further result in premature failure in adhesively bonded joints. It has been reported that for manual degreasing, solvents with a faster evaporation rate are preferable (Baldan, 2012). The challenges encountered in practical applications, such as working in dusty environments, have led to the consideration of acetone as a suitable option for many adhesive applications. Acetone exhibits a high level of wettability, making it an attractive choice for mixing with adhesives in such scenarios.

2.4.3.1.3.2. Surface pre-treatment: Mechanical abrasion methods

Mechanical abrasion, also referred to as grinding, can be performed on smooth surfaces to create a rough texture that can affect the adhesion performance of adhesively bonded joints. Some prevalent mechanical treatment techniques comprise sandpaper or emery cloth abrasion, and sandblasting. It has been advised that degreasing should be repeated after mechanical abrasion treatments to remove any loose particles that may remain on the abraded surface (Paz et al., 2016). The resultant surface texture after performing any mechanical abrasion method differs from the physical and chemical properties of the bulk material. The new form of surface is normally referred to as the interfacial zone, in which different surface characteristics are expected (see Figure 8).

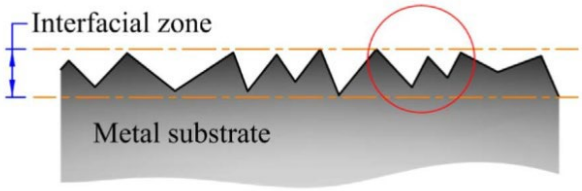

Figure 8: Cross-section diagram of the interfacial zone after mechanical treatment with an average depth of 10μm (Wang et al., 2017)

The influence of different surface roughness of the interfacial zone developed after mechanical abrasion on the cleavage strength was first studied by Shahid and Hashim (Shahid & Hashim, 2002). The results suggested that two surface roughness parameters, R_a and $R_{max,}$ can be assessed to predict the trend of improvement in the strength of the adhesively bonded joints. Furthermore, the study by Ghumatkar et al. (Ghumatkar et al., 2016) conducted a shear strength between two different adherend materials, aluminium and steel, to investigate the influence of the surface roughness on the shear strength of the adhesively bonded joints. Studies mentioned above have indicated that increasing surface roughness can have a positive impact on the initial performance of adhesively bonded joints, up to a certain threshold. The efficacy of mechanical abrasion in enhancing shear

strength exhibits a correlation with the adhered materials, demonstrating a comparable trend of improvement, as illustrated in Figure 9. Therefore, the shear strength reaches its optimal value for both aluminium and steel for a Ra value of 2μm before dropping the strength with extensive roughness. It is outlined that high roughness reduces the adhesive's ability to travel all the way to the bottom of irregularities and merge with the surface texture, increasing the chance of air bubble formation and therefore initiating localised stress concentration (Prolongo et al., 2006; Rudawska et al., 2016).

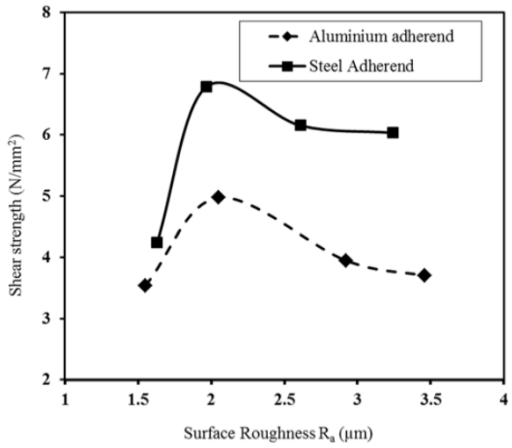

Figure 9: Shear strength with respect to the adherend surface roughness of two different metallic materials (Ghumatkar et al., 2016)

The results aforementioned highlight the significance of the surface roughness parameter for exploring the efficacy of various mechanical treatment methods in improving the adhesive strength of the bonded joints. The characterisation of surface roughness parameters can serve as a robust method for analysing the surface topography resulting from various surface treatments. Indeed, a pronounced reduction in strength is observed when the interface is overly roughened. Consequently, the association between surface roughness and adhesion performance is not straightforward. The most favourable surface texture is adhesive-specific and is influenced by the applied stress type.

The critical value for optimal surface roughness depends on several parameters, such as the type of adherend and adhesive, the geometry of samples and the type of load. Dry blasting is another mechanical abrasion method that is generally used for metallic components. However, it has been found that surface roughening using the blasting method can introduce physical and chemical modification, which is named a physio-chemical change. Physio-chemical modification can influence the thermodynamic characteristics of the treated surface, such as wettability and surface free energy (Da Silva et al., 2010). Different fine materials can be used as the abrasive particle, such as sand, shot, garnet, metal, etc. However, sand had been the most common grinding particle.

Sandblasting is suggested to be considered for surface treatment of a wide range of materials prior to adhesive bonding. These materials include aluminium alloys (Bresson et al., 2012; Critchlow & Brewis, 1996), titanium alloys (Golaz et al., 2013) and steel (Bouazaoui & Li, 2008). In spite of the fact that sandblasting develops mechanical effects similar to those of manual sandpapering, it was found that sandblasting could also influence the chemical composition (Harris & Beevers, 1999), micro-rigidity (Wang et al., 2014) and microstructure of interface (Multigner et al., 2009) of the treated surfaces. Also, the depth and location of surface modification due to this surface treatment usually is inhomogeneous (Okada et al., 2019). This may introduce some level of difficulty where a controlled surface texture is required.

2.4.3.1.3.3. Surface pre-treatment: Chemical treatment methods

In the realm of advanced engineering applications involving adhesive bonding, mechanical treatments alone are often insufficient to produce a robust adhesive bond (Narbon et al., 2019). Hence, chemical treatments are often necessary to achieve durable adhesive bonding in advanced engineering applications (van Dam et al., 2020). Although chemical treatments are generally considered a straightforward process, in practical applications, various competing reactions may occur, and even small variations in treatment conditions, such as solution concentration, bath temperature, and ion content of substrate metals, can render chemical treatments more intricate than mechanical pre-treatments. A further concern associated with chemical treatments is the generation of toxic waste, which may pose a substantial environmental challenge. The majority of chemical treatments involve the use of potent oxidising agents, necessitating cautious handling and complex disposal procedures. Consequently, prior to application, all selected chemical solutions must undergo careful evaluation in accordance with the Material Safety Data Sheet (MSDS). Hence, there is a growing trend in this field to search for new environmentally friendly agents for chemical treatments of adhesively bonded joints.

One of the commonly employed chemical surface treatment methods for preparing substrates prior to adhesive bonding is etching and pickling. The main objective of these treatments is to transform the topmost layer of metallic surfaces into a new and more stable oxide layer that is suitable for effective bonding. This process is especially effective for metallic materials that are prone to instability and degradation due to microstructure abnormalities like oxide layers, changes in chemical composition, and smaller grain size. The etching process can be performed in either alkaline or acidic solutions. In the study by van Dam et al. (van Dam et al., 2020), the influence of both acidic and alkaline treatment on the steel-bonded joints' initial and exposed performance

were investigated. It was found that the alkaline treatment of the polished surface shows the shear strength was even lower than the untreated and polished ones for steel substrate. However, according to the surface characterisation results obtained in this study, it was found that alkaline treatments have the ability to eliminate the passive oxide layer of steel substrates and form a fresh hydroxyl group on the surface of the treated samples. Alternatively, acid treatment results in a significant improvement in shear strength compared to the polished surface. The conclusion drawn from the study suggests that the enhancement in shear strength of the adhesively bonded joints is primarily attributed to the alteration in the quantity of interactions occurring between the adhesive and the interface of the substrate. In line with these results, Pohl et al. (Pohl et al., 2016) addressed in their study that acid treatment can lower the presence of hydroxyl groups in the treated samples.

In addition to the aforementioned etching processes, anodising has been identified as an effective method for forming porous anodic oxide films on titanium and aluminium alloys, with widespread use in commercial applications. The formed layers provide a nano-porous texture for infiltration by adhesive, thereby improving interface and bonding stability. However, it was also found that the irregularities produced after this treatment may be too deep for most of the available adhesive to reach the bottom of the porous layer. The questionable concern about the anodising methods is their environmental impact. It is worth mentioning that the complexity of the anodising method can introduce significant difficulties in ease of adaptation for various applications.

2.4.3.1.3.4. Surface post-treatment: Adhesion promoters

Any subsequent steps that are undertaken after the mechanical and chemical pre-treatment methods, are commonly referred to as surface post-treatments. One of the prevalent post-treatment methods of surfaces is the utilisation of adhesion promoters, which are commonly referred to as coupling agents. Organic materials such as polymer and adhesive are significantly different from inorganic materials in many ways, for instance, in chemical reactivity, coefficient of thermal expansion, and most importantly, surface properties, thereby forming an adequate chemical bond between these two different materials is arduous. Herein, surface post-treatment can promote the adequate adhesion interaction between inorganic substrates and adhesive by enhancing the stability of the interface through the formation of strong chemical bonds (i.e., covalent bonding). Furthermore, coupling agents can impart a notable level of resistance against environmental factors, such as moisture and temperature, which often impair the performance of the adhesively bonded joints by adversely affecting the strength of the interfacial interactions between the two substrates.

Coupling agents are typically selected with dual functionality based on their compatibility with substrate and adhesive (Figure 10). A metallic atom at the centre of the coupling agent's molecular structure, including silicon, titanium, zirconium, and aluminium, will provide a site for inorganic reactivity, especially if hydroxyl groups are presented at the metallic surface. On the other hand, the organofunctional group can condense with themselves and form a rough oligomeric structure. This fundamental principle of chemistry and the reaction mechanisms involved in coupling agents has provided valuable insights into the improvement of adhesively bonded joint performance. Different coupling agents with various practicalities and applications have been studied in the literature to improve the instability of the interface of the metallic materials and adhesives (Abel et al., 2006; Bertho et al., 2010; Guo et al., 2019; Mohseni et al., 2006; Plueddemann, 1982; Rider, 2006; Rider & Arnott, 2000). Upon deposition of the coupling agent onto a pre-treated inorganic surface, the surface properties undergo a transformation, resulting in the formation of a new interfacial layer with unique characteristics. Therefore, different coupling agents with different surface characteristics can be selected to develop the desired surface for the intended use.

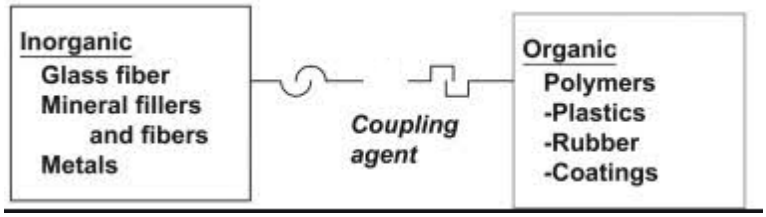

Figure 10: Schematic diagram of dual functionality of the coupling agents (Ebnesajjad & Ebnesajjad, 2013)

A substantial body of literature has established that a silane-based coupling agent can serve as an effective adhesion promoter owing to its ability to undergo reactions with both metallic adherends and polymers. The performance of the conventional silane on the resultant durability of the adhesively bonded joint was studied comprehensively by Abel et al. (Abel et al., 2006). It was concluded that the nature of the solvent (water or methanol), the pH of the solution, the concentration of silane and hydrolysis time prior to application are crucial to the performance of the silane coupling agent. This promising result was achieved when the durability of the silane-treated specimens was compared to a chromic acid anodised treatment.

2.4.3.1.3.5. Silane

The silicon-based coupling agent, also known as silane, typically possesses a monomeric molecular structure with a silicon core atom bonded to four substituents. The most conventional structure has one organofunctional group (Y) and three inorganic-reactive methoxys, ethoxy or alkoxy groups (X) in the form of $X_3Si(CH_2)_nY$ as shown in

Figure 11. Silicon is a chemical element located in the same group as carbon in the periodic table. However, the chemical reactivity of silicon is significantly different from carbon. Despite the similarities between carbon and silicon, silicon does not form double bonds and, because of its strong electropositive characteristics is capable of strong and unique chemical reactions, which increases its usefulness as an adhesion promoter. A silanol, -Si-OH, part of the silane is usually unstable and easily condenses to siloxane, -Si-O-Si-. In general, silane polymerisation is a complicated reaction consisting of three different stages. In the first stage, the silane solution will be hydrolysis, in which the hydroxyl group (OH) substitutes the alkoxy groups in an acidic medium in the presence of selected solvents. Then, the formation of siloxane takes place by condensing a water or alcohol molecule from organofunctional silane molecules. Hence, the incorporation of both organic and inorganic substituents in the chemical structure of silane makes it an attractive candidate for use as a coupling agent.

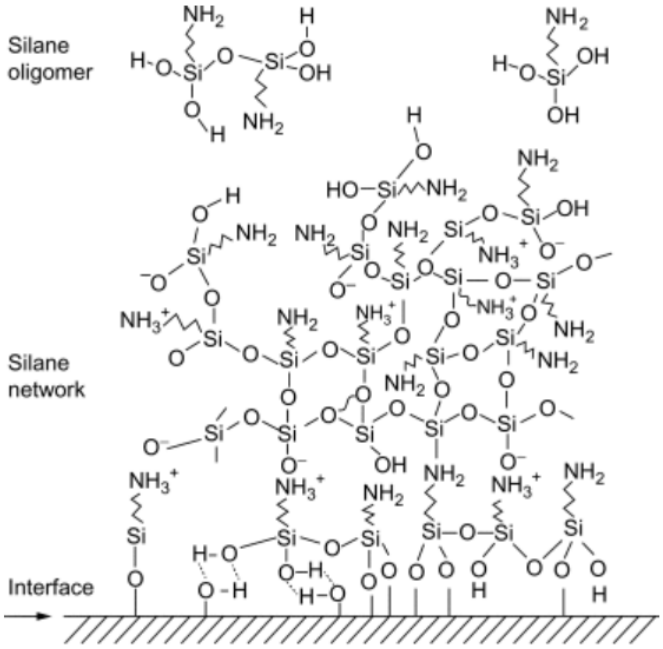

Figure 11: Schematic presentation of different layers of the silanol after condensation (Mohseni et al., 2006)

2.4.3.1.3.6. Dipodal silane

The term dipodal refers to the Greek word which means ‘two feet.’ Dipodal silanes can be differentiated from conventional silane, based on their chemical compositions. In most conventional silane surface modifications, only one of the three hydroxyl groups, on each silicon atom formed during hydrolytic deposition, condenses with silanol on the treated substrate to form a siloxane bond (Figure 12). As mentioned earlier and seen in Figure 11, the remaining silanols condense into the silsequioxane structures or remain as unbound or hydrogen-bonded silanols. Disregarding the formation of silsequioxane, an estimated improvement in the stability of the treated surface on a silane with two silicon

atoms and therefore double the chance to form siloxane bonds, could potentially enhance the durability of the bond 100-fold (Arkles et al., 2014). This discussion is mainly simplified but appears to be consistent with improvements in the hydrolytic stability observed with dipodal silane. It was also concluded that there are distinct advantages which can be achieved by using dipodal silanes in comparison with conventional silane in terms of maintaining the integrity of surface coating in aggressive environments. Theoretically, according to the equilibrium constant for ≡Si-O-Si≡ dissociation to silanols, dipodal silanes can provide greater resistance, almost 10,000 times, than conventional silanes. However, the number of empirical studies of the investigation of dipodal silane, despite the fact that they may potentially perform better than conventional silanes as a coupling agent is rare, especially in the field of adhesive bonding. In the study by Singh et al. (Singh et al., 2014), the resistance of treated surfaces with hydrophobic alkyl functionality in acidic and brine environments was studied and compared with conventional silane coupling agents. The conducted static immersion durability test was undertaken in a very harsh solution, and the results suggested the advantages of using a dipodal silane over the analogous conventional silane coupling agent as a coating. However, the improvement in actual mechanical and adhesive strength has not been studied.

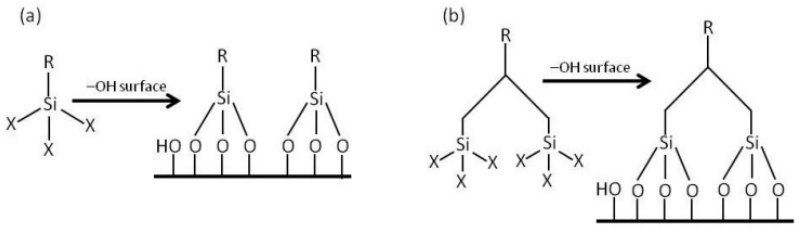

Figure 12: Different layout of covalent bond formation to a hydroxylated organic surface by (a) conventional silane and (b) dipodal silane (Singh et al., 2014)

2.4.3.1.3.7. Zirconate

Many coupling agents other than those based on silicon have been evaluated over the years. However, there has been limited research on the surface characteristics of samples treated with these coupling agents. These materials are based on the same principles as silicon-based coupling agents but have a different metallic core element. In this case, zirconate has been advanced as an adhesion coupling agent. Zirconate-based coupling agents are able to act as a chemical bridge for bonding two dissimilar species via proton coordination without the need for water condensation as it would happen with silanes (Monte, 2002). There is some debate regarding the effectiveness of zirconate in improving the treated surface's stability compared to silane. The main reason behind the statement that zirconate may be a more efficient adhesion promoter than conventional silanes lays in the unique multifunctional chemistry of zirconate. A zirconate coupling

agent has no pH sensitivity as with silane, and no hydroxyl group is required to be presented at the surface of the treated samples to complete the bonding.

The effect of zirconium conversion treatment on the adhesive bonding strength and surface characteristics of a steel substrate was studied by van Dam et al. (van Dam et al., 2020). They have found that modifying the surface chemistry of the steel substrate with zirconium-based coupling agents significantly affects the initial shear strength of adhesively bonded joints utilising epoxy adhesive. However, a clear comparison between zirconate and silane coupling agents has not been developed.

2.4.3.2 Environmental factors

The durability and stability of adhesively bonded joints depend significantly on the robustness of the interface between the adherend and the adhesive. Therefore, the interface between the adhesive and adherend is considered as the crucial region for preserving the adhesive strength and adhesion properties over the joints' service life. The durability of adhesive bonded joints, especially in high moisture conditions, is a crucial aspect that is widely considered in various applications of this joining technique (Tatar et al., 2018). While achieving high initial bond strength is comparatively straightforward, forming durable adhesively bonded joints that can withstand severe environmental conditions is relatively complex and challenging. Depending on the application, adhesively bonded joints may be exposed to various environmental conditions during their service life. It is imperative to conduct a comprehensive investigation on the effect of environmental conditions on adhesively bonded joints, particularly on their exposed performance. Research has shown that the exposed mechanical behaviour of adhesively bonded joints is significantly influenced by two distinct environmental factors, namely temperature and humidity (Fevery et al., 2021).

The influence of these two environmental factors was studied by Fevery et al. (Fevery et al., 2021) by exposing the aluminium-epoxy single-shear samples to multiple environmental factors acting simultaneously. The impact of temperature on the residual strength of the single lap joints was found to be substantial, resulting in a three-fold reduction. The findings suggest that moisture and dynamic loading are also significant factors that impact the mechanical properties of adhesively bonded joints, although their effect is less severe compared to temperature. In addition to this, moisture can be recognised as one of the primary external factors influencing the exposed integrity of the adhesively bonded joints. In the case of epoxy-based adhesive, which is the most studied type of adhesive in the literature, the modulus in the transition region reported by Jurf and Vinson (Jurf & Vinson, 1985) was reduced in the presence of moisture. This study suggests that the effect of moisture on epoxies may be irreversible.

Furthermore, the impact of moisture on the degradation of the interface between the adhesive and substrate can be exacerbated by high temperatures. It is broadly admitted that moisture diffusion follows the Arrhenius equation in the structural adhesives, in which the diffusion rate significantly increases with a subsequent increase in temperature (Heshmati et al., 2015). Therefore, the ageing condition in most of the studies in the literature was set to be coupled with high temperature to accelerate it by increasing the diffusion rate to evaluate the result in a shorter time (Bai et al., 2014; Correia et al., 2018; Costa et al., 2017; Possart & Brede, 2019).

Bai et al. (Bai et al., 2014) performed fatigue tests on steel-to-CFRP joints under elevated temperatures. Strength reduction of 50% and 20-30% reduction in residual stress were observed for specimens glued with epoxy adhesive compared to room temperature. In general, to make reliable prognostication about the durability of the adhesive bond, the conditions of the testing should be selected as close to real-life conditions as possible. In the study by Possart and Brede (Possart & Brede, 2019), the complex correlation between the failure behaviour of adhesive joints and artificial ageing was described. In addition to that, the statement was made by Costa et al. (Costa et al., 2017) that no consistent trends are discovered in the effect of humidity and temperature on the strength of the adhesive bonds. Besides that, it was stated in the latest study about the influence of different environmental conditions on the durability of the adhesively bonded joints that different ageing parameters such as moisture and temperature cannot be viewed independently (Fevery et al., 2021). Therefore, clear insights into the ingrained correlations between environmental conditions can be provided by further studies. The dominant trend of epoxies' application for investigating the performance of the adhesively bonded joint, can be seen from the previously cited literature. Considering there is an urge for applications of more environmentally friendly adhesives, there is considerable concern about the limited number of studies on this topic.

As mentioned previously, moisture is a critical factor that can significantly impact the durability of adhesively bonded joints. It is challenging, if not impossible, to prevent water from coming into contact with an adhesively bonded structure that is exposed to any environmental conditions. Water molecules can diffuse through the interface between adhesive and adherend surfaces at the weakest point of the structure if necessary considerations such as proper surface treatment have not been considered. Once water molecules find their way to diffuse into the interface layer, the integrity of the bonded joints can be significantly reduced by substituting the interaction between surface molecules with unstable hydrogen bonds. In this case, the locus of failure has been reported to migrate from the cohesive zone to the adhesive zone near to the interface. For

instance, due to the polar nature of metal oxide surfaces which refers to the presence of metal atoms with a partially positive charge, water molecules are attracted across the interface and disrupt any dispersive bonds. From the thermodynamic perspective, the positive work of adhesion can indicate a stable interface, while the negative value indicates the opposite (Kinloch & Kinloch, 1987). As shown in Table 2, it is seen that the presence of moisture can change the work of adhesion at the metals-adhesive interface from stable to unstable. On the other hand, it is seen that the moisture reduces the work of adhesion in the interface between the epoxy adhesive and polymeric adherend but thermodynamically remains stable.

Table 2: Calculated work of adhesion in their normal situation and the presence of moisture for different sets of adhesively bonded joints and their failure mode (Kinloch & Kinloch, 1987)

Interface	Work of Adhesion (mJ/m^2)		Interfacial Debonding After Immersion in Water
	In Inert Medium	In Water	
Epoxy/ferric oxide (mild steel)	291	−255	Yes
Epoxy/alumina	232	−137	Yes
Epoxy/silica	178	−57	Yes
Epoxy/CFRP	88–99	22–44	No

The information presented in Table 2 illustrates the detrimental consequences that may arise when the interface forces are predominantly based on dispersive interactions in metal-adhesive bonds. This type of the intermolecular forces which arise due to the temporary fluctuations in electron distribution within the metal and adhesive molecules can lead to a temporary dipole and potentially enhancing the interface forces at the interface. Hence, strengthening the interface zone is deemed the most efficient approach to address the issue of interface degradation resulting from moisture presence. As stated by David and Bond (Davis & Bond, 1999), establishing adequate surface chemistry can be considered to be the most important step in the surface preparation process.

The selection of surface treatment should be based on the type of adherend material due to the varying forms and conditions of degradation observed in different materials. In the case of aluminium adherents, the presence of moisture can cause surface hydration which leads to an increase in the volume of the interface, resulting in high levels of internal stress. This increase in stress can initiate and propagate cracks near or at the adhesive/metal interface, as illustrated in Figure 13. It is important to consider the specific material properties and the conditions in which they will be used when selecting the appropriate surface treatment to prevent such issues.

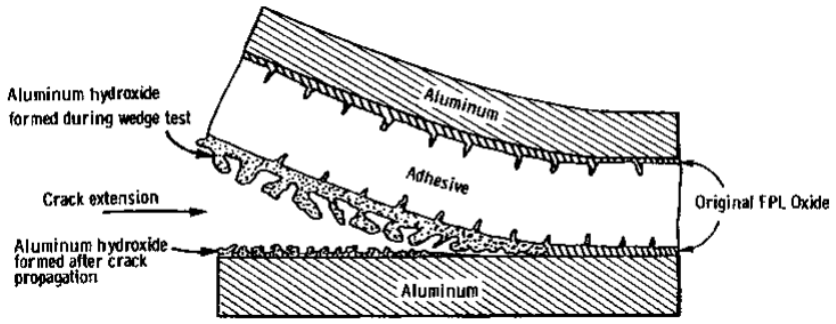

Figure 13: Schematic representation of hydration causing crack propagation in a wedge test specimen (Jahn et al., 2016)

The rate of hydration of aluminium oxide is a complex process that can be influenced by multiple factors. These factors include the surface chemistry of the material after treatment, the presence of hydration-resistant compounds in the selected promoter, temperature, and the level of environmental humidity. Understanding these factors and their impact on the rate of hydration is critical in the development of effective surface treatments for aluminium adherents. Failure to properly address this issue can lead to significant internal stress within the interface, which can result in crack initiation and propagation near the adhesive/metal interface. In the study by Abel et al. (Abel et al., 2006), the influence of silane pretreatment as a selected surface treatment was addressed comprehensively. All the samples were examined under different silane solution conditions. The results suggested that under all silane treatment conditions, failure within the regions of crack propagation after the ageing conditions, appeared to be interfacial. In this study, from the XPS analysis, the existence of metallic material as well as silicone elements on both sides of failed surfaces can imply the location of failure within an oxide/silane/adhesive zone (Figure 14). Similar behaviour was also observed in the locus of failure in the study by Rider and Arnott (Rider & Arnott, 2000). Such observation evidently delivers interesting indications as to how greater enhancements in the durability of the adhesively bonded joints could be achieved from appropriate surface modifications to both the silane and oxide layers.

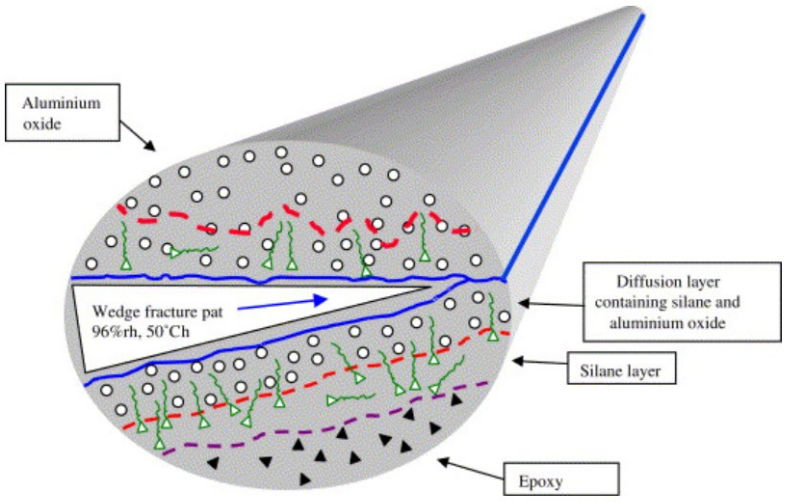

Figure 14: Schematic of a sectional wedge joint showing the apparent failure path (Abel et al., 2006)

2.5 Aluminium surface

Aluminium alloys have been selected as one of the primary materials for lightweight structural applications due to their exceptional mechanical properties, including advanced high strength and non-ferrous characteristics. Specifically, it has been observed that the average usage of aluminium alloys in passenger cars has doubled, and this trend is expected to continue based on the recent design concept (Hirsch, 2014; Njuguna, 2016; Ribbens et al., 2009). Compared to steel, aluminium alloys can provide 65% less density, which can be a huge advantage for lightweight structural frameworks. However, to reach the same stiffness as steel structures, thicker aluminium parts are required, while the average elastic modulus of aluminium is less than steel. Aluminium-based structures pose a challenge in terms of joining through spot welding due to the high activity of the oxide layer on the aluminium surface, which interferes with spot weld electrodes. In addition, the high temperature involved in welding can reduce the strength of the bonded joints. Thus, the replacement of steel with aluminium alloys is not a straightforward process and necessitates design and process adaptation.

As previously mentioned, the limitations of hot bonding (e.g., welding) can be overcome by selecting cold bonding methods, such as mechanical fastening and adhesive bonding, as alternatives. The dependency of the adhesively bonded joint's strength and durability has been well-known among researchers in this field. Therefore, a good understanding of the substrate's surface characteristics can enhance the confidence level in better performance of the bonded system. In the subsequent section, an in-depth analysis of the fundamental characteristics of aluminium and its alloys is presented. Emphasising the paramount importance of these base materials, a comprehensive examination of the surface appearance of aluminium alloys is provided. Furthermore, the

latest advancements in surface treatments specifically tailored for aluminium alloys in the context of aluminium adhesive bonded joints are thoroughly discussed.

2.5.1 Aluminium and its alloys

Aluminium exhibits high chemical reactivity owing to its strong electro-affinity for oxygen, as evidenced by the exothermic nature of the oxide formation process. Despite its abundance in the earth's crust, aluminium was not utilised extensively until the late 1800s due to the technical challenges associated with extracting the metal from its oxide form. Nonetheless, alumina (Al_2O_3) was already familiar to scientists in the eighteenth century, as demonstrated by Danish worker H.C. Oersted's successful production of aluminium powder through the reduction of anhydrous aluminium chloride with sodium amalgam (Sheasby & Pinner, 2001). Many researchers devoted considerable efforts to the development of aluminium metal, but it took several years before the metal was produced on a commercial scale.

It can be fair to name the French scientist as a father of the light metal industry, Henri Sainte-Claire Deville, who in 1850 replaced potassium with sodium to improve Wohler's method and consider aluminium and sodium as his main source of metal, thereby directing the production of the aluminium alloys into a commercial proposition. However, the main drawback of using metal back in that time was its high price which was sometimes equivalent to the price of gold.

To be able to decrease the cost of production of aluminium alloys, in 1886, Heroult and Hall invented a new method of aluminium production from alumina and molten cryolite. Additionally, the modern industrial production of aluminium involves a complex process starting from bauxite, a mineral containing approximately one-fourth of aluminium's chemical composition. Bauxite is first digested with a solution of sodium hydroxide under pressure, commonly referred to as the Bayer process, to produce purified alumina. The purified alumina is then added to a molten mixture of cryolite and fluorspar, and an electric current is passed through the mixture to produce molten aluminium (Sheasby & Pinner, 2001). This process, known as the Hall-Heroult process, was first developed in the late 19th century and is still widely used today.

2.5.2 Aluminium alloy 6061-T6 properties

Aluminium, in its pure condition, is a relatively soft metal with a maximum yield strength of only 34.5N/mm^2 and tensile strength of 90N/mm^2 (Nettikaden, 2008). Thanks to the development of aluminium alloys, varied strength and stiffness can be achieved based on the requirement of different applications. In its pure state, aluminium exhibits a relatively low corrosion rate once it forms oxide layer, and consequently, it requires less

protection compared to aluminium alloys. In order to enhance the mechanical properties of pure aluminium, various alloying elements are utilised, such as magnesium, silicon, copper, manganese, nickel, and zinc. In total, aluminium alloys can be categorised into two classes. The first category is called “cast alloys” due to the manufacturing method, in which the product is cast directly into their desired forms. The second class is called “wrought Al alloys,” which manufacturing takes place over hot and cold extrusion, forging, etc. The main classes of alloys are coded as 2000 series (Al-Cu alloys), which have mainly been used in aircraft applications due to their high strength properties; the 3000 series (Al-Mn alloys), which have mainly been used in the canning industry, the 5000 series (Al-Mg alloys), which are used unprotected for architectural and structural applications, the 6000 series (Al-Mg-Si alloys), which are the most common extrusion alloys, and the 7000 series (Al-Zn-Mg alloys) which are high strength alloys (Sheasby & Pinner, 2001).

2.5.3 Surface layer composition

Typically, the surface of various metals is coated with a layer characterised by a complex composition, comprising contaminants such as residual lubricants and remnants resulting from manufacturing processes (Cavezza et al., 2020). For instance, to manufacture aluminium sheet plates, aluminium must be subjected to a cold or hot rolling process in which the complex layer can be developed on the aluminium surface, as shown in Figure 15.

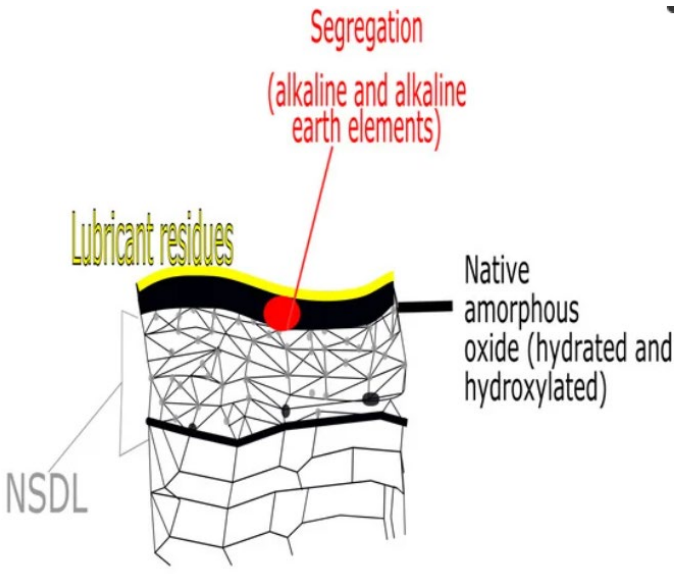

Figure 15: The complex top layer of the aluminium surface after rolling (Cavezza et al., 2020)

In the process of rolling, various lubricants are employed to prevent the formation of a solid film on the roll's surface and workpiece. The primary function of these lubricants is to reduce the friction forces between the roll and workpiece, and to prevent

potential damage to the workpiece surface resulting from the applied pressure. Generally, lubricants are composed of paraffin, which is volatilised either through natural evaporation or annealing. However, a certain degree of contamination is expected to remain on the rolled aluminium's surface, necessitating further treatment through a degreasing process (King, 2014).

On the contrary, due to the high reactivity of aluminium at various temperatures, the formation of a thin oxide layer on the surface of aluminium is unavoidable. The oxide layer at low temperatures is composed of a very thin amorphous Al_2O_3, which forms beside the hydrated surfaces of the metal and hydroxide on top. Aluminium hydroxides have been identified as a highly effective agent for interacting with polar acid components of polymers. However, it is important to note that the hydration of the aluminium surface can result in a decrease in overall adhesion performance, as it generates a weaker interaction on the top surface. Additionally, the oxidation and hydration of the aluminium surface can be accelerated by the presence of alkaline earth elements, such as sodium and magnesium, which may become isolated at the surface of the metal. In general, the presence of magnesium can promote crystalline growth for $\gamma - Al_2O_3$. Therefore, a complex oxide layer can be formed in Mg-rich alloys.

2.5.4 Surface treatment of aluminium alloy

Every metal has its own unique surface characteristics, leading to specific behaviour. The passive film quality is highly dependent on the alloying types of the metal. At the same time, it is also influenced by other factors such as surface morphology, surface topography, the manufacturing process and selected surface treatments (Baldan, 2012). The properties and stability of this passive layer can be highly influenced by its environment due to the dynamic nature of the system. Therefore, the metal surface will be covered with an oxide layer almost instantly after exposure to the atmosphere and hydroxylated after exposure to water. This layer can further be covered by the oxide layer, which has an affinity to absorb contamination like water (Leena et al., 2016).

The importance of the surface treatment has been addressed herein, referring to the experimental studies that were undertaken in several investigations (Heshmati et al., 2015; Islam et al., 2014; Pramanik et al., 2017). Additionally, Rhee et al. (Rhee et al., 2003) discussed the shear strength of the plasma-treated CFRP/Al adhesively bonded joint. The strength of the treated samples was six times higher than those with no specific treatment (Pramanik et al., 2017). As shown in Figure 16, the influence of the surface treatment is significant based on the traditional load-displacement curve for four adhesively bonded joints with different sets of surface treatments. The specimens reach their highest stiffness when both CFRP and aluminium surfaces are treated (curve 1).

Although the surface treatment of each side of the adhesively bonded joint in dissimilar bonding (curves 2 and 3) showed a certain level of strength in the bonded joints, a higher level of improvement was recorded in the case of the treated aluminium compared to the composite side.

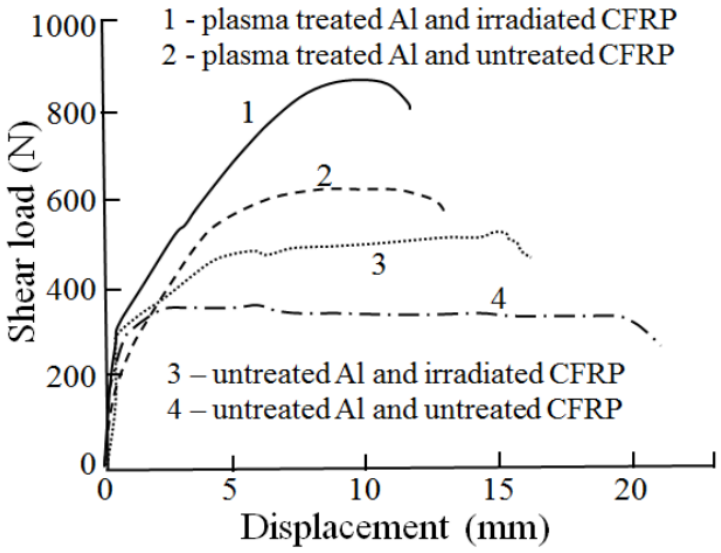

Figure 16: Shear-load versus displacement curves for adhesively bonded joints of CFRP and aluminium subjected to different surface treatment (Pramanik et al., 2017)

In conclusion, the enhancement of the overall performance of adhesively bonded joints relies significantly on the surface treatment of aluminium. From the general perspective, various surface treatments have been studied in the literature (Guo et al., 2019; Leena et al., 2016; Lunder et al., 2002; Saleema et al., 2012)

Saleema et al. (Saleema et al., 2012) investigated the influence of a simple surface treatment of aluminium by immersing a substrate in a diluted sodium hydroxide solution into the adhesion performance of the bonded joints using epoxy resin. The traditional anodising of aluminium was selected in their study for the sake of comparison. A considerable improvement was observed in the bonded joints' initial and exposed performance (about 20%).

Leena et al. (Leena et al., 2016) revealed that superior strength for aluminium joints can be attained by a combination of factors including high surface energy, ideal surface texture, and a high level of adhesive wettability. In this investigation, the authors examined the impact of three distinct surface treatments, namely solvent degreasing, etching, and priming, on the initial performance of the bonded joints. However, the study did not assess any exposed effects regarding the durability and stability of the bonded joints. Given the effects of different surface characteristics on the adhesion performance of the bonded joints, Zhang et al. (Zhang et al., 2008) studied the influence of a

combination of the grit blasting method with phosphoric acid anodising on the initial adhesively bonded joints' performance. Based on the studies mentioned above, it can be inferred that a systematic combination of various surface treatments may enhance the performance of adhesively bonded joints, as compared to individual surface treatments. The meticulous selection of appropriate surface treatments can prevent any added complexity in the treatment process and, in some cases, can simplify the complex surface treatments while achieving satisfactory adhesion characteristics.

Rider (Rider, 2006) conducted experimental tests on the treated aluminium substrate, examining the potential factors that could impact the durability of adhesively bonded joints, including mechanical and chemical aspects. The results revealed that both mechanical and chemical surface treatments are important for achieving a certain level of success in adhesively bonded joints. Silane primer was found to act as a coupling agent, preventing water molecules from integrating into the aluminium and epoxy adhesive interface. However, further studies are needed to investigate the impact of combined surface treatments on the initial and exposed adhesion performance of adhesively bonded joints.

Kim et al. (W.-S. Kim et al., 2010) investigated the contribution of mechanical interlocking to the adhesion strength of a composite-metal adhesively bonded joint system by creating micro-patterned dimensions on the surface of the steel substrate. The outcome of the study indicates a significant correlation between the effectiveness of the adhesion bond and the employed surface treatment methods. A schematic diagram depicting the patterned surface of the substrate was presented in the study, as there was an unclear association between surface roughness and adhesion strength (see Figure 17). The scanning electron microscope (SEM) analysis presented in Figure 18 supported the schematic diagram. The SEM observation demonstrated that the total area related to cohesion and adhesion failure is closely related to the inverse relationship between surface roughness and adhesion performance (Figure 19).

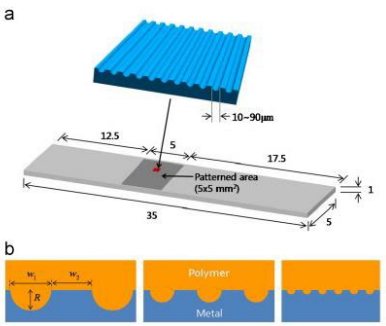

Figure 17: (a) schematic diagram of a uniform patterned metal specimen, (b) schematic diagram of the interface between substrate and adhesive (Kwon et al., 2019)

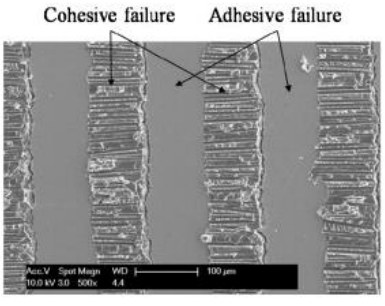

Figure 18: Fracture surface of ENF specimens on the metal side with patterned irregularities (Kwon et al., 2019)

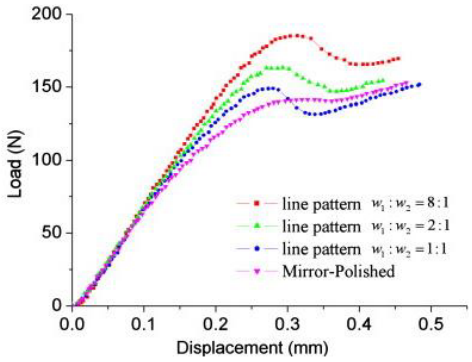

Figure 19: Typical load-displacement curves of treated ENF specimens with different pattern width ratio (Kwon et al., 2019)

Kwon et al. (Kwon et al., 2019) conducted an investigation on the effect of mechanical surface treatment with varying curing times of epoxy adhesive on the adhesion strength of bonded joints. The adhesion performance of the joints was measured using a single-lap joint testing method. The study reported that an increase in the curing time of the adhesive led to a decrease in the number of active functional groups present on the adhesive surface, which reduced its surface tension. The study also examined the influence of surface roughness developed by different mesh sizes and sanding durations. The results revealed that the smaller mesh size abrasive paper produced higher surface roughness values, while longer sanding durations led to a more uniform surface and higher adhesion strength. This was attributed to the formation of a fresh oxide layer after extended sanding. Contrary to the mechanical theory, the study found that increasing the surface roughness did not necessarily improve the adhesion performance of the bonded joints. Therefore, further research is needed to understand the influence of sanding on the surface characteristics of the treated surface and the adhesion performance of the bonded joints.

2.6 Composite surface

Various surface treatment methods have been proposed in the literature for composite materials, including sand blasting and peel-ply. Sanding and sandpapering are among the very early methods developed for the treatment of composite materials due to their excellent ability to remove the contaminators of the surface. This provided a rougher surface and increased the available surface area for efficient bonding between the polymer surface and adhesive. However, excessive sanding can lead to damage in the fibre structure of composite materials, resulting in a decrease in the strength of the bonded joints. The peel-ply method also has limitations, as improper design considerations can cause significant damage to the fibre structure (Nasreen et al., 2021). The utilisation of peel plies is inherently intricate, presenting challenges in their removal,

particularly when composed of nylon fibers. Notably, during the elevated cure process of a composite component, the polyamide within the nylon peel ply fibers can actively participate in the polymerisation of the matrix resin as a comonomer, leading to an arduous adherence to the underlying laminate (Kanerva & Saarela, 2013). Additionally, when evaluating the mechanical properties, such as shear strength or fracture toughness, the resultant strength of a joint post-peel ply treatment seldom equals that achieved through pre-treatment via abrasive mechanical means. Following the removal of a peel ply from a composite surface, residual irregularities in the form of rough ridges and bumps persist, potentially exerting adverse effects on the overall bond strength.

The influence of simple surface treatment for CFRP utilising sandpaper was conducted by Yang et al. (Yang et al., 2019). It was found that the surface characteristics of the CFRP influence the adhesively bonded joint in a CFRP-to-CFRP adhesively bonded joint system. In their study, three different directions and four different grit sizes were used to alter the surface texture of the CFRP. The experimental results revealed that sanding in a random direction would result in the highest bonding strength. On the other hand, the grit size of the sandpapering can profoundly influence the CFRP's surface energy, its surface topography, and other thermodynamic surface characteristics.

Many studies have been conducted for different surface treatments of composite material to enhance the adhesion performance of these materials. However, it has been reported that chemical modifications of polymeric surfaces are expensive and not environmentally feasible (Awaja et al., 2009; Mühlhan et al., 1999; Shrivastava, 1995). Naturally, composite materials have low surface free energy, which can result in weak adhesion performance (Critchlow & Brewis, 1996). To overcome this issue, different treatments have been applied on the surface of the composite material to enhance the surface energy (Guo et al., 2019), surface roughness (Baldan, 2012), and surface chemistry (Benard et al., 2009) and thereby improving the bond strength and its durability for composite materials.

2.7 Effect of Surface Characteristics on the Performance of the Adhesively Bonded Joints

As previously mentioned, various surface treatments can modify the substrate's properties to enhance the adhesively bonded joint's initial and exposed performance. The characteristics of a treated surface can be defined by two primary factors: surface roughness and surface chemistry. It is crucial to carefully evaluate and select suitable surface treatments for a specific adhesive-bonded joint system based on the intended application. Effective surface treatment is only beneficial if an appropriate adhesive is

chosen. Therefore, it is important to comprehend the impact of various surface characteristics of the treated surface on the adhesion performance of the adhesively bonded joint. Consequently, many studies have been focused on developing appropriate surface treatments. Surface roughness parameters are commonly used in the literature to describe the finish after mechanical treatment methods, and some of the most frequently mentioned parameters are listed below.

Surface characterisation of treated surfaces is typically evaluated based on various statistical parameters. The literature has introduced up to 50 parameters for quantifying the finish of the substrate following any surface modification (De Chiffre et al., 2000; Leach, 2013). However, only a few of these parameters have been frequently addressed in the literature (Leach et al., 2015). The most common statistical parameter that has been used in literature is the arithmetical average peak height from the mean line of the roughness profile R_a. Another expression of the surface height is maximum peak height, R_p. Besides this parameter is the Root mean square height of the defined area, R_q, also known as the standard deviation of the heights alongside the treated surface. Based on the information that can be extracted from the skewness and kurtosis value, it would be beneficial to compare the value of these parameters with the abovementioned parameters to examine the final surface conditions after selected treatments. On one side, skewness S_{sk} provides information on whether the final surface profile is biased towards valleys or summits. Therefore, it can be a helpful parameter correlating adhesives' ability to fill deep valleys or cover the highest summits. For example, a skewness of zero can indicate a rough surface with a symmetric surface finish. Conversely, the symmetric surfaces can be indicated by kurtosis, S_{ku} of 3. The lower kurtosis value indicates a skewed surface distribution with fewer outliers; a higher value indicates the opposite.

2.7.1 Influence of surface roughness on adhesively bonded joints

Despite the abundance of studies examining the influence of different surface characteristics, there remains an ongoing need to deepen our understanding of the specific contributions of individual surface properties, including surface roughness and chemistry, to the adhesion performance within bonded systems. Although it has been reported that surface roughening prior to adhesive bonding can improve bonded strength, the actual relationship between adhesion and roughness is not fully comprehended. This correlation may be attributed to either the increased effective surface area or the introduction of mechanical interlocking (van Dam et al., 2020).

One of the earliest published numerical and experimental studies which quantitively related the surface roughness and its parameters to the strength of adhesively bonded joints was conducted by Shahid and Hashim (Shahid & Hashim, 2002). The

attempt was to relate three different surface roughness parameters, R_a, $R_{l0,}$ and $R_{dq,}$ to the cleavage strength of steel-to-steel adhesively bonded joints. Steel surfaces were polished and then grit-blasted by four different grit sizes, and surface roughness parameters were measured using a surface line profilometer prior to cleavage testing. The results illustrated the linear relationship between the cleavage strength and R_a value due to possible enlargement of the surface area. However, it should be noted that grit-blasting not only changes the morphology of the treated surfaces, but surface chemistry can also be altered.

The impact of surface roughness on the strength of adhesive-bonded joints was examined in a study conducted by Ghumatkar et al. (Ghumatkar et al., 2016). Two adherends, mild steel and aluminium, were treated mechanically using sandpapers with varying mesh sizes to produce different surface roughness before bonding with epoxy adhesive. Two-dimensional surface roughness parameters, R_a and R_z, were employed to assess the surface quality of the treated surfaces. The researchers found that the increased adhesion strength was potentially due to mechanical interlocking. The trend of strength enhancement was similar for both materials, despite the difference in magnitude, in relation to the produced surface roughness. A 40% strength improvement was observed for treated aluminium surfaces with a roughness range of 2.05μm as compared to the untreated surface. However, it was noted that high surface roughness did not significantly enhance the initial performance of adhesively bonded joints. The researchers also concluded that shear strength could not be explained solely by increased roughness characteristics as other parameters could contribute to strength improvement. Additionally, all adhesively bonded joints experienced adhesion failure, regardless of surface roughness.

Van Dam et al. (van Dam et al., 2020) conducted a study to investigate the impact of surface roughness on the initial strength and exposed durability of steel-to-steel adhesively bonded joints under various loading and environmental conditions. The steel adherend used in this study was subjected to mechanical treatments such as abrasion and grit blasting. The effect of each treatment on the surface characteristics was observed using different analytical tools. Three different surface roughness parameters, S_a, S_{sk} and $S_{dr,}$ were used to describe the treated surface. It becomes apparent that S_a values growth with rougher abrasive paper. Subsequently, that negative value of S_{sk} indicates the presence of a greater number of valleys than peaks in the treated surface. Additionally, a higher surface area with the use of a rougher abrasive paper was reported. From the single lap joint shear test, it becomes evident that the surface roughness of treated steel is the dominant factor in the initial adhesion performance of the adhesively bonded joints.

In another study by Safari et al. (Safari et al., 2020), the authors investigate the effect of different surface preparations on the initial strength of adhesively bonded joints in aluminium alloys. The surface roughness of the aluminium alloys was modified using manual sandpapering with seven different mesh sizes, as well as shot and sandblasting. The arithmetic average of profile height from the mean line, Ra, was used to determine surface roughness. Two different adhesives with varying viscosities were used in the single lap joint experiment. The results indicated that the initial strength of the adhesively bonded joints increased as the degree of surface roughness increased through manual sandpapering, but then decreased as further roughness was further increased due to insufficient adhesive penetration into the extensive valleys of surface profile. In contrast, the strength of the bonded joints continuously increased as surface roughness increased through shot and sandblasting methods. The study concluded that the optimal surface roughness and strength of the adhesively bonded joints could be adjusted based on the viscosity of the adhesive.

Given the importance of the correlation between surface roughness and viscosity of the adhesive and their effect on the overall performance of adhesively bonded joints, Paz et al. (Paz et al., 2016) conducted an experimental study using two different acrylic adhesives with an aluminium substrate. Two different acrylate adhesives with different viscosities were manufactured and applied over the mechanically abraded aluminium surfaces with two different levels of roughness, R_a = 0.2µm and R_a = 2µm. A smaller contact angle for an adhesive with low viscosity was recorded for the roughest surface. This was stated to be in accordance with Wenzel's equation. However, the opposite result for the high viscosity was reported to be against the fundamentals in Wenzel's equation. The increased viscosity of the selected adhesive also caused a higher bond strength. It was stated that this behaviour could be due to improved adhesive toughness, lower chance of shrinkage prior to curing, and higher strength and uniformity of the chemical bonds.

Reina et al. (Reina et al., 2009) analysed the influence of surface roughness using three different surface roughness parameters, R_a, S_m, and $R_{mr[c],}$ on the mechanical performance of the 6061 aluminium alloy adhesively bonded joints utilising acrylic adhesive. Substrates were treated by three different methods, included of rough machining with an angle grinder to obtain the surface roughness range between 5-6µm, manual sanding utilising abrasive paper to obtain a roughness range between 1-4µm, and finally, polishing to obtain roughness range between 0.1-0.4µm. In addition, the value analysis technique was used to quantitatively assess the corresponding cost for each surface treatment to propose the best use/cost ratio. The results showed that a higher

strength value was reached for specimens treated with emery paper than grinding surface-treated specimens. The value analysis was employed considering the cost involved in the specimens' manufacturing processes, such as labour, machinery, and tools costs. The results from value analysing in this study indicated satisfactory values for sandpapering of aluminium surfaces considering both the cost associated with the manufacturing process and the mechanical performance of the adhesively bonded joint.

In the study by Croll and Payne (Croll & Payne, 2020), the aim was established to evaluate the effectiveness of different surface roughness parameters on steel substrates. To achieve this, rough surface profiles were developed, and two methods were used to measure the surface roughness in two dimensions (line scan) and three dimensions (surface scan). A stylus profilometer and scanning electron microscopy were used for the measurements. The results obtained from both methods were consistent, but the data from the 3D scan were much more numerous than from the 2D scan. The researchers concluded that the surface scan parameters can provide scientific insight into the way that the features of rough surfaces can contribute on improving adhesion performance by conducting further destructive method such as single lap joint tensile test.

In the study by Li et al. (Li et al., 2018), a new type of aluminium alloy, Al-Li alloy, was sandblasted under different conditions to further study the influence of mechanical surface treatment on an aluminium substrate. Four different surface roughness parameters, i.e., R_a, R_z, R_q and R_t, were recorded for each set of treated samples and compared with sandpapered surfaces. The influence of sandblasting on the abovementioned surface roughness parameters was identified as a function of rougher abrasive materials. Accordingly, the results from bond strength in this study indicated a significant improvement in a rough surface produced by sandblasting. It was found that the turning point of the adhesion performance of the bonded joints is the value of 3.85 μm. It was reported that the strength and surface energy values showed different behaviour before and after this turning point. This unique dependency was addressed using the method of Pearson correlation coefficient in which an increase in R_a value has led to the higher surface free energy of the treated surface before the turning point. By contrast, the results after the turning point suggested the exact opposite correlation between R_a, surface energy and the initial performance of the adhesively bonded joints. It was therefore claimed that the intermediate surface roughness has a greater positive influence on the bonded system's surface free energy and shear strength.

In a similar study by Rudawska et al. (Rudawska et al., 2016), the influence of sandblasting on the surface properties of steel in favour of better adhesion, was studied in detail. The effect of different sandblasting variables was addressed, such as blasting

pressure and abrasive size, on surface free energy, work of adhesion and surface roughness. Different surface roughness parameters were employed to define the developed texture after the selected surface treatment. This study clearly stated the importance of utilising different line surface roughness parameters simultaneously beside R_a. For instance, examining the obtained surface roughness parameters led them to a clear conclusion of negligible influence of sandblasting pressure on the surface roughness profile. Also, the correlation between different surface roughness parameters and surface free energy of the treated samples was studied due to the dependency found between them. Significant dependency was observed between the polar component of the treated samples and R_p (maximum peak height of the roughness profile).

In terms of combined surface treatments of the aluminium alloy, Li et al. (Li et al., 2019) investigated the effect of grit blasting and phosphoric acid anodisation on the surface characteristics and the performance of the adhesively bonded aluminium joint. Parameter R_a was used to address the roughness of the developed surface as well as the surface energy measurements to obtain the wettability of the final surface. It was stated that rough surfaces were developed by grit blasting, followed by producing porous structures on the rough surface via phosphoric acid anodising (PAA). Thus, surfaces subjected to combined treatments promoted greater initial adhesion performance in comparison to single surface treatments. The statement was further supported by an experimental study conducted by the authors in which a 119.4% improvement was obtained for combined surface treatment compared to individual treatments.

2.7.2 Influence of surface chemistry on adhesively bonded joints

The significance of chemical conversion to ideal surface characteristics of aluminium alloys through specific surface treatments in automotive applications is an excellent illustration. Smooth and less profiled surfaces are generally preferred, but in the absence of a self-passivated metal interface, increased corrosion rates may result due to the larger surface area exposed to the environment compared to a smooth surface (Li & Li, 2006). In adhesive-bonded joints, metallic substrates are often prone to oxide formation and hydroxide group adsorption at the interface, which can lead to moisture absorption and subsequent degradation of the joint's integrity.

The functional domains of metals, copper, steel and aluminium in particular, extend beyond the purview of their physico-mechanical and tribological attributes, encompassing crucial near-surface properties, with wettability holding a paramount position. Wettability, a significant determinant (Jixue Zhou et al., 2019), influences diverse functional characteristics such as self-cleaning (Ahmad Kamal et al., 2021; Fürstner et al., 2005), resistance to icing (Volpe et al., 2020), fogging (Jiannotti & Ji,

2020), corrosion (Feoktistov et al., 2021), biofouling (Choi et al., 2017), as well as abrasive and cavitation wear , and protection against bacterial intrusion (Emelyanenko et al., 2020).

Jang et al. (Jang et al., 2011) conducted a study to examine the effect of surface preparation at both nano- and micro-scales on the adhesion performance of the aluminium-to-CFRP adhesively bonded joint system. The researchers developed micro-patterns on aluminium surfaces through etching and formed nano-scale surface patterns by anodising. The results of the single leg bending test indicated a strengthening of the adhesion due to the higher mechanical interlocking effect caused by micro-scale irregularities. However, the study did not analyse any surface roughness parameters to describe the characteristics of the treated surfaces. Given the effects of surface irregularities and roughness on adhesively bonded joint strength, Haghpanah et al. (Haghpanah et al., 2014) fabricated a control surface texture with a zigzag interface containing interlocking teeth. Furthermore, the tensile behaviour of the bonded joints was tested and can compare with polished samples' performance. The experimental results suggest in this study that surface interlocking can change the stress distribution along the bondline. Thereby the tendency of a crack to propagate along the bond depends strongly on the morphology of the surface.

The phenomenon of wetting is contingent upon both the elemental composition of the subsurface layer and its topographical intricacies, including roughness (texture) (Malijevský, 2014). While extensive research has been dedicated to elucidating wetting behaviour on molecularly smooth and chemically homogeneous surfaces (Svoboda et al., 2015), it is imperative to acknowledge that the surfaces of metals deployed in various industries as technological surfaces exhibit chemical inhomogeneity and significant roughness.

The determination of wetting properties on surfaces exhibiting chemical inhomogeneity and significant roughness involves the application of the Wenzel (or Wenzel-Deryagin) equation (Wenzel, 1936) for predicting apparent contact angles in cases of homogeneous wetting. In instances of heterogeneous wetting, the Cassie-Baxter equation (Werner et al., 2005) is employed. Despite numerous experimental studies validating the applicability of these equations (Kuznetsov et al., 2020), a discordance arises from conflicting results found in other investigations (Foadi et al., 2019; Hu et al., 2019).

The complexity further amplifies during surface modification endeavors, wherein deciphering the influence of roughness on alterations in wettability properties becomes

challenging, especially when coupled with simultaneous variations in the elemental composition of the near-surface layer. A comprehensive study of the impact of roughness on wettability properties of metal surfaces necessitates extensive variations in roughness within stable elemental compositions over time post-modification.

Conventional methods for metal surface modification, such as chemical vapor deposition (Sun et al., 2021), etching (Khodaei & Shadmani, 2019), and laser radiation (Kuznetsov et al., 2019), have demonstrated the ability to induce extreme alterations in wettability (superhydrophilicity/superhydrophobicity). However, these methods invariably induce concurrent changes in both surface roughness and elemental composition. Likewise, abrasive processing of metal surfaces, a widely employed technique, also influences both roughness and elemental composition, as the near-surface layer undergoes modification (Cadien & Nolan, 2012), and carbon contaminants are adsorbed from the environment (Boinovich et al., 2016). Yet, it remains unexplored whether variations in elemental composition occur when employing abrasive materials characterised by different average sand paper sizes.

Regarding the influence of surface treatments on surface chemistry of the treated surfaces, Zain et al. (Zain et al., 2014) studied the effect of two different chemical treatments on the bond performance of the aluminium-bonded joint system. The researchers employed two different chemical surface treatments, i.e., alkaline etching and warm water treatment, followed by salinisation into the aluminium substrate. One surface roughness parameter was used to address the morphological modification of the treated surface in addition to contact angle measurements. They concluded that, in general, surface treatments could influence the mechanical and chemical characteristics of the aluminium surface with a certain level of detail. However, the actual contribution of these factors did not address systematically. It was found that NaOH treatment is not sufficient on its own to be considered as a suitable surface treatment for application under elevated environmental conditions such as high humidity and temperature.

2.8 Thermodynamic characteristics of the surface

The importance of the interface in determining the adhesion performance of adhesively bonded joints has been previously discussed in this chapter. The present section aims to provide a more comprehensive understanding of the surface characteristics and their relationship with the adhesion mechanism. The interfaces in adhesively bonded joints often serve as weak boundary links in the load transfer chain, leading to stress singularities at their edges due to differences in material properties. Hence, enhancing the surface topography at the interfaces is critical to increase the

maximum load-bearing capacity and deformational characteristics of such joints. The quality of the interface is, therefore, a crucial factor influencing the adhesion performance of such joints.

In the field of adhesion, interfaces can be discussed in two distinct areas. The first area concerns the existence of an "interphase," which is a region intermediate to two contacting solids that possess distinct structural and mechanical characteristics from either of the two contacting phases. The interphases can control the overall mechanical behaviour of macrosystems such as adhesive joints and coating substrate systems. The second area of focus is on the surface characteristics of the microstructure phenomena. The surface of a material has unique properties that differ from the bulk material. A better understanding of intermolecular forces at the interfaces can lead to improved adhesion between substrates, resulting in higher adhesively bonded joint strength. The literature provides various parameters, such as surface free energy, which is defined by Young's contact angle and work of adhesion (WA), to characterise the thermodynamic properties of a surface. The upcoming sections will delve into the significance of surface free energy and its correlation with contact angle and work of adhesion. Additionally, different methods for measuring the surface free energy of solids will be discussed. Suitable surface treatments for adhesively bonded joints can be evaluated using various methods, including measuring the treatment's impact on mechanical properties and surface characteristics parameters. These parameters include surface free energy, surface roughness, and chemical composition. Each parameter affects the adhesive bond performance to a different degree, and the following subsections will provide a more detailed analysis of each.

The polar surface component plays a pivotal role in surface energy considerations and adhesive bonding. Surface energy is often dissected into polar and dispersive components, with the former stemming from interactions involving polar or ionic forces. This component significantly influences wettability and adhesive properties. Polar surfaces, characterised by the presence of functional groups such as hydroxyl (-OH) or carbonyl (C=O), exhibit enhanced adhesive characteristics due to their capacity for forming strong polar interactions with other polar molecules. Consequently, in adhesive bonding applications, selecting materials with compatible polar surface components becomes paramount to fostering robust and durable adhesive bonds. Understanding the interplay between the polar surface component and adhesive behaviour is integral to optimising adhesion performance across diverse material interfaces (Belyaeva et al., 2018).

Conversely, the dispersive surface component constitutes another crucial facet in the realm of surface energy and adhesive bonding. Originating from van der Waals forces, this component reflects the non-polar nature of certain surfaces, where interactions are primarily governed by electron dispersion. Materials with dispersive surface characteristics, often lacking pronounced polar groups, interact through van der Waals forces, influencing wettability and adhesive strength. In adhesive bonding scenarios, recognising and addressing the dispersive surface component is vital for achieving effective adhesion across non-polar interfaces. Tailoring adhesive formulations to accommodate the dispersive nature of specific surfaces ensures optimal molecular interactions and, consequently, robust adhesion in applications where dispersive forces dominate the intermolecular interactions (Harikrishnan et al., 2017).

2.9 Review on adhesive bonding characterisation tests and standards

Several standards and guidelines have been developed to investigate the surface characteristics of treated samples, the performance of adhesively bonded joints, and the exposed durability of the joints.

The general adhesive and adhesive bonding terminology can be found in ASTM D907-15 (ASTM, 2005).

In terms of the determination of different surface characteristics of the treated surfaces, ISO 25178-2 (Standardization, 2012) specifies all the terms, definitions and surface texture parameters in detail. Different characteristics such as height parameters, spatial parameters, and hybrid parameters to define the surface texture by areal methods are discussed in this standard. This is done to provide informative data about the treated samples in terms of their roughness and surface texture characteristics.

ASTM D7490-08 is a standard method used to determine the total surface free energy of treated surfaces. The method involves measuring the contact angle of polar and dispersive liquids, such as DI water and diiodomethane, on the surface. The total surface free energy of the substrate is calculated by adding the polar and dispersive surface components. The polar and dispersive components, along with the total solid surface energy, can be used to predict and explain the adhesion performance of the selected surface treatments. The standard also outlines the procedure for contact angle measurements.

ASTM D1002-10 is a standard test method that can be used to determine the shear strength of the metal-to-metal adhesively bonded joints under single-lap joint

configuration. The test can determine the mechanical properties of the adhesively bonded joint system, such as strength, surface preparation parameters, and environmental durability. There are various other methods based on D1002-10 in the case of different substrate materials, like ASTM D3163, which is for plastic joints, and ASTM D5868, which is for composite materials against itself or metal. According to this method, two metal plates are manufactured with selected adhesive, which is then placed in the grips of a universal testing machine and pulled at a constant speed. Different valuable data can be extracted from the disbanded joints, such as load at failure, approximate shear strength at failure and type of failure.

To evaluate how adhesively bonded joints respond to challenging environmental conditions, we consider peel loading as an ideal method, applying a localized load to the interface. On the other hand, lap shear loading distributes the load more evenly. Therefore, for a initial assessment of adhesively bonded joints, the single lap joint test proves to be effective. On the other hand, the peel test can be a practical way to evaluate the effectiveness of the selected surface treatment to enhance the bond strength at the interface. Various peel tests are available to determine the mechanical properties of an adhesive for bulk specimens and bonded joints (Adams et al., 1997). These include the contoured double cantilever beam (DCB), the T-peel, the tapered DCB, and so on. In addition to these methods, in the 1970s, Boeing introduced the wedge test for the first time to assess the effectiveness of the different surface treatments on bonded aluminium alloys used in aircrafts and evaluate the durability of the selected surface treatments in various harsh environmental conditions (Marceau et al., 1977). Since then, this test method has become an integral part of virtually all metal-bond manufacturing programmes (Abel et al., 2006; Armstrong, 1997; Hart-Smith, 1999; Rider, 2006; van Dam et al., 2020; Zain et al., 2014), and it is described in ASTM D3762 and ISO 10354. The Boeing wedge test (BWT) comprises two substrates bonded with adhesive in the middle. The wedge test involves the insertion of a wedge into one end of the specimens, which are then forced open with the edge in a fixed position. The propagation of the crack is then monitored over time. This test is cost-effective, repeatable, and allows for multiple specimens to be conditioned simultaneously.

2.10 Conclusion

Deciding on where to draw the conclusion for the history of adhesive bonding is a challenging task, much like determining its beginning. However, shifting the focus to the 21st century can be a suitable endpoint. The underlying principles of modern structural adhesives have undergone significant technological advancements, making them more

sophisticated and mature. In parallel to these developments, there have been significant advancements in surface analysis techniques, analytical tools, stress analysis, and evaluation methods necessary for realising their full potential.

In most of the studies, the effect of the surface roughness on initial and exposed performance of the adhesively bonded joints was assessed by relating the initial strength of the bonded joints to the single roughness parameter, R_a, in two-dimensional investigations and S_a in the three-dimensional investigation. Although these surface roughness parameters are a good estimator of the average height of the treated surface, these parameters do not additionally define the height, shape and density of the peaks and valleys. Therefore, it is essential to use other surface roughness parameters simultaneously with R_a or S_a to precisely describe the surface morphology of the treated surfaces. An adequate definition of surface roughness requires as least three different surface parameters considering both horizontal and vertical parameters. For this reason, different roughness parameters were used in this study to define the surface finish characteristics with greater precision following the selected surface treatments. To the best of the author's knowledge, no study was dedicated to systematically examining the correlation between the different surface parameters. These include surface roughness parameters and thermodynamic characteristics of the treated adherend's surface, with the initial and exposed performance of the adhesively bonded joints. The importance of the dissimilar bonding of aluminium-to-composite materials was outlined in this chapter. However, the more problematic aluminium surface characteristics make these materials more interesting for further study than composite materials. There is no doubt that surface treatments can develop desired surface characteristics to hold the integrity of the adhesively bonded joints. Hence, the question is not about "will" the surface treatment improve the surface strength for better adhesion performance of the adhesively bonded joints. Instead, the remaining concern is "how" different surface treatments with different natures improve the stability of the adherend-adhesive interface. Different preparation methods should be undertaken to develop different surface characteristics, each with its own requirements such as tools, time, etc., and different costs. This association consideration can be an interest of study to compare the industrial use of adhesively bonded joints in terms of their compatibility with other traditional joining methods.

The majority of research on surface treatments in adhesion has focused on the use of epoxy adhesives, with relatively limited attention paid to the use of polyurethane (PU) as an adhesive resin. This knowledge gap motivated the author of the present study to explore the impact of surface treatments on the properties of PU adhesive/aluminium bonds considering the unique characteristics of this particular type of adhesive. Its ability

to cured rapidly upon cooling and forming a strong bond as well as offering high bond strength and durability in diverse component besides their versatility and simplified processing can be named as a few aspects that make this type of adhesive interesting for further investigations.

CHAPTER 3

Surface Characteristics of the Treated Surfaces

3.1 Chapter overview

The previous chapter's overview has indicated a research gap that warrants further investigation into the effect of various surface treatments on diverse surface characteristics of the aluminium alloy. It has been observed that the combination of different types of surface treatments may lead to different modes of modifications in the surface characteristics of the adherend. However, a comprehensive and conclusive recommendation on optimal surface characteristics for adhesion cannot be made based on the literature, as there is a lack of a systematic approach in this area of research interest. In this chapter, various combinations of surface treatments are introduced to explore their impact on the surface characteristics of aluminium. The aim is to provide a systematic approach towards identifying the optimal surface characteristics for improving the adhesive bond performance of aluminium. By systematically varying the types and order of surface treatments, it is possible to obtain a better understanding of their individual and combined effects on surface roughness, surface free energy, and chemical composition. This will enable the development of a comprehensive understanding of the optimal surface characteristics for aluminium substrates, which can in turn lead to the development of improved surface treatment methods and more effective adhesively bonded joints. For this chapter, suitable surface treatment variables were selected based on the literature review, including mechanical abrasion with varying mesh sizes and deposition of different coupling agents. These variables were deemed ideal for investigating their influence on the surface characteristics of the aluminium alloy. The specimens are fabricated according to relevant standards. Different conditioning scenarios are developed for aluminium surfaces using simple, cost-effective preparation methods. Different analysing techniques such as 3D surface scanning, contact angle measurement,

and energy-dispersive X-ray spectroscopy are utilised to study the different surface parameters of the treated surfaces. Roughness characteristics of the treated aluminium surface are addressed based on five different parameters: S_a, S_p, S_q, S_{sk} and S_{ku}. In addition, the wettability of the aluminium surface was evaluated by calculating the total surface free energy, as well as its polar and dispersive components, using the recorded contact angle. To assess the efficacy of the chosen treatments in modifying the properties of the treated samples, the surface characteristics of the aluminium were documented both prior to and following the application of the treatments. This allows for the identification of the influence of each treatment and its overall effectiveness in modifying the surface properties of the treated samples. A statistical analysis using two-way analysis of variance (ANOVA) is performed to show the effect of different surface treatments on the characteristics of the treated samples. Lastly, the Pearson correlation between the surface roughness parameters and surface energy and its component in terms of different treatments is addressed.

3.2 Introduction

To date, various methods of aluminium surface preparation prior to adhesive bonding (i.e., chemical, mechanical, and electrochemical) are studied in the literature, as mentioned in Chapter 2. Each of these methods, changes the overall morphology of the aluminium surface to some extent, which in succession influences the adhesion performance of the metallic interface with the adhesive. The alterations made to the surface may result in improved initial adhesion performance, which can be attributed to the increased surface energy and mechanical interlocking between the metal surface and adhesive (Packham, 2003; Zielecfei et al., 2013). Given the current literature on the influence of diverse treatments on the surface properties of aluminium alloys, there exists a necessity to conduct in-depth investigations into innovative approaches for synergistically combining these treatments in a more holistic manner. This would introduce favourable surface characteristics to improve the adhesion performance at the metal-composite interface. To accomplish this goal, further investigation is required to identify the influence of individual mechanical and chemical surface treatments and their combination to improve adhesion performance.

Drawing upon the latest technological advancements, it is evident that surface treatment of aluminium plays a pivotal role in establishing a robust interface between the metal surface and adhesive, thereby enhancing adhesion performance. Hence, it is imperative to conduct research on surface modification of aluminium alloys to enhance the level of comprehension in this area. While each of the selected surface

treatments may have been previously investigated in the literature with respect to their impact on the surface characteristics of the metallic material, further exploration is required to assess the effects of their combinations on the adhesive performance of the material (Abel et al., 2006; Rider & Arnott, 2000; Saleema et al., 2012). However, the best combination of these surface treatments is not addressed in the literature. Additionally, it is essential to identify the underlying reasons for their sole effectiveness in improving the surface characteristics of the treated substrate.

3.3 Objective of this chapter

The primary objective of this chapter is to provide a comprehensive analysis of the impact of various pre- and post-surface treatments on the characteristics of treated substrates. The experimental program involved measuring the contact angle and calculating surface free energy, as well as determining three-dimensional surface roughness parameters of the specimens before and after each set of treatments. Additionally, the surface chemistry of the specimens was recorded, and the correlations between different treatments and roughness were identified.

3.4 Experimental materials and methods

3.4.1 Materials

Aluminium alloy 6061-T6 (Manufactured by Ullrich Aluminium, New Zealand)was used in this study as a selected substrate to investigate relevant surface modifications and their characteristics. The manufacturer reported yield stress of 276MPa, ultimate strength of 310MPa, average elasticity modulus of 68.9GPa and Poisson's ratio of 0.33. Furthermore, the chemical compositions of this alloy are listed in Table 3.

Table 3: Elemental composition of aluminium alloy 6061-T6

Element	Al	Mg	Si	Fe	Cu	Cr	Zn	Ti	Mn
wt%	Balance	0.8 - 1.20	0.4 – 0.8	0 - 0.7	0.15 – 0.4	0.04 – 0.35	0 - 0.25	0 - 0.15	0 - 0.15

3.4.2 Fabrication of specimens for surface analysing

Aluminium sheets were laser cut to 101.6mm x 25.4mm x 1.62mm specimen dimensions. These dimensions are identical to those used to cut the coupons for conducting single lap joints in Chapter 4. All as-received aluminium sheets were cleaned after cutting to the abovesaid dimensions with an ultrasonic cleaner in acetone for 10 minutes. This will ensure the cleanliness of the substrate surface from any external contamination. Following ultrasonic cleaning with acetone, the surfaces were subjected to various mechanical and chemical treatments to create distinct textures and chemistries, utilising a single-factor experimental approach. Table 4 presents the grouping of the samples based on their respective surface treatment methods.

Table 4: Sample coding based on relative surface treatments

Group name	Sample code	Treatment method
A	A0	Polished
	A1	Polished (A0) + NaOH
	A2	Same treatment as A1 + #240
	A3	Same treatment as A1 + #120
	A4	Same treatment as A1 + #80
B	B0	Polished + Silane
	B1	Polished + NaOH + Silane
	B2	Surface treatment as A2 + Silane
	B3	Surface treatment as A3 + Silane
	B4	Surface treatment as A4 + Silane
C	C0	Polished + Dipodal Silane
	C1	Polished + NaOH + Dipodal Silane
	C2	Same as A2 + Dipodal Silane
	C3	Same as A3 + Dipodal Silane
	C4	Same as A4 + Dipodal Silane
D	D0	Polished + Zirconate
	D1	Polished + NaOH + Zirconate
	D2	Same treatment as A2 + Zirconate
	D3	Same treatment as A3 + Zirconate
	D4	Same treatment as A4 + Zirconate

To modify the mechanical surface characteristics of aluminium alloy, three different aluminium oxide (Al_3O_2) sandpapers with mesh sizes of 80, 120 and 240 were used (3M abrasive sheets, UK). The samples were ground in the pattern of 0˚, ±45˚ and 90˚ (Ghumatkar et al., 2016). To eliminate the influence of other extraneous variables, such as the pressure in the sandpaper and the number of passes, the trial test was conducted with the designed preparation mould to hold the samples in place while the

sandpapering was progressing as shown in Figure 20. In order to mitigate the impact of pressure variations during sandpapering, a custom-made weighted holder was developed and employed. In addition, a preliminary study was conducted to determine the optimal number of passes required to achieve a reproducible surface roughness using the selected material as the substrate. It was found that excessive sandpapering could result in undesirable peaks and valleys, thereby diminishing the effectiveness of mechanical interlocking. Hence, it was important to strike a balance between the number of passes and the desired surface texture. To determine the primary surface roughness value of the sandpapered surfaces, a Taylor Hobson Talysurf 2D surface profilometer was employed in this section. The surface roughness was measured in different selected areas along two different directions to ensure the uniformity of the surface, and the average value was selected as the final result. The 5mm and 10mm transverse lengths were selected for measurement, and the profilometer range was set to be 0.05-10µm. The cut length of 0.8mm, while the speed was 0.25mm/s, was selected for the device to measure the surface roughness. The mesh size #120 sandpaper was selected for the trial test, and the result suggests that 50 passes can achieve the best result. Furthermore, sandpapered samples were cleaned using an ultrasonic cleaner with acetone for another 10 minutes to ensure the leftover sand was removed.

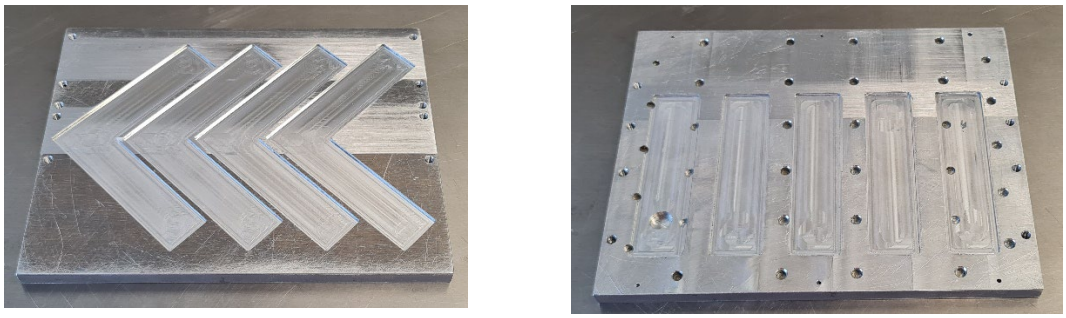

Figure 20: Sand papering mould

To perform NaOH treatment, a diluted sodium hydroxide solution was prepared by dissolving NaOH pellets in deionised water at a concentration of 0.1M. This method was initially introduced by Saleema et al. (Saleema et al., 2012) in which the specimens were ultrasonicated in the solution at room temperature for varying immersion times. Then Zain et al. (Zain et al., 2014) used 1.2M NaOH solution for the etching process and applied different polyurethane adhesives. In the most recent study in this area, Hu et al. (Hu et al., 2019) etched aluminium alloy in different concentrations of the NaOH solution at 55˚C for a duration of 10 minutes. The studies conducted in this area have demonstrated varying surface characteristics following NaOH treatment, indicating that

the efficacy of alkaline etching is influenced by several factors, including solution concentration, etching temperature, and treatment duration time. Consequently, a preliminary trial was conducted to ensure the appropriate variables were chosen for this investigation. A key objective of the NaOH treatment trial test is to establish appropriate parameters, such as temperature and duration, for the alkaline solution. Taking into account the most recent studies in this field, an investigation was carried out on the effect of NaOH treatment on aluminium alloy 6061-T6. The specimens were subjected to etching in a 0.1M NaOH solution at different temperatures (25˚C/35˚C/45˚C/55˚C) for a period of 10 minutes. After etching, the specimens were rinsed in deionised water. The results indicated that the surface etched in 0.1M NaOH solution at 55˚C appeared to have a pitted topography as shown in Figure 21(d), which is a typical characteristic of aluminium alloy after successful alkaline etching.

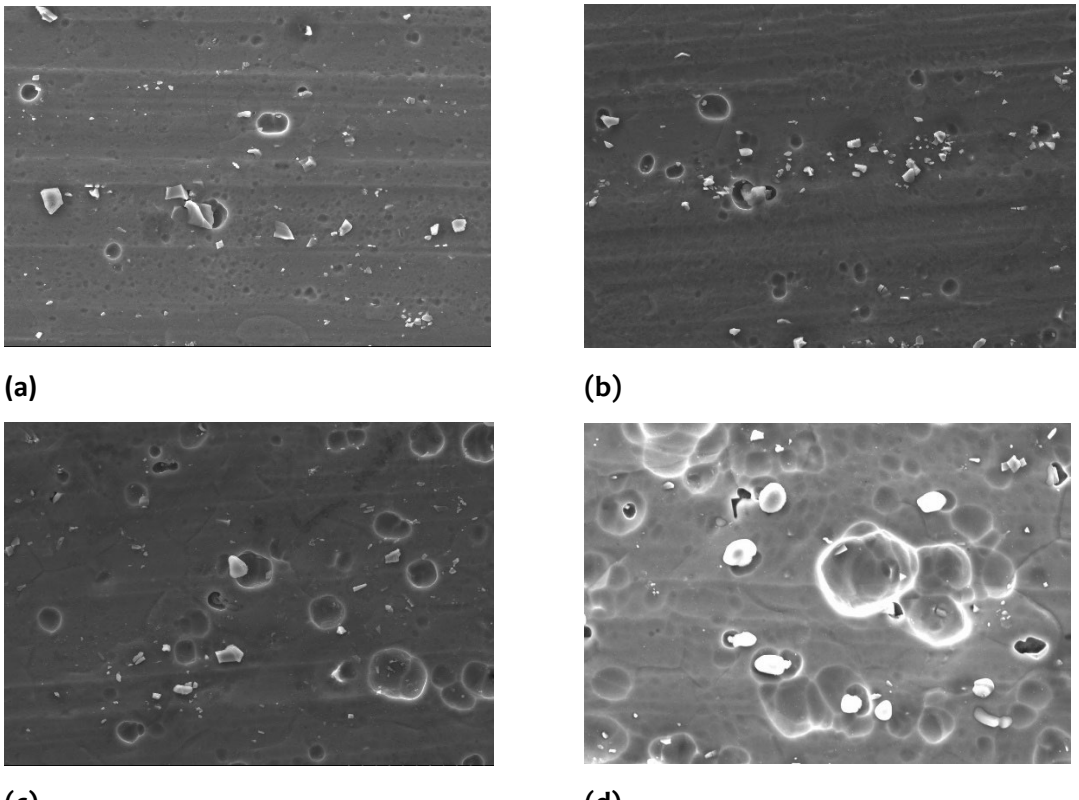

Figure 21: SEM images of NaOH treated aluminium surface at (a) 25˚C, (b) 35˚C, (c) 45˚C, (d) 55˚C all magnification is set to be X250

As can be seen in Table 4, three distinct coupling agents were chosen as the final group of surface treatments in this investigation to examine their efficacy in conjunction with the previous treatments. The first coupling agent used in this study was Bis(trimethoxysilylpropyl)amine silane, a secondary amino-functional methoxy-silane with two symmetric silicon atoms (Evonik Dynasylan 1124, Germany). Secondly, Tris[3-(trimethoxysilyl)propyl]isocyautrate was selected as a dipodal silane to compare its

effectiveness with other coupling agents (Evonik VPS 7161, Germany). VPS 7161 is an isocyanurate silane with a high concentration of trimethoxysilyl groups. Dipodal silane possesses two silicon atoms in the core of its molecular structure, promoting a strong covalent bond with a substrate. Theoretically, the primary reason that dipodal silane might favour better durability and strength than conventional silane is its higher cross-link density on the treated sample's surface. Dipodal silanes can create six Si-O bonds compared to traditional silane, creating only three bonds. The silane and dipodal silane solutions were prepared by following the method proposed by Abel et al. (Abel et al., 2006) and manufacturer recommendations. The pH of a 1% silane and dipodal solution in a 95:5 ratio ethanol/DI water mixture was adjusted to 4.5 using acetic acid and was hydrolysed for 1 hour at room temperature being continuously stirred using a magnetic stirrer. Then the samples were immersed in the solution for a duration of 60 seconds. After deposition, the samples were cured at 100°C for 1 hour. Thirdly, zirconate was selected as the last coupling agent. The procedure for the zirconate treatment of the aluminium surfaces was discussed with the manufacturer. Based on their advice, the following steps were taken to prepare the zirconate coupling agent solution. The cross-linking agent was zirconium triethanolamine, which can react with -OH and -COOH groups on the surface to act as an adhesion promoter and coupling agent (Borica Tytan AQZ30, Hong Kong). In this case, the pH of a 1% zirconate solution in a 90:10 ratio ethanol/DI water mixture was adjusted to 4.5 and was hydrolysed for 1 hour. The final step was the same for groups B and C.

3.4.3 Surface analysis methods and testing set up to evaluate the surface characteristics of the treated surface

Several analytical methods were utilised to examine the effect of various treatments on the physicochemical properties of the aluminium surface. The surface characteristics such as roughness parameters, surface free energy, and chemistry were evaluated using a 3D profilometer, contact angle measurements, and energy-dispersive X-ray spectroscopy (EDX), respectively. These surface analysis techniques were found to be effective in defining the properties of the modified surfaces. As a result, they provided valuable information on the potential impact of the selected surface treatments on the physical and chemical texture of the treated aluminium.

3.4.3.1 Determining surface topography

The Bruker three-dimensional (3D) profilometer system was employed to capture the 3D microscopic topography of the treated surfaces. The measurements of surface roughness were taken at five different points for each sample, with an area of 500μm x

500µm and a magnification of 10x. Visual 60 software was used to experiment and measure the selected surface roughness parameters.

The parameters for measuring surface roughness were determined in accordance with ISO 25178 standard (Standardization, 2012). Each measurement was repeated five times in different locations for every surface treatment variant, and the average value was calculated. All average values were taken after acceptable standard deviations were recorded. All measurements were taken a few hours after each treatment to avoid any absorption of contaminants on the treated aluminium surface.

3.4.3.2 Contact angle measurement and surface energy calculation

An Attention Theta Lite optical tensiometer (Biolin Scientific, Germany) was used to measure the static contact angles between the treated aluminium surfaces and the selected liquids via the sessile drop technique. The surface free energy of the aluminium samples was calculated based on the contact angles recorded from the sessile drop technique. The Owens, Wendt, Rabel, and Kaelble (OWRK) method (Li et al., 2018) was applied in this study to determine the surface free energy, which considers the different components of the treated surface, including polar, dispersive, and total surface free energy. To calculate the surface free energy, two measuring liquids with known surface free energies and polar and dispersive characteristics (listed in Table 5) were used.

Table 5: Surface free energy and their components of DI water and diiodomethane at room temperature (Jaganathan et al., 2016)

Liquid	γ_l^p	γ_l^d	γ_l^t
Distilled water	51.0	21.8	72.8
Diiodomethane	0	50.8	50.8

The ASTM D7490-13 standard was used to determine the appropriate amounts of distilled water and diiodomethane for contact angle measurements, with 2µL and 1µL selected for each liquid, respectively (Etzler, 2018). Five measurements were conducted for each treatment at various locations on the surface of the aluminium, as illustrated in Figure 22.

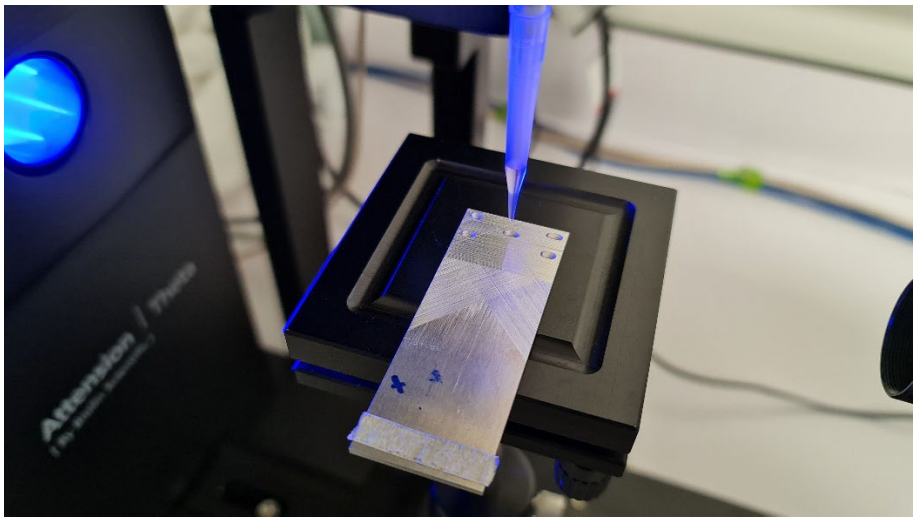

Figure 22: Contact angle measurements set-up

The droplet images capture 10 seconds after the deposition of the liquid on the surface using a 1280 x 1024 resolution and 2068 frames per second by a CCD camera system with an optical magnification of 10, coupled with suitable PC image software. The complete measurement setup can be seen in Figure 23. The final contact angle was measured from the average values of all five measurements considering the acceptable standard deviation range of ±4˚. Then, the average value of each base liquid was used to calculate the polar and dispersive components of each selected surface treatment. Six replicates of the contact angle measurements were carried out for each treatment. Finally, the experimental results were analysed through a two-way analysis of variance (ANOVA).

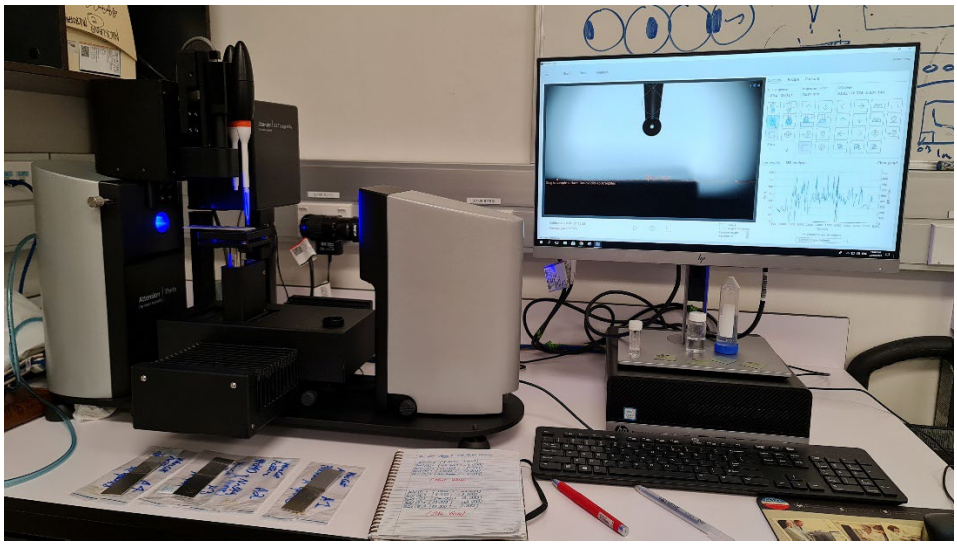

Figure 23: Experimental apparatus for contact angle measurement

According to the OWRK method, Equations (1) and (2) will be employed for the sake of this calculation as shown below (Rudawska, 2012):

$$(\gamma_s^d)^{0.5} = \frac{-\gamma_w\sqrt{\frac{\gamma_d^p}{\gamma_w^p}}(1+\cos\theta_w)+\gamma_d(1+\cos\theta_d)}{2(\sqrt{\gamma_d^d}-\sqrt{\gamma_d^p\frac{\gamma_w^d}{\gamma_w^p}})} \quad (1)$$

$$(\gamma_s^d)^{0.5} = \frac{\gamma_w(1+\cos\theta_w)-2\sqrt{\gamma_s^d\gamma_w^d}}{2\sqrt{\gamma_w^p}} \quad (2)$$

where γ_w- total surface energy of water, γ_d- total surface energy of diiodomethane, γ_w^p- polar component surface energy of water, γ_d^p- polar component surface energy of diiodomethane, γ_s^p- polar component surface energy of the aluminium surface, γ_w^d- dispersive component surface energy of water, γ_d^d- dispersive component surface energy of diiodomethane, γ_s^d- dispersive component surface energy of the aluminium surface, θ_w- average contact angle of water, θ_d- average contact angle of diiodomethane.

Furthermore, the total surface energy of the treated aluminium based on different groups can be calculated from Equation (3):

$$\gamma^t = \gamma^p + \gamma^d \quad (3)$$

3.4.3.3 Elemental composition analysis

The chemical modifications of the aluminium surface after each treatment were analysed by using scanning electron microscopy (SEM) coupled with energy-dispersive X-ray spectroscopy (EDX) using a Hitachi 70. Micrographs and spectra of the treated surfaces were captured at a magnification of x250 with an acceleration voltage of 20kV.

3.5 Experimental result and discussion

3.5.1 Surface roughness parameter measurements

In order to describe the surface topography using various surface roughness parameters, more than 50 different parameters have been identified (Croll, 2020). This study examined five surface roughness parameters to assess the characteristics of the aluminium surface, and the average values were selected as the results for comparison according to ISO 25178. The primary surface roughness parameter used in this study is S_a, also known as the arithmetic mean height. This parameter is defined as the average absolute deviation of the roughness features from the mean line over one sampling length, as illustrated in Figure 24(a). While the S_a parameter provides useful information about surface roughness, it is not enough to fully characterise the surface texture. This is because different surface profiles can exhibit similar S_a values, which means that additional surface roughness parameters must be examined in conjunction with S_a to obtain a more comprehensive understanding of the surface's texture. Examining different surface roughness parameters simultaneously can provide a more comprehensive understanding of the surface topography and texture. By considering multiple parameters, it is possible to obtain a more complete picture of the surface's characteristics, which can aid in the evaluation of its performance and suitability for different applications. Another useful surface roughness parameter is S_p, which represents the height of the highest peak within a defined area, as illustrated in Figure 24(b). In addition to S_p, S_q can be considered for further investigation, where S_q represents the root mean square value of the ordinate value within the defined area, which is also known as a standard deviation of heights (Figure 24(c)). Studies have revealed that the surface energy and roughness parameters of a treated surface can be affected by the shape of tips and the depth of valleys (Shahid & Hashim, 2002). In this manner, this study included two additional parameters, namely skewness (S_{sk}) and kurtosis (S_{ku}), to evaluate the shape and degree of asymmetry of the treated surface around the mean plane, as demonstrated in Figure 24(d) and (e), respectively. The negative skewness value indicates the height distribution is placed above the mean plane, which can identify the surface with holes. By contrast, the positive value of skewness stands for the surface with peaks above the mean plane. The last selected surface roughness parameter is S_{ku}, which can define the shape of the peaks and valleys based on their degree of sharpness. A kurtosis of more than 3 indicates a sharp tip appearance, while a value less than 3 is assigned to the tip geometry with a smoother appearance. A better surface profile can be illustrated using all these parameters for treated aluminium surfaces. Therefore, this study used the combination of all the above-mentioned parameters to study the influence of different surface treatments on the

aluminium surface. Before measuring the value of the selected surface roughness in this study, it is crucial to investigate the respective benchmark substrate on which the surface treatments will be undertaken.

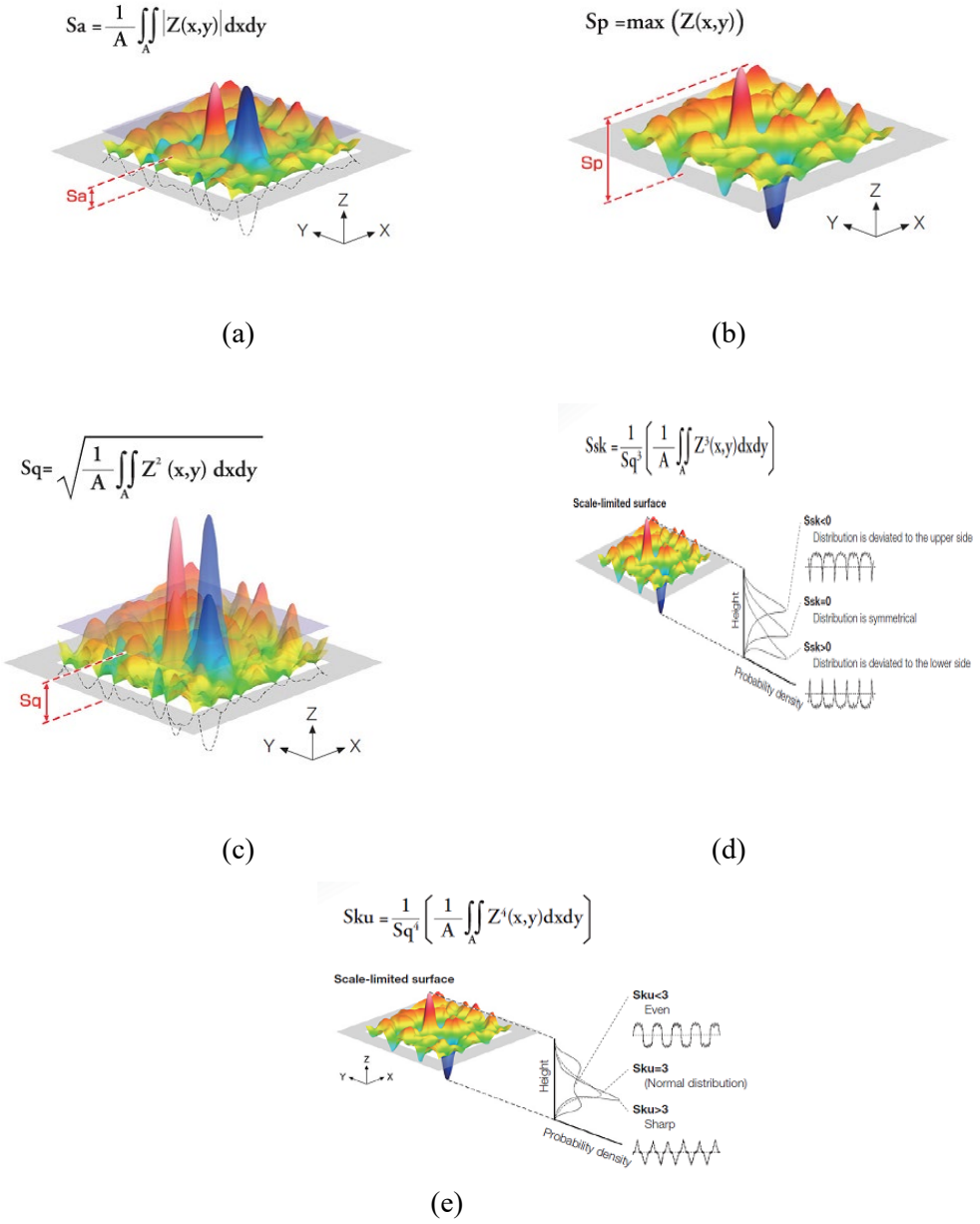

Figure 24: Geometrical feature of different aerial surface roughness parameters: (a)S_a,(b)S_p,(c)S_q,(d)S_{sk} and (e)S_{ku} (Harcarik & Jankovych, 2016)

Table 6 shows the final values of all selected surface roughness parameters along with their sample codes. The polished surface A0 reveals the lowest S_a value of 0.154µm with the smallest standard deviation of height (S_q) equal to 0.218 µm. The observation of a negative skewness value for sample A0 suggests the presence of holes, despite the polishing applied to the surface. This may be due to the high sensitivity of the 3D

profilometer used, as negative skewness values can also be associated with the presence of holes in the nanometre scale. The high kurtosis value, which signifies the presence of steep tips or deep valleys in the polished sample's surface topography, could also account for the negative skewness value, which indicates the existence of holes on the surface. In light of the findings, the polished aluminuim surface emerges as a commendable benchmark in this study, characterized by favourable attributes. These attributes encompass minimal values for surface roughness, emphasizing the avoidance of any surface characteristics indicative of roughness, such as elevated S_a values. After NaOH treatment, there was a significant increase in the surface roughness parameters S_a and S_q, with values for A1 approximately fourteen times greater than those for A0. This suggests a marked alteration in the texture of the aluminium surface resulting from this alkaline treatment approach. Previous studies by Yu et al. (Yu et al., 2019) and Saleema et al. (Saleema et al., 2012) have also investigated the impact of NaOH treatment on surface roughness parameters of aluminium. However, the selection of the as-received condition of the aluminium surface as a reference point for comparison in those studies may have led to a misjudgement of the true effect of the NaOH treatment on the surface. It should be noted that the as-received surface may possess certain irregularities that can significantly influence the measured surface roughness parameters as mentioned in chapter 2. Therefore, the accuracy of the insights into the effect of the NaOH treatment could be compromised. The one-factor ANOVA method also showed the NaOH treatment's significant influence on S_a, S_p and S_q of the treated aluminium surface.

Likewise, the skewness value of A1 has demonstrated a twofold increase in comparison to the polished surface. The decrease in kurtosis value can be attributed to the attainment of a uniform surface finish resulting from the NaOH treatment of the polished aluminium surface. As a result, the tips and valleys are formed more uniformly on the surface of A1. However, one-way ANOVA did not show a significant effect of the NaOH treatment on the S_{ku} and S_{sk} of the treated aluminium surface.

Table 6: Average surface roughness parameters for different groups of surface treatments

Sample code	S_a (µm)	S_p (µm)	S_q (µm)	S_{ku}	S_{sk}
A0	0.154	1.488	0.218	14.19	-1.801
A1	2.294	7.581	3.245	8.805	-2.283
A2	2.901	8.552	3.799	5.049	-1.313
A3	2.994	9.611	3.994	3.176	-0.70
A4	3.049	15.480	4.765	3.510	-0.397
B0	0.232	2.081	0.328	13.729	-1.159
B1	1.801	6.481	2.812	13.783	-2.932
B2	2.333	8.664	3.257	7.950	-1.861
B3	2.606	9.381	3.267	6.561	-1.463

B4	2.966	17.657	3.703	4.263	-0.612
C0	0.186	1.363	0.271	10.784	-0.440
C1	1.337	9.488	2.436	24.868	-4.358
C2	2.132	8.886	2.922	8.845	-1.192
C3	2.495	12.049	3.539	4.653	-1.119
C4	2.824	16.164	3.772	3.482	-0.475
D0	0.172	1.349	0.238	12.510	-1.006
D1	1.215	5.082	2.110	30.995	-4.335
D2	2.104	7.801	2.942	10.700	-2.141
D3	2.427	11.208	3.274	7.879	-1.605
D4	2.794	14.332	3.432	2.872	0.313

Various results were yielded when three different surface roughening conditions were taken into account prior to the NaOH treatment of the polished aluminium surface. The results indicate that the S_a value increases as the roughness of the abrasive paper increases, as illustrated in Figure 25. Nonetheless, the extent of the increase in the surface roughness parameters S_a and S_q is not proportionate to the increase in the NaOH-treated specimens compared to the polished surface. The skewness value also continuously increases, indicating a higher number of valleys compared to peaks by rougher abrasive paper. Based on the results evaluated for group A, the effectiveness of the NaOH treatment on surface roughness parameters can be compared with the polished surface (A0) and in combination with the different roughened conditions before NaOH treatment. The experimental results suggest that the combination of NaOH treatment and sandpapering, as applied to samples A2 to A4, may be effective in addressing some of the limitations associated with the sole use of sandpapering in the surface treatment of aluminium, as identified in previous studies. (Croll, 2020). The surface roughness parameters of sample A4 exhibit the highest values, with a S_a of 3.049 μm, indicating extensive surface roughness after mechanical abrasion. Nevertheless, the application of NaOH treatment after mechanical abrasion reduces the kurtosis value by increasing the roughness of the sandpaper. Despite the kurtosis reduction, the S_q parameter increases with the roughness of the sandpaper, indicating an increase in surface area and a potential increase in adhesion strength.

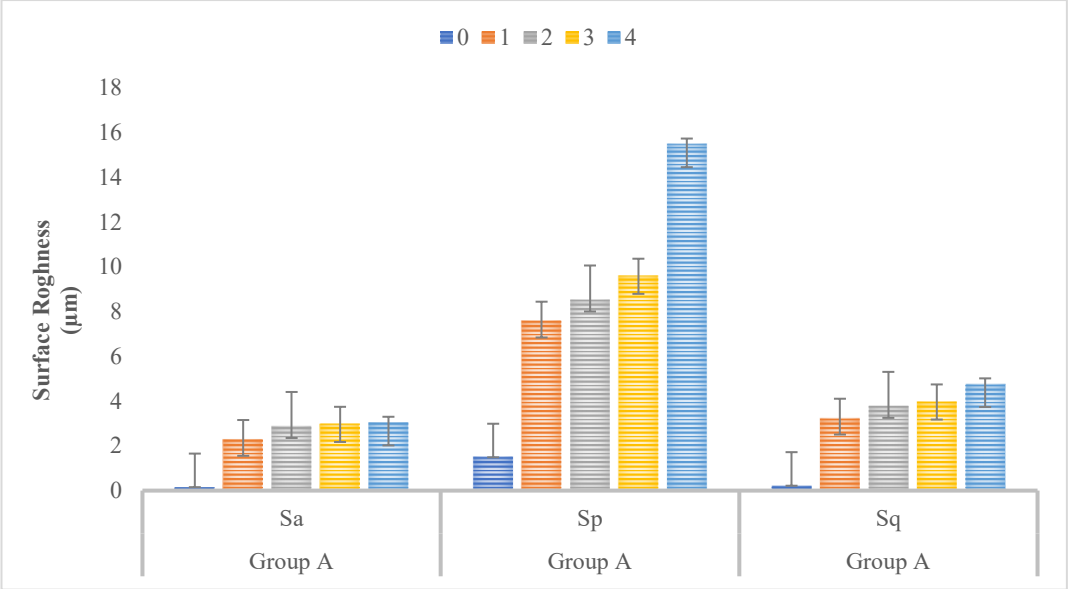

Figure 25: Surface roughness values of S_a, S_p and S_q for group A

To ensure the accuracy of the results, one factor ANOVA analysis was undertaken and concluded that the combination of NaOH treatment with sandpapering with different mesh sizes did not show a significant effect on measured surface roughness parameters S_a, S_q and S_{sk}. In contrast, a significant effect was observed on Sp and Sku, indicating that the surface roughness prior to NaOH treatment may not influence the arithmetical mean height of the aluminium surface. As this parameter is commonly used to evaluate surface roughness, it can be concluded that NaOH treatment has the ability to dissolve the sharp tips produced by sandpapering and reform the final surface with a more even topography. This conclusion is supported by the results obtained for S_{sk} and S_{ku}. Thus, considering the findings presented in this section in conjunction with the existing body of literature, it can be asserted that a 0.1M NaOH solution has a high degree of interaction with the aluminium surface, resulting in the formation of a uniform topography with a greater depth size for irregularities and a larger hydroxide zone (-OH).

The findings from Table 6 for group B demonstrate the impact of silane deposition on the surface roughness parameters of aluminium. Specifically, the S_a value increased to 0.232µm for B0 compared to A0. This increase in surface roughness can be attributed to the successful deposition of silanol on the aluminium surface, leading to the formation of clustered silane oligomers. This finding is consistent with previous research by Kono et al. (Kono et al., 2001), silane deposition on the aluminium surface can promote roughness due to the presence of OH groups. which suggests that silane deposition on aluminium surfaces can increase surface roughness due to the presence of hydroxyl (OH) groups. However, the NaOH treatment can also increase the number of hydroxide groups on the surface and create a better surface for silane deposition. Comparing the surface roughness

parameters of B0 and A0, it is evident that the silane treatment (as a result of silane oligomer formation (J. G. Kim et al., 2010) alters the surface morphology differently than the NaOH treatment. Specifically, the alkaline treatment produces more valleys, while the silane treatment forms more peaks on the polished surface.

The results indicate that the silane deposition on the aluminium surface can result in a smoother surface when compared to group A. This can be attributed to the filling of valleys by the silane oligomers and the formation of a silanol deposit. Additionally, the reduction in skewness suggests that the surface treated with silane oligomers appears to have a smoother topography with fewer sharp features. The statistical analysis using the one-way ANOVA method indicated that silane deposition has a significant impact on the S_a, S_p, and S_q values of the polished aluminium surface in group B. However, it should be noted that a similar effect was observed in group A1 treated with NaOH only, suggesting that the NaOH treatment is the primary factor influencing the surface roughness parameters. The silane deposition appears to primarily affect the surface chemistry of the aluminium surface rather than its roughness, as evidenced by the lack of significant effect on the S_{ku} and S_{sk} values.

Based on the results presented in Table 6, it is apparent that the surface treatment of group C has caused changes in the surface roughness parameters. A significant observation is the similarity in surface roughness parameters between C0 and A0, which suggests the unsuccessful deposition of dipodal silane on the polished aluminium surface. However, a successful deposition of dipodal silane was observed on the NaOH treated surface, similar to group B. Therefore, it can be concluded that a higher level of hydroxide groups on the aluminium surface is necessary for the successful deposition of dipodal silane. Furthermore, a natural aluminium oxide layer after polishing is insufficient for ensuring successful deposition of dipodal silane on an aluminium alloy. Group C, which was treated with dipodal silane, showed a similar effect to that of group B, which was subjected to silane deposition. However, the surfaces treated with dipodal silane were found to be less rough and more uniform in comparison. Comparing the surface roughness parameters of group A and group C indicates an overall reduction in surface roughness. This can be attributed to the better interaction between the dipodal silane and the NaOH-treated aluminium surface at the interface. This finding is consistent with a study by Zhou et al. (Zhou et al., 2019), where the surface roughness was decreased due to the deposition of a coupling agent. For group C, the statistical analysis, employing a one-way ANOVA, shows a significant effect of surface treatments used for group C. However, the primary influence can be mentioned as NaOH treatment, in the same manner as group B.

Referring back to Table 6, it is apparent that the surface roughness parameters continue to increase with NaOH treatment and surface roughening prior to etching and coupling agent deposition in group D. As a result of the different surface roughness parameters, it can be observed that the highest values of S_a, S_p, and S_q were obtained for D4, while the lowest values were observed for D0. Despite the distinct molecular structures of the zirconate coupling agents, similar surface roughness characteristics were observed in comparison to silane and dipodal silane, indicating that coupling agents may have a similar impact on surface roughness parameters. A one-way ANOVA analysis method was employed for group D, and it concluded that the selected surface treatment in group D significantly affected selected surface roughness parameters. However, NaOH treatment can be considered the main driving factor in altering the surface roughness parameters.

Furthermore, the trend for changes in the surface roughness parameter S_a is similar for all groups A, B, C, and D, as shown in Figure 26. This suggests that the deposition of coupling agents results in a gradual reduction of surface roughness. The lower surface roughness for groups B-D compared to group A can be attributed to the smoothing effect of the last layer of molecules on the treated surface or the ability of the coupling agent to fill the valleys of the roughened surface. Moreover, the reduction in surface roughness parameters such as S_a after the deposition of coupling agents indicates good interfacial interaction between the deposited solution and the aluminium surface, as reported in the literature (Zhou et al., 2019).

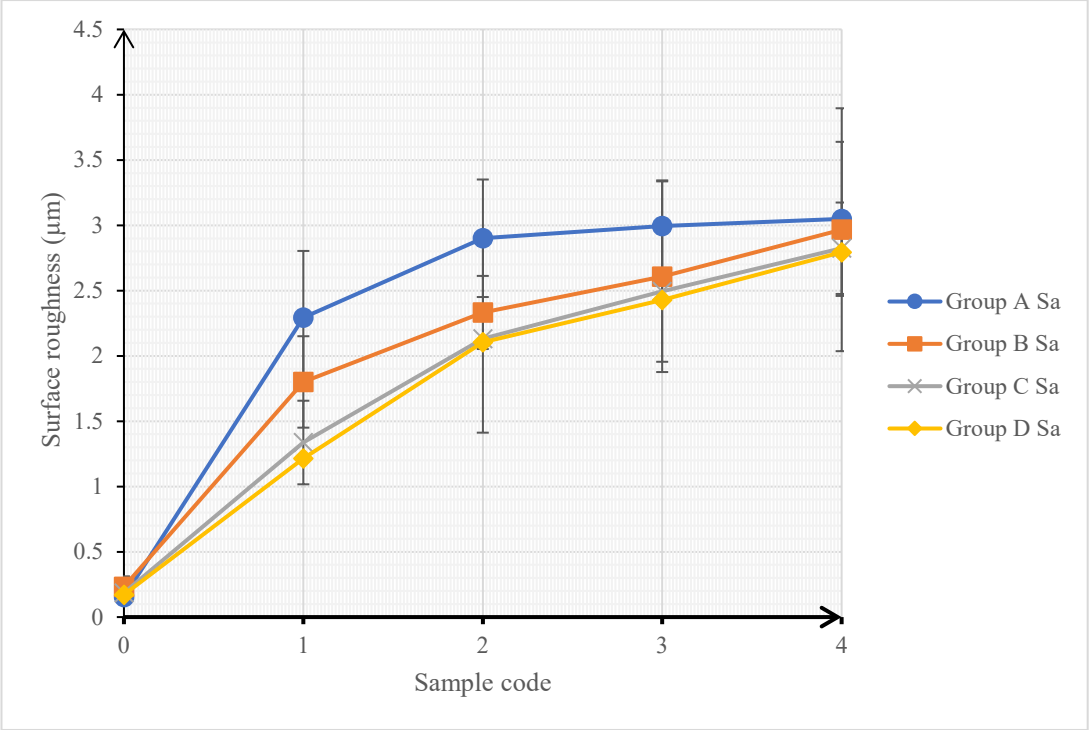

Figure 26: Comparison of the surface roughness parameter S_a of the differently treated samples

3.5.2 Surface energy calculated for each surface treatment

Surface free energies of different treated specimens were calculated after the relative contact angles were measured. The values of surface free energy and their corresponding components acquired thereafter the employment of different surface treatments are given in Table 7.

Table 7: Relative contact angle, surface free energy, and its components of the aluminium surface after each specific treatment

Sample code	θ_w(°)	θ_d(°)	γ_s^p (mJ/m²)	γ_s^d (mJ/m²)	γ_s^t (mJ/m²)	Polar ratio (P_S)
A0	49.80	50.62	20.97	33.93	54.90	0.382
A1	75.63	55.71	7.40	31.04	38.44	0.192
A2	72.16	57.05	9.37	30.27	39.64	0.236
A3	59.99	58.51	16.8	29.43	46.23	0.363
A4	73.33	67.87	11.23	24.07	35.3	0.318
B0	69.11	50.51	9.63	33.99	43.62	0.221
B1	82.86	59.15	4.73	29.06	33.78	0.140
B2	83.34	62.11	5.15	27.36	32.51	0.158
B3	91.25	66.85	3.03	24.65	27.68	0.109
B4	76.21	66.82	9.39	20.27	29.66	0.316
C0	53.36	43.90	17.06	37.59	54.65	0.312
C1	73.38	60.77	9.53	28.13	37.66	0.253
C2	86.62	62.87	4.02	26.92	30.94	0.130
C3	89.37	64.81	3.35	25.81	29.16	0.115
C4	72.04	66.99	11.75	24.57	36.32	0.323
D0	81.99	66.89	6.57	24.62	31.19	0.211
D1	73.18	66.71	11.03	24.72	35.75	0.308

D2	62.16	78.22	21.83	18.41	40.24	0.542
D3	60.15	83.82	25.54	15.58	41.12	0.621
D4	75.80	84.44	14.38	15.28	29.66	0.484

The findings for group A reveal that the utilisation of NaOH treatment in conjunction with sandpapering engenders a distinctive impact on the surface energies and their components of the AA6061-T6 alloy surface. Specifically, the surface energy values exhibit a considerable reduction to 38.44mJ/m^2 on the NaOH-etched surfaces (group A1) in comparison to 54.90mJ/m^2 on the polished surfaces (group A0), which corresponds to a 30% decrease in total surface free energy. Moreover, a comparison of the surface energy components between A0 and A1 indicated a decrease in both polar and dispersive components, as depicted in Figure 27. The reduction was more pronounced for polar components, which decreased to 7.40mJ/m^2 on A1 compared to 20.97mJ/m^2 on A0, corresponding to a 65% decrease in the polar component of the surface energy. The changes in surface free energy after NaOH treatment may be attributed to alterations in surface chemistry and modifications in surface roughness during the etching process. Previously, it has been reported by Hu et al. (Hu et al., 2019) that NaOH treatment can form a thin layer of hydroxide on the aluminium surface, which could influence its surface free energy. It is worth mentioning that in their study, the influence of NaOH treatment was compared with as-received samples and not polished samples. This comparison may neglect the influence of NaOH treatment on the surface roughness of treated aluminium. Therefore, a reference point has been set for polished samples to understand the effect of NaOH treatment on aluminium specimens.

Similarly, in another study, it has been stated that the NaOH treatment can remove the native oxide layer and replace it with fresher and more active aluminium oxide and hydroxide (Saleema et al., 2012). This also confirms the passivation of the aluminium surface before NaOH treatment to produce surface with less polarity characteristics, producing better initial dry adhesion (Kim & Ajersch, 1994). The solid's Ps (polar ratio) was calculated by the ratio of the polar component to overall surface energy, and values are shown in Table 5. In the A0 and A1 comparison case, the polar ratio decreases by 50% with the NaOH treatment.

To obtain a more precise analysis of the results, a one-factor analysis of variance (ANOVA) was conducted with a significance level of 0.05. The ANOVA results revealed that the polar components of the aluminium surface were significantly affected by NaOH treatment. However, the statistical analysis showed that the NaOH treatment did not have a significant impact on the dispersive component of the aluminium surface. Furthermore,

the ANOVA results indicated a significant influence of NaOH treatment on the total surface free energy.

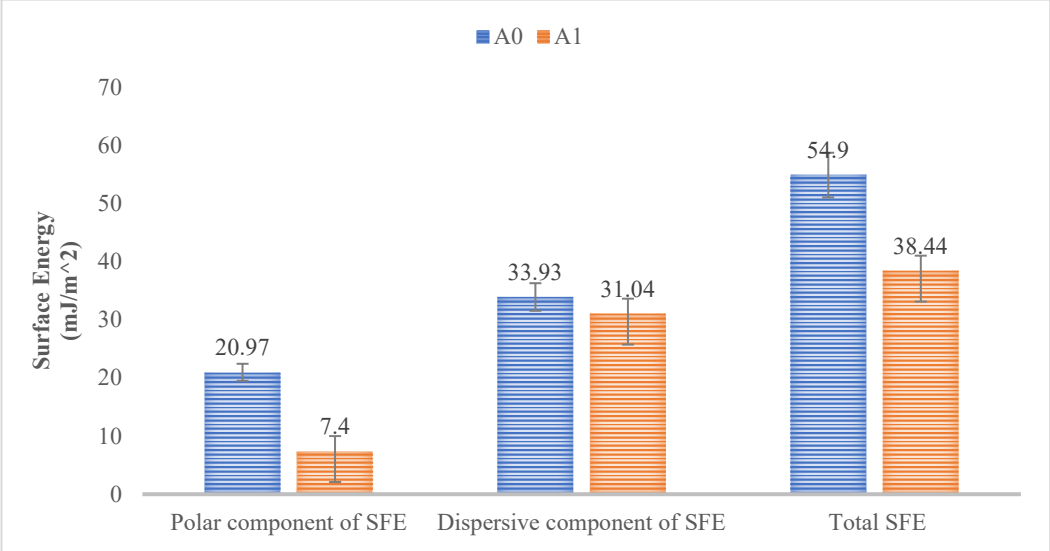

Figure 27: Effect of NaOH treatment on surface free energy (SFE) and its components of polished aluminium surface

The effect of the combination of surface treatment methods, including sandpapering with different mesh sizes and NaOH treatment, on the surface energy and its components were analysed and presented in Figure 28. The data was obtained from the additional information provided in Table 7, which includes the results of samples A2 to A4. The data indicates that roughening the surface using different sandpapers leads to a slight increase in the value of total surface free energy. The increase in surface free energy is mainly attributed to the increase of the polar component of the treated surface, while the dispersive component decreases gradually. The surface free energy for the NaOH treated sample (A1) increased to 39.64mJ/m^2 for A2**.** As mentioned earlier, this change is mainly due to the increases in the polar component, which increased from 7.40mJ/m^2 for group A1 to 9.37mJ/m^2 for group A2. The surface free energy and its polar component of A3 increase further to 46.23mJ/m^2 and 16.8mJ/m^2, respectively. Based on the potential of NaOH treatment to generate a thin layer of hydroxide groups on the treated surface and their polar nature, the results indicate that combining surface roughening with NaOH etching is an effective approach to enhance the surface energy and polar ratio of the aluminium surface. Roughening with a lower mesh size can form a rougher surface (based on recorded surface roughness parameters in this study); a higher surface area can therefore be expected. Increasing the surface area can improve the efficacy of NaOH treatment by providing more surface area for reaction with sodium hydroxide as further explore in section 3.5.3. However, it is noteworthy that the surface energy reached a maximum value for A3 before decreasing to 35.3mJ/m^2 for A4, despite

the increase in surface area achieved by using a finer mesh sandpaper. As stated above, the more macro- and micro-irregularities, the higher the aluminium surface area in contact with the NaOH treatment to produce further micro-texture and potentially a higher number of active sites to react with the coupling agents. However, the higher roughness values may have a negative effect on the ability of liquids to penetrate the deep valleys or cross the high tips. This can explain the reduction in the total surface free energy of A4, specifically for the polar component.

The one-factor ANOVA method showed a significant effect of the combination of the NaOH treatment and surface roughening treated aluminium's polar and dispersive components. However, the one-factor ANOVA test results are only limited to confirming the existence of a difference between two variables. Therefore, the test will not reveal what these differences are. Consequently, the post-hoc test should be performed. Post-hoc analysis using a Bonferroni test revealed that there is a significant difference between the A3 ($16.8 \pm 2.58 mJ/m^2$, $p<0.001$) polar component of the aluminium surface compared with those roughening factors in A2 ($9.37 \pm 3.07 mJ/m^2$, $p<0.001$) and A4 (11.23 ± 3.11 mJ/m^2, $p<0.001$). The same post-hoc analysis was undertaken for the dispersive component of the treated aluminium surface. The results revealed that the A4 (24.07 $mJ/m^2 \pm 2.34$, $p<0.001$) surface preparation could significantly influence the dispersive component of the treated aluminium surface compared with the roughening factor developed in A2 ($30.27 mJ/m^2 \pm 1.4$, $p<0.001$) and A3 ($29.43 mJ/m^2 \pm 1.62$, $p<0.001$).

Based on the findings of the study, it can be inferred that the surface roughening of the aluminium substrate prior to NaOH treatment results in a higher concentration of polar hydroxide groups on the treated surface, as evidenced by the contact angle analysis, which showed an increase in total surface free energy, particularly the polar component. Moreover, it is evident that the NaOH treatment can interact with both polished and roughened aluminium surfaces to form a uniform and homogenous surface with depth valleys, which can be beneficial in the case of complete adhesive penetration, leading to an improvement in adhesion performance. The study highlights the potential of combining surface roughening and NaOH treatment to enhance the surface energy and adhesion properties of aluminium alloys. The surface characteristic described above, namely the increased presence of polar hydroxide groups and the formation of a uniform and porous surface, can be considered an ideal condition for the deposition of coupling agents with the aim of improving adhesion performance (Engelkemeier et al., 2019).

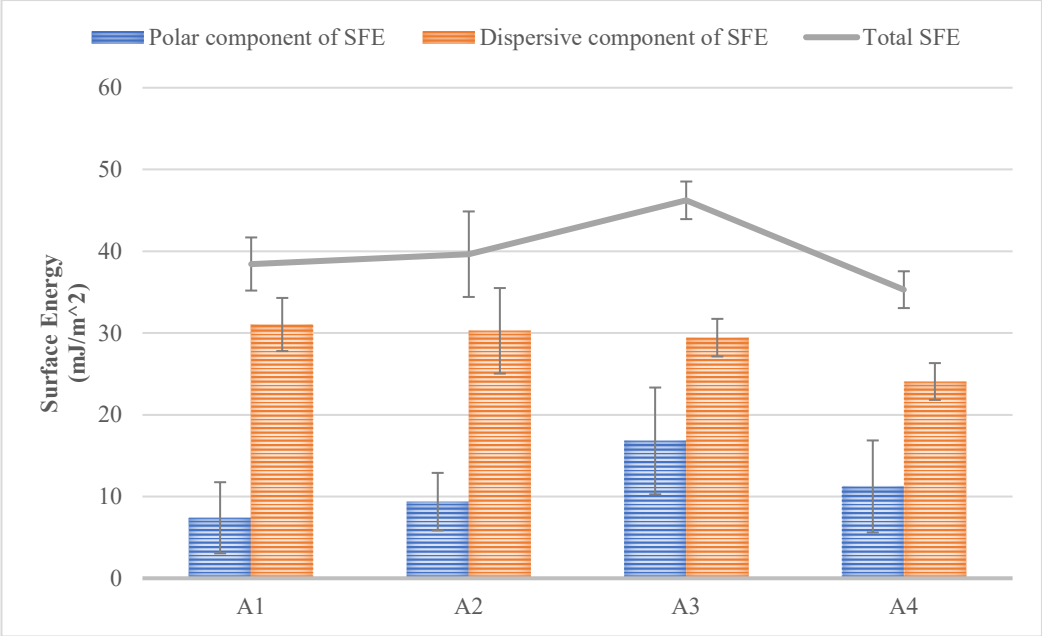

Figure 28: Effect of abrasive mesh size on surface free energy and its component in a combination of NaOH treatment

In order to examine the aforementioned proposition, the study proceeded to investigate the effectiveness of various coupling agents on the treated surfaces employed in group A, leading to the formation of group B to D. These agents were carefully selected based on their distinct molecular structures and the potential to create a robust layer of molecules on top of the metal surface. Different trends for different coupling agents were recorded based on their surface energies and components. Based on the analysis presented in Table 7, it can be observed that the application of silane deposition over the polished surface in group B resulted in a reduction of the surface free energy from 54.90mJ/m^2 for A0 to 43.62mJ/m^2 for B0. This reduction can primarily be attributed to the reduction in the polar component of the aluminium surface due to the deposition of silane, while the dispersive component remained unchanged. The reduction in the polar component of the surface after silane deposition can be attributed to the lower polarity of the silane coupling agent on the surface of B0 compared to the aluminium oxide on A0, as illustrated in Figure 29.

Likewise, the silane coupling agent deposition following NaOH treatment resulted in a further decrease in the surface free energy and the polar component on the treated aluminium surface. This implies that NaOH treatment can create favourable underlying conditions for enhancing the interaction between the aluminium surface and the silane coupling agent. The one-factor ANOVA method was employed to investigate the statistical significance of the silane deposition on both the polished aluminium and

NaOH-treated surfaces, and it revealed a significant effect of the silane deposition on both types of surfaces.

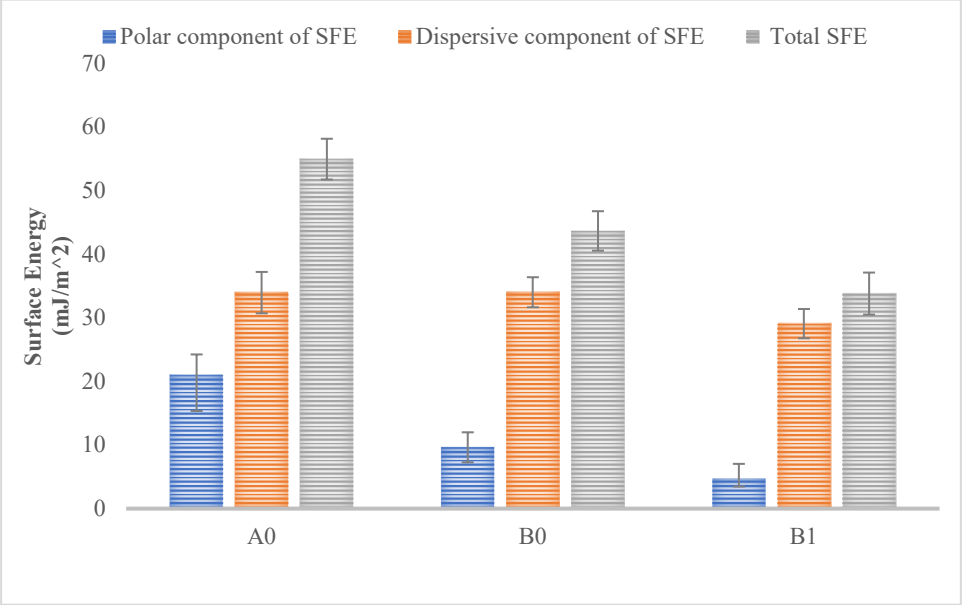

Figure 29: Effect of silane deposition over the polished aluminium surface and in a combination of NaOH treatment

Similarly, Figure 30 shows a comparable pattern between groups A (as shown in Figure 28) and B regarding the influence of different surface roughening conditions. The lowest polar ratio contribution in group B3 can be attributed to the highest level of surface salinisation. Furthermore, the optimal surface area was obtained using sandpaper with a mesh size of 120 before NaOH treatment, which is consistent with the results of group A. The use of highly rough surfaces, such as B4, hindered complete liquid penetration and resulted in high contact angle readings. The one-factor ANOVA analysis indicated that the surface irregularities formed by different sandpapers did not have a direct effect on silane deposition. However, the greater surface area produced by different sandpapers increased the available area for NaOH solution to react with the aluminium surface, which improved the underlayer surface area. Similar findings were also reported in (van Dam et al., 2020).

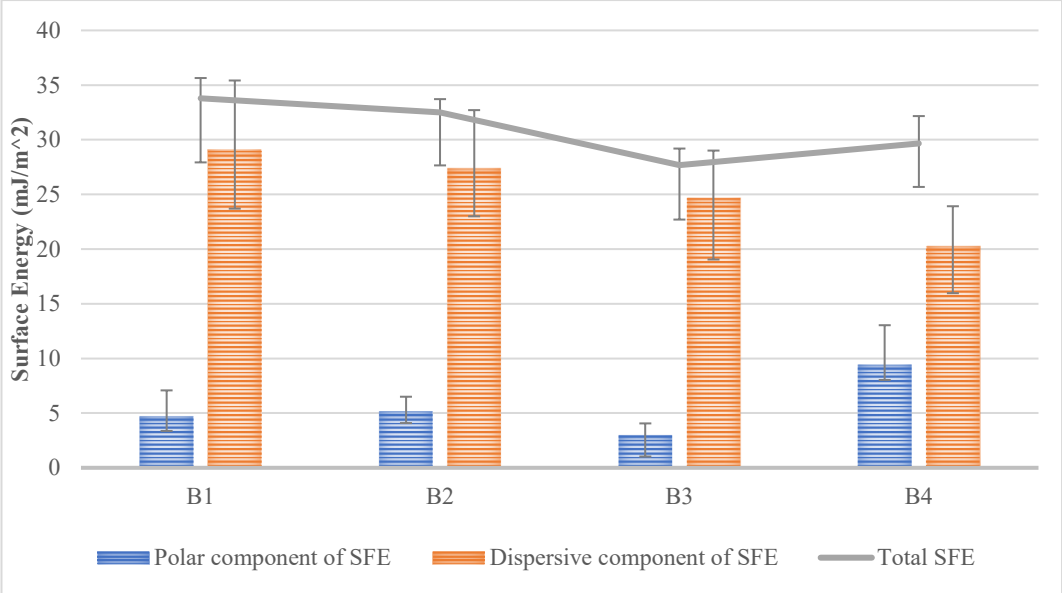

Figure 30: Effect of silane deposition in a combination of NaOH treatment under different roughness conditions

A similar approach was employed to study the influence of dipodal silane deposition over the polished aluminium surface (C0), NaOH-treated surface (C1) and in combination with different sandpaper (C2 to C4). By contrast, different results were recorded after dipodal silane (C0) deposition compared to A0 and B0, where similar surface free energy was measured for C0 with A0, as shown in Figure 31.

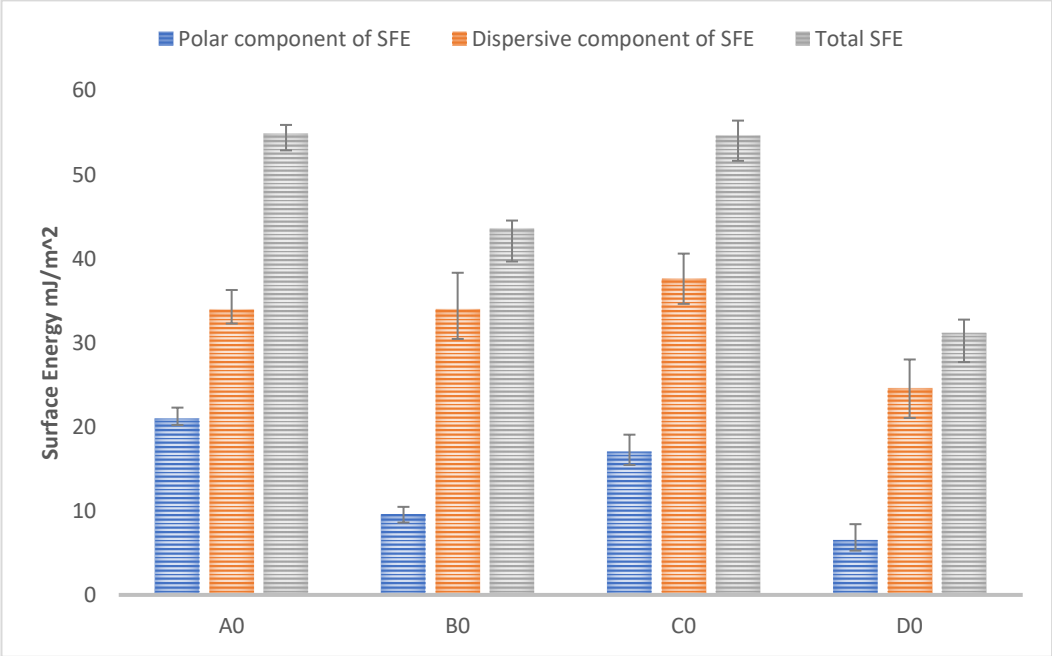

Figure 31: Effect of different coupling agents on surface energy and its component of polished aluminium surface

The unexpected finding of a lack of change in the polar component of the polished aluminium surface after dipodal silane deposition suggests that the deposition process

may have been unsuccessful. This is because, based on the molecular structure of dipodal silane, a reduction in the polar component is expected to occur on the aluminium surface, similar to what was observed for C0 (as shown in Figure 29) (Singh et al., 2014). On the other hand, the result for C1 can indicate the successful deposition of the dipodal silane on the NaOH-treated aluminium substrate. In the same trend as group B, the dipodal silane group (group C) follows the same trend of decreasing and increasing surface energies and their components, as shown in Figure 32. Hence, group B significantly reduces polar components more than dipodal silane. The lowest polarity ratio was recorded for B3. In the same manner, the lowest polarity ratio among group C was recorded for C3 as well as total surface free energy. This can be mainly due to the high silanol presence at the top layer of the treated aluminium surface. A low level of polarity ratio can also indicate the hydrophobicity of the final treated surface. The sudden increase in C4 can also be explained by the rose petal effect. It can be the higher presence of the silanol zone interacting with the adhesive in the next stage of assembly, but due to this effect, water drop is not able to travel over the tips produced as a result of rough overall surface morphology.

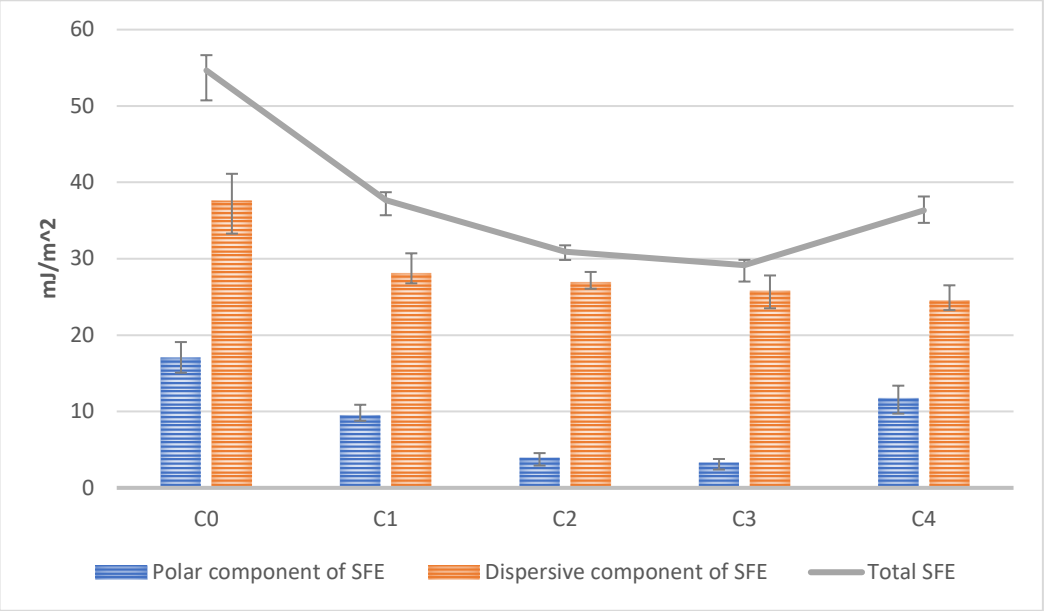

Figure 32: Influence of dipodal silane deposition on surface energy and its component of aluminium alloy

Zirconate, in contrast to silane and dipodal silane, possesses distinct chemical characteristics with a more polarised nature. As a result, zirconate exhibits a higher surface free energy than silanol (Monte, 2002). The results suggest that zirconate can effectively reduce the polar and dispersive components of the treated surface, as demonstrated by the significant reduction in these components observed in D0 compared to A0. Moreover, the similarity in polarity ratio between D0 and B0 suggests that

zirconate may be as effective as silane in reducing surface polarity. It is noteworthy that the addition of NaOH treatment prior to zirconate deposition increases the polar component, which enhances the reactivity of zirconate with active hydroxide groups that are formed after alkaline etching. As previously mentioned, NaOH treatment alone reduces surface polarity, while the addition of zirconate increases it from 7.40 mJ/m^2 for A1 to 11.03mJ/m^2 for D1. The one-factor ANOVA method also did show a significant effect of the zirconate coupling agent on the polar component of the treated aluminium surface. According to the research by Monte (Monte, 1982), organometallic coupling agents containing titanium and zirconium provide different coupling mechanisms compared to silanes. The multifunctional chemistry of zirconates makes them potentially better adhesion promoters than silanes. Such an effect on the surface energy of the treated aluminium surface in combination with other selected surface treatments can be seen in Figure 33. The different overall trend in polar component, and surface energy for group D are clearly seen. A significant increase in polar component and surface energy of the treated aluminium surface is achieved by depositing zirconate over the NaOH-treated aluminium surface.

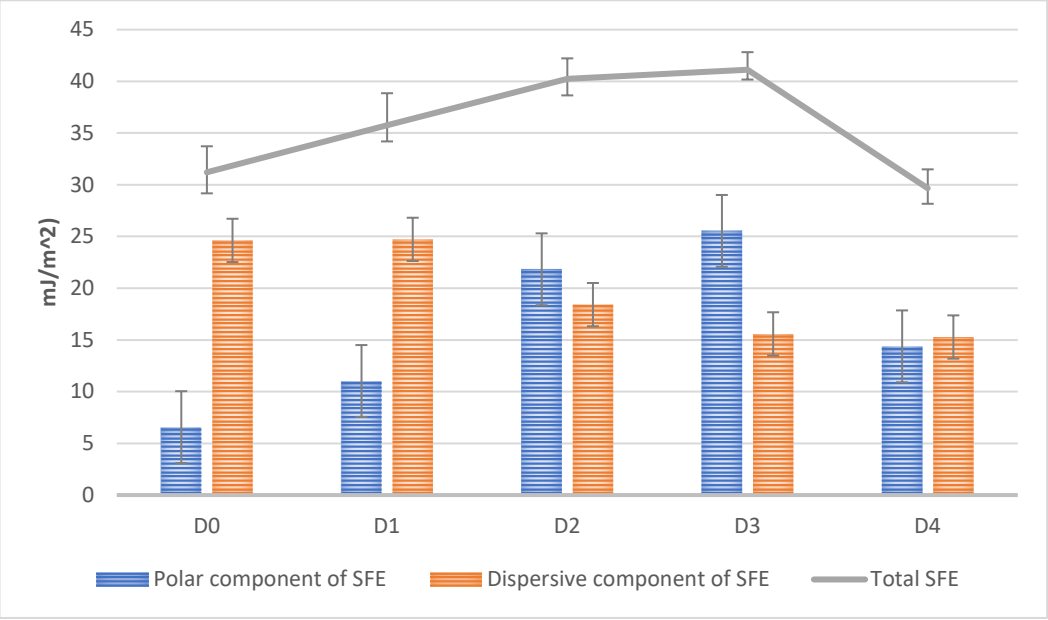

Figure 33: Influence of zirconate coupling agent on surface energy and its component of aluminium alloy in combination with other selected surface treatments

Interestingly, the zirconate deposition also trends like other coupling agents in the case of a combination of NaOH and rougher surface texture. Similarly, the optimal case for zirconate is D3, with the highest polarity ratio among all other sample groups (P_s = 0.621). Even with the high level of polarity, the total surface energy of A0 is the highest among the other groups. These findings reveal that the zirconate deposition prior to NaOH treatment of the aluminium surface could effectively increase its surface energy.

This can possibly be explained by the zirconate coupling agent's hydroxide components which could form strong hydrogen bonds with water molecules, leading to better spreading for a diluted water drop.

It can be concluded that NaOH treatment could effectively passivate the aluminium surface and prepare a positive underlying surface condition for the effective deposition of coupling agents selected in this study. This can be mainly due to the metal oxide conversion during NaOH treatment which can produce strong chemical bonds with high polarity existing in the coupling agents. It can further be stated that the roughening of the aluminium surface can be an effective, simple method to increase the roughness parameters which favour better deposition of the coupling agents. However, in the following section, an in-depth analysis is undertaken to record the different surface roughness parameters and expand the level of understanding of their influence of them on surface wettability.

3.5.3 Surface chemistry and elemental compositions analysis

SEM micrographs presented in Figure 34 were utilised to investigate the impact of different surface treatments on the surface morphology of the aluminium alloy. The SEM images of the polished surface exhibited a relatively flat surface, containing micro-scratches and small holes (Figure 34 (a-d)). These micro-scratches were found to be the result of hand polishing, which was supported by the high value of Sku obtained in the preceding section. The small holes observed in the SEM micrographs might have been produced by the manufacturing defects of aluminium sheets. Patterned scratches were observed after sandpapering (Figure 34 (j-w)), demonstrating the formation of rougher surface texture with greater control over the final surface texture by using rougher abrasive paper. The dominant pattern direction of the last sandpapering action can be attributed to the higher material removal when rougher sandpaper was used. The effect of NaOH treatment on the polished aluminium surface was evident in the SEM images shown in Figure 34 (e). The surface of the aluminium treated with a diluted alkaline solution displayed a wide and shallow pitted topography, which is the typical aspect of an aluminium-treated surface using an alkaline solution (Hu et al., 2019). This was supported by the higher value of S_a obtained in the previous section. Consequently, it can be concluded that 3D surface roughness parameters can effectively and precisely describe the surface topography of the aluminium alloy to a greater extent.

The higher corrosion rate of aluminium grain boundaries causes the formation of microcracks. The number of pitted holes was increased by decreasing the mesh size of the abrasive paper. This can clearly support increasing the surface area using rougher

abrasive paper favouring the higher area available for NaOH treatment; this increases the hydroxide groups on the aluminium surface. Surfaces after silane, dipodal silane, and zirconate treatments are shown in Figure 34 (b-d, f-i, k-m, o-q, and s-w, respectively). All solutions were able to alter the aluminium-treated surface to some extent. However, this alternation becomes more significant in combination with other methods, especially after NaOH treatment. The NaOH treatment can significantly increase the density of the hydroxide group across the treated aluminium surface (Saleema et al., 2012). These hydroxide sites can react with silane to form silanol. The silane oligomers and zirconium oxide can be observed across the surface of the NaOH-treated substrate (white dots). The increased number of white dots is achieved by increasing the roughness.

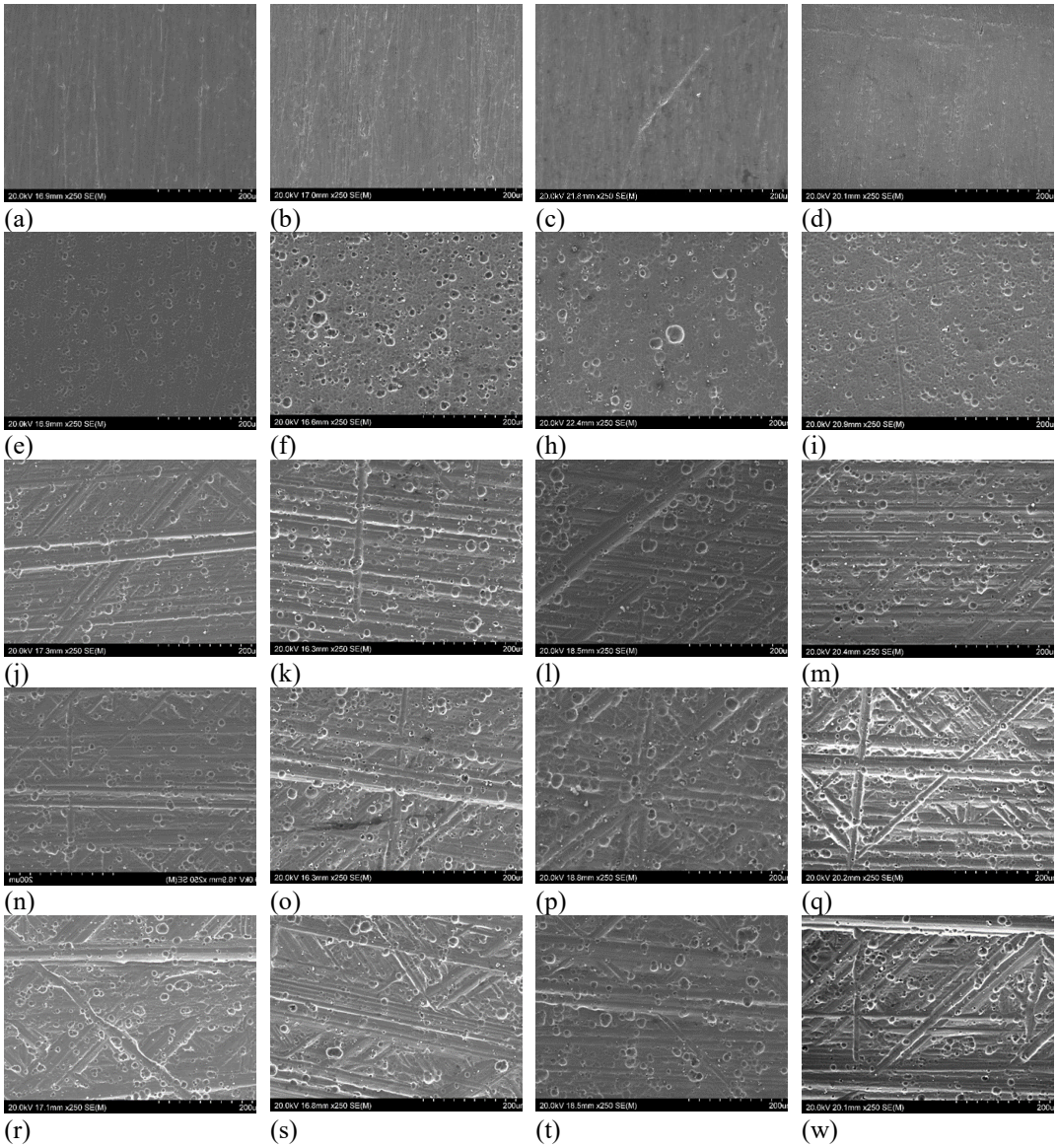

Figure 34: SEM images for different surfaces after specific surface treatment (a) A0, (b) B0, (c) C0, (d) D0, (e) A1, (f) B1, (h) C1, (i) D1, (j) A2, (k) B2, (l) C2, (m) D2, (n) A3, (o) B3, (p) C3, (q) D3, (r) A4, (s) B4, (t) C4 and (w) D4

EDX analysis was used to evaluate the elemental composition of the treated samples to confirm the surface chemistry alternation after each treatment. Figure 35 shows the comparison of atomic weight concentrations of each element composition after different surface treatments based on their group codes. It should be noted that the elemental compositions completed by EDX could be affected due to the surface metal hydroxides and bulk aluminium. It is seen that the NaOH treatment did not leave any intermetallic particles on the treated surface of the treated surface. NaOH eventually removed the native surface oxide presented across the treated aluminium surface and fresh reform hydroxide through the surface. The improvement of the hydroxide group after NaOH treatment can be seen after the deposition of the coupling agent. The silane atomic weight over the aluminium surface significantly improves for NaOH treatment groups before the coupling agent treatment. Also, the increased surface area and NaOH treatment cause higher deposition of the coupling agents. The spectrum of the silane and dipodal silane specimens show that the high silane signal confirms the silanol oligomers' deposition; for the zirconate treated samples, the precise zirconium specimen is also detected with spectrum.

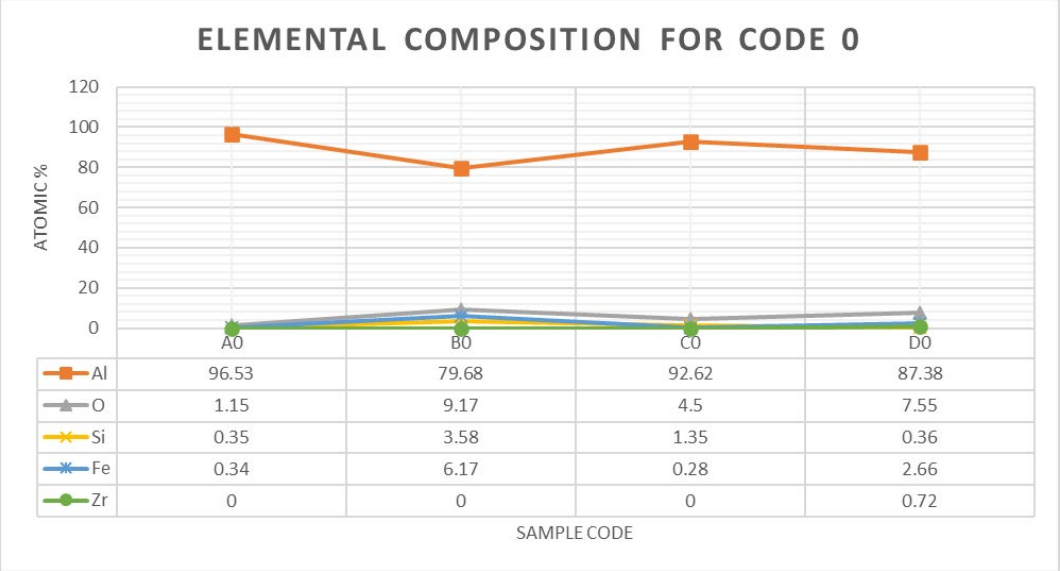

(a)

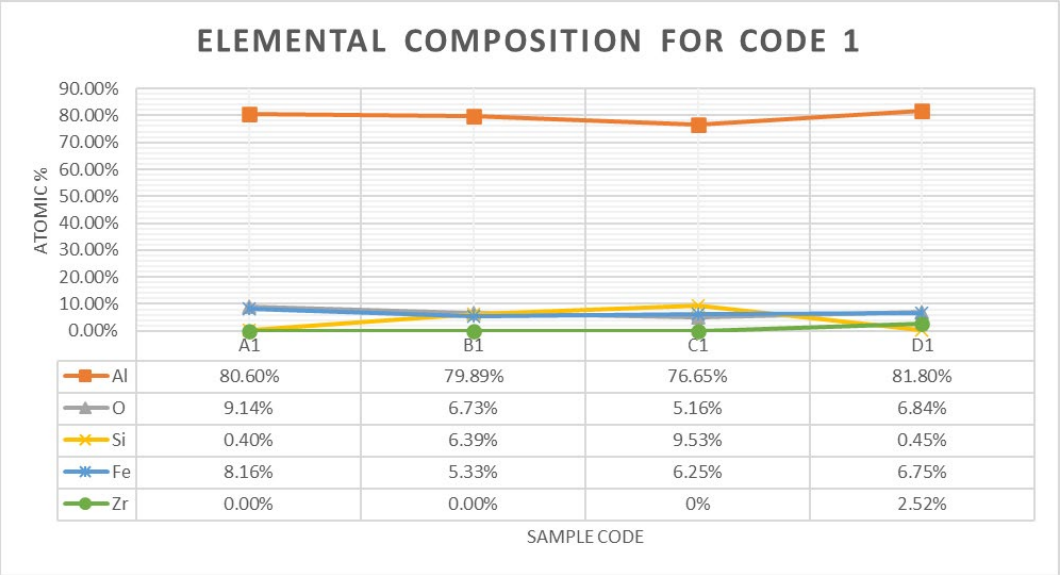
ELEMENTAL COMPOSITION FOR CODE 1
ATOMIC %
90.00%
80.00%
70.00%
60.00%
50.00%
40.00%
30.00%
20.00%
10.00%
0.00%
A1 B1 C1 D1
Al 80.60% 79.89% 76.65% 81.80%
O 9.14% 6.73% 5.16% 6.84%
Si 0.40% 6.39% 9.53% 0.45%
Fe 8.16% 5.33% 6.25% 6.75%
Zr 0.00% 0.00% 0% 2.52%
SAMPLE CODE

(b)

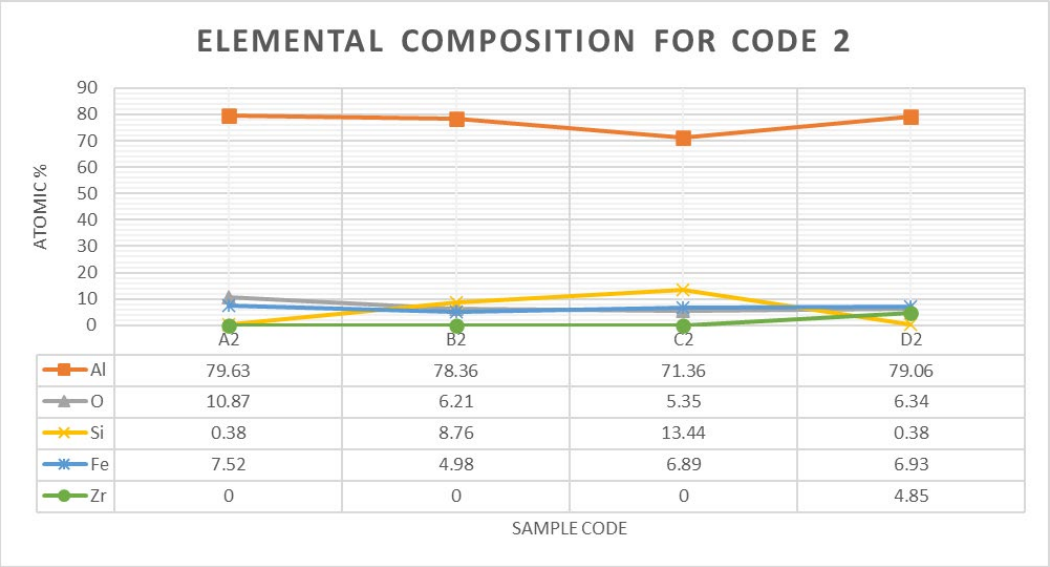
ELEMENTAL COMPOSITION FOR CODE 2
ATOMIC %
90
80
70
60
50
40
30
20
10
0
A2 B2 C2 D2
Al 79.63 78.36 71.36 79.06
O 10.87 6.21 5.35 6.34
Si 0.38 8.76 13.44 0.38
Fe 7.52 4.98 6.89 6.93
Zr 0 0 0 4.85
SAMPLE CODE

(c)

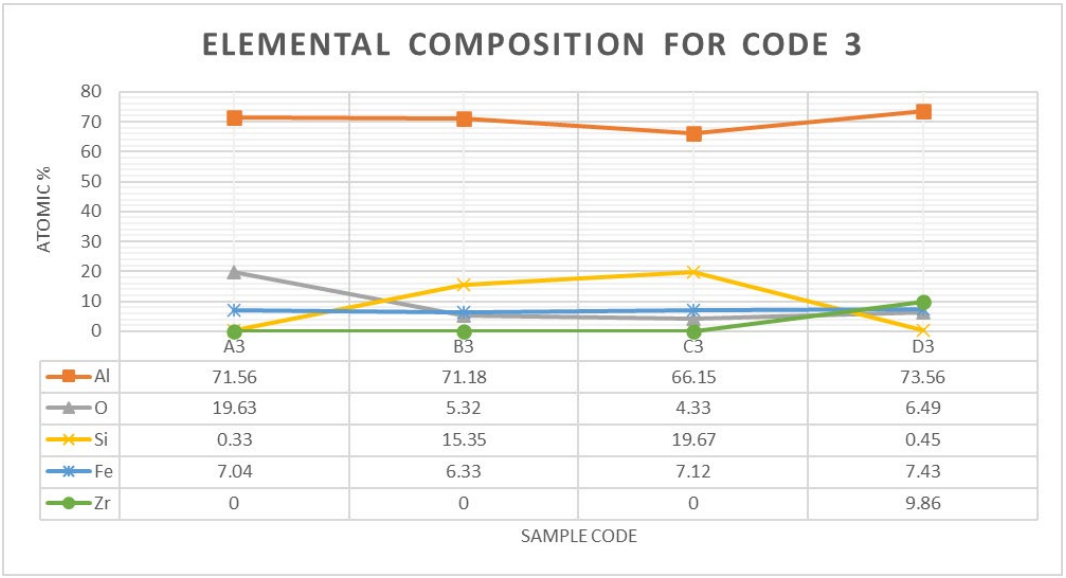

(d)

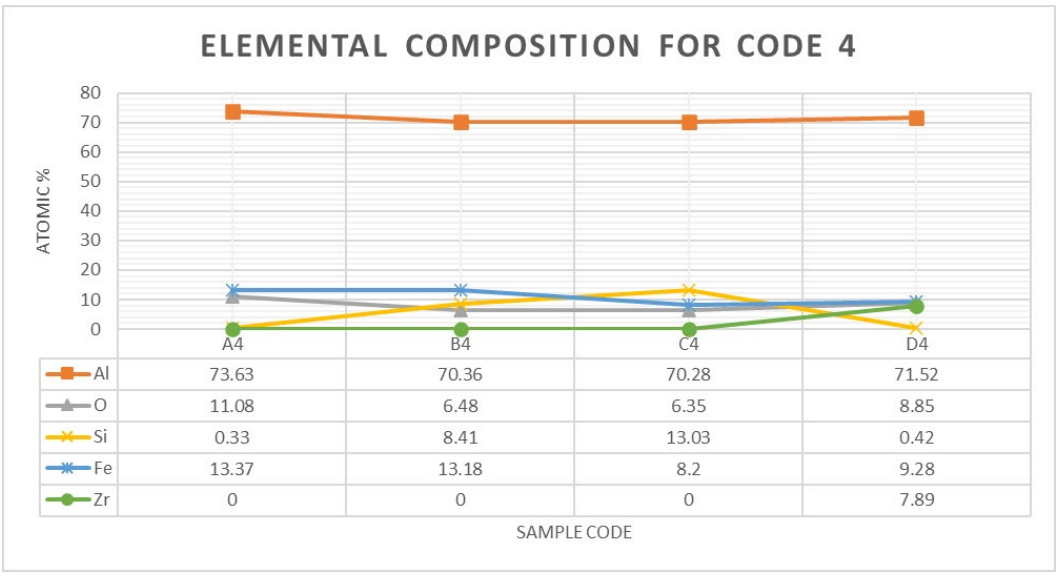

(e)

Figure 35: Elemental compositions analysis using the EDS for the treated aluminium surfaces shown in Figure 34 for five elements based on (a) code 0, (b) code 1, (c) code 2, (d) code 3, and (e) code 4.

3.5.4 Correlation between the surface free energy and its components and different selected surface roughness parameters

Referring to the results presented in the previous section, it can be noted that there are different levels of dependencies between the surface free energy and its components with different selected surface roughness parameters. This section addresses the existing correlation between these two dependent variables (i.e. surface roughness and surface energy and its components) in terms of the different employed surface treatments.

In order to identify the correlation between the surface free energy and its components on the initial performance of the bonded joint, the Pearson correlation coefficient (Rodgers & Nicewander, 1988), which has a high sensitivity to the linear correlation between two variables, was employed in this chapter and it will be referred to as the correlation coefficient. The Pearson correlation coefficient can be calculated by dividing the covariance of two variables by the product of their standard deviations (Rudawska et al., 2016). In general, the Pearson correlation coefficient between two random variables X and Y with an anticipated value of ξ_X and ξ_Y and standard deviations of σ_X and σ_Y is defined as:

$$\rho X,Y = corr(X,Y) = \frac{cov(X,Y)}{\sigma_X \sigma_Y} = \frac{E[(X-\mu_X)(Y-\mu_Y)]}{\sigma_X \sigma_Y} \quad (1)$$

where E is the anticipated value operator, *cov* stands for covariance, and *corr* is a well-known notation for the correlation coefficient.

The Pearson correlation value ranges in the scale of +1 in the case of a perfect direct correlation (linear relationship) to -1 in the case of a perfect anticorrelation (linear relationship) (Rodgers & Nicewander, 1988). As the value reaches closer to zero, there is less of a relationship, and it can be named as uncorrelated. More specifically, the overall correspondence between the range of Pearson correlation coefficients' values and correlations are given in words in Table 8.

Table 8: Corresponding Pearson value range and correlation wording

Coefficient of correlation	Correlation in words
0.0 - ±0.2	Little correlation
±0.2 - ±0.4	Weak correlation
±0.4 - ±0.7	Correlated
±0.7 - ±0.9	Strong Correlation
±0.9 - ±1.0	Very strong correlation

A comparison was made between the surface characteristics of specimens A0 and A1 in group A, as depicted in Figure 36. The results indicate that the highest Pearson correlation coefficient value (-0.88) was observed between the polar surface component of the NaOH-treated aluminium surface and S_q. The analysis of the correlation between the surface free energy components and selected surface roughness parameters revealed that polar components exhibit a strong negative correlation with all the chosen parameters, while the dispersive component showed a relatively weaker negative correlation. Additionally, a noticeable negative correlation was observed between the total surface treatment and surface roughness parameters. Based on these findings, it can be inferred that an increase in surface roughness due to the NaOH treatment results in a corresponding decrease in the total surface free energy and its components. Rudawska et al. (Rudawska et al., 2016) presented that, in general, with the mechanical abbreviation variants investigated, parameters that increase surface roughness decrease the values of the polar component of surface free energy due to NaOH treatment. This can be linked explicitly to the NaOH treatment effect in which the higher surface roughness parameters can be used as an excellent indicator for a higher number of -OH zone on the aluminium surface. Furthermore, it was stated in the study by (Wang & Zhang, 2020) that the opposite correlation between surface roughness and surface energy can indicate the hydrophobicity of the developed surface. Therefore, it is essential to investigate the surface characteristics of physiochemical surface treatment methods like NaOH treatment by considering surface roughness parameters and surface energy.

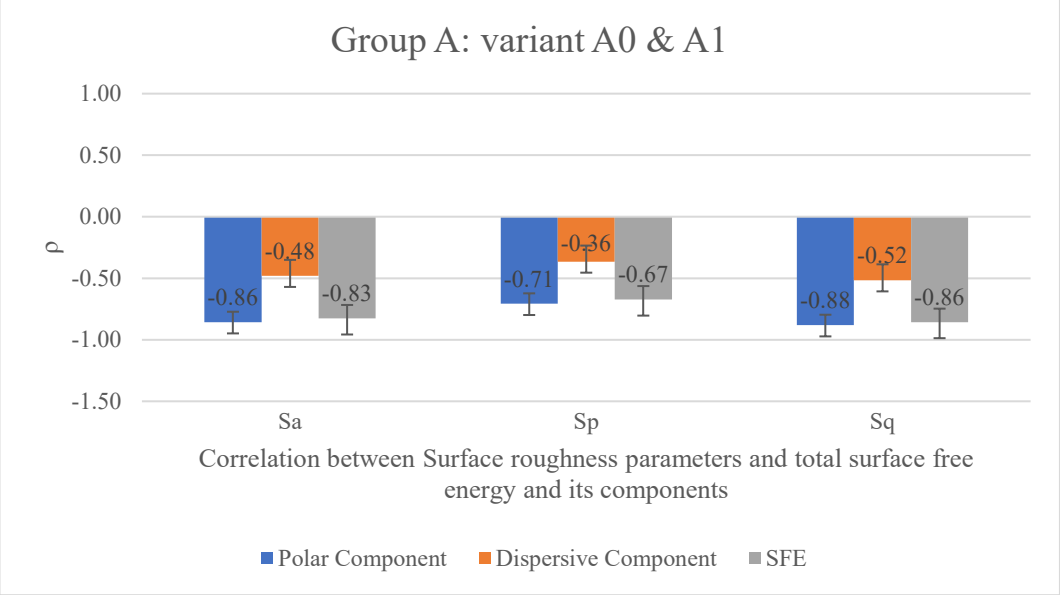

Figure 36: The Pearson correlation coefficient between the different surface roughness parameters and the total surface free energy and its component for variants A0 and A1

In addition, the comparison of surface roughness parameters, surface energy, and its components for specimens A1 to A4 was conducted, as demonstrated in Figure 37. The results indicate that mechanical abrasion of aluminium prior to NaOH treatment alters the correlation between the selected surface roughness parameters and the calculated total surface energy and its component of the treated aluminium. Specifically, the surface roughness parameter S_a exhibits a positive correlation with polar and total surface energy and is uncorrelated with the dispersive component. The significant difference between the Pearson correlation for A0 and A1 variant and A1 to A4 variant implies that mechanical abrasion (manual sandpapering) may have a different correlation with the surface energy of treated aluminium than the alteration in surface roughness parameters resulting from NaOH treatment. It is widely acknowledged that surface wettability of the treated substrate is a crucial factor in ensuring good interface adhesion strength. The surface morphology evaluation is known to affect the surface roughness characteristics of the aluminium surface and thus, the performance of water transport (Wang et al., 2022). According to the adhesion theory, the greater the surface energy of the treated surface in comparison to the selected adhesive, the better wettability can be excepted and, consequently, better adhesion performance (Gonzalez-Canche et al., 2018). Adhesive infiltration follows different mechanisms, which can develop some controversy about the driving factor in improving adhesion performance. In the study by Xu et al. (Xu et al., 2016), a similar statement was made based on the observation that suggested that increasing surface roughness and surface free energy cannot always promote a high adhesion performance. A similar outcome can be observed in the study by Saleema et al. (Saleema et al., 2012) regarding the effect of NaOH treatment on the surface energy of the aluminium.

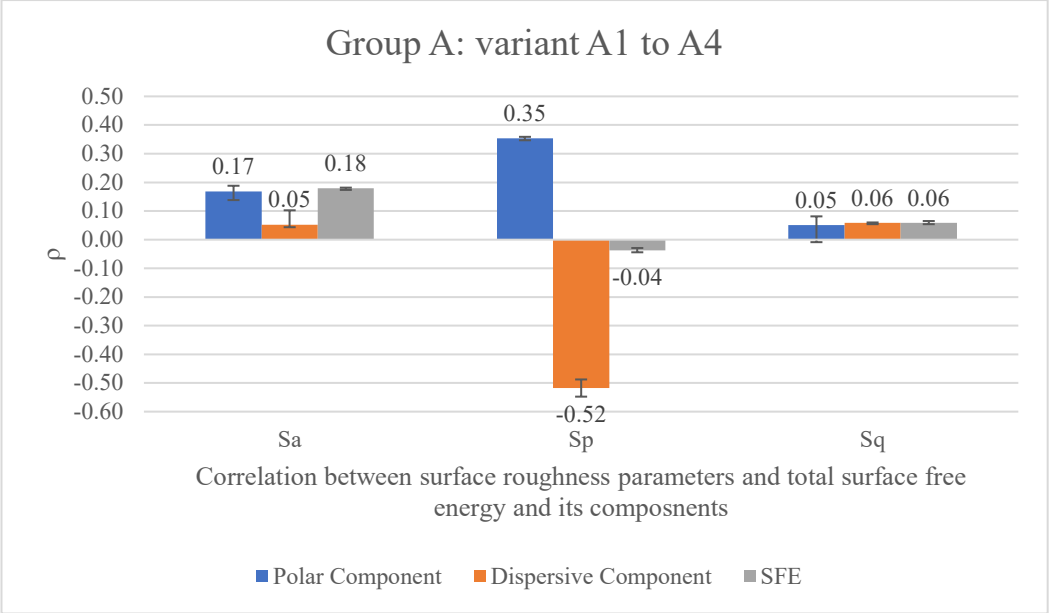

Figure 37: The Pearson correlation coefficient between the different surface roughness parameters and the total surface free energy and its component for variants A1 to A4

Similar to group A, a similar trend was observed between the surface roughness parameters and surface free energy and its components for variant B0 and B1 in group B in Figure 38. The lowest Pearson coefficient value (-0.87) was obtained between the total surface free energy of the NaOH + silane treated aluminium surface and S_q. The results showed that almost all selected surface roughness parameters had a strong negative correlation coefficient with surface free energy and its components. Therefore, an increase in the surface roughness parameters of S_a, S_p, and S_q leads to a decrease in the surface free energy, polar component, and dispersive component in group B.

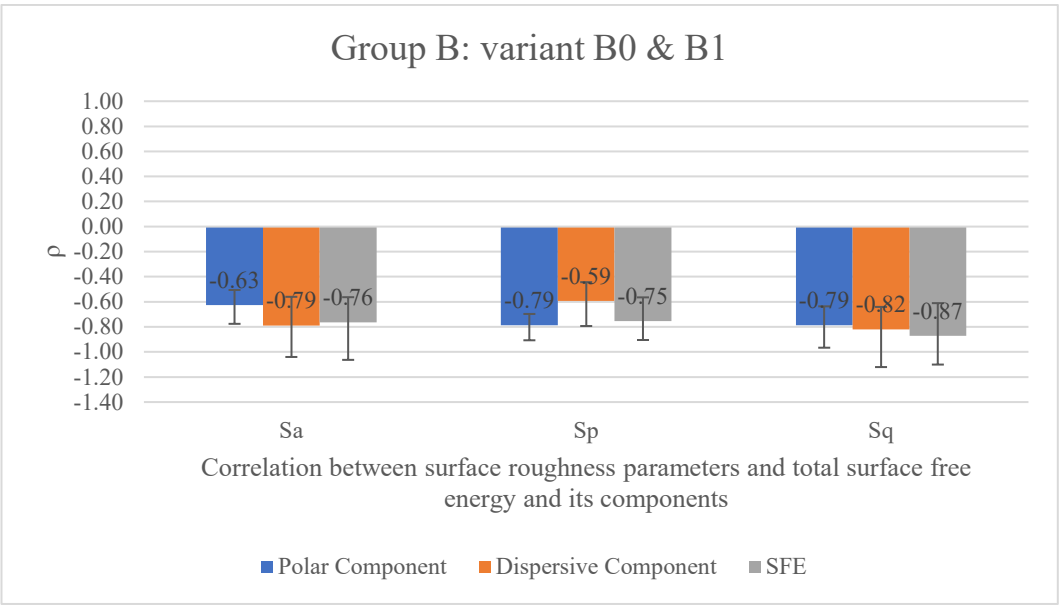

Figure 38: The Pearson correlation coefficient between the different surface roughness parameters and the total surface free energy and its component for variants B0 and B1

Furthermore, a comparison between the surface roughness parameters, surface energy and its component of specimens B1 to B4 was determined, as shown in Figure 39. Similarly, a correlation was found between the surface roughness parameters and surface energy and its component in group A and group B. As stated in Figure 39, the polar component of the variant B1 to B4 has a weak-moderate positive correlation with selected surface roughness parameters. This means that increasing the roughness parameters before the NaOH treatment and silane deposition can form a surface with greater polarity. However, it is seen that, in total, surface free energy has a negative correlation coefficient. This can be defined based on the rose petal effect (Bhushan & Her, 2010). Based on this effect, roughening of the aluminium surface prior to NaOH treatment and silane deposition developed the surface, which can be categorised in the Cassie impregnating wetting regime (Saleema et al., 2012). This means that the water drop gets stuck to the rough surface and does not wet it on the inclined surface.

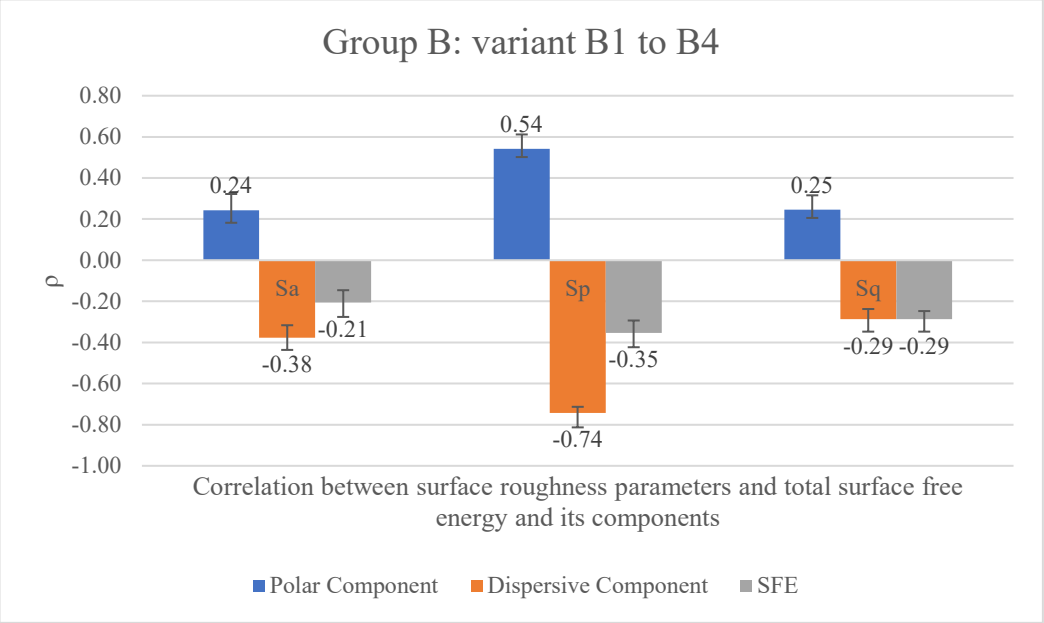

Figure 39: The Pearson correlation coefficient between the different surface roughness parameters and the total surface free energy and its component for variants B1 to B4

For variants C0 and C1 from group C, complementary results were observed to find the correlation between the surface roughness parameters and surface energy and its component between the polished aluminium surface and NaOH treatment in addition to the silane deposition and dipodal silane. As shown in Figure 40, it is seen that all the surface roughness parameters have a strong negative correlation with surface energy and its components. This means that by increasing the roughness due to NaOH treatment and surface chemistry alternation due to dipodal silane deposition, the surface energy and its component decrease.

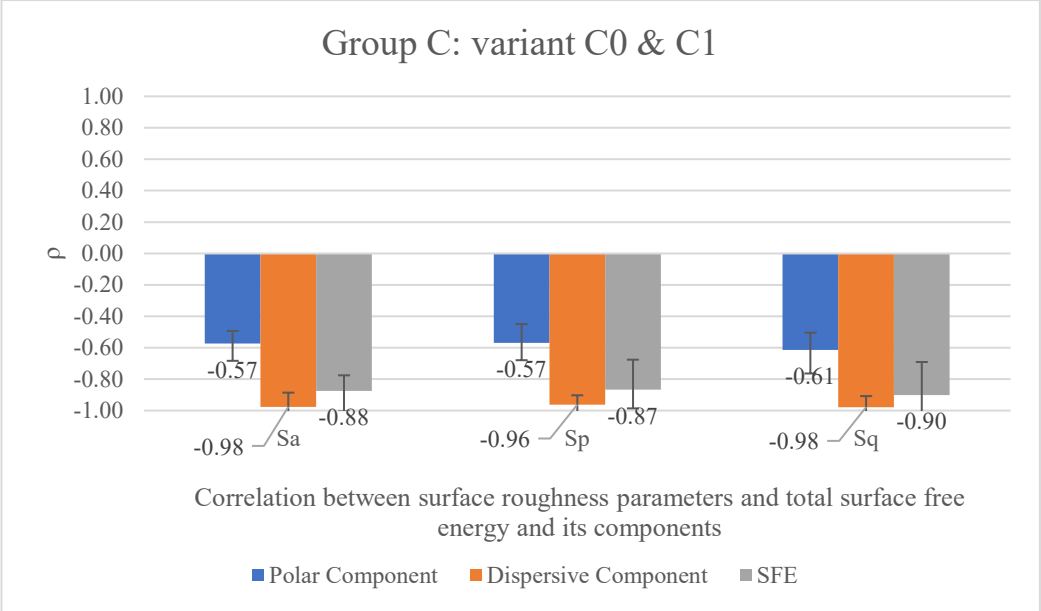

Figure 40: The Pearson correlation coefficient between the different surface roughness parameters and the total surface free energy and its component for variants C0 and C1

Moreover, a comparison of the variant C1 to C4 reveals an interesting correlation between the surface roughness parameters and surface energy and its component, as shown in Figure 41. Note that surface roughening prior to NaOH treatment and dipodal silane deposition, can develop a direct relationship between the polar component and surface roughness parameter S_p. This can be seen with the Pearson correlation coefficient of S_a and when the polar component is sitting at 0.47, which can be stated as a relatively correlated variable.

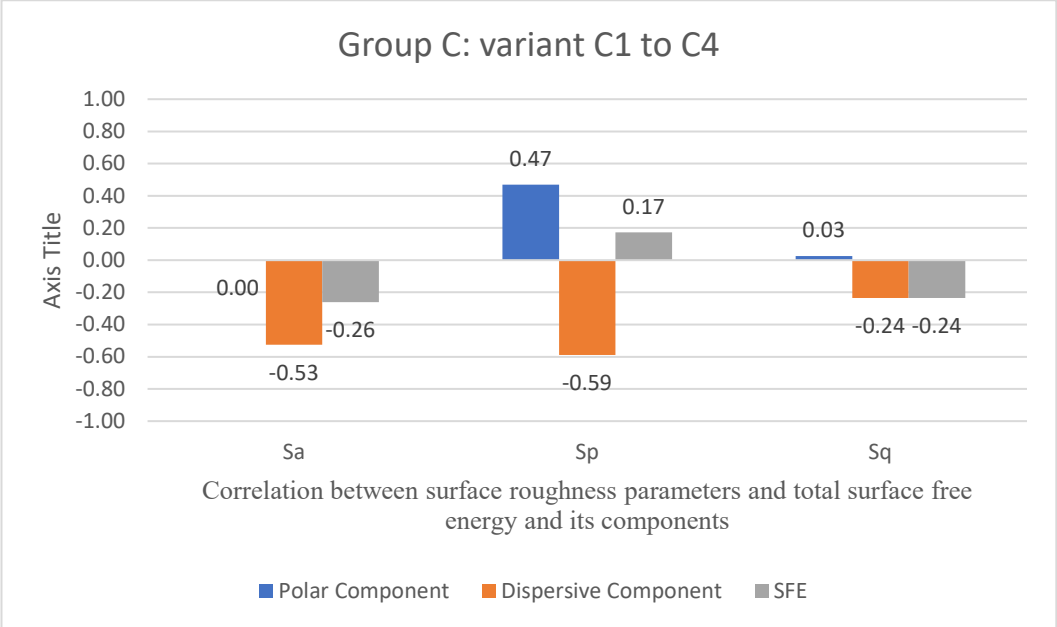

Figure 41: The Pearson correlation coefficient between the different surface roughness parameters and the total surface free energy and its component for variants C1 to C4

The dissimilarities between zirconate coupling agents and silanes were considered to identify the correlation between surface roughness parameters and surface energy in group D. The comparison between variants D0 and D1 shows a positive correlation between surface roughness parameters S_a, S_p, and S_q and the polar component of the treated aluminium surface, which suggests that an increase in surface roughness parameters due to NaOH treatment before zirconate deposition can enhance the polar component of the treated surface, leading to a stronger interaction between the zirconate coupling agent and the developed surface (see Figure 42). The dispersive component of variants D0 and D1 displays a negligible correlation with the different surface roughness parameters. Moreover, the total surface energy of the variant D0 and D1 moderately strongly correlates with the selected surface roughness parameters.

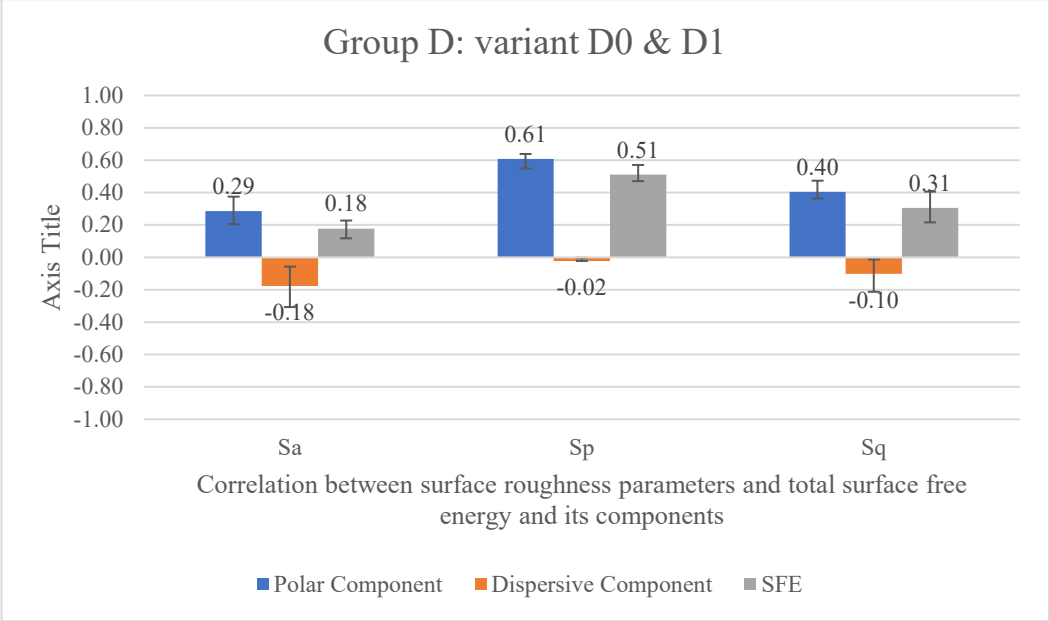

Figure 42: The Pearson correlation coefficient between the different surface roughness parameters and the total surface free energy and its component for variants D0 and D1

Furthermore, comparison in variants D1 to D4 also discloses a different correlation between surface roughness parameters and surface energy and its components. As shown in Figure 43, observe that the polar component shows a moderate positive correlation with the surface roughness parameter S_a and S_q, where it is employed prior to NaOH treatment and zirconate deposition.

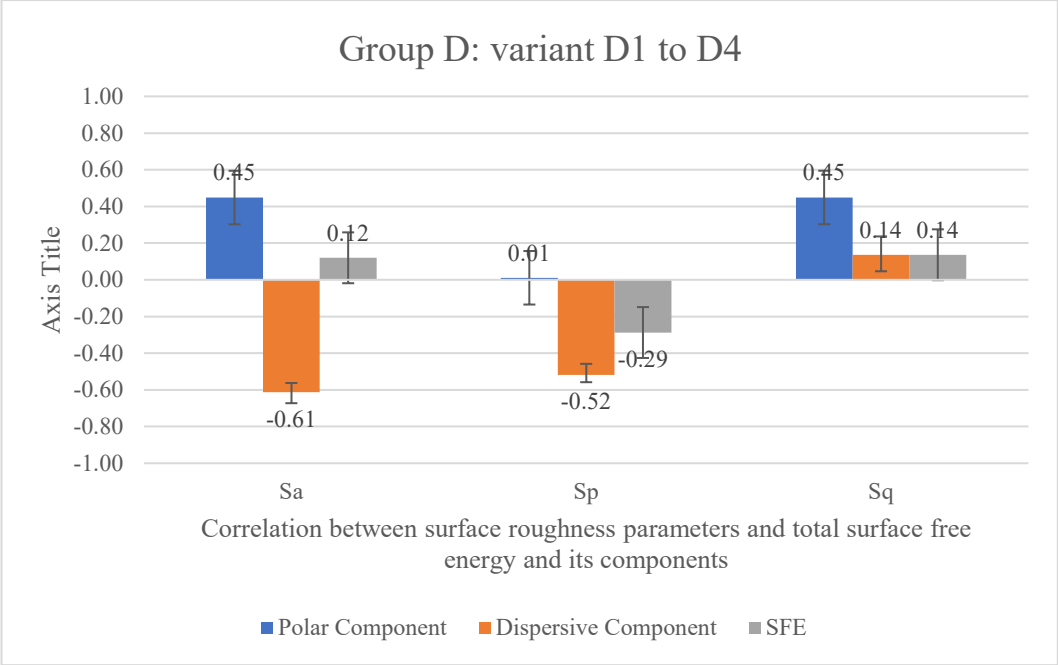

Figure 43: The Pearson correlation coefficient between the different surface roughness parameters and the total surface free energy and its component for variants D1 to D4

3.6 Conclusion

The primary goal of this work was to assess the influence of different surface treatments utilised in this study on surface morphology and surface chemistry of the aluminium alloy 6061-T6. A proposed set of surface treatment combinations allowed a detailed assessment of the surface characteristics of each sample, considering the importance of selected surface treatments. The following conclusions can be drawn.

- 0.1M NaOH treatment can significantly alter the surface roughness parameters such as S_a and S_q of the polished aluminium surface, which was misjudged in the literature due to the lack of systematic comparison.
- The deposition of the coupling agents, such as silane and dipodal silane, can be significantly influenced by NaOH treatment. NaOH treatment can form a suitable surface condition by increasing the hydroxyl group on the aluminium surface to promote significant reactivity between the aluminium surface and silane.
- To ensure the successful deposition of dipodal silane on aluminium alloy, the NaOH treatment is required.
- Roughening the aluminium surface prior to NaOH treatment can effectively increase the underlying available surface for NaOH treatment reaction and provide a higher range of hydroxyl groups.
- The results reveal that 3D surface roughness parameters can effectively be used to describe the surface roughness of the treated aluminium surface.
- The NaOH treatment can significantly increase the density of the hydroxide group across the surface of the treated aluminium surface. These hydroxide sites can react with silane to form silanol.
- NaOH treatment reduces the surface free energy of the polished aluminium surface mainly by reducing the surface energy of polar components. This can lead to a more stable aluminium surface against water.
- It can be argued that the rough surface texture developed by sandpapering can enhance the effectiveness of NaOH treatment and depositing the coupling agents. First, it provides a larger surface area for NaOH treatment to react with the aluminium surface. Secondly, it can facilitate mechanical interlocking, which can favour higher adhesion between adhesive and adherend in the case of adhesive bonding.
- The elemental analysis results reveal that the NaOH treatment will not leave any intermetallic particles on the aluminium surface. It only affected the number of hydroxyl groups available for bonding and removing the

native oxide layer and replacing it with active and fresh aluminium hydroxide on the treated surface.

- Silane and dipodal can form a hydrophobic surface, while the zirconate treatment forms a hydrophilic surface.
- It can be suggested that the silane and dipodal silane can be used for the application where the surface is in close contact with water or exposed to a harsh environment. At the same time, zirconate can be a good candidate as an alternative method for silane coating on surface materials that may not respond well to silane coupling agents.
- The proposed surface treatment group set allows us to identify the influence of different surface treatments individually and in combination with other methods studied in this chapter. The results in this chapter can be used for more competent surface treatment selection based on variables such as selected adhesive and other product requirements.
- The surface chemistry of the final treated aluminium surface has a higher level of influence on surface energy and wettability than surface roughness.

CHAPTER 4

Initial Performance

THE INFLUENCE OF DIFFERENT ROUGHNESS PARAMETERS, ENERGY AND CHEMISTRY OF THE TREATED SURFACE ON INITIAL-TERM PERFORMANCE OF THE REACTIVE PUR BONDED ALUMINIUM-TO-ALUMINIUM JOINTS

4.1 Overview

The aim of this chapter is to demonstrate the impact of selected surface treatments on the performance of adhesively bonded aluminium-to-aluminium joints using the one of the latest environmentally friendly adhesives. The influence of various roughness parameters and polar and dispersive components of the treated surface on the strength of the adhesive joints is examined. The adhesively bonded specimens are manufactured in accordance with the relevant standard, and single-lap joint tensile tests are conducted on the adhesive coupons to evaluate the initial performance of the bonded joints. Pearson correlation coefficient is used to identify the relationship between the surface parameter and different treatments and to analyse the impact of various surface finishes on the initial performance of the adhesively bonded joints. In addition, the multivariate analysis of variance (MANOVA) method is employed to investigate the effect of different surface parameters on the initial performance of the bonded joints.

4.2 Introduction

4.2.1 Influence of surface roughness on the initial performance of the adhesively bonded joint

Existing experimental results in the literature have demonstrated that the surface roughening of aluminium alloys plays a critical role in determining the initial performance of single lap joints. The influence of different surface roughness on the bonding performance of the steel and aluminium surface was studied by Ghumatkar et al. (Ghumatkar et al., 2016). Various levels of surface roughness were produced utilising

different sandpaper, and an optimal roughness was identified at 1.97μm. Possible mechanical interlocking was assigned as the dominant factor in improving the adhesion performance. Alternatively, Zielecki et al. (Zielecfei et al., 2013) investigated the impact of mechanical roughening on the shear strength of adhesively bonded joints. In their conclusion, the statement was made that the effective surface area produced by mechanical abrasion is the primary factor influencing the performance of adhesively bonded joints. Subsequently, they refute the notion of supplementary mechanical interlocking, which was proposed by Ghumatkar et al. (Ghumatkar et al., 2016). However, in the similar study by Rudawska (Rudawska et al., 2016), the impact of mechanical treatment on various roughness parameters revealed that the geometrical characteristics of the treated surface holds greater significance than the surface area. It is clear from the aforementioned studies that there exists a debate regarding the effect of roughness alone, without even taking into account the impact of the chemistry of the treated surface.

4.2.2 Influence of surface energy and its components on the initial performance of the adhesively bonded joint

Similar to the studies on surface roughness, numerous research efforts have been devoted to investigating the effect of wettability and surface chemistry on the performance of adhesives and metallic materials. For instance, in the study by Wielant et al. (Wielant et al., 2010), the adhesion performance of polished steel was found to be the highest for the highly hydroxylated surfaces due to the formation of the solid acid-base interaction at the interface. Of a similar school of mind, Sababi et al. (Sababi et al., 2017) studied the influence of the surface coupling agent zirconium on the interfacial bonding properties of the polished steel surface. In their conclusion, the chemistry of the treated surface was indicated as the profound influencer on the stability of the metallic surface. Similarly, organo-silane-based coupling agents have been known for some decades to promote acceptable adhesion performance in various applications by forming covalent bonds across the polymer-substrate interface (Issa & Luyt, 2019). In the study by Xu et al. (Xu et al., 2016), the data for the surface energy and its component reveals the importance of the surface wettability of the treated aluminium. A higher surface energy can generally promote better wettability; however, the infiltration of different adhesives differs from that of water. Thus, a high surface energy does not always benefit better adhesion strength.

4.2.3 Objective of this chapter

The present chapter seeks to examine the impact of diverse attributes of the modified aluminium surface, utilising the treatments introduced in Chapter 3, on the

initial performance of the single lap adhesively bonded joints. The adhesive used for fabricating the single lap joints in this study is a reactive hot melt polyurethane (PUR). Although this type of adhesive exhibits superior characteristics, most of the literature on surface treatment and investigation of the effect on adhesion performance of adhesively bonded joints focuses on epoxies. Thus, we were motivated to examine the impact of various surface characteristics, as discussed in Chapter 3, on the initial adhesion performance of the bonded joints bonded with this type of adhesive. The experimental program involved the evaluation of the tensile strength of single-lap aluminium-to-aluminium joints. Pearson correlation coefficient was utilised to examine the effect of various surface parameters on the initial performance of the adhesively bonded joints and the extent of their contribution to enhancing the adhesion performance. Further, statistical analysis was performed to confirm the impact of various surface characteristic parameters, including roughness, surface energy, and its components resulting from the selected treatments.

4.3 Experimental programme

4.3.1 Materials

The material used as a substrate to manufacture the single lap joints was similar to that in Chapter 3, aluminium alloy 6061-T6, as shown in Table 3. This study selected one commercially available PUR adhesive with shown mechanical properties in Table 9 for further investigation. After each treatment, the selected adhesive has a long set time to ensure good penetration into the surface irregularities. It is a one-component adhesive that can form high-strength and flexible bonds with similar and dissimilar materials.

Table 9: Mechanical Properties of 3M PUR TS 115 HGS Adhesive as Specified by Manufacturer

Properties	**Values**
Viscosity (Uncured)	16,000 cP
Open Time	10 mins
Time to handling strength	60 s
Shore D Hardness	47 (In accordance with ASTM D2240)
T-Peel Adhesion	145 KPa
Application Temperature	121 C

4.3.2 Fabrication of adhesively bonded joints

Single lap joints were produced by employing custom-made aluminium mould that adhered to the guidelines set forth in ASTM D1002, which aimed to determine the shear strength of the adhesively bonded joints (Appendix 1a-c) . The geometry of the specimens was established based on the specified dimensions outlined in the aforementioned standard. Figure 44 depicts the assembly illustration of the single lap joint.

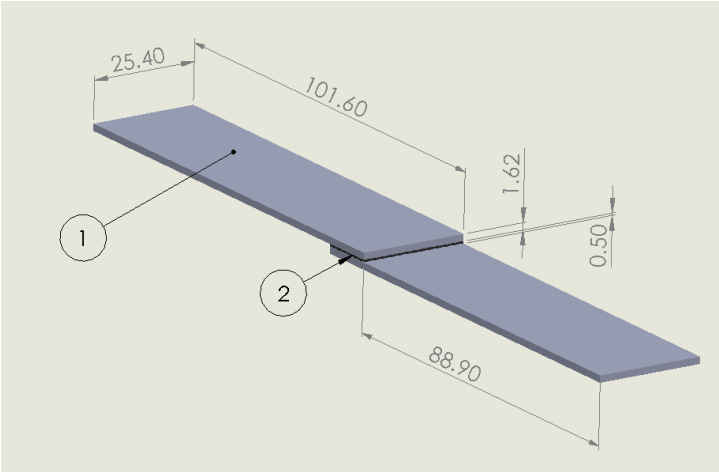

Figure 44: ASTM D1002 single lap joint configuration, (1) aluminium alloy; (2) PUR adhesive. All the values are in mm.

The coupon configuration of the single lap joints is often criticised due to the number of set-up parameters that can negatively affect the consistency of the test results unless they are carefully controlled. Two such key parameters are the correct alignment of the substrate before adhesive application and controlling its thickness across the bondline. Due to the potential for high stress concentration at the edges of the bondline, it is essential to ensure that an adequate amount of adhesive reaches these regions to ensure consistency in the joint setup. Hence, a customised mould was designed to ensure precise alignment of the coupons, controlled adhesive thickness, and uniform pressure across the bondline area, thereby reducing the chances of errors within a single batch and enabling a reliable comparison between batches. The adhesive thickness was selected based on the optimal thickness as studied by Boutar et al. (Boutar et al., 2018). The mould was coated with PTFE to prevent the samples from sticking to the bond rig due to adhesive over-fill once pressure was applied using the security bars. The 3M Scotch-Weld PUR Easy 250 applicator dispensed the PUR cartridges at 121˚ C. To obviate potential hindrances to adhesive penetration caused by temperature differentials between the aluminuim and PUR, all aluminuim laps underwent a preheating process at 100°C in the oven for 10 minutes, ensuring elevation of the substrate temperature prior to adhesive application. Tabs were carefully attached to the ends of each specimen using adhesive tape to ensure accurate alignment in the testing machine. The thickness of each single lap joint was measured using a micrometre to confirm the reproducibility of the custom-designed mould. The measurement procedure followed the guidelines specified in ISO 25217:2009. The thickness of the bonded joint at the bondline area was measured using a pro-grade electronic digital calliper at five different locations. Five specimens were prepared and tested for each of the different surface treatment groups, and a curing period of seven days at room temperature was allowed before testing.

4.3.3 Single lap joint testing

A universal tensile testing machine with a maximum capacity of 20kN was employed to conduct the single lap joint tests. Ensuring proper load string alignment is a key challenge in the tensile testing of single lap joint configurations, primarily due to the offset configuration of the specimen at each side. To achieve uniform load application, each specimen was meticulously aligned vertically using the alignment tab located at each side of the coupon. The grips were then tightened to eliminate any specimen movement, while minimising the creation of stress concentrations at the ends of the coupons. To prevent any inaccuracies in the results or premature failure due to misalignment of specimen ends, an alignment tab gripping solution was employed. Displacement-control mode was used to test all specimens at a constant displacement rate of 1.3mm/min. Any specimens that failed at the grips were deemed invalid, and the coupons were remade to maintain the same number of repetitions for each testing condition. The tensile force at rupture was converted into shear stress by dividing the value by the adhesive area. The results consisted of failure load, and the failure mode was recorded.

4.4 Experimental results and discussion

4.4.1 Single lap joint shear test

Figure 45 presents the overall results of the initial performance of the adhesively bonded single lap joints in relation to various surface treatments. The data indicates that the adhesion performance of the aluminium-to-aluminium bonded joint using PUR adhesive is significantly affected by the type of surface treatment applied.

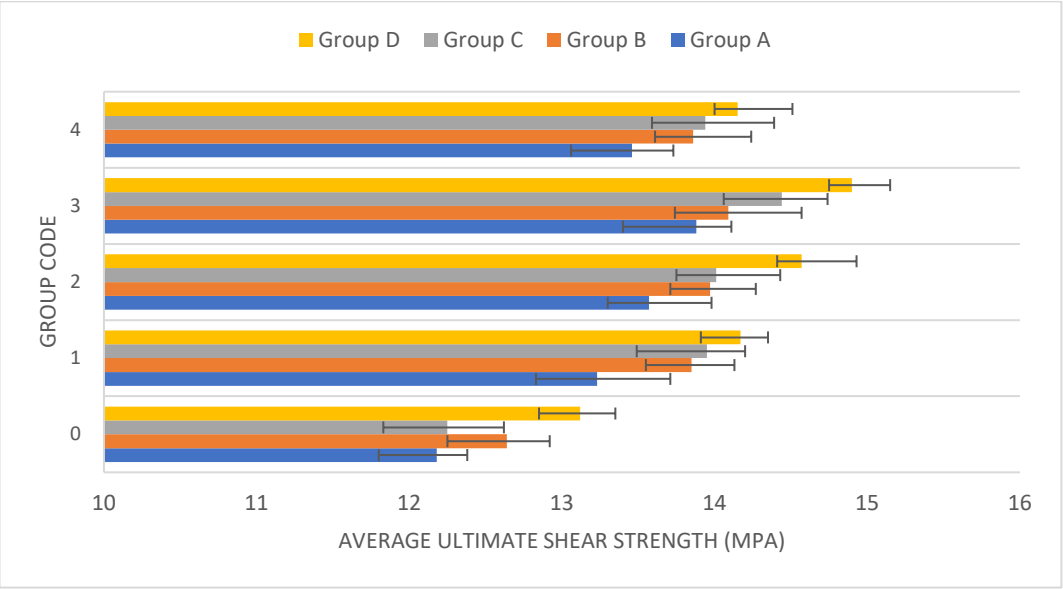

Figure 45: Average ultimate shear strength of single lap joint specimens based on different surface treatments

Group A exhibited an increase in the average ultimate shear strength of the bonded joint by 8.62% from 12.18MPa for A0 to 13.23MPa for A1 when the polished aluminium surface was etched in dilute NaOH solution. The results indicate that introducing roughening to the surface treatment combination led to a further increase in the ultimate shear strength of the adhesively bonded joint. The increasing trend was observed for groups A2 and A3, before a reduction in ultimate strength occurred for group A4. The highest ultimate shear strength among all measured samples for group A was achieved through the combination of NaOH etching and surface roughening with the mesh size of #120, resulting in an average ultimate shear strength value of 13.88MPa. This value is 13.96% higher than the strength of polished aluminium lap joints. The results indicate that excessive roughening of the aluminium surface can lead to a decrease in the peak strength achieved by the surface treatment combination. For instance, in group A3, further roughening caused a reduction in the ultimate shear strength to 13.46 MPa, which is a 3.03% decrease compared to group A2 and a 0.81% decrease compared to group A1. The varying trend in ultimate strength observed for group A can be attributed to the different surface treatment combinations applied. This may be explained by examining the recorded free energy and its components, as well as roughness parameters of the surface treatment. These aspects will be further discussed in the subsequent section of this chapter.

The results for group B demonstrate the impact of coupling agent deposition on the initial performance of the adhesively bonded joints, marking the first set of surface treatments to do so. The results indicate that the deposition of silane on the aluminium surface leads to a certain degree of improvement in the recorded average ultimate strength of the lap joints of the aluminium alloy, as compared to the results for group A. It should be noted that a similar trend is observed for groups A and B. By comparing the results for A0 and B0, it can be observed that the deposition of silane on the polished aluminium surface can increase the average ultimate strength of the bonded joints by 3.78%, from 12.18MPa to 12.64MPa, respectively. The results indicate that the combination of NaOH treatment and sandpapering with abrasive paper of #120 (B3) before silane deposition produces the highest average ultimate shear strength for group B. This combination results in a 15.68% increase in shear strength of the bonded joint compared to B1. This trend is consistent with group A, which also showed an increase in strength with surface roughening. To further elaborate, the result of group B confirms that the use of silane deposition can improve the initial performance of the adhesively bonded joints. The comparison between groups A and B indicates that the silane deposition has a greater

impact on group B, resulting in a higher increase in average ultimate shear strength compared to group A. Specifically, the average increase in ultimate shear strength between groups A and B after silane deposition was 3.038%. The results suggest that silane deposition can mitigate the adverse effects of excessive surface roughening. Comparing the results for A0, A4, and B4, it is evident that the ultimate shear strength of the joints treated with silane deposition (B4) increased by 2.97% compared to the joints without silane deposition (A4). Moreover, the comparison of B3-B4 and A3-A4 indicates that the negative impact of surface roughening has been reduced by 50% with the introduction of silane deposition. Based on the results, it is evident that the combination of NaOH treatment and surface roughening can produce a more robust initial adhesion performance compared to silane deposition alone. This is shown by the higher average ultimate shear strength values recorded for groups A1, A2, A3, and A4 compared to B0. Therefore, the NaOH treatment combined with surface roughening can be considered a more effective surface treatment for adhesively bonded single lap joints of aluminium alloys. This means that the results significantly agree with the rose petal effect reported in the literature (Bhushan & Her, 2010; Teisala et al., 2011), in which high contact angle (low surface energy) for group A can coexist with relatively strong initial adhesion performance.

Similar to groups A and B, the results for group C demonstrate an increasing trend in ultimate shear strength by depositing the dipodal silane on the aluminium surface prior to adhesive bonding. However, the C0 variant, which involved depositing dipodal silane on a polished aluminium surface, showed only a slight improvement compared to the A0 reference point. This was expected since the surface characteristics of polished aluminium could not effectively interact with the dipodal silane to create the desired surface. Excluding the result for variant C0, the findings suggest that the ultimate average shear strength for group B and group C is nearly identical. The only notable difference is in variant C3, where the average ultimate shear strength is 14.44MPa, representing an increase of 2.48% and 4.03% compared to B3 and A3, respectively. This result suggests that the dipodal silane deposition can promote the adhesion performance of the aluminium-to-aluminium bonded joints to some extent. However, the effectiveness of dipodal silane deposition seems to reach a plateau when combined with surface roughening. This can be seen in the result for variants C4 and B4, where both show a reduction in ultimate shear strength compared to their respective surface roughening variants without dipodal silane deposition. Overall, the results indicate that the type and combination of surface treatments play a significant role in the initial performance of adhesively bonded single lap joints, with the highest average ultimate shear strength

observed for a combination of NaOH treatment and surface roughening with #120 abrasive paper, followed by dipodal silane deposition.

Based on the results of the last group, which involved using zirconate as the selected coupling agent, a significant level of improvement was observed, with a similar trend to other groups, in terms of the average ultimate shear strength. This improvement was observed in the polished surface variants A0, B0, C0, and D0, where the zirconate-treated surfaces exhibited the highest shear strength of 13.12MPa. Expressed as a percentage, the application of zirconate on average increases the ultimate strength of aluminium adhesively bonded joints by 3.37% compared to group A. This improvement can be attributed to the better compatibility between the surface characteristics of the developed surface and the selected adhesive. The reactive PUR adhesive has moisture-curing properties that can react efficiently with the polar components of the substrate surface. In the previous chapter, it was reported that the zirconate-deposited aluminium surfaces in group D had the highest polar ratio.

Table 10 presents the average ultimate shear strength changes for different surface treatments, where the green colour indicates a positive improvement in shear strength due to the respective surface treatments applied in each group. A valid comparison can be made by comparing the different surface treatments with the polished aluminium surface. However, to provide a better reference point for future applications, it is crucial to thoroughly comprehend each improvement. The surface treatments that resulted in the highest improvement in shear strength were NaOH treatment + roughening with #120 and zirconate deposition, with 22.33% improvement compared to the polished surface. Zirconate was found to be more effective than silane in increasing the shear strength of the bonded joint, with double the improvement observed for zirconate compared to silane. The lack of improvement seen in dipodal silane-treated samples (C0) can be attributed to insufficient deposition of the coupling agent on the polished aluminium surface. The results also showed that dipodal silane was more effective in improving strength compared to conventional silane, likely due to the higher number of interaction sites and covalent bonding. The level of improvement increased with rougher sandpaper used for surface roughening, but excessive roughness resulted in decreased shear strength for all treatments. Variant 3 was identified as the turning point, beyond which further surface roughening led to reduced initial performance of the adhesively bonded joints. A similar trend of ultimate shear strength concerning surface roughness was found by Budhe et al. (Budhe et al., 2015) for aluminium and Sekercioglu et al. (Şekercíoğlu et al., 2003) for steel under shear load.

The findings of the study indicate that the developed textured surfaces exhibit a higher average ultimate shear strength in the single lap joint test as compared to the polished surfaces. The average level of improvement between different developed textured surfaces after appropriate treatment for the selected group is presented in Table 10. The level of improvement is found to vary depending on the surface condition. However, all the improvements support the aforementioned statement. The most significant level of improvement occurs between groups D and A0, exhibiting an average shear strength improvement of 18.75%. Conversely, the lowest level of improvement resulting from surface texturing/roughening is observed between groups A and D0, demonstrating only a 3.16% average shear strength improvement.

Table 10: Level of improvement on ultimate shear strength as a result of the surface texturing/roughening

Level of improvement for the textured surfaces

Textured Groups	Polished Groups A0	B0	C0	D0
A1	8.62%	4.67%	8.00%	0.84%
A2	11.41%	7.36%	10.78%	3.43%
A3	13.96%	9.81%	13.31%	5.79%
A4	10.51%	6.49%	9.88%	2.59%
Average	11.13%	7.08%	10.49%	3.16%
B1	13.71%	9.57%	13.06%	5.56%
B2	14.70%	10.51%	14.04%	6.48%
B3	15.68%	11.47%	15.02%	7.39%
B4	13.79%	9.65%	13.14%	5.64%
Average	14.47%	10.30%	13.82%	6.27%
C1	14.53%	10.36%	13.88%	6.33%
C2	15.02%	10.84%	14.37%	6.78%
C3	18.86%	14.24%	17.88%	10.06%
C4	14.45%	10.28%	13.80%	6.25%
Average	15.72%	11.43%	14.98%	7.36%
D1	16.34%	12.10%	15.67%	8.00%
D2	19.62%	15.27%	18.94%	11.05%
D3	22.33%	17.88%	21.63%	13.57%
D4	16.70%	11.95%	15.51%	7.85%
Average	18.75%	14.30%	17.94%	10.12%

4.4.2 Single lap joint failure modes

The failure modes observed in the adhesively bonded joint can be utilised to assess the efficacy of the surface treatments and the overall performance of the joint. While the single lap joint failure mode may not be the most accurate method to determine the shear strength of the bonded joint, it can serve as an excellent indicator of the effectiveness of the various surface treatments (Banea & da Silva, 2009). Consequently, a thorough analysis of both sides of the aluminium adherents was performed in this study to determine the failure mode corresponding to the different specimen groups following the

single-lap joint test. The results of this examination are presented in Table 11. A discernible trend has been observed in the failure modes of the samples tested in the single lap joint test in this study. Samples with average ultimate shear strength values exceeding 13MPa have shown cohesion failure as the predominant mode of failure. This includes samples A2 and A3 from Group A, B1, B2 and B3 from Group B, C1, C2 and C3 from Group C, and D1, D2, D3 and D4 from Group D. On the other hand, samples A1, A4, B4, C4 and D0 exhibit a mixed failure mode, which may be attributed to the extensive surface roughening, leading to decreased adhesive penetration in samples with a number 4 designation in their initiations (Rudawska et al., 2016).

On the other hand, the results indicate that polished specimens for groups A, B, and C demonstrate a dominant adhesion failure mode, which appears as a mirror-polished surface after failure, similar to its appearance before the single lap joint testing. This suggests that the deposition of various coupling agents can effectively increase the strength of the bonded joint, and good compatibility between the adhesive and selected coupling agent can overcome some of the limitations of surface roughening. Furthermore, it can be observed that, despite the extensive surface roughening exhibited by D4, the good compatibility between zirconate and PUR resulted in a strong bonded joint with cohesive failure mode. The results also show that depositing zirconate prior to NaOH treatment over the polished aluminium surface can still promote different failure modes in comparison to other polished subcategories, such as A0, B0, and C0, where a mixed mode failure was recorded for D0.

The results of the study demonstrate that NaOH treatment of the aluminium surface can improve the bonding strength at the interface between aluminium and PUR adhesive, but to achieve cohesion failure, either surface roughening or deposition of the coupling agent is required. Furthermore, it was observed that extensive surface roughening can lead to a mixed mode failure. The effectiveness of silane and dipodal silane treatments in mitigating the negative impact of extensive surface roughening was found to be inferior to that of zirconate. A comparison between A1 and A0 also indicates that the addition of NaOH treatment can enhance the bonding strength, but it may not be enough to achieve the desired failure mode without further treatment.

Table 11: Different failure modes corresponding to different surface treatments of adhesively bonded joints

	Sample ID	Ultimate Shear Strength (MPa)	Failure mode
Group A	A0-1	11.94	A
	A0-2	12.59	A
	A0-3	12.93	A
	A0-4	12.23	A
	A0-5	11.22	A

	Average	**12.18**	**Adhesion Failure Mode**
	A1-1	13.01	M
	A1-2	12.42	A
	A1-3	13.58	M
	A1-4	13.82	M
	A1-5	13.31	M
	Average	**13.23**	**Mixed Failure Mode**
	A2-1	13.28	M
	A2-2	13.64	C
	A2-3	13.64	C
	A2-4	13.66	C
	A2-5	13.63	C
	Average	**13.57**	**Cohesion Failure Mode**
	A3-1	13.94	C
	A3-2	13.97	C
	A3-3	14.05	C
	A3-4	13.94	C
	A3-5	13.53	C
	Average	**13.88**	**Cohesion Failure Mode**
	A4-1	12.95	A
	A4-2	13.64	M
	A4-3	13.85	M
	A4-4	13.38	M
	A4-5	13.50	M
	Average	**13.47**	**Mixed Failure Mode**
Group B	B0-1	12.83	A
	B0-2	12.61	A
	B0-3	12.44	A
	B0-4	12.78	A
	B0-5	12.56	A
	Average	**12.64**	**Adhesion Failure Mode**
	B1-1	13.80	C
	B1-2	13.89	C
	B1-3	14.21	C
	B1-4	13.82	C
	B1-5	13.57	C
	Average	**13.85**	**Cohesion Failure Mode**
	B2-1	14.23	C
	B2-2	13.83	C
	B2-3	14.13	C
	B2-4	14.01	C
	B2-5	13.67	M
Group B	**Average**	**13.97**	**Cohesion Failure Mode**
	B3-1	13.74	C
	B3-2	14.14	C
	B3-3	14.26	C
	B3-4	14.30	C
	B3-5	14.02	C
	Average	**14.09**	**Cohesion Failure Mode**
	B4-1	13.69	M
	B4-2	13.85	M
	B4-3	13.93	M
	B4-4	13.95	M

	B4-5	13.87	M
	Average	**13.85**	**Mixed Failure Mode**
Group C	C0-1	11.76	A
	C0-2	12.28	A
	C0-3	12.48	A
	C0-4	12.38	A
	C0-5	12.37	A
	Average	**12.25**	**Adhesion Failure Mode**
	C1-1	13.89	C
	C1-2	14.00	C
	C1-3	13.96	C
	C1-4	13.99	C
	C1-5	13.89	C
	Average	**13.94**	**Cohesion Failure Mode**
	C2-1	14.11	C
	C2-2	14.37	C
	C2-3	13.45	M
	C2-4	14.02	C
	C2-5	14.11	C
	Average	**14.02**	**Cohesion Failure Mode**
	C3-1	14.30	C
	C3-2	14.46	C
	C3-3	14.48	C
	C3-4	14.51	C
	C3-5	14.44	C
	Average	**14.44**	**Cohesion Failure Mode**
	C4-1	13.67	M
	C4-2	13.81	C
	C4-3	13.91	C
	C4-4	14.11	C
	C4-5	14.17	C
	Average	**13.93**	**Mixed Failure Mode**
Group D	D0-1	12.96	M
	D0-2	13.06	C
	D0-3	13.27	C
	D0-4	13.14	C
	D0-5	13.21	C
	Average	**13.13**	**Cohesion Failure Mode**
	D1-1	14.44	C
	D1-2	13.97	C
	D1-3	13.98	C
	D1-4	14.04	C
	D1-5	14.41	C
Group D	**Average**	**14.17**	**Cohesion Failure Mode**
	D2-1	14.54	C
	D2-2	14.55	C
	D2-3	14.70	C
	D2-4	14.49	C
	D2-5	14.57	C
	Average	**14.57**	**Cohesion Failure Mode**
	D3-1	13.67	M
	D3-2	15.44	C
	D3-3	15.44	C

	D3-4	15.14	C
	D3-5	14.76	C
	Average	**14.89**	**Cohesion Failure Mode**
	D4-1	14.11	C
	D4-2	14.30	C
	D4-3	14.03	C
	D4-4	14.15	C
	D4-5	14.17	C
	Average	**14.15**	**Cohesion Failure Mode**

4.4.3 The correlation between surface roughness parameters and initial performance bonded joints

To gain a deeper understanding of the impact of various surface roughness parameters on the adhesion performance of adhesively bonded joints, the results from the initial adhesion testing of single lap joints were compared to selected surface roughness parameters obtained in Chapter 3. The surface roughness characteristics of the treated specimens were measured in terms of different parameters, including S_a, S_p, S_q, S_{ku}, and S_{sk}. However, in this chapter, the focus was mainly on S_a, S_p, and S_q. The polished specimens (A0, B0, C0, and D0) were used as a central reference point for interpreting the results of both the surface roughness parameter values and the average ultimate shear strength of the joints.

Figure 46 illustrates the relationship between the average ultimate shear strength of group A and the surface roughness parameter S_a. The results show a positive correlation between the two variables, where an increase in surface roughness parameter S_a leads to an increase in the average ultimate shear strength. However, the highest surface roughness parameter S_a measured among group A results in a decrement in strength. These findings are consistent with prior research reported in the literature (Ghumatkar et al., 2016; Pereira et al., 2009; Saleema et al., 2012). This phenomenon can be attributed to the negative impact of extensive surface roughening, which diminishes the adhesive's ability to replicate the adherend's surface topography and penetrate into the surface irregularities.

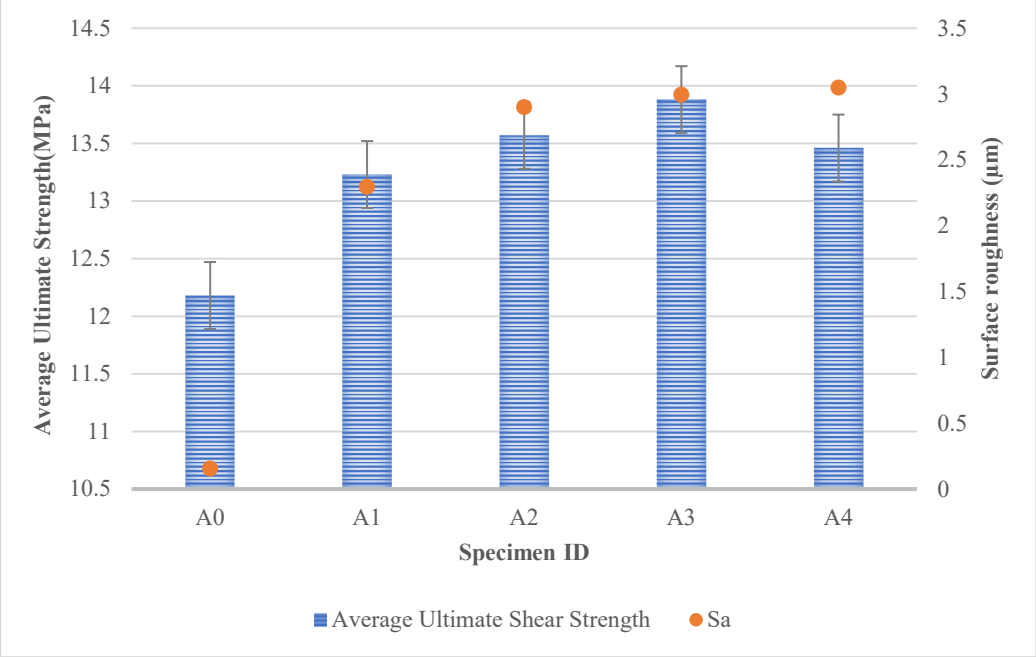

Figure 46: Average ultimate shear strength with respect to the surface roughness parameter S_a of group A

The shear strength of group A with respect to the surface roughness parameter S_p is presented in Figure 47. It is observed that the initial performance of the aluminium-to-aluminium adhesively bonded joint using PUR adhesive is affected by a similar trend to that of the arithmetical mean height of a line, S_a, and the maximum peak height, S_p. Extremely high values of surface roughness parameters, such as S_p and S_a, can hinder the ability of the adhesive to conform to and penetrate the treated aluminium surface, leading to adhesive being trapped on the tips' sides. This can create a high-stress concentration zone, leading to premature failure in single-lap joints. Such behaviour can be considered as the primary cause of the drop in the shear strength of A4.

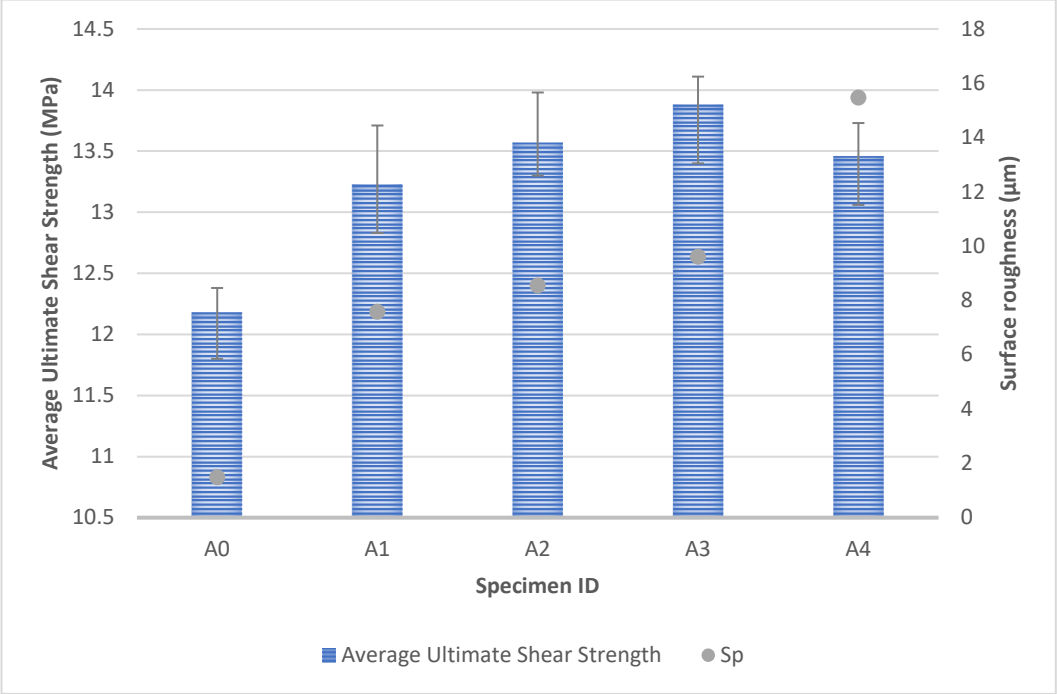

Figure 47: Average ultimate shear strength with respect to the surface roughness parameter S_p of group A

Figure 48 displays the average ultimate shear strength of group A concerning the surface roughness parameter Sq. It is evident that a comparable trend is observed for the variations in Sq. Thus, it can be inferred that the surface roughness parameters S_a, S_p, and S_q exhibit a direct correlation with initial performance, albeit the extensive surface roughening imposes certain restrictions.

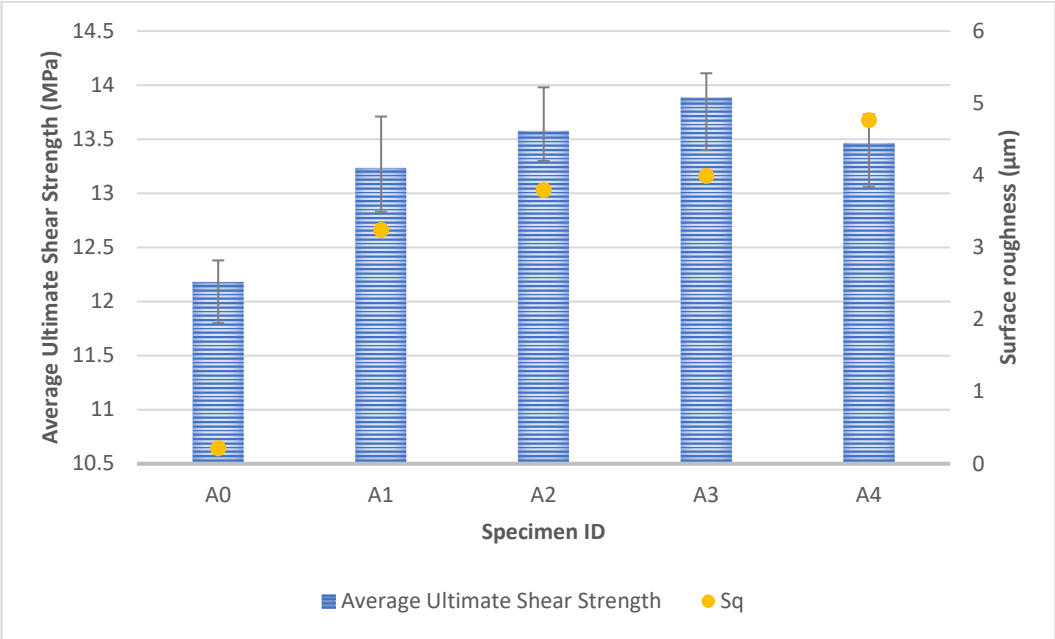

Figure 48: Average ultimate shear strength with respect to the surface roughness parameter S_q of group A

In addition, a comparison between group A's results expressed in percentage terms is depicted in Figure 49, where 100% was assigned to the polished aluminium surface. The correlation between S_a and ultimate shear strength was calculated to be 0.97, indicating a strong positive correlation between these two parameters. This means that the average ultimate strength of the adhesively bonded joint between aluminium substrates increases with an increase in S_a. Similarly, the correlation coefficients for Sp and Sq with ultimate shear strength were calculated to be 0.75 and 0.92, respectively.

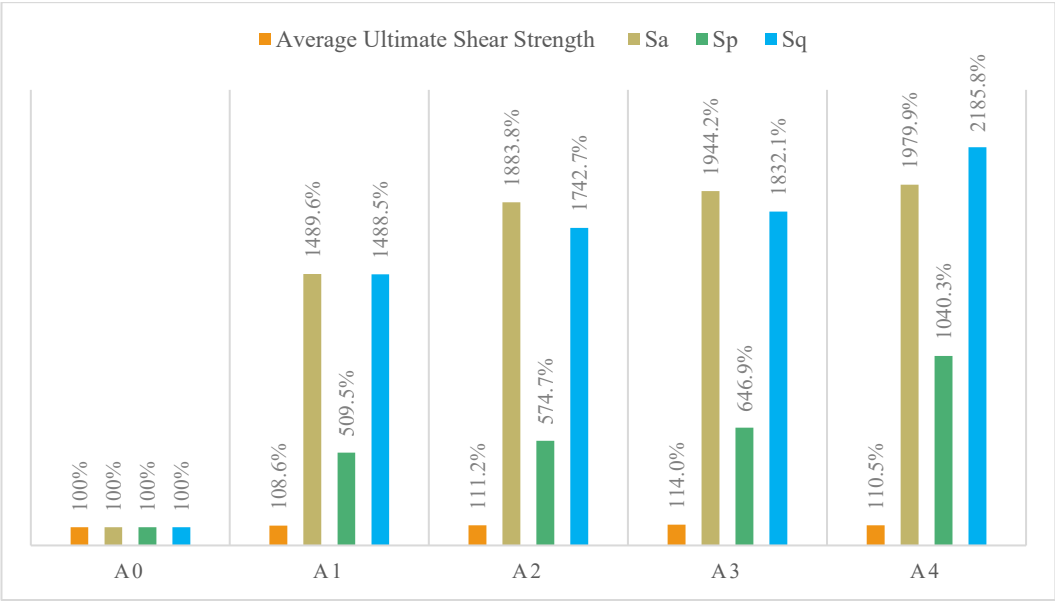

Figure 49: Comparison of resultant average ultimate shear strength of the aluminium bonded joints and selected surface roughness parameters for group A

In this study a multivariate analysis of variance (MANOVA) was conducted to determine the significant effects of surface treatments on the initial performance of adhesively bonded joints and surface roughness parameters. The MANOVA test develop several important statistical outputs, including Wilks' Lambda, Pillai's Trace, Hotelling's Trace, and Roy's largest root. These statistics parameters provide information about the overall significance of the model, the effect of each independent variable on the dependent variable, and the significance of the individual dependent variables. The comprehensive explanation about these parameters has been already demonstrated in the study by Todorov and Filzmoser (Todorov & Filzmoser, 2010). To test the null hypothesis of this study that there are no significant differences in the means of the dependent variable (surface characteristics of the treated specimens) across different groups of surface treatment, Wilks' Lambda can be used. Associated value ranges from 0 to 1 can be defined for this parameter, where a value closer to 0 indicates a stronger relationship between the selected independent and dependent variables. In addition to that, the significance of Wilks' Lambda is assessed using the F distribution. If the p-value associated with Wilks' Lambda is less than a predetermined significance level, the null hypothesis is rejected, and it can be concluded that there are significant differences in the means of the dependent variables across groups. Given the aims and objectives of this research, it is evident that employing MANOVA analysis would be highly appropriate for the current investigation.

The MANOVA results indicated a significant difference between A0 and A1, considering both the average ultimate shear strength and S_a variables jointly. The Wilks' Λ value was 0.147, with an F-value of 20.359 and partial η^2 of 0.853. Additionally, a separate analysis of variance (ANOVA) was performed for each dependent variable (i.e. surface roughness parameters) at an alpha level of 0.05. The results of a separate ANOVA for the dependent variable of average ultimate shear strength revealed a significant difference between A0 and A1, with A1 (M = 13.23) showing a higher score than A0 (M = 12.18), $F(1,8) = 7.586$, p = 0.025, partial η^2=0.487. There was also a significant difference between A0 and A1 on the surface roughness parameter S_a value, $F(1,8) = 28.543$, $p < 0.01$, partial η^2=0.781. For the S_p, Wilks' Λ= 0.255, $F(2,7)$=10.23, partial η^2=0.745, the MANOVA shows that there was no significant difference between A0 and A1, $F(1,8) = 1.986$, $p = 0.196$, partial η^2=0.199. Lastly, the result suggests that there was a significant difference between the A0 and A1 on the value of S_q, Wilks' Λ= 0.118, $F(2,7)$=26.18, partial η^2=0.882 for the initial performance and $F(1,8) = 40.806$, $p < 0.01$, partial η^2=0.836.

Upon comparing the Pearson correlation coefficient, a notable correlation was observed between the selected surface roughness parameters and average ultimate shear strength. Specifically, in the NaOH treatment of the polished aluminium surface, a positive correlation was found between the various surface roughness parameters and the initial performance of the bonded joints. The Pearson correlation coefficient was calculated to be 0.47, 0.32, and 0.52 for S_a, S_p, and S_q, respectively. As a result of NaOH treatment, an increase in different surface roughness parameters can potentially increase the average ultimate shear strength of PUR aluminium-to-aluminium adhesively bonded joints. However, the Pearson correlation coefficient obtained between variant A1 to A4 suggests that the direct impact of manual surface roughening of the aluminium surface before NaOH treatment on the initial performance of the bonded joints is minimal, as there is little correlation. Therefore, roughening the aluminium surface before NaOH treatment enhance the initial performance of the bonded joint by effectively increasing the available surface area for the reaction between the etching agent and the aluminium. Notwithstanding the minimal Pearson correlation coefficient observed among variants A1 to A4, a preliminary inference can be drawn regarding the limited direct influence of manual surface roughening on the aluminuim surface before NaOH treatment on the initial performance of the adhesively bonded joints, given the marginal correlation. Nonetheless, it is posited that the augmentation of initial performance in the bonded joints through the practice of roughening the aluminuim surface before NaOH treatment is underpinned by an effective increase in available surface area. This increase facilitates a heightened interaction between the etching agent and aluminuim, consequently yielding a more extensive hydroxide zone on the aluminuim surface.

A comparable statistical analysis was conducted to investigate the effect of surface roughening on the aluminium surface prior to NaOH treatment on the selected roughness parameters and the initial performance of the adhesively bonded joint. This analysis was performed on specimens A1, A2, A3, and A4. Examining the results from the MANOVA analysis, it can be noted that there is a significant difference between specimen A1 to A4 when considered jointly on the variables average ultimate shear strength and recorded value for S_a, Wilks' Λ= 0.350, $F(6,30)=3.454$, partial $\eta^2=0.409$. However, the MANOVA analysis does not provide information regarding the specific groups that exhibit significant differences. Therefore, post-hoc tests, namely the Least Significant Difference (LSD) and Bonferroni tests, were employed to determine the differences in means among the selected specimen groups. Referring to the Table 12, it is evident that the LSD post-hoc method identifies a significant difference in the average ultimate shear strength between specimens A1 and A3. In addition to this, it can be noted that the Bonferroni result agrees with the LSD result; therefore, the identified significance of the LSD

method for ultimate shear strength between selected specimens is satisfactory. However, there was no significant difference between the same specimens on S_a of the treated aluminium surface, in which $F(3,16) = 1.83$, $p = 0.217$, partial η^2=0.236. As stated in the Table 12 , S_a did not significantly affect the initial performance of the bonded joints using the LSD post-hoc method. Herein, the Bonferroni result agrees with the LSD, and it can be concluded that the obtained results for S_a using MANOVA and LSD are satisfactory. For the S_p, Wilks' Λ= 0.160, $F(6,30)$=7.519, partial $\eta^2 = 0.601$, the MANOVA shows that there was a significant difference between selected specimens, $F(3,16)$ =3.452, $p = 0.001$, partial η^2=0.716. As stated in the Table 12, for most of the comparisons, a significant effect was identified except for A2 and A3. Likewise, the Bonferroni result agrees with the LSD, and it can be concluded that the obtained results for S_p using the MANOVA analysis and LSD are satisfactory results. Lastly, referring to the MANOVA analysis of surface roughness parameter S_q, it can be concluded that there was no significant difference between selected specimens on total surface free energy, Wilks' Λ= 0.466, $F(6,30)$=2.327, partial η^2=0.058 for the initial performance and $F(3,16) = 0.730$, $p = 0.549$, partial η^2=0.120.

Table 12: Values for post-hoc analysis in terms of shear strength of the adhesively bonded joints and different surface roughness parameters for variants A1 to A4

Shear Strengh	LSD			
	A1	A2	A3	A4
A1		0.14	0.008	0.297
A2	0.14		0.166	0.641
A3	0.008	0.166		0.072
A4	0.297	0.641	0.072	

Shear Strengh	Bonferroni			
	A1	A2	A3	A4
A1		0.84	0.05	1
A2	0.84		0.994	1
A3	0.05	0.994		0.431
A4	0.002	0.81	0.431	

Sa	LSD			
	A1	A2	A3	A4
A1		0.134	0.087	0.067
A2	0.134		0.81	0.705
A3	0.087	0.81		0.889
A4	0.067	0.705	0.889	

Sa	Bonferroni			
	A1	A2	A3	A4
A1		0.804	0.522	0.402
A2	0.804		1	1
A3	0.522	1		1
A4	0.402	1	1	

Sp	LSD			
	A1	A2	A3	A4
A1		0.001	0.003	0.001
A2	0.001		0.599	0.04
A3	0.003	0.599		0.014
A4	0.001	0.04	0.014	

Sp	Bonferroni			
	A1	A2	A3	A4
A1		0.006	0.018	0.001
A2	0.006		1	0.239
A3	0.018	1		0.081
A4	0.001	0.239	0.081	

Sq	LSD			
	A1	A2	A3	A4
A1		0.248	0.36	0.198
A2	0.248		0.8	0.888
A3	0.36	0.8		0.694
A4	0.198	0.888	0.694	

Sq	Bonferroni			
	A1	A2	A3	A4
A1		1	1	1
A2	1		1	1
A3	1	1		1
A4	1	1	1	

In order to evaluate the distinct impact of surface roughening on the aluminium surface prior to NaOH treatment on the initial performance of the adhesively bonded joints, a comparison was made between the variants A1 to A4 in group A. The Pearson correlation coefficient of these variants was examined, and it was observed that there existed a negative correlation between the initial performance of the adhesively bonded joint and Sa, and Sq, with values of -0.16 and -0.22, respectively. However, the

correlation coefficient between the initial performance of the adhesively bonded joint and Sp was positive but very weak, with a value of 0.07.

In reference to Group B, it is evident from Figure 50 that the trend for the sample with supplementary silane deposition is comparable to that of Group A regarding the S_a surface roughness parameter.

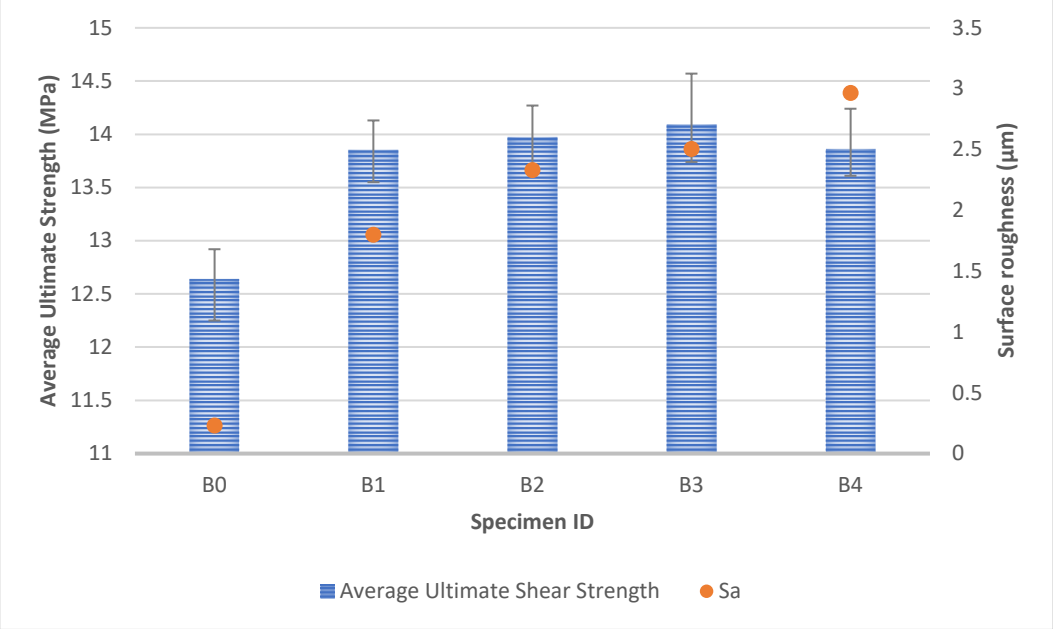

Figure 50: Average ultimate shear strength with respect to the surface roughness parameter S_a of group B

The findings indicate that despite the application of silane deposition, significant surface roughening continues to have a negative impact on the average ultimate shear strength, underscoring the importance of ensuring compatibility between surface roughness and adhesive viscosity. Nonetheless, it is worth noting that the initial performance of the adhesively bonded joint shows improvement compared to group A, albeit with a steady trend. This result is in great agreement with the study outcome by van Dam et al. (van Dam et al., 2020). However, Khan et al. (Khan et al., 2016) reported a decrease in surface roughness leading to higher shear strength in aluminium adhesively bonded joints, while Boutar et al. (Boutar et al., 2016) found that rougher surfaces can result in weaker shear strength due to decreased wettability. Based on the existing literature and the results of this study, it can be concluded that the combination of NaOH treatment and silane coupling agent application can mitigate the negative impact of surface roughness characteristics on the performance of adhesively bonded joints in aluminium structures.

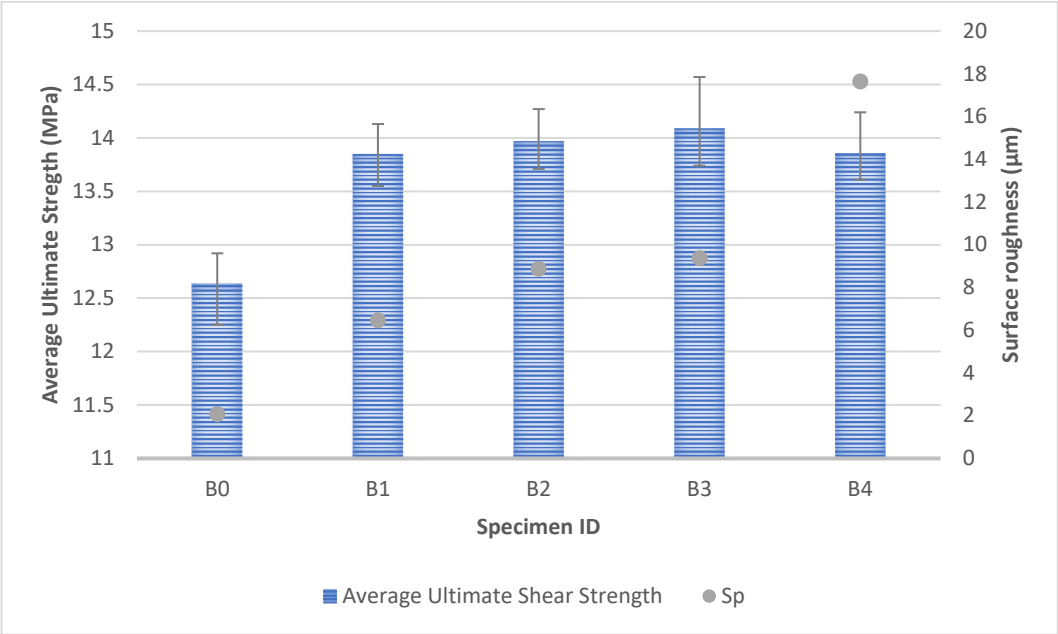

Figure 51: Average ultimate shear strength with respect to the surface roughness parameter S_p of group B

As illustrated in Figure 51 and 52, there is a clear trend of increasing shear strength as the S_p and S_q value increases, respectively. This trend is similar to that observed in group A, but with a greater degree of improvement, as evidenced by the reduction in shear strength observed in the last specimen, B4, which is less pronounced than that observed in specimen A4. These results indicate that the deposition of silane coupling agents can help to reduce the gap between surface roughness parameters and improve the resulting initial performance of the adhesively bonded joints.

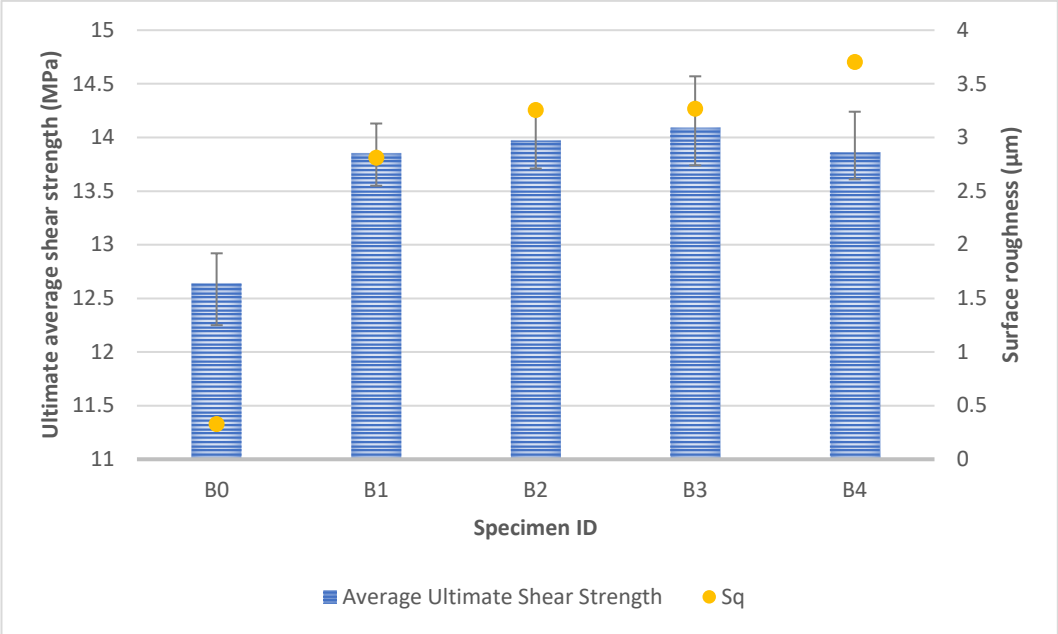

Figure 52: Average ultimate shear strength with respect to the surface roughness parameter Sq of group B

In Figure 53, the percentage-wise comparison of average ultimate shear strength and selected surface roughness parameters for group B is depicted. By analysing the results shown in Figure 49 and comparing the resultant average ultimate shear strength and different surface roughness parameters, it can be observed that a relatively similar correlation was obtained to those evaluated for group A. This implies that the influence of surface roughness on the initial performance of the adhesively bonded joints is consistent for both groups A and B. It is noteworthy that the silane coupling agent deposition leads to an improvement in the initial performance of the adhesively bonded joints for both groups A and B, as seen in the increased ultimate shear strength values. Moreover, the reduction in surface roughness parameters appears to have a positive impact on the shear strength of aluminium adhesively bonded joints, which is consistent with some of the previous studies. However, this trend is not observed in the current study, as the surface roughness reduction did not lead to an increase in ultimate shear strength.

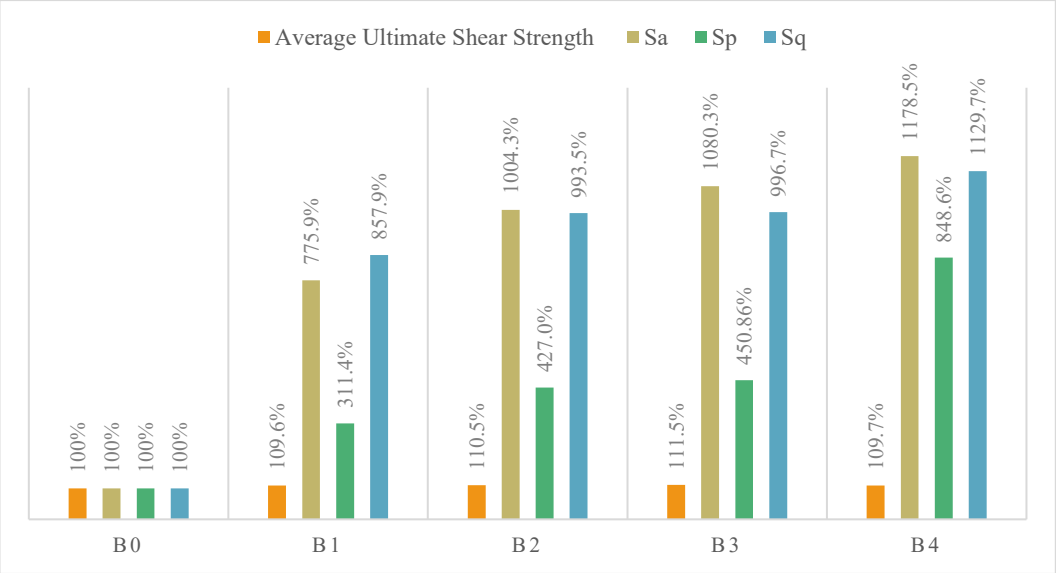

Figure 53: Comparison of resultant average ultimate shear strength of the aluminium bonded joints and selected surface roughness parameters for group B

The multivariate analysis of variance (MANOVA) was employed to investigate the impact of surface treatments on group B in terms of the initial performance of the adhesively bonded joints and selected surface roughness parameters. The findings indicate a substantial difference between B0 and B1 in terms of average ultimate shear strength and S_a when evaluated together, Wilks' Λ= 0.082, $F(2,7)$= 39.436, partial η^2= 0.918. Subsequently, individual ANOVA tests were performed on each dependent variable (i.e. surface roughness parameters) at a significance level of 0.05. There was a significant difference between B0 and B1 on average ultimate shear strength, $F(1,8)$ = 89.252, p = 0.001, partial η^2= 0.918, with B1 (M = 13.85MPa) scoring higher than B0 (M = 12.64MPa). There was also a significant difference between A0 and A1 on the value of

the surface roughness parameter S_a, $F(1,8) = 28.531$, $p < 0.001$, partial η^2=0.781. For the S_p, Wilks' Λ= 0.08, $F(2,7)$= 40.421, partial η^2=0.92, the MANOVA shows that there was significant difference between B0 and B1, $F(1,8) = 15.377$, $p = 0.004$, partial η^2=0.658. Lastly, the result suggests that there was a significant difference between the B0 and B1 on the value of S_q, Wilks' Λ= 0.009, $F(2,7)$=369.163, partial η^2=0.991 for the initial performance and $F(1,8) = 257.063$, $p < 0.01$, partial η^2=0.970. The findings suggest that the combination of NaOH treatment and a silane coupling agent has a notable impact on both initial performance and selected surface roughness parameters. However, it remains unclear whether the changes are due to the etching process or the deposition of the coupling agent. To investigate this, cross-analysis was conducted between variants A0 and B0, and A1 and B1. The results indicate that silane deposition alone does not account for the observed significant effect. Specifically, the comparison between A0 and B0 revealed no significant effect of silane deposition on surface roughness parameters and shear strength of the bonded joints, which was also confirmed by the comparison between A1 and B1. Hence, it can be concluded that silane deposition alone is insufficient in promoting good initial performance for the adhesively bonded joints.

In analysing the influence of surface roughening prior to the NaOH treatment and silane deposition on the aluminium surface, a similar statistical method was used between specimens B1 to B4. Based on the MANOVA analysis, it was found that there is no significant effect of surface roughening in variant B1 to B4 when considered jointly on the variable average ultimate shear strength and the measured value of S_a, Wilks' Λ=0.670 $F(6,30)$=1.109, partial η^2=0.182. However, with the assistance of the LSD and the Bonferroni post-hoc method, it has been found that there is a significant difference between B1 and B4 in the S_q value.

Similar to the analysis conducted for group A, the Pearson correlation coefficient between variants B0 and B1 and B1 to B4 was calculated. This was done to gain further insight into the actual relationship between selected surface roughness parameters and the initial performance of the aluminium-bonded joints in group B. The Pearson correlation coefficient of surface roughness parameters S_a, S_p and S_q and the average ultimate shear strength of the bonded joint between variant B0 and B1 are 0.93, 0.82 and 0.91, respectively. The analysis indicates that the selected surface treatments exhibit a positive correlation with the initial performance of the aluminium adhesively bonded joints. When comparing these findings with the Pearson correlation coefficient obtained for variants A0 and A1, it is observed that NaOH treatment prior to silane deposition can enhance the correlation coefficient for all three surface roughness parameters with average ultimate shear strength. Moreover, for variants B1 to B4, S_q was found to have a negative

correlation coefficient with the initial performance of the bonded joints, while S_a and S_p were found to have a negligible correlation with the shear strength of the bonded joints. Hence, it can be inferred that the mechanical abrasion of the polished aluminium surface before NaOH treatment and silane deposition may not have a significant impact on the initial performance of the aluminium bonded joint.

In Figure 54, it is apparent that an increase in the surface roughness parameter S_a leads to an increase in the average ultimate shear strength for group C. However, similar to group A and group B, the shear strength value decreased for extensively roughened surfaces. This finding suggests that despite the potential improvement in the aluminium surface's chemistry due to the dipodal silane deposition, the negative impact of excessive surface roughness cannot be ignored. As previously suggested, adjusting the viscosity of the adhesive could be a potential solution to ensure that the adhesive completely infiltrates different irregularities on the surface.

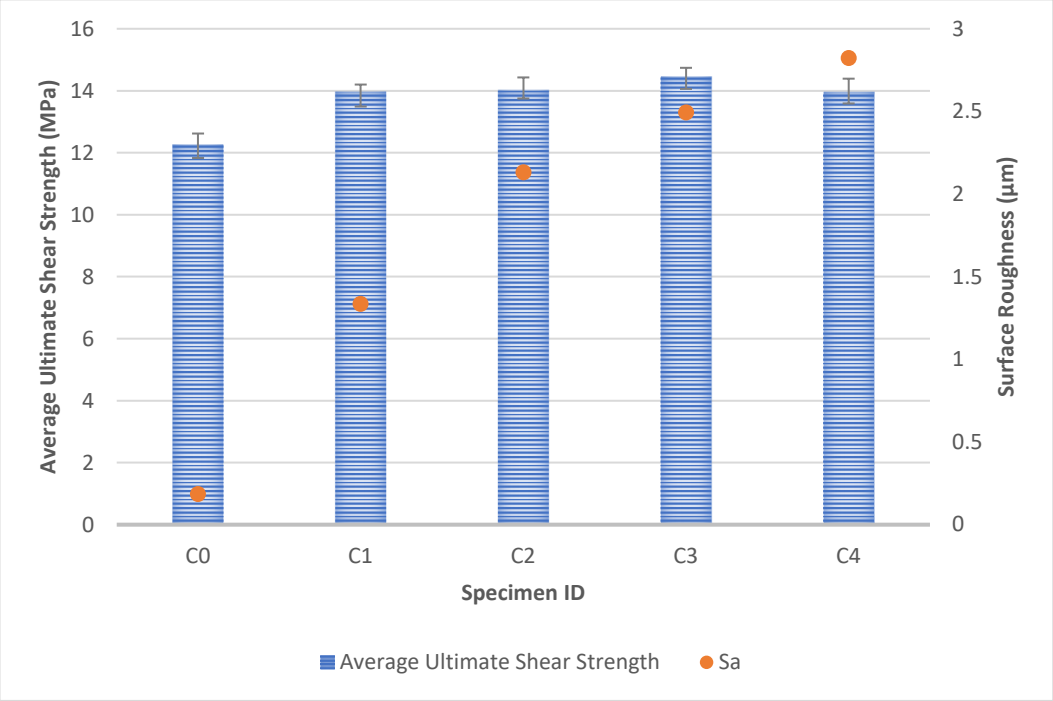

Figure 54: Average ultimate shear strength with respect to the surface roughness parameter S_a of Group C

An analogous method was employed to investigate the possible correlation between the surface roughness parameter S_p and the average ultimate shear strength of the adhesively bonded joint, as depicted in Figure 55. As a result, it is evident that there exists a direct relationship between Sp and the average ultimate shear strength.

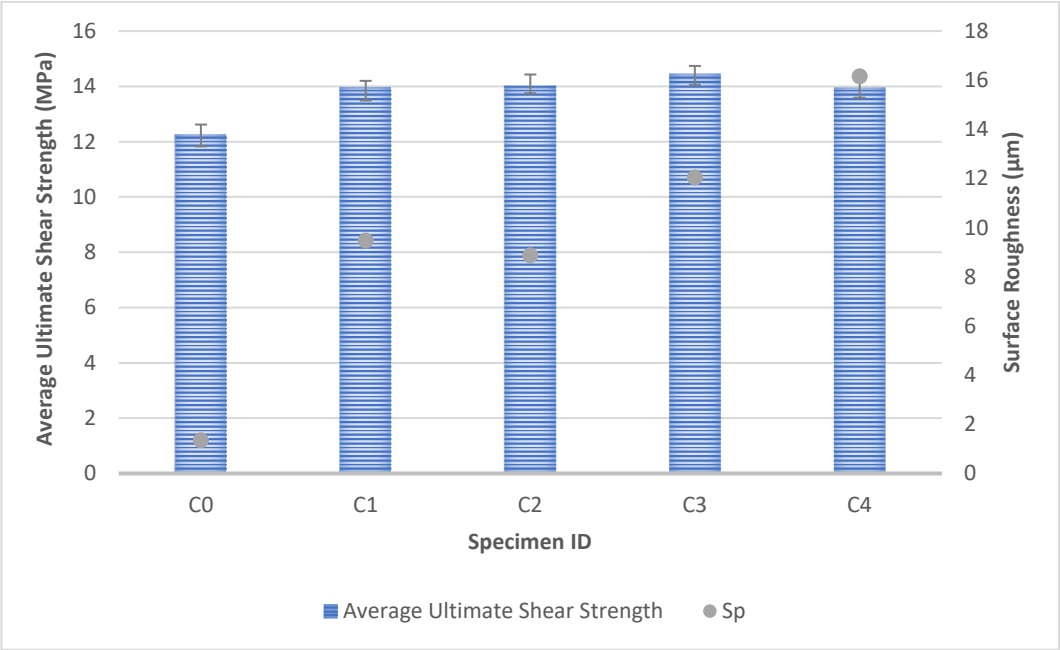

Figure 55: Average ultimate shear strength with respect to the surface roughness parameter Sp of group C

Upon analysing the surface roughness parameter S_q for group C, as depicted in Figure 56, it is evident that the trend obtained is akin to those observed for group A and group B.

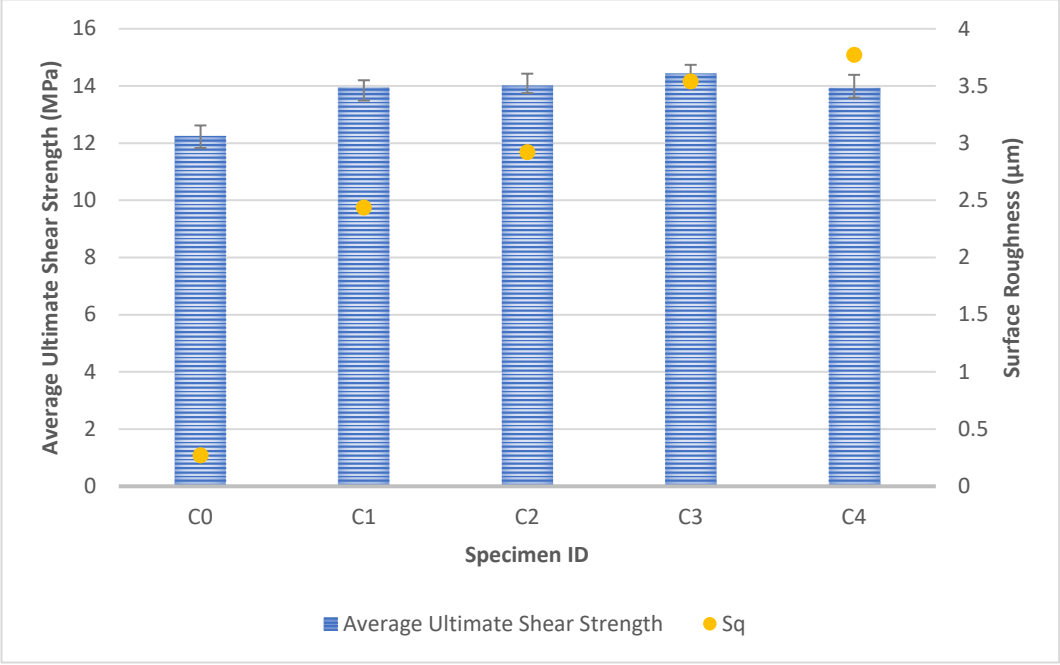

Figure 56: Average ultimate shear strength with respect to the surface roughness parameter Sq of Group C

The comparison of the selected surface roughness parameters and average ultimate shear strength for group C (expressed in percentage) can be seen in Figure 57.

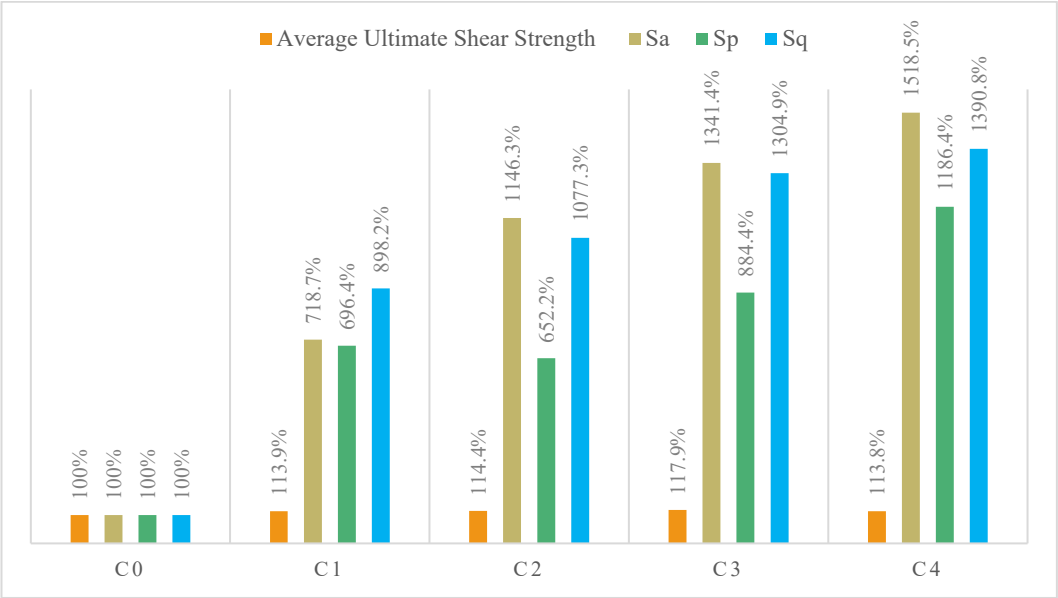

Figure 57: Comparison of resultant average ultimate shear strength of the aluminium bonded joints and selected surface roughness parameters for group C

Based on the comparison of ultimate shear strength and relative selected surface roughness parameters for group C, as shown in Figure 57, it can be inferred that the findings are consistent with the results obtained in Figures 49 and 53.

Herein, the multivariate analysis of variance (MANOVA) method was utilised to investigate the impact of surface treatments on the initial performance of the adhesively bonded joints and the measured surface roughness parameters in group C. The MANOVA analysis revealed a statistically significant difference between the experimental groups C0 and C1 when examined together for both the average ultimate shear strength and the S_a parameter, Wilks' Λ= 0.035, $F(2,7)$= 95.655, partial η^2= 0.965. An individual ANOVA was carried out for each dependent variable (i.e. surface roughness parameters) at a significance level of 0.05. The analysis indicated a statistically significant difference between C0 and C1 in terms of the average ultimate shear strength, $F(1,8) = 171.117$, $p = 0.001$, partial η^2= 0.955, with C1 (M = 13.94 MPa) scoring higher than C0 (M = 12.25 MPa). There was also a significant difference between C0 and C1 on the value of the surface roughness parameter S_a, $F(1,8) = 65.473$, $p < 0.001$, partial η^2=0.891. For the S_p, Wilks' Λ= 0.021, $F(2,7)$= 164.376, partial η^2=0.979, the MANOVA shows that there was significant difference between C0 and C1, $F(1,8) = 189.708$, $p = 0.001$, partial η^2=0.960. Lastly, the result suggests that there was a significant difference between the C0 and C1 on the value of S_q, Wilks' Λ= 0.029, $F(2,7)$=118.622, partial η^2=0.971 for the initial performance and $F(1,8) = 109.036$, $p < 0.01$, partial η^2=0.932. It has been suggested that the combination of NaOH treatment and dipodal silane coupling agent has a significant effect on the initial performance and selected surface roughness parameters of the

aluminium-to-aluminium adhesively bonded joint, as previously stated. However, it remains unclear whether the changes observed are primarily due to the etching or coupling agent deposition. Therefore, cross-analysis between variant A0 and C0 and A1 and C1 were performed to clear the doubt about this uncertainty. Both analyses suggest that dipodal silane deposition is not a driving factor for this significant effect. Based on the comparison between variants A0 and B0, it can be inferred that the application of dipodal silane coupling agent did not have any noticeable effect on the surface roughness parameters and shear strength of the bonded joints. Similarly, the comparison between variants A1 and B1 yielded similar results, supporting the conclusion that dipodal silane deposition alone cannot improve the initial performance of the adhesively bonded joints.

To investigate the impact of surface roughening prior to NaOH treatment and dipodal silane deposition on the aluminium surface, a similar statistical methodology was applied to specimens C1 to C4. Based on the MANOVA analysis, surface roughening significantly affects variants C1 to C4 when considered jointly on the variable average ultimate shear strength and the measured value of S_a, Wilks' Λ=0.335, $F(6,30)$=3.642, partial η^2=0.421. Hence, individual analysis of variance (ANOVA) was performed for each dependent variable (i.e. surface roughness parameters), and the significance level for each ANOVA was set at alpha=0.05. Interestingly, there was no significant difference between C0 and C4 on average ultimate shear strength, $F(1,8) = 1.211$, $p = 0.338$, partial $\eta^2 = 0.85$. However, the result from the ANOVA analysis indicates a significant effect of surface roughening of aluminium prior to NaOH treatment and dipodal silane deposition on S_a, $F(1,8) = 9.263$, $p = 0.001$, partial $\eta^2 = 0.635$. For S_p, Wilks' $\Lambda = 0.416$, $F(6,30) = 2.750$, partial η^2=0.355, the MANOVA shows that there was significant difference between C0 and C1, $F(1,8) = 5.107$, $p = 0.011$, partial η^2=0.489. Lastly, the result suggests a significant difference between the C0 and C1 on the value of S_q, Wilks' Λ= 0.428, $F(6,30)$=2.640, partial η^2=0.345 for the initial performance and $F(3,16) = 5.955$, $p = 0.006$, partial η^2=0.528.

By using a similar approach, the potential correlation between the selected surface roughness parameters and the average ultimate strength for group D was investigated. The obtained results, as presented in Figure 58, demonstrate a similar trend to those obtained for other groups. Specifically, an increase in the surface roughness parameter S_a up to 2.5µm is observed to result in an increase in the ultimate shear strength, followed by a decrease for S_a values beyond 2.5µm. Furthermore, it is worth noting that the gap between the S_a value and the ultimate strength is at its highest compared to the other specimens in groups A, B, and C.

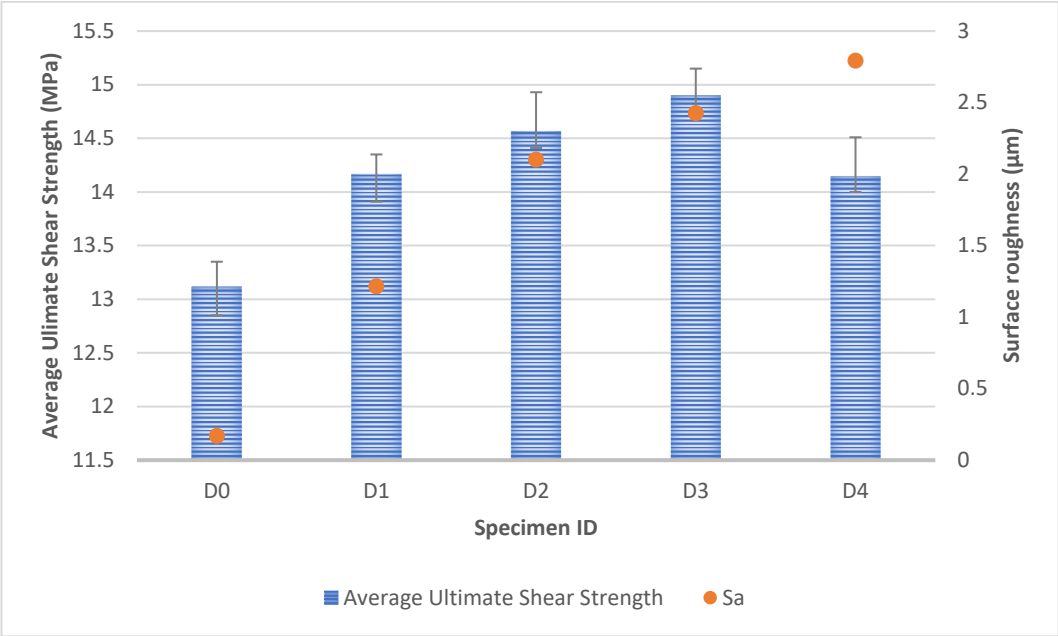

Figure 58: Average ultimate shear strength with respect to the surface roughness parameter S_a of Group D

In contrast, Figure 59 indicates that the average ultimate shear strength of group D increases with increasing values of the surface roughness parameter S_p up to 12µm, beyond which it begins to decrease. It is noteworthy that the drop in shear strength for group D beyond the threshold S_p value is more significant than other groups in the same variant.

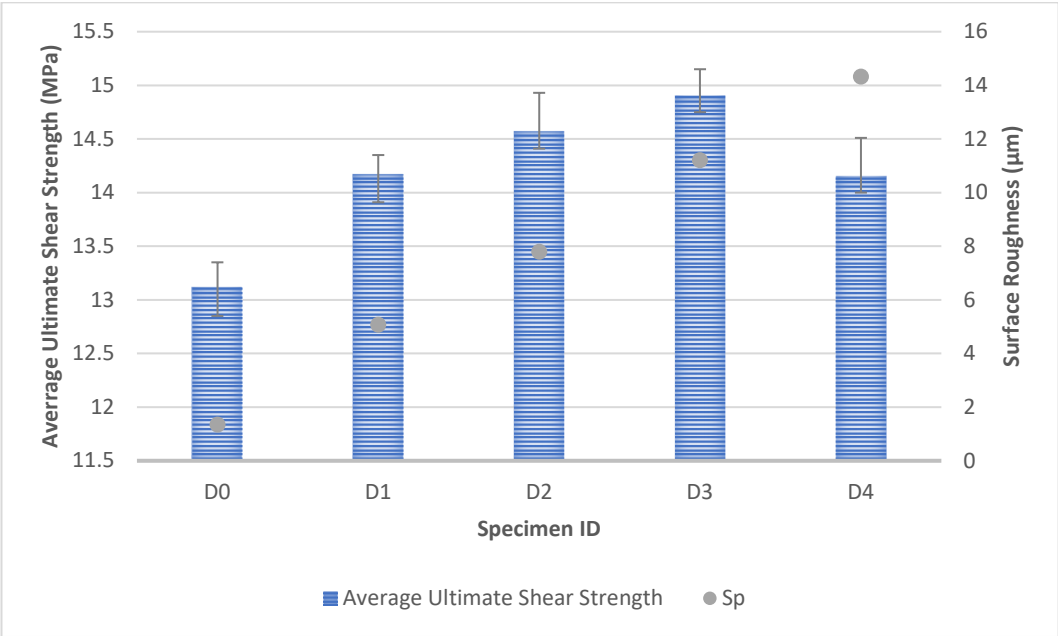

Figure 59: Average ultimate shear strength with respect to the surface roughness parameter Sp of Group D

Based on the data presented in Figure 60, it is evident that maintaining the surface roughness parameter Sq within the range of 3.27µm can lead to optimal shear strength for Group D. However, excessive surface roughening can have a negative impact on the

initial performance of the adhesively bonded joints, as indicated by a reduction in shear strength for S_q values beyond 3.27µm. This trend is consistent with the results observed in other variants within the A, B, and C groups.

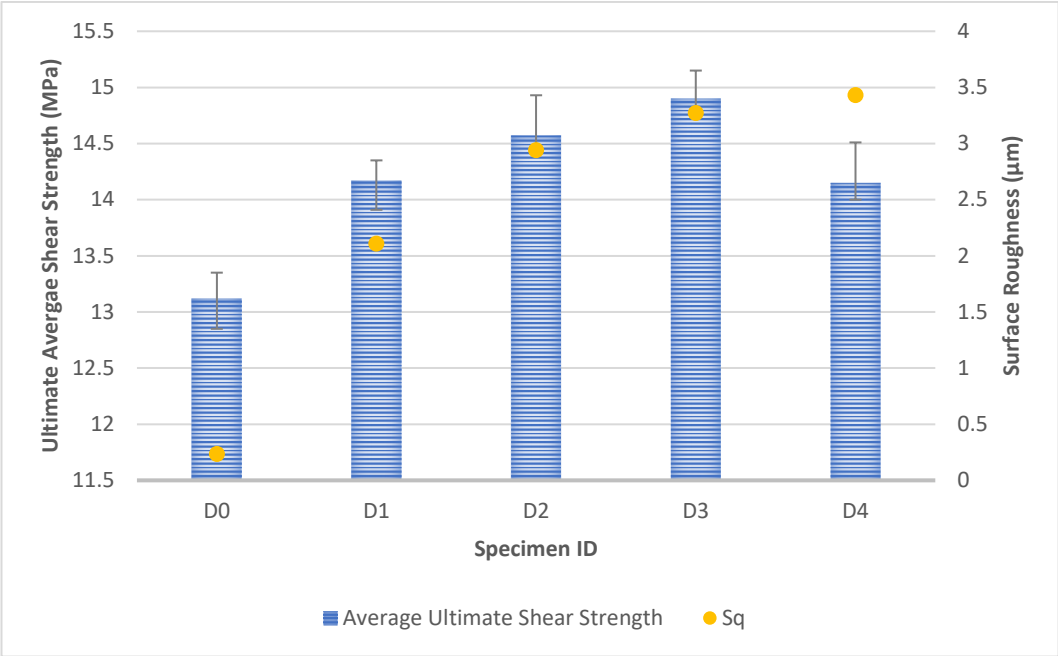

Figure 60: Average ultimate shear strength with respect to the surface roughness parameter Sq of Group D

The comparison of selected surface roughness parameters and average ultimate shear strength for group D (expressed in percentage) is provided in Figure 61.

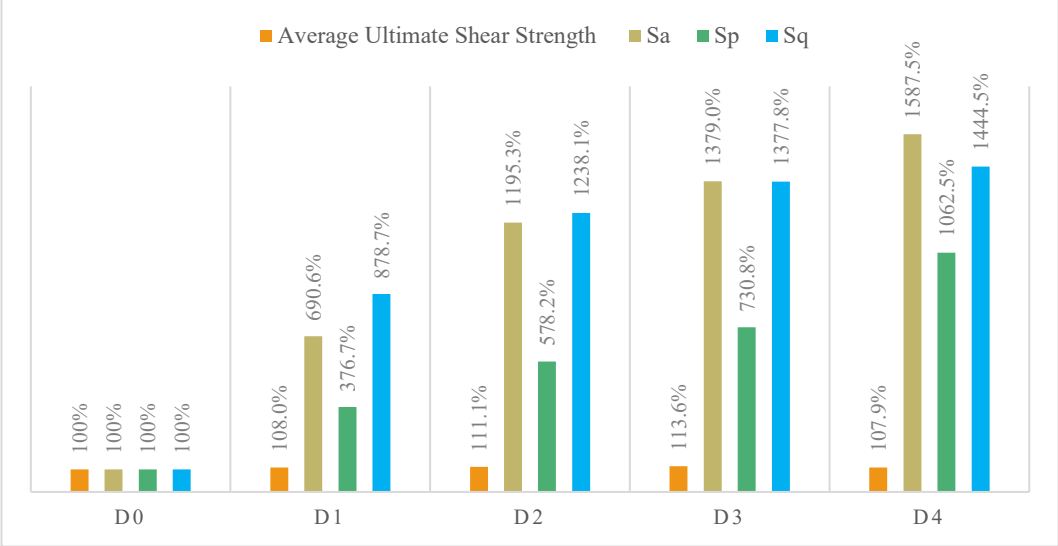

Figure 61: Comparison of resultant average ultimate shear strength of the aluminium bonded joints and selected surface roughness parameters for Group D

Upon evaluation of the results presented in Figure 61, it can be observed that the relationship between the selected surface roughness parameters and average ultimate shear strength for Group D follows a similar trend as the relationships observed in

Figures 49, 53, and 57. The Pearson correlation coefficient between the surface roughness parameters S_a, S_p, S_q, and the average ultimate shear strength of the bonded joint for Variant D0 and D1 are 0.84, 0.71, and 0.92, respectively. The findings suggest that there is a strong positive correlation between the selected surface roughness parameters and the initial performance of adhesively bonded joints. Hence, it can be concluded that increasing the surface roughness parameters using a combination of NaOH treatment and zirconate coupling agents can lead to stronger bonded joints. Moreover, the study highlights that surface roughening before NaOH treatment and zirconate deposition also positively correlates with the initial performance of the adhesively bonded joints. This correlation is supported by the Pearson correlation coefficients for surface roughness parameters S_a, S_p, and S_q. The average ultimate shear strength of the bonded joint between variants D1 and D4 shows coefficients of 0.45, 0.15, and 0.45, respectively.

To investigate the impact of surface treatments on the initial performance of adhesively bonded joints and surface roughness parameters, the multivariate analysis of variance (MANOVA) method was employed for group D. The results of the MANOVA indicate a significant difference between D0 and D1 in terms of their average ultimate shear strength and S_a when considered jointly as variables, Wilks' Λ= 0.071, $F(2,7)$= 45.753, partial η^2= 0.929. For each dependent variable (i.e. surface roughness parameters), a separate ANOVA was carried out with a significance level of 0.05. The results indicate a significant disparity between the average ultimate shear strength of D0 and D1, $F(1,8) = 77.689$, $p = 0.001$, partial η^2= 0.907, with D1 (M = 14.17 MPa) scoring higher than D0 (M = 13.12MPa). There was also a significant difference between A0 and A1 on the value of the surface roughness parameter S_a, $F(1,8) = 28.827$, $p < 0.001$, partial η^2=0.783. For the S_p, Wilks' Λ= 0.062, $F(2,7)$= 53.359, partial η^2=0.938, the MANOVA shows that there was significant difference between D0 and D1, $F(1,8) = 14.256$, $p = 0.005$, partial η^2=0.641. Lastly, the result suggests that there was a significant difference between the D0 and D1 on the value of S_q, Wilks' Λ= 0.054, $F(2,7)$=61.052, partial η^2=0.946 for the initial performance and $F(1,8) = 76.968$, $p < 0.01$, partial η^2=0.906. In the previous discussion, it was suggested that the NaOH treatment in combination with zirconate coupling agent influence the initial performance and selected surface roughness parameters. However, it was unclear whether the observed changes were driven by the etching or the coupling agent deposition. To address this uncertainty, cross-analysis was conducted between variant A0 and D0 and A1 and D1. The findings from both analyses indicated that zirconate deposition was not the primary factor contributing to the significant effect. Specifically, the comparison between A0 and D0 showed no significant effect of zirconate deposition on surface roughness parameters and shear strength of the bonded joints. Similarly, the comparison between A1 and D1 confirmed

this statement. Therefore, it can be concluded that zirconate deposition alone cannot enhance the initial performance of the adhesively bonded joints. These findings suggest that the observed changes are primarily attributed to the NaOH treatment, which plays a significant role in improving the surface roughness and initial performance of adhesively bonded joints.

A similar statistical analysis was conducted on variants D1, D2, D3, and D4 to examine the impact of surface roughening on the aluminium surface before NaOH treatment and zirconate coupling agent deposition on the selected surface roughness parameters and initial performance of the adhesively bonded joint. Referring to the results from the MANOVA analysis, it can be noted that there is a significant difference between specimen D1 to D4 when considered jointly on the variables average ultimate shear strength and recorded value for S_a, Wilks' Λ= 0.385, $F(6,30)=3.056$, partial $\eta^2=0.379$. In order to evaluate the effect of each dependent variable (i.e. surface roughness parameters), separate ANOVA analyses were conducted for each of them. Each ANOVA was evaluated at an alpha level of 0.05 to determine statistical significance. There was no significant difference between D1 to D4 on average ultimate shear strength, $F(3,16) =1.387$, $p = 0.283$, partial $\eta^2= 0.206$. However, there was a significant difference between D1 to D4 on the value of the surface roughness parameter S_a, $F(3,16) = 7.292$, $p = 0.003$, partial $\eta^2=0.578$.

However, the aforementioned result does not indicate where difference lies. To determine the difference between the means of selected specimen groups, the least significant difference (LSD) and Bonferroni post-hoc tests were performed. According to the table, the LSD post-hoc method did not reveal any significant difference in average ultimate shear strength. However, the Bonferroni test produced results that are consistent with those of the LSD method. Thus, the LSD method's results for ultimate shear strength between selected specimens are considered satisfactory. Based on the results given for S_a values by LSD analysis, a significant difference existed between variant D1 to D4, where the reference point is D1. Again, the agreement between the result between LSD and Bonferroni can be considered satisfactory. For the S_p, Wilks' Λ= 0.40, $F(6,30)=2.909$, partial $\eta^2 = 0.368$, the MANOVA shows that there was a significant difference between selected specimens, $F(3,16) =1.367$, $p = 0.009$, partial $\eta^2=0.505$. As indicated, the significance is found between the variant D3 and D4 in comparison to D1. Likewise, the Bonferroni result agrees with the LSD, and it can be concluded that the obtained results for S_p using MANOVA and LSD are satisfactory. Lastly, referring to the MANOVA analysis of surface roughness parameter S_q, it can be concluded that there was no significant difference between selected specimens on total surface free energy, Wilks' Λ=

0.440, $F(6,30)=2.536$, partial $\eta^2=0.337$ for the initial performance and $F(3,16) = 5.889$, $p = 0.007$, partial $\eta^2=0.525$. Similarly, the result for surface roughness parameter S_q shows a similar trend as surface roughness parameter S_a with a satisfactory outcome for LSD and Bonferroni analysis.

4.4.4 The correlation between surface energy and its components and the initial performance of bonded joints

This section aims to establish a correlation between the surface energy of the aluminium surface, including its polar and dispersive components, after undergoing selected surface treatments and the average ultimate shear strength of adhesively bonded joints. As discussed in the previous chapter, the energy characteristics of the treated surface were determined by measuring the total surface energy, polar component, and dispersive component. The polished specimens (A0-B0-C0-D0) were used as a reference point for interpreting the results of both surface energy parameters and average ultimate shear strength. All treated specimens were analysed systematically to determine the driving factor for the improved initial performance of the adhesively bonded joints using PUR adhesive.

Figures 62-64 present the outcomes of the average ultimate shear strength of the bonded joint in group A, in relation to the recorded polar component, dispersive component, and total surface free energy. The assessment of the results indicates significant associations between the total surface free energy and its components, as well as the ultimate shear strength that was recorded. The existence of such associations can be defined by employing correlation coefficient (r) or (ρ).

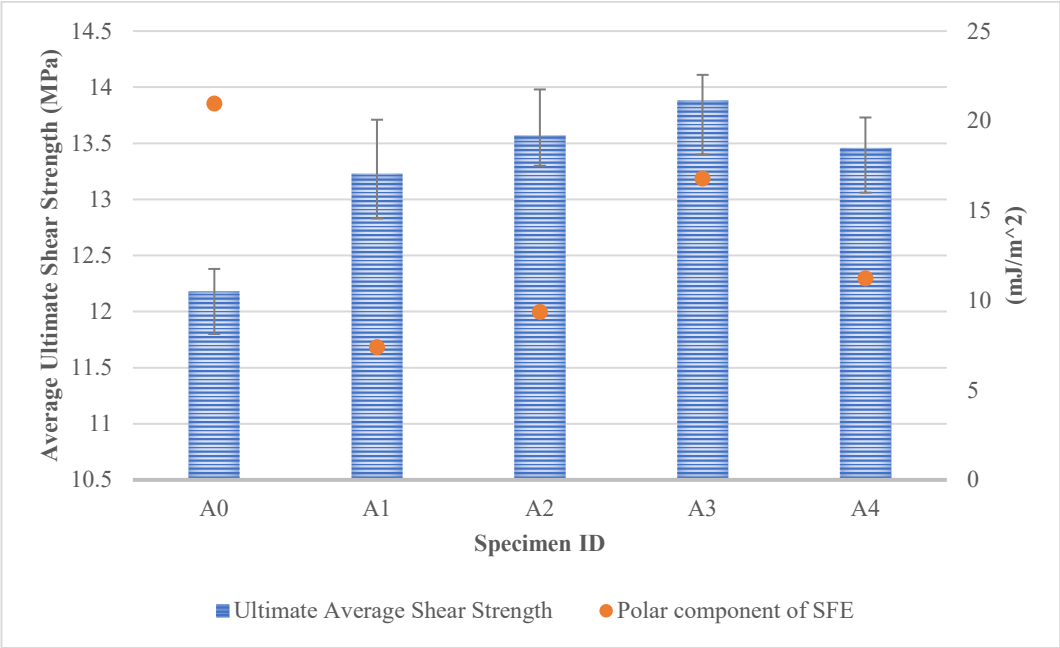

Figure 62: Average ultimate shear strength with respect to the polar component of group A

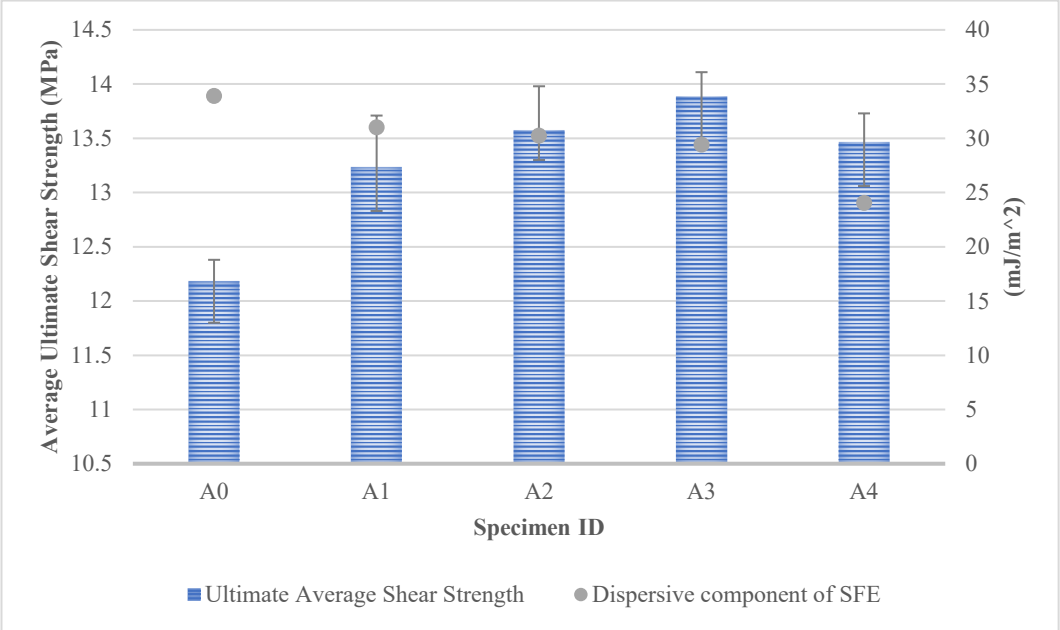

Figure 63: Average ultimate shear strength with respect to the dispersive component of group A

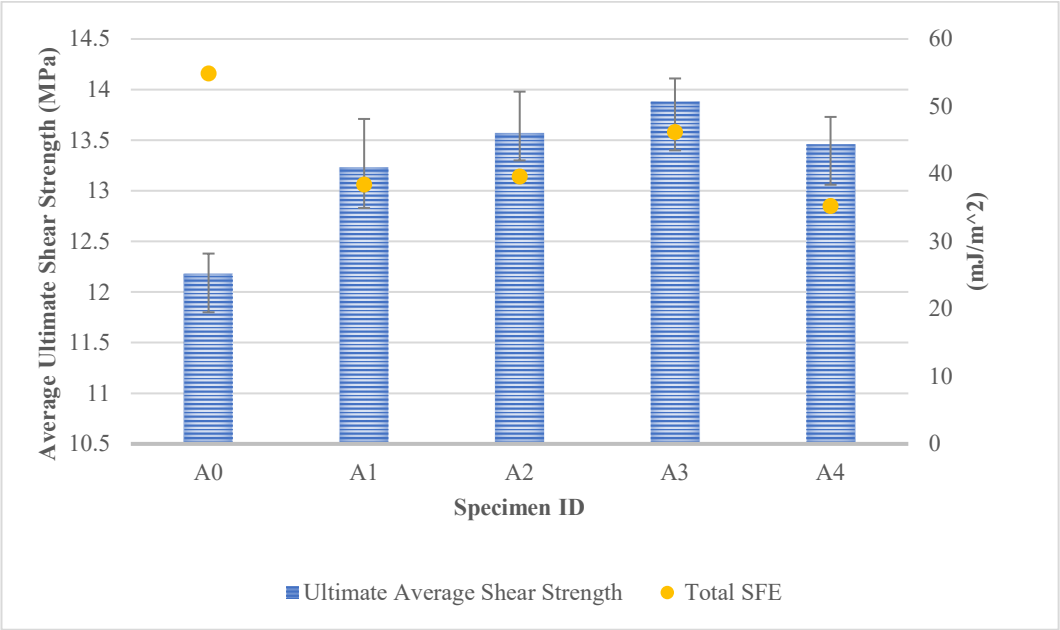

Figure 64: Average ultimate shear strength with respect to the total surface free energy of group A

Based on the comparison between A0 and A1, it can be inferred that there is a negative correlation between the initial performance of adhesively bonded joints and the polar component, dispersive component, and total surface free energy. The Pearson correlation coefficient values for these relationships are -0.55, -0.41, and -0.56, respectively, which indicates that an increase in surface energy and its components results in a decrease in average ultimate shear strength. These findings are consistent with the results presented in Section 4.5.2, which compare the correlation between various surface roughness parameters and ultimate shear strength. These results suggest that surface roughness parameters are more crucial to the initial performance of adhesively bonded joints using PUR adhesive in the aluminium-to-aluminium system than total surface energy and its components. Overall, NaOH treatment has been shown to improve the initial adhesion performance of aluminium and PUR.

The effect of surface treatments on the initial performance of adhesively bonded joints and the value of surface energy and its components of treated aluminium surfaces in Group A was examined using the multivariate analysis of variance (MANOVA) method. The results of the MANOVA analysis revealed a significant difference between A0 and A1 in terms of the average ultimate shear strength and polar component when considered jointly., Wilks' Λ= 0.081, $F(2,7)$=39.553, partial η^2=0.919. A separate ANOVA was conducted for each dependent variable (i.e. surface free energy and its components), with each one evaluated at an alpha level of 0.05. There was a significant difference between A0 and A1 on average ultimate shear strength, $F(1,8) = 7.586$, $p = 0.025$, partial η^2=0.487, with A1 ($M = 13.23$) scoring higher than A0 ($M = 12.18$). There

was also a significant difference between A0 and A1 on polar surface energy components, $F(1,8) = 79.518$, $p < 0.01$, partial $\eta^2=0.909$. For the dispersive component, Wilks' $\Lambda= 0.346$, $F(2,7)=6.63$, partial $\eta^2=0.654$, the MANOVA shows that there was no significant difference between A0 and A1, $F(1,8) = 4.899$, $p = 0.58$, partial $\eta^2=0.38$. This can be associated with a relatively low Pearson correlation coefficient. Lastly, it was concluded that there was a significant difference between the A0 and A1 on total surface free energy, Wilks' $\Lambda= 0.928$, $F(2,7)=45.342$, partial $\eta^2=0.928$ for the initial performance and $F(1,8) = 83.607$, $p < 0.01$, partial $\eta^2=0.913$.

A comparison between variants A1 to A4 in group A was conducted to investigate the influence of surface roughening on the aluminium surface prior to NaOH treatment and its effect on the initial performance of the adhesively bonded joints. The Pearson correlation coefficient was used to determine the relationship between the initial performance of the adhesively bonded joint and the polar component, dispersive component, and total surface free energy of these variants. The analysis revealed that the coefficient values between the initial performance of the adhesively bonded joint and polar component, dispersive component, and total surface free energy are 0.46, -0.17, and 0.28, respectively. This result indicates a new relationship between the total surface free energy and its component with the initial performance of the adhesively bonded joints. An increase in polar components led to an increase in the initial performance of the bonded joints. Moreover, the low correlation value between the dispersive component and initial performance suggests that the effect of dispersive components on the adhesion performance of the bonded joints is negligible.

As a result, it can be inferred that the surface roughening of the aluminium did not have a direct impact on the initial performance of the adhesively bonded joints. However, it could enhance the efficacy of the NaOH treatment by providing a greater surface area for the etching solution and aluminium surface.

A multivariate analysis of variance (MANOVA) was conducted on specimens A1 to A4 to investigate the effect of surface roughening of the aluminium substrate prior to NaOH treatment on surface energy and its components. The results from the MANOVA analysis revealed a significant difference between specimens A1 to A4 when jointly considering the variables of average ultimate shear strength and polar component, Wilks' $\Lambda= 0.375$, $F(6,30)=3.161$, partial $\eta^2=0.387$. This statistical analysis provides evidence of the influence of surface roughening on the surface energy and adhesion properties of the aluminium substrate in the context of adhesively bonded joints. A separate ANOVA was conducted for each dependent variable (i.e. surface free energy and its components), with each ANOVA evaluated at an alpha level of 0.025. There was no significant difference

between selected group A specimens on average ultimate shear strength. However, there was a significant difference between the identical specimens on polar components of treated aluminium surface, $F(3,16) = 5.912$, $p = 0.006$, partial $\eta^2=0.526$. For the dispersive component, Wilks' $\Lambda= 0.267$, $F(6,30)=4.681$, partial $\eta^2=0.484$, the MANOVA shows a significant difference between selected specimens from group A, $F(3,16) = 6.549$, $p = 0.004$, partial $\eta^2=0.551$. Therefore, it can be concluded that there was a significant difference between selected specimens from group A on total surface free energy, Wilks' $\Lambda= 0.363$, $F(6,30)=3.302$, partial $\eta^2=0.398$ for the initial performance and $F(3,16) = 4.654$, $p = 0.016$, partial $\eta^2=0.466$.

Figures 65-67 display the recorded average ultimate shear strength of the adhesively bonded joints of group B, in relation to the polar component, dispersive component, and total surface free energy. These figures illustrate a clear correlation between the energy components of the treated aluminium surface and the initial performance of the bonded joints.

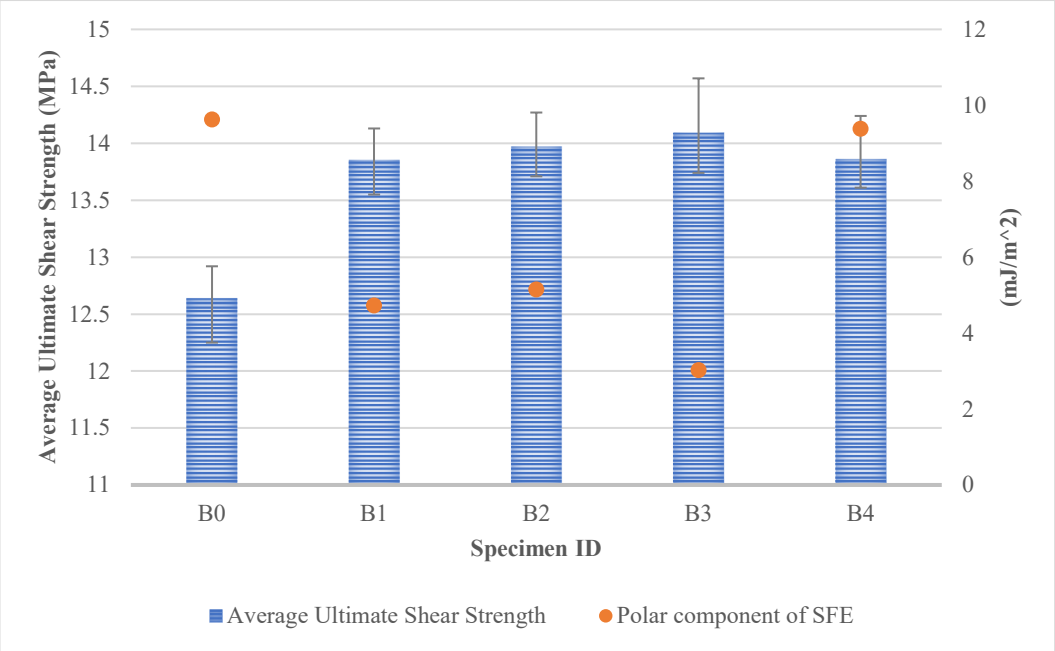

Figure 65: Average ultimate shear strength with respect to the polar component of group B

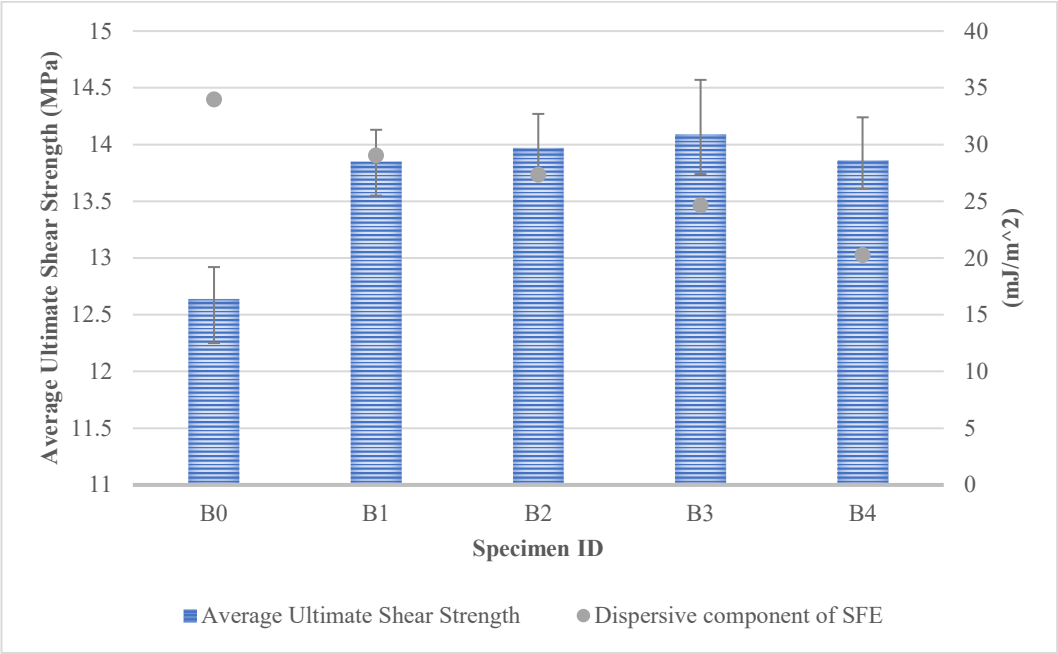

Figure 66: Average ultimate shear strength with respect to the dispersive component of group B

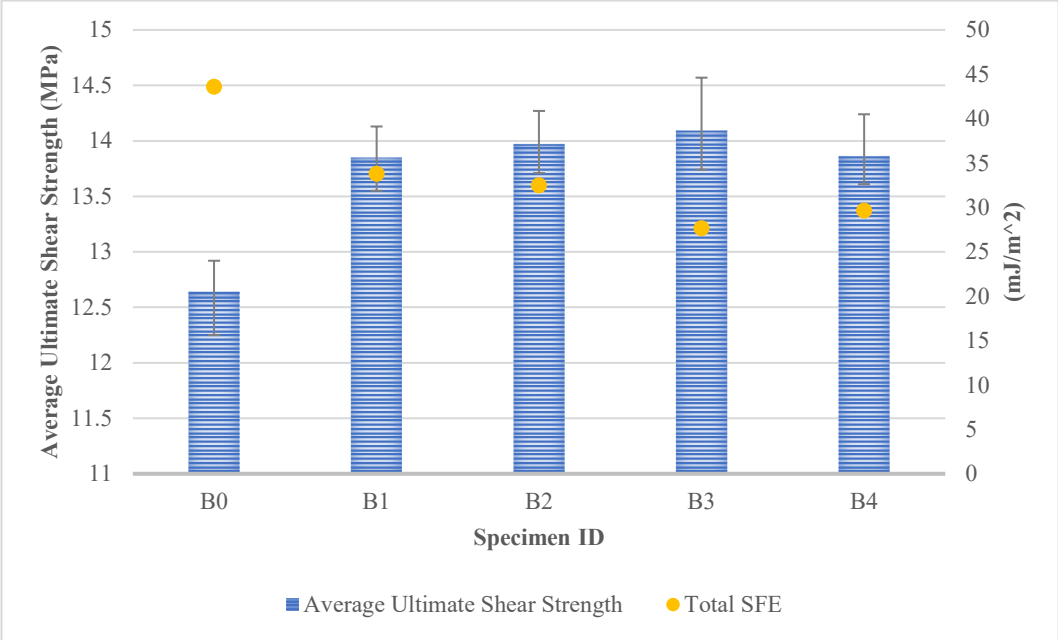

Figure 67: Average ultimate shear strength with respect to the total surface free energy of group B

By comparing the surface free energy and its components with the average ultimate shear strength of the adhesively bonded joints after the application of NaOH treatment and silane deposition on a polished aluminium surface, it can be asserted that a strong negative correlation exists between the initial adhesion performance of the bonded joints and the polar component, dispersive component, and total surface free energy. This is supported by the Pearson correlation coefficient values of -0.61, -0.76, and -0.75, respectively. The increase in surface free energy and its components can lead to a weaker initial performance of the adhesively bonded joints, which explains the negative

correlation. Thus, it can be concluded that the negative correlation between the surface energy component and the initial performance of the adhesively bonded joints still falls under the rose petal effect, as seen in the results for group A.

Based on the MANOVA analysis, it was observed that there is a significant difference between B0 and B1 concerning the average ultimate shear strength and the polar component of the surface free energy when considered together, Wilks' Λ= 0.04, $F(2,7)$=84.558, partial η^2=0.960. or each dependent variable (i.e. surface free energy and its components), a separate ANOVA was performed with an alpha level of 0.05. The results show a significant difference between B0 and B1 on the average ultimate shear strength, $F(1,8) = 89.252$, p <0.001, partial η^2=0.918, with B1 (M = 13.85) scoring higher than A0 (M = 12.64). There was also a significant difference between B0 and B1 on polar surface energy components, $F(1,8) = 60.152$, $p = 0.012$, partial η^2=0.587. For the dispersive component, Wilks' Λ= 0.052, $F(2,7)$=63.778, partial η^2=0.948, the MANOVA shows that there was significant difference between B0 and B1, $F(1,8) = 19.983$, p = 0.002, partial η^2=0.714. Ultimately, it was concluded that there was a significant difference between the B0 and B1 on total surface free energy, Wilks' Λ= 0.031, $F(2,7)$=107.822, partial η^2=0.969 for the initial performance of adhesively bonded joint and $F(1,8) = 23.618$, $p = 0.01$, partial η^2=0.747.

Conversely, the effect of surface roughening on the aluminium surface before NaOH treatment and silane deposition was evaluated by comparing variants B1 to B4 regarding the initial performance of adhesively bonded joints. The Pearson correlation coefficient analysis showed a negligible correlation between the polar component of variants B1 to B4 and the ultimate shear strength of the bonded joint, as evidenced by the correlation value of -0.07. However, there was a relatively weak positive correlation between the dispersive and total surface free energy and initial performance of the bonded joint, as indicated by Pearson correlation coefficients of 0.16 and 0.11, respectively. These results suggest that surface roughening may have a limited effect on the adhesion performance of the bonded joints in this context.

Corresponding statistical analysis occurred between specimens B1, B2, B3 and B4 to identify the influence of surface roughening of the aluminium prior to NaOH treatment and silane deposition on surface energy and its components. Referring to the results from MANOVA analysis, it can be observed that a significant difference between specimen B1 to B4 when considered jointly on the variables average ultimate shear strength and polar component, Wilks' Λ= 0.337, $F(6,30)$=3.608, partial η^2=0.419Each dependent variable (i.e. surface free energy and its components) underwent a separate ANOVA, with an alpha level of 0.05. The results revealed no significant difference in average ultimate

shear strength among the selected group B specimens. However, there was a significant difference between the identical specimens concerning the polar components of the treated aluminium surface, $F(3,16) = 6.37$, $p = 0.005$, partial $\eta^2=0.544$. For the dispersive component, Wilks' $\Lambda= 0.124$, $F(6,30)=9.222$, partial $\eta^2=0.648$, the MANOVA shows that there was a significant difference between selected specimens from group A, $F(3,16) = 23.363$, $p < 0.001$, partial $\eta^2=0.814$. Therefore, it can be concluded that there was a significant difference between selected specimens from group A on total surface free energy, Wilks' $\Lambda= 0.421$, $F(6,30)=2.703$, partial $\eta^2=0.351$ for the initial performance and $F(3,16) = 3.072$, $p = 0.048$, partial $\eta^2=0.366$.

Based on the data presented in Figure 68-70, it is observed that dipodal silane-treated specimens in group C and silane-treated samples in group B exhibit a similar trend. It becomes evident that the initial performance of the aluminium-to-aluminium bonded joints is dependent on the surface energy and its components.

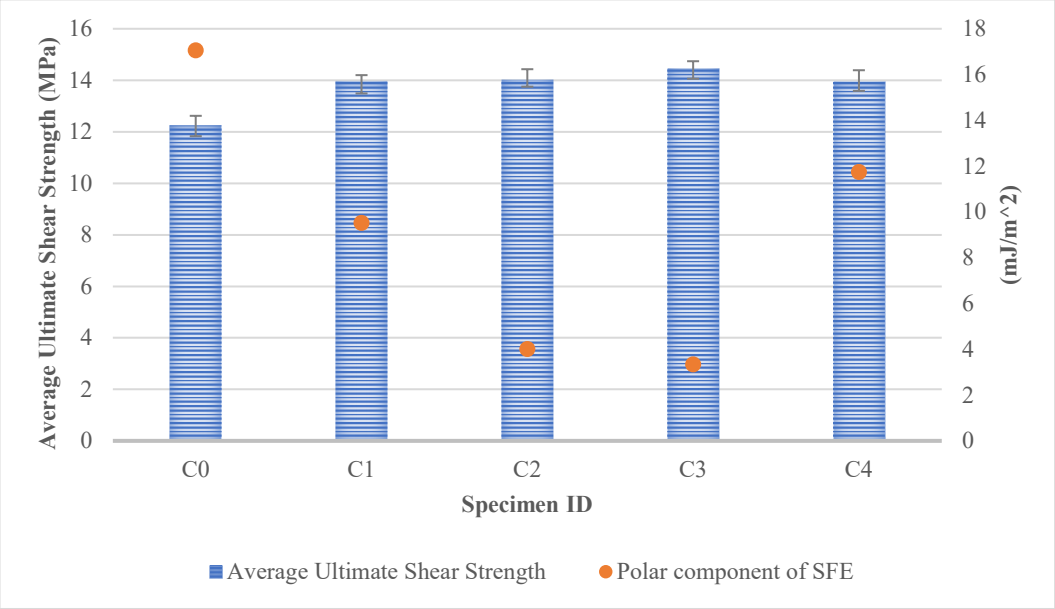

Figure 68: Average ultimate shear strength with respect to the polar component of group C

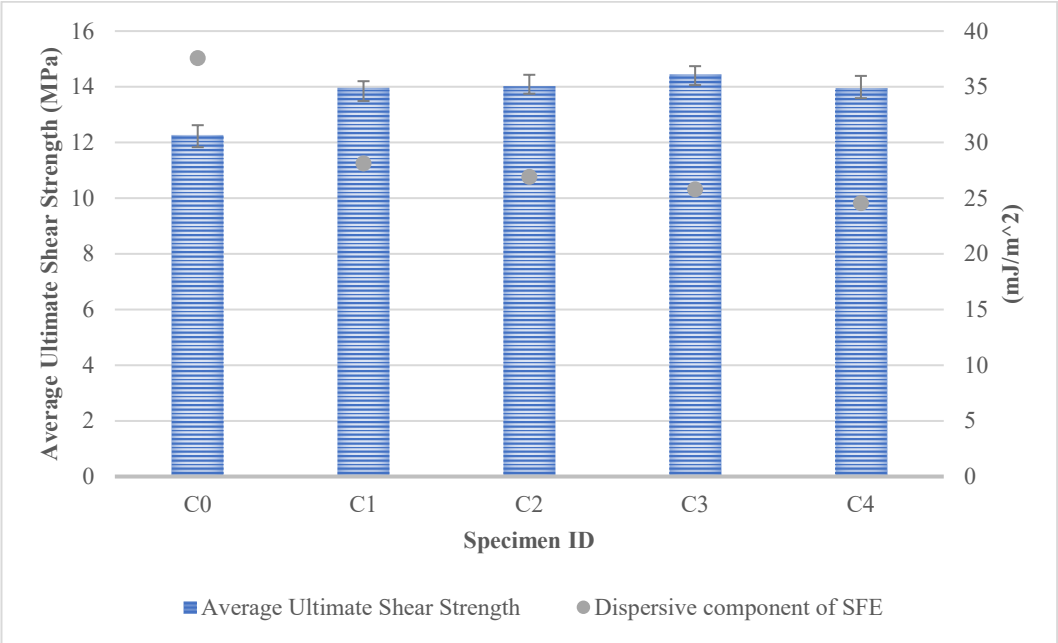

Figure 69: Average ultimate shear strength with respect to the dispersive component of group C

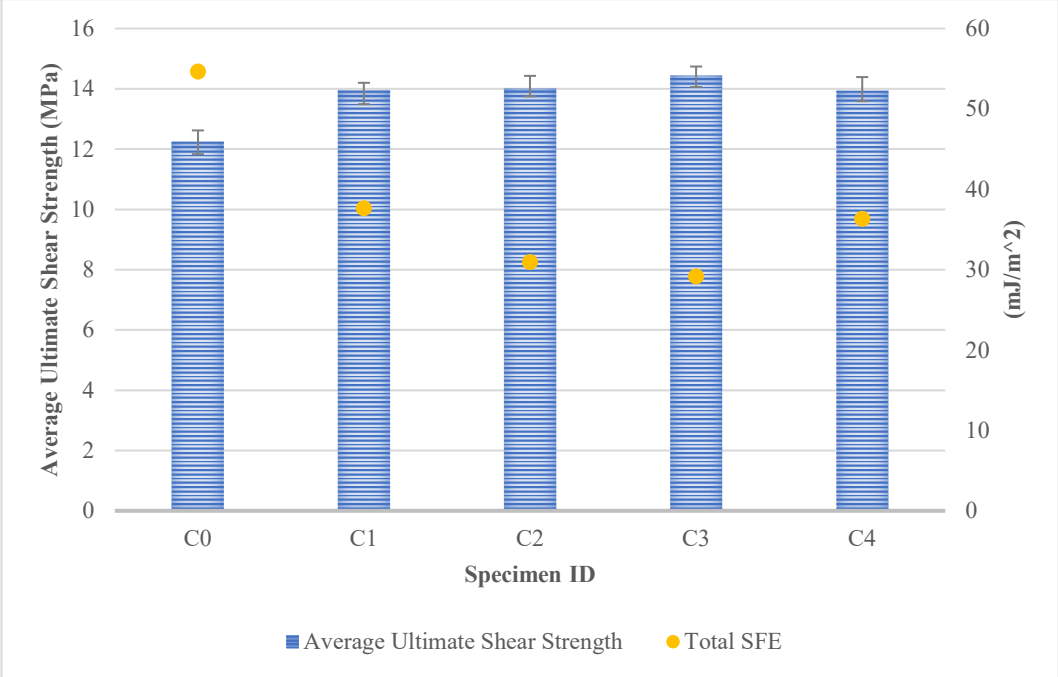

Figure 70: Average ultimate shear strength with respect to the total surface free energy of group C

The results of the analysis reveal a strong negative correlation between the polar component, dispersive component, and total surface free energy of specimens in group C, and the initial performance of the adhesively bonded joints, after the combination of NaOH treatment and dipodal silane deposition on polished aluminium surfaces. The Pearson correlation coefficients are -0.62, -0.96, and -0.90, respectively. The influence of the selected coupling agent, dipodal silane deposition, can explain this finding, as it was previously established that this agent effectively decreases the surface energy of the

aluminium surface. Although the comparison between C0 and C1 variants includes the influence of NaOH treatment, this correlation can also be attributed to the rose petal effect.

The MANOVA analysis results reveal a statistically significant difference between the average ultimate shear strength and the polar component of the surface free energy when C0 and C1 variants are considered together, Wilks' Λ= 0.04, $F(2,7)$=83.688, partial η^2=0.960. Each dependent variable (i.e. surface free energy and its components) was subjected to a separate ANOVA with an alpha level of 0.05 for evaluation. The analysis indicated that there was a statistically significant difference in the average ultimate shear strength between C0 and C1, $F(1,8) = 171.117$, $p < 0.001$, partial η^2=0.955, with C1 (M = 13.94) scoring higher than C0 (M = 12.25). There was also a significant difference between C0 and C1 on polar surface energy components, $F(1,8) = 6.268$, $p = 0.037$, partial η^2=0.439. For the dispersive component, Wilks' Λ= 0.039, $F(2,7)$=87.127, partial η^2=0.961, the MANOVA shows that there was significant difference between C0 and C1, $F(1,8) = 109.247$, $p < 0.001$, partial η^2=0.932. Ultimately, it was concluded that there was a significant difference between the C0 and C1 on total surface free energy, Wilks' Λ= 0.035, $F(2,7)$=95.788, partial η^2=0.965 for the initial performance of adhesively bonded joint and $F(1,8) = 46.054$, $p < 0.01$, partial η^2=0.852.

In addition, the study investigated the impact of surface roughening of the aluminium surface prior to NaOH treatment and dipodal silane deposition on the initial performance of the adhesively bonded joint by comparing the variants C1 to C4. The results from the Pearson correlation coefficient analysis suggest that a weak to moderate negative correlation exists between the surface free energy and its components and the initial performance of the bonded joint. The correlation coefficients between the polar component, dispersive component, and total surface free energy with the initial performance of the bonded joints are -0.32, -0.18 and -0.42, respectively.

Corresponding statistical analysis was performed between specimens C1, C2, C3 and C4 to identify the influence of surface roughening of the aluminium prior to NaOH treatment and dipodal silane deposition on surface energy and its components. Referring to the results from MANOVA analysis, it is apparent that a significant difference between specimen C1 to C4 when considered jointly on the variables average ultimate shear strength and polar component, Wilks' Λ=0.399, $F(6,30)$=2.918, partial η^2=0.368. Each dependent variable (i.e. surface free energy and its components) was subjected to a separate ANOVA analysis with an alpha level of 0.05. The results showed no significant difference between the chosen group C specimens concerning their average ultimate shear strength. However, there was a significant difference between the identical specimens

when it comes to the polar components of the treated aluminium surface, $F(3,16) = 5.988$, $p = 0.006$, partial $\eta^2=0.529$. For the dispersive component, Wilks' $\Lambda= 0.628$, $F(6,30)=1.307$, partial $\eta^2=0.207$, the MANOVA shows that there was no significant difference between selected specimens from group C, $F(3,16) =1.810$, $p = 0.186$, partial $\eta^2=0.253$. However, referring to the MANOVA analysis of surface free energy, it can be concluded that there was a significant difference between selected specimens from group C on total surface free energy, Wilks' $\Lambda= 0.439$, $F(6,30)=2.544$, partial $\eta^2=0.337$ for the initial performance and $F(3,16) = 5.66$, $p = 0.008$, partial $\eta^2=0.515$.

Figures 71-73 illustrate the average ultimate shear strength of the aluminium-to-aluminium adhesively bonded joint concerning the variations in the polar component, dispersive component, and total surface free energy for group D. The data presented in these figures highlight a significant correlation between the value of total surface free energy and its components in this group and the initial performance of the bonded joints. Additionally, it is evident that the changes observed due to zirconate deposition on the polished and treated aluminium surface energy and polar component are distinct from those observed in groups B and C.

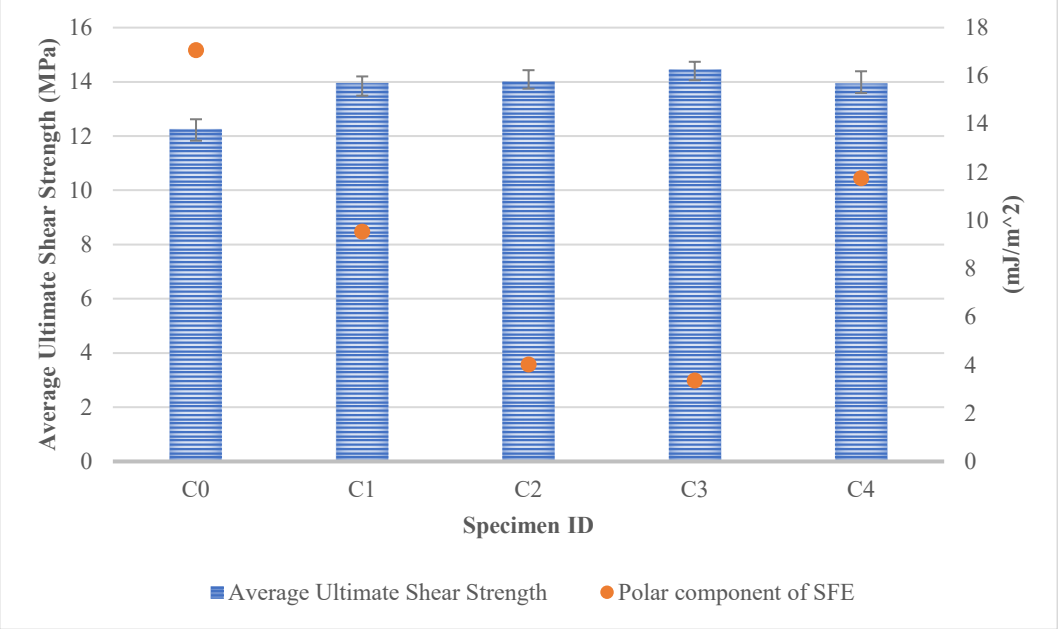

Figure 71: Average ultimate shear strength with respect to the total surface free energy of group C

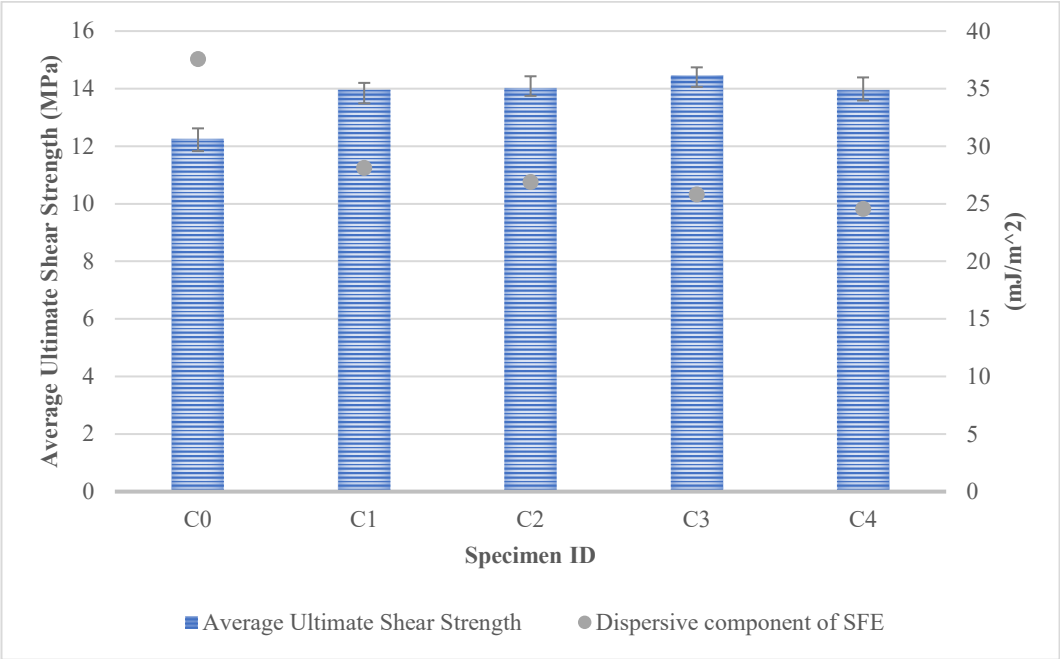

Figure 72: Average ultimate shear strength with respect to the total surface free energy of group C

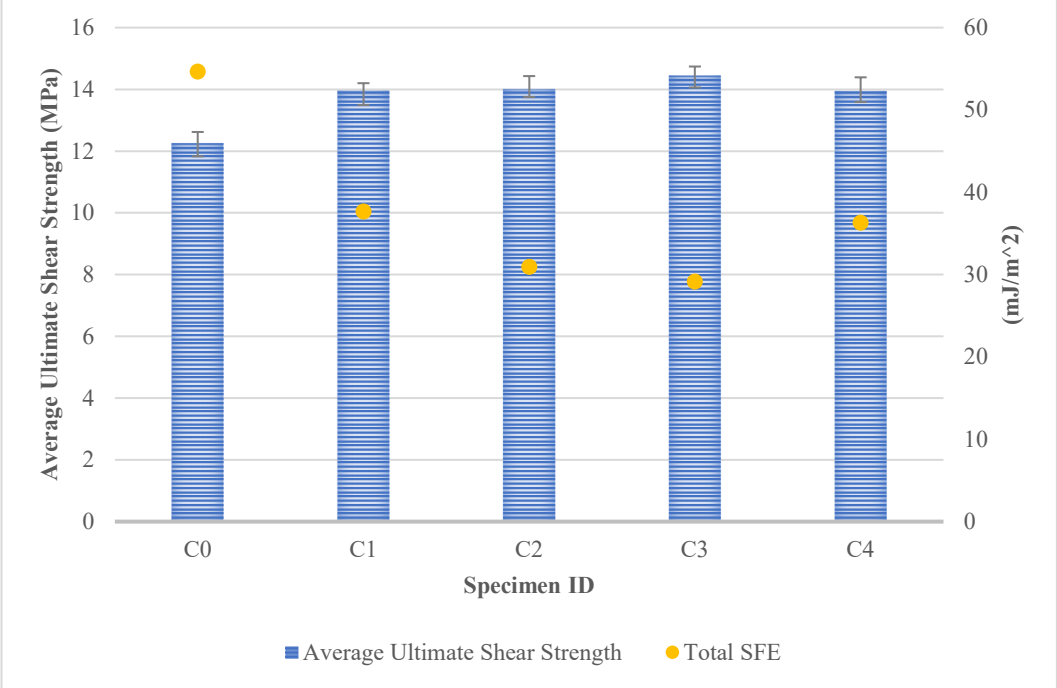

Figure 73: Average ultimate shear strength with respect to the total surface free energy of group C

Upon comparing the surface free energy and its components with the average ultimate shear strength of variants D0 and D1, it was observed that the Pearson correlation coefficient for the polar component, dispersive component, and total surface free energy were 0.54, 0.23, and 0.55, respectively. This indicates that the initial performance of adhesively bonded joints can be enhanced by increasing the surface free energy through NaOH treatment and zirconate deposition. This finding differs relatively from the results obtained for groups A, B, and C. Notably, variant D1 exhibited an

increase in surface free energy and polar component, leading to better adhesion performance. Considering the high rate of improvement in the initial performance of the adhesively bonded joint between group D and other groups, it can be concluded that high surface free energy is associated with high initial performance in a PUR aluminium-to-aluminium adhesively bonded joint. Furthermore, the polar component of variants D1 to D4 showed a relatively positive correlation with substrate surface roughening prior to NaOH treatment and zirconate deposition. Conversely, the dispersive component of variants D1 to D4 showed the opposite effect.

According to the MANOVA analysis, a significant difference was observed between D0 and D1 with respect to the joint consideration of the average ultimate shear strength and the polar component of the surface free energy variable, Wilks' Λ= 0.076, $F(2,7)=42.509$, partial $\eta^2=0.924$. An ANOVA was conducted separately for each dependent variable (i.e. surface free energy and its components) with an alpha level of 0.05 for evaluation. The analysis showed that a significant difference exists between D0 and D1 regarding the average ultimate shear strength, $F(1,8) = 77.699$, $p < 0.001$, partial $\eta^2=0.907$, with D1 ($M = 14.17$) scoring higher than C0 ($M = 13.12$). By way of contrast, there was no significant difference between D0 and D1 on polar components of the surface energy, $F(1,8) = 5.073$, $p = 0.054$, partial $\eta^2=0.388$. For the dispersive component, Wilks' Λ= 0.055, $F(2,7)=59.982$, partial $\eta^2=0.945$, the MANOVA shows that there was also no significant difference between D0 and D1, $F(1,8) = 0.008$, $p = 0.93$, partial $\eta^2=0.001$. Ultimately, it was concluded that there was no significant difference between the D0 and D1 on total surface free energy, Wilks' Λ= 0.093, $F(2,7)=34.332$, partial $\eta^2=0.907$ for the initial performance of adhesively bonded joint and $F(1,8) = 3.343$, $p = 0.105$, partial $\eta^2=0.295$.

Relevant statistical analysis was taken between specimens D1, D2, D3 and D4 to identify the influence of surface roughening of the aluminium prior to NaOH treatment and zirconate silane deposition on surface energy and its components. Refereeing to the results from MANOVA analysis, it is apparent that a significant difference between specimen D1 to D4 when considered jointly on the variables average ultimate shear strength and polar component, Wilks' Λ=0.368, $F(6,30)=3.243$, partial $\eta^2=0.393$. A separate ANOVA was conducted for each dependent variable (i.e. surface free energy and its components), with each ANOVA evaluated at an alpha level of 0.05. There was no significant difference between selected group D specimens on average ultimate shear strength $F(3,16) = 1.387$, $p = 0.283$, partial $\eta^2=0.206$. However, there was a significant difference between the same specimens on polar components of the treated aluminium surface, $F(3,16) = 6.463$, $p = 0.005$, partial $\eta^2=0.548$. For the dispersive component,

Wilks' Λ= 0.200, $F(6,30)=6.173$, partial $\eta^2 = 0.552$, the MANOVA shows that there was also a significant difference between selected specimens from group D, $F(3,16) =17.154$, $p = 0.001$, partial $\eta^2=0.763$. Thereafter, referring to the MANOVA analysis of surface free energy, it can be concluded that there was a significant difference between selected specimens from group D on total surface free energy, Wilks' Λ= 0.490, $F(6,30)=2.142$, partial $\eta^2=0.30$ for the initial performance and $F(3,16) = 3.289$, $p = 0.048$, partial $\eta^2=0.381$.

The findings presented in Figures 74-76 demonstrate the impact of changes in the polar component, dispersive component, and total surface free energy on the average ultimate shear strength of aluminium-to-aluminium adhesively bonded joints for variant A0, B0, C0, and D0. These results suggest a significant relationship between the total surface free energy and its components with the initial performance of the bonded joints in this variant. Furthermore, the figures indicate that the deposition of the coupling agent with varying molecular structures can lead to different effects on the surface energy and its components of the aluminium surface.

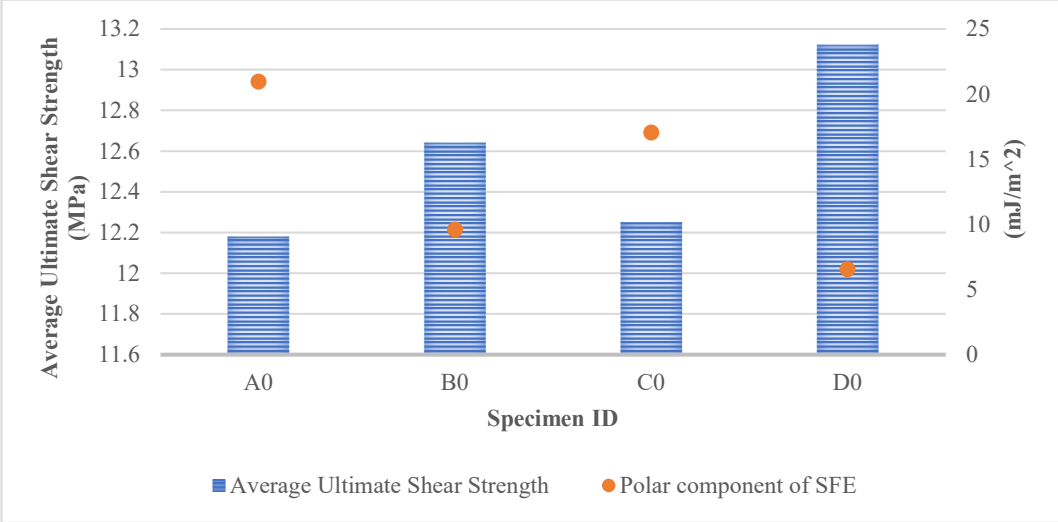

Figure 74: Average ultimate shear strength with respect to a polar component of Variants A0, B0, C0 and D0

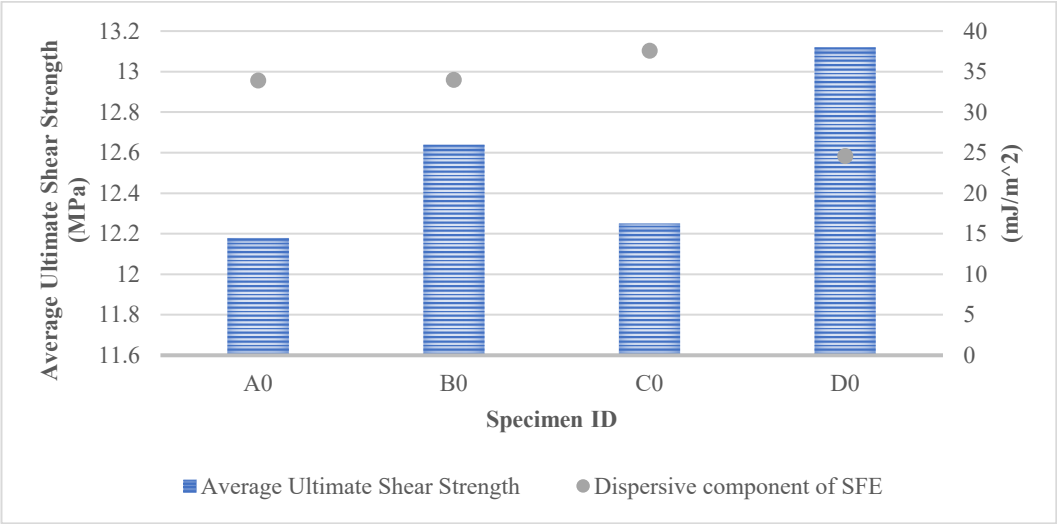

Figure 75: Average ultimate shear strength with respect to a dispersive component of Variants A0, B0, C0 and D0

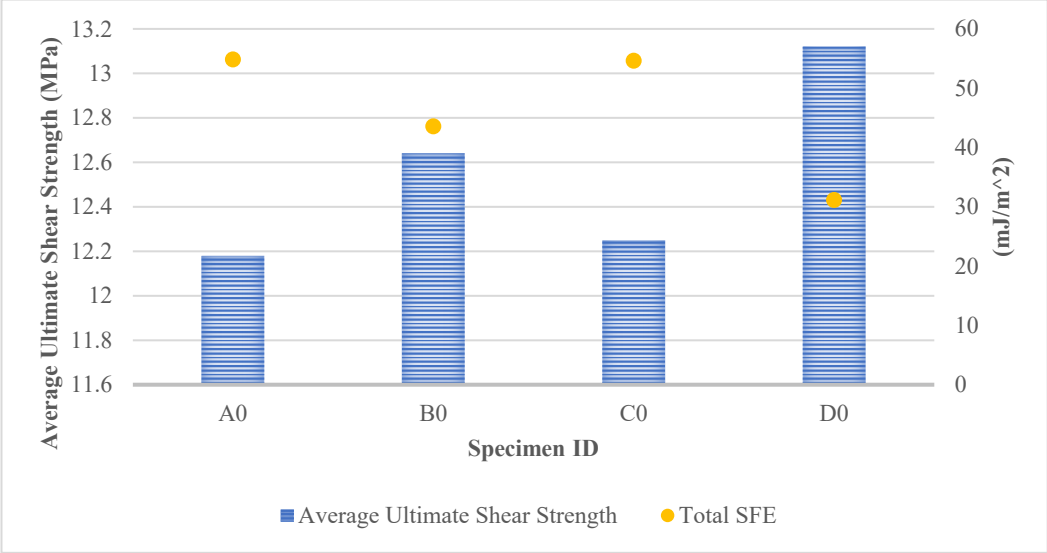

Figure 76: Average ultimate shear strength with respect to the total surface free energy of Variants A0, B0, C0 and D0

Based on the statistical analysis conducted between specimens A0, B0, C0, and D0, it was aimed to investigate the impact of different coupling agents on the polished aluminium surface energy and its components. The results obtained from the MANOVA analysis revealed that there was a significant difference between specimens A0, B0, C0, and D0, when assessed together on the variables of average ultimate shear strength and polar component, Wilks' Λ=0.145, $F(6,30)$=8.123, partial η^2=0.619. The average ultimate shear strength of the selected specimens was analysed through separate ANOVA for each dependent variable, with each ANOVA assessed at an alpha level of 0.05. The results indicated a significant difference between the selected specimens in terms of average ultimate shear strength, $F(3,16) = 6.845$, $p = 0.004$, partial η^2=0.562. Nevertheless, this result cannot specify the location of the significant difference. Therefore, the least

significant difference (LSD) and Bonferroni post-hoc test were employed to evaluate the difference between the means of selected specimen groups. The Table 13 shows that the significant difference in average ultimate shear strength is obtained by the LSD post-hoc method between A0 and D0. A significant difference exists between the ultimate shear strength of C0 and D0. Still, this result can be linked to the lack of dipodal silane over the polished surface and its relatively similar surface characteristics with A0. In addition, it can be noted that the Bonferroni result agrees with the LSD result; therefore, the identified significance of the LSD method for ultimate shear strength between selected specimens is the satisfactory result.

However, there was a significant difference between the identical specimens on the polar component of the treated aluminium surface, in which $F(3,16) = 22.360$, $p = 0.001$, partial η^2=0.807. According to Table 13, there was no significant difference in the polar component between A0 and C0, which can be explained by the absence of dipodal silane deposition on the polished aluminium surface. In contrast, LSD did not reveal a significant difference between the polar component of B0 and D0. The Bonferroni result supports the LSD result, and it can be concluded that the polar component results obtained using MANOVA and LSD are satisfactory. For the dispersive component, Wilks' Λ= 0.056, $F(6,30)$=16.089, partial η^2 = 0.763, the MANOVA shows that there was also a significant difference between selected specimens, $F(3,16)$ =67.752, p = 0.001, partial η^2=0.927. The data presented in Table 13 indicates that only the application of silane treatment to the aluminium surface did not result in significant changes to the dispersive component of the polished aluminium surface. However, based on the MANOVA analysis of surface free energy, it can be concluded that there was a significant difference observed between the selected specimens in terms of their total surface free energy, Wilks' Λ= 0.055, $F(6,30)$=16.320, partial η^2=0.765 for the initial performance and $F(3,16) = 53.177$, $p = 0.001$, partial η^2=0.909. After comparing the results presented in Table 13, it can be concluded that the use of different coupling agents had an effect on the surface energy of polished aluminium.

Table 13: Values for post-hoc analysis in terms of shear strength of the adhesively bonded joints and different surface roughness parameters for variants A0, B0, C0, and D0

Shear Strengh	LSD			
	A0	B0	C0	D0
A0		0.067	0.763	0.001
B0	0.067		0.116	0.056
C0	0.763	0.116		0.002
D0	0.001	0.056	0.002	

Shear Strengh	Bonferroni			
	A0	B0	C0	D0
A0		0.4	1	0.006
B0	0.4		0.697	0.335
C0	1	0.697		0.011
D0	0.006	0.335	0.011	

Polar Component	LSD			
	A0	B0	C0	D0
A0		0.001	0.065	0.001
B0	0.001		0.002	0.158
C0	0.065	0.002		0.001
D0	0.001	0.158	0.001	

Polar Component	Bonferroni			
	A0	B0	C0	D0
A0		0.001	0.39	0.001
B0	0.001		0.01	0.95
C0	0.39	0.01		0.001
D0	0.001	0.95	0.001	

Dispersive Component	LSD			
	A0	B0	C0	D0
A0		0.931	0.001	0.001
B0	0.931		0.002	0.001
C0	0.001	0.002		0.001
D0	0.001	0.001	0.001	

Dispersive Component	Bonferroni			
	A0	B0	C0	D0
A0		1	0.008	0.001
B0	1		0.01	0.001
C0	0.008	0.01		0.001
D0	0.001	0.001	0.001	

Total Surface Free Energy	LSD			
	A0	B0	C0	D0
A0		0.001	0.001	0.001
B0	0.001		0.011	0.001
C0	0.001	0.011		0.003
D0	0.001	0.001	0.003	

Total Surface Free Energy	Bonferroni			
	A0	B0	C0	D0
A0		0.001	0.001	0.001
B0	0.001		0.048	0.001
C0	0.001	0.048		0.018
D0	0.001	0.001	0.018	

In a similar fashion to the previous analysis of specimens A0, B0, C0, and D0, a statistical analysis was conducted between specimens A1, B1, C1, and D1 to investigate the impact of NaOH treatment prior to each different coupling agent on the initial performance of the adhesively bonded joint, surface energy, and its components. Referring to the results from MANOVA analysis, it is apparent that a significant difference between specimens A1, B1, C1 and D1 when considered jointly on the variables average ultimate shear strength and polar component, Wilks' Λ=0.254, $F(6,30)$=4.929, partial η^2=0.496. Each dependent variable underwent a separate ANOVA, with a significance level of 0.05. The results indicate a significant difference between the selected specimens regarding their average ultimate shear strength, $F(3,16) = 7.945$, $p = 0.004$, partial η^2=0.598. To identify the exact location of the significant difference in the means of the selected specimens, LSD and Bonferroni post-hoc tests were conducted. Based on Table 14, it is apparent that the LSD post-hoc test indicates a significant difference in the average ultimate shear strength between all the NaOH-treated aluminium surfaces before the selected coupling agents. Furthermore, the Bonferroni post-hoc test result supports this finding. As a result, it can be concluded that NaOH treatment prior to the application of coupling agents can effectively enhance their influence on the initial performance of adhesively bonded joints. Also, there was a significant difference between the same specimens on the polar component of the treated aluminium surface, in which $F(3,16) = 3.755$, $p = 0.032$, partial η^2=0.413. As stated in the Table 14, the polar

component did not differ significantly from those with significant initial performance differences.

On the other hand, LSD shows a significant polar component difference between B1 and C1, but Bonferroni's result did not support this finding. For the dispersive component, Wilks' Λ= 0.149, $F(6,30)=7.963$, partial η^2 = 0.614, the MANOVA shows that there was also a significant difference between selected specimens, $F(3,16) =8.752$, p = 0.001, partial $\eta^2=0.621$. According to the findings presented in Table 14, a strong correlation was observed between the dispersive component and shear strength of the adhesively bonded joint, with the exception of the specimen treated with silane deposition. Moreover, based on the Bonferroni results, it can be inferred that the outcomes for this aspect of the study are likely to be inconclusive. On the opposite side, referring to the MANOVA analysis of surface free energy, it can be seen that there was no significant difference between selected specimens on total surface free energy, Wilks' Λ= 0.258, $F(6,30)=4.837$, partial $\eta^2=0.001$ for the initial performance and $F(3,16) =$ 23.562, p = 0.219, partial $\eta^2=0.236$. Despite the "not significant" result for this section, post-hoc analyses were employed to investigate the reliability of this answer. Comparing the result in the Table 14, it is seen that a similar trend was recorded in the effect of selected surface treatment on the aluminium total surface free energy. Also, Bonferroni's result suggests that the result from LSD analysis is reliable and satisfactory. Based on the findings, it can be inferred that the polar and dispersive components of the surface free energy may not provide a reliable indicator for studying the impact of surface treatments on the initial performance of the adhesively bonded joint. Nonetheless, total surface free energy can be considered a dependable surface parameter for examining the efficacy of chemical-based surface treatments on the aluminium surface.

Table 14: Values for post-hoc analysis in terms of shear strength of the adhesively bonded joints and different surface roughness parameters for variants A1, B1, C1, and D1

Shear Strengh	LSD			
	A1	B1	C1	D1
A1		0.007	0.003	0.001
B1	0.007		0.641	0.135
C1	0.003	0.641		0.288
D1	0.001	0.135	0.288	

Shear Strengh	Bonferroni			
	A1	B1	C1	D1
A1		0.043	0.016	0.002
B1	0.043		1	0.81
C1	0.016	1		1
D1	0.002	0.81	1	

Polar Component	LSD			
	A1	B1	C1	D1
A1		0.21	0.251	0.092
B1	0.21		0.024	0.007
C1	0.251	0.024		0.556
D1	0.092	0.007	0.556	

Polar Component	Bonferroni			
	A1	B1	C1	D1
A1		1	1	0.552
B1	1		0.143	0.041
C1	1	0.143		1
D1	0.552	0.041	1	

Dispersive Component	LSD			
	A1	B1	C1	D1
A1		0.137	0.031	0.001
B1	0.137		0.44	0.003
C1	0.031	0.44		0.018
D1	0.001	0.003	0.018	

Dispersive Component	Bonferroni			
	A1	B1	C1	D1
A1		0.819	0.188	0.001
B1	0.819		1	0.02
C1	0.188	1		0.106
D1	0.001	0.02	0.106	

Total Surface Free Energy	LSD			
	A1	B1	C1	D1
A1		0.007	0.003	0.001
B1	0.007		0.641	0.135
C1	0.003	0.641		0.288
D1	0.001	0.135	0.288	

Total Surface Free Energy	Bonferroni			
	A1	B1	C1	D1
A1		0.043	0.016	0.002
B1	0.043		1	0.81
C1	0.016	1		1
D1	0.002	0.81	1	

4.5 Conclusion

An experimental investigation was conducted to evaluate the impact of various mechanical and chemical surface treatments on the adhesively bonded joints of aluminium-to-aluminium using a PUR adhesive. The study also examined the effects of surface roughness, wettability, and chemistry of treated aluminium on the initial performance of the single lap joints. Based on the findings presented in this chapter, it can be concluded that:

- the success of adhesively bonded joints of aluminium-to-aluminium with different surface treatments relies heavily on the compatibility between the treated surface chemistry and polarity with the selected adhesive. Therefore, it is important to carefully select the adhesive based on the polar and dispersive components of the treated surface. The present study found that the PUR adhesive demonstrated the highest compatibility with the zirconate coupling agent, which had the highest recorded polar component in the previous chapter.
- The surface roughening of aluminium surface prior to NaOH treatment and coupling agent application can enhance initial adhesion performance compared to polished specimens, as observed in this study. The most significant improvement, with a 22.33% increase of ultimate shear strength, was achieved by roughening the aluminium surface with #120

grit prior to NaOH treatment, followed by zirconate deposition. This finding highlights the importance of surface preparation in achieving optimal adhesion performance in aluminium-to-aluminium bonding.

- there is a limit to the trend of increasing the ultimate shear strength by increasing the surface roughness. For each type of surface treatment, there exists a plateau at which further increases in the surface roughness of the treated aluminium do not result in an increase in the average shear strength of the bonded single lap joints.
- A combination of simple surface treatments can lead to achieving cohesion failure in the adhesively bonded single lap joints of aluminium-to-aluminium. However, this outcome cannot be achieved with a polished aluminium surface when using PUR adhesive.
- The results reveal that the NaOH treatment can significantly enhance the ultimate shear strength of adhesively bonded joints. This enhancement can be accurately predicted by the combination of surface roughness parameters S_a and S_q, as a direct relationship was observed. Furthermore, it was found that surface roughening of the aluminium alloy can indirectly affect the initial adhesion performance of the bonded joint. Specifically, roughening the aluminium surface can increase the reaction zone for NaOH treatment, thereby leading to an increase in the shear strength of the bonded joint.

CHAPTER 5

Exposed Performance

THE INFLUENCE OF DIFFERENT ROUGHNESS PARAMETERS, ENERGY AND CHEMISTRY OF THE TREATED ALUMINIUM SURFACE ON EXPOSED PERFORMANCE OF THE PUR BONDED ALUMINIUM-TO-ALUMINIUM JOINTS

5.1 Overview

In the previous chapter, the initial performance of PUR adhesively bonded joints was systematically studied with respect to different surface roughness parameters and their energy and components. This chapter aims to evaluate the influence of the previously studied surface characteristics, such as surface roughness parameters and surface energy components, on the exposed performance of aluminium-to-aluminium PUR adhesively bonded joints. This study is restricted to analysing the impact of three surface roughness parameters (S_a, S_p, and S_q) and the polar, dispersive, and total surface free energy of the treated aluminium surface on the exposed durability of the aluminium-to-aluminium PUR adhesively bonded joint under humid environmental conditions. Adhesively bonded aluminium-to-aluminium specimens are manufactured according to the wedge Boeing standard, ASTM D3762. The specimens are subjected to accelerated aging inside an environmental chamber under controlled conditions of elevated temperature and specific humidity. The aim of this investigation is to determine how specific surface treatments and their corresponding surface characteristics affect the exposed performance of adhesively bonded joints by measuring the crack growth rate under humid condition. The Pearson correlation coefficient (ρ) is used to study the dependency between the measured surface parameters as a result of selected surface treatments with the recorded fracture toughness of the bonded joint. In addition, MANOVA analysis is employed to investigate the statistical effect of various surface treatments on the exposed performance of the adhesively bonded joints. To determine differences among groups of surface treatments based on their surface properties and

fracture toughness data, post-hoc analysis using the Bonferroni method in combination with the least significant difference (LSD) is conducted.

5.2 Introduction

5.2.1 Influence of surface roughness on the durability of the adhesively bonded joint

Undoubtedly, the exposed performance of the adhesively bonded joint is a critical aspect of all modern engineering structures, regardless of their applications. As previously noted in this study, the pre-bonding surface treatment of the adherend is recognised in the literature as crucial for enhancing the initial strength, durability, fracture toughness, and failure modes of adhesively bonded joints.
The surface roughness condition of the treated adherend is a notable characteristic aspect that can influence the performance of adhesively bonded joints. The relationship between surface roughness and the initial and exposed performance of these joints is believed to be complex and still requires further understanding. Critchlow and Brewis (Critchlow & Brewis, 1995) conducted research that identified a significant influence of surface roughness on the durability of adhesively bonded joints in aluminium. They used grit blasting to modify the roughness of the aluminium surface before applying epoxy adhesive, and their conclusion was that the durability of the epoxy-based adhesively bonded joints was significantly affected by surface roughness. In contrast, van Dam et al. (van Dam et al., 2020) found that surface roughening of an epoxy and steel substrate prior to adhesive bonding can enhance the initial strength of the bonded joint, but it has a minor effect on the exposed performance of the bonded joints. Therefore, it can be concluded that in the present literature there is no universal trend linking surface roughness to the exposed performance of adhesively bonded joints. The ideal surface morphology for achieving high exposed performance of adhesively bonded joints varies depending on the specific adhesive-adherend combination. Thus, there may be a different relationship between surface roughness and bond durability for different adhesive-adherend joints. Therefore, it is important to examine the effects of various roughness characteristics from a diverse set of surface treatments that involve different adhesives.

5.2.2 Influence of surface wettability and chemistry on the durability of the adhesively bonded joint

Numerous studies highlight the significance effect of surface treatment on surface properties of the adhesively bonded joint, which can chemically alter the properties of the treated substrate. Such chemical treatments can affect the thermodynamic characteristics

of the treated aluminium surface. In the study by van Dam et al. (van Dam et al., 2020), it was stated that the presence of the complex texture and morphology provides a more profound effect on both the initial and exposed performance of the epoxy adhesively bonded joint. The results obtained from the wedge test indicate that surface treatment can modify the chemistry of the substrate, leading to stronger and more durable bonded joints. The study suggests that chemically altered silane and zirconium surfaces exhibit better exposed performance, especially in the absence of a complex texture resulting from mechanical treatment. While the significance of surface treatment in improving the exposed of adhesively bonded joints is well-established, to the best of the author's knowledge, no research has systematically investigated the impact of thermodynamic characteristics of the treated aluminium surface, such as surface energy and its components, on the exposed performance of adhesively bonded joints.

5.2.3 Objective of this chapter

The objective of this chapter is to investigate the impact of surface characteristics on altered aluminium surface, achieved through the surface treatments discussed in Chapter 3, on the exposed performance of adhesively bonded joints using PUR adhesive. Although the literature mainly focuses on epoxy adhesives, the author chose to investigate the behaviour of adhesively bonded joints using the same PUR adhesive in chapter 4 and selected surface treatments to identify any possible correlations between surface phenomena and durability. The experimental programme involved measuring initial crack length and fracture toughness of wedge tests under controlled environmental conditions. Statistical analysis was conducted using the MANOVA method with LSD and Bonferroni post-hoc methods. The investigation aimed to determine the correlation between various characteristics of the treated aluminium surface, including three different surface roughness parameters, polar component, dispersive component, and total surface free energy.

5.3 Experimental programme

5.3.1 Materials

The material used as an adherend to manufacture the wedge beam coupons was similar to that noted in previous chapters – aluminium alloy 6061-T6. Its mechanical characteristic was shown in Table 3, including one-component commercially available PUR (3M PUR TS115 HGS) which was used in this study as a selected adhesive for investigation of the exposed performance of the bonded joints.

5.3.2 Fabrication of the Wedge Specimen

One of the most common testing methods to assess the durability of the adhesively bonded joint is the ASTM D3762 metal-to-metal wedge crack durability test. The specimen's geometry was set based on the defined dimensions and additional considerations in regards to fabrication of wedge coupons and cutting the samples into separate specimens in the abovementioned standard. According to this standard, the suggested specimen geometries must be 203 x 25 x 3.2 mm. However, due to the lack of guidance provided in this standard regarding specifics on testing conditions and specimen fabrication, additional reference (Adams et al., 2012) was used to ensure: (1) acceptable metal bonds were manufactured, and (2) the reliability of the conducted test was within the acceptable/reproducible range. Also, two other issues need to be taken care of while fabricating the wedge specimens: (1) controlling the bondline thickness, and (2) appropriate machining of the specimens from the test panel.

To address these concerns, a custom mould was designed to ensure accurate alignment of specimens and sufficient control of adhesive thickness to prevent premature failure or unreliable testing results. The design was based on recommendations from the literature (Adams et al., 2009). With the help of the custom mould, an adhesive thickness of 0.5mm was achieved. The spacer (with a thickness of 0.5mm) was positioned at the tip of each specimen to create the necessary space for inserting the wedge once the adhesive had cured. Another spacer was also placed at the end of the specimen to ensure a consistent bond line thickness. Prior to bonding, the substrates were heated in an oven to 100°C for 60 minutes to minimise thermal effects between the aluminium surface and the adhesive due to temperature differences. The 3M Scotch-Weld PUR Easy 250 applicator was used to dispense the PUR cartridges at 121℃ to fabricate the specimens. The manufacturer recommended a curing period of seven days at room temperature for complete curing and maximum strength. To avoid any permanent attachment between the tip spacer and adhesive, the top spacer was removed carefully after 48 hours of gluing. The thickness of the bonded joint at the bondline area was measured at eight critical points, three at the tip, three at the tail, and two in the middle, using a pro-grade electronic digital calliper. The adhesive thickness was found to be reproducible in accordance with ISO 25217:2009. For each variant of surface treatment, five specimens were prepared and tested.

5.3.3 The Boeing Wedge testing

The Boeing wedge test is a widely used method for evaluating the exposed performance of adhesively bonded joints, and it has been recognised by ASTM D3762. As the need for a better understanding of the durability aspects of adhesively bonded

joints has increased in recent decades, reliable testing setups like the Boeing wedge test have become essential to investigate the behaviour of such joints. The reason for its frequent use is its high dependability in assessing and displaying the bonded joint's longevity under varying environmental circumstances (Adams et al., 2009). The test involves using double cantilever testing coupons, which were loaded by inserting a wedge into the gap between the beams, as illustrated in the Figure 77.

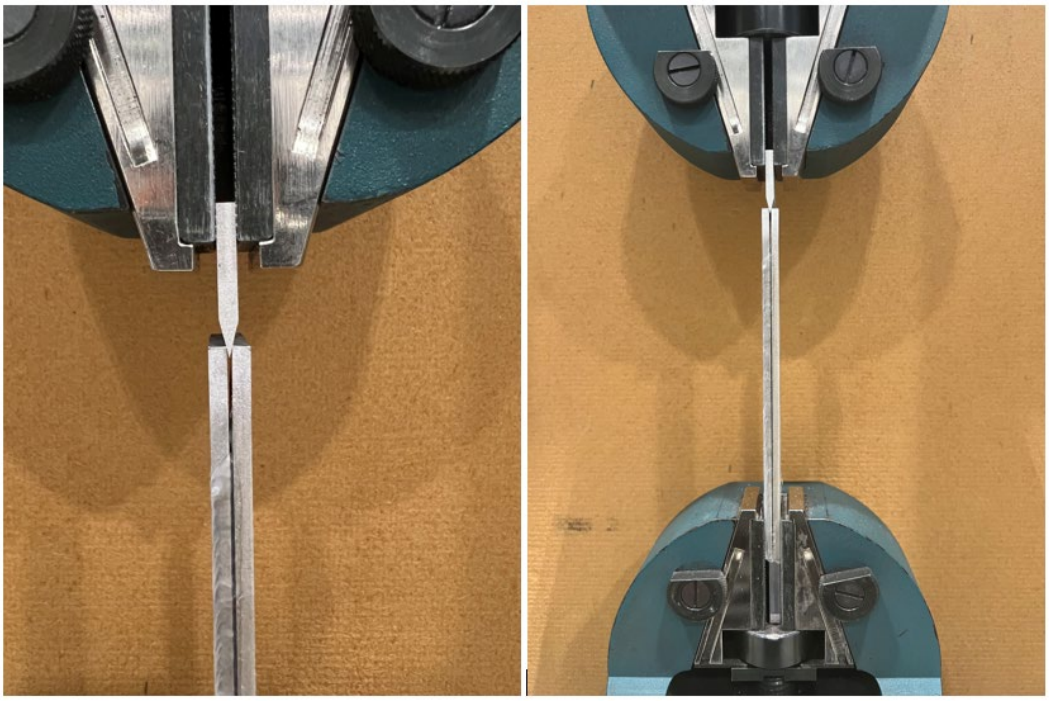

Figure 77: Wedge force inserting into the assembled cured wedge specimens

By using the wedge test, the interface between the adhesive and adherend can be subjected to high tensile strength, making it a reliable method to determine the durability of the bonded joint under various environmental conditions. After inserting the wedge into the gap between the beams of the double cantilever testing coupons, the assembly was placed into the environmental chamber for testing. The growth of the crack was measured every third day for a total exposure time of 30 days. The qualitative nature of this test enables it to predict the environmental durability of adhesively bonded joints effectively. Moreover, it is the most suitable method to compare different surface treatments in terms of the degree of enhancement in the exposed performance of bonded joints.

In this study, the insertion of the wedge into the gap between the beams was carried out at a constant speed of 1.3mm/min by holding onto the tail end of the specimen. The wedge was carefully positioned to ensure that its end and sides were aligned precisely with the specimen's sides to prevent any bending or early deformation. The initial crack length was measured one hour after inserting the wedge to allow the specimen to stabilise

(Davis et al., 2007). After measuring the initial crack length, the specimens were lined up and placed in a temperature and humidity-controlled chamber. Based on the recommendation provided by Davis et al. (Davis et al., 2007), any specimens with an initial crack length of 52mm and more will be disregarded. Once the specimens were placed in the environmental chamber, the crack lengths were measured every third day during the 30 days of exposure time. The specimens were exposed to 50̊ C, 95% humidity and noncondensing conditions for the entire duration of the test.

Based on the measured crack length and the geometry of the specimens, the fracture toughness values, $G_I(J/m^2)$, were estimated using simple beam theory expression as shown in Equation 4. (Sargent, 2005):

$$G_I = \frac{3Eh^3w^2}{16a^4} \quad (4)$$

where E is Young's modulus of aluminium alloy 6061, which is 69GPa, w is the opening displacement of the crack, which can be defined as the wedge's thickness (3.2 mm), h is the thickness of the substrate (3.2mm), and a is the measured crack length at the specific intervals.

Despite this equation's simplicity, the resulting effectiveness is reliable for the sake of comparison and not actual fracture toughness (Zain et al., 2014). Considering the main aim of this chapter, the abovementioned equation was selected as the central one to calculate the fracture toughness of the bonded joint based on the recorded crack length. At the end of the exposure period of thirty days, the wedge specimens were forced opened for visual inspection of the fracture surfaces.

5.4 Experimental results and discussion

5.4.1 Wedge Test Results (Bond Durability Measurement)

Figures 78 and 79 show the average crack length and growth of the wedge test specimen in terms of the different surface treatments. The trends shown in both figures a strong correlation between the recorded crack length and growth and the chosen surface treatments. The trend observed in both graphs is similar, as the lowest crack length and growth are consistently recorded for variant C3 across all exposure times. The results indicate that roughening the aluminium surface with #120 sandpaper mesh size prior to NaOH treatment and dipodal silane leads to a strong interface interaction, preventing quick crack initiation and propagation in controlled environmental conditions. However, it should be noted that significant differences in the recorded initial crack length are observed in the first few days prior of a wedge insertion. Additionally, a rapid

increase in crack length can be observed in the first ten days of environmental exposure for all variants in groups A and C0. Among these variants, the trend of high crack growth (A0 > C0 > A1 > A2 > A3 > A4) can be obtained during the abovementioned exposure time. The results show that the polished sample exhibited the lowest performance compared to other variants in terms of crack growth, with the crack length continuing to increase rapidly even during the exposed exposure stage. Variants A0, A1, and A2 were identified as the "rapid increase variants" due to their similar high levels of crack growth, with final crack lengths ranging from 111mm for A2 to approximately 118mm for A0 after 30 days of exposure time. The trend for the moderate crack growth samples is that the initial crack length growth was the highest in the first ten days of exposure time. In this group, the samples with coupling agents showed moderate to low increases in crack length and growth. The trend for the moderate increase samples is B0 > D0 > B1 > B4 > B2 > D4 > C4. The term "moderate increase variant" refers to the variants with moderate crack growth. The results showed that these variants had lower crack growth after ten days of exposure, and their final crack length ranged from 71 mm for C4 and B1 to around 87mm for D0. Thus, it can be inferred that the use of coupling agent in conjunction with NaOH treatment and surface roughening can impact the durability of the adhesively bonded joint, which is dependent on the molecular structure of the coupling agent, the pre-treatment of the aluminium surface with NaOH, and the degree of surface roughness prior to these treatments. This issue will be examined more thoroughly by analysing the relationship between the surface roughness parameters and the surface free energy and its constituents in the upcoming sections. It can be observed that variants such as B3, C1, and D1 exhibit relatively low increases in crack growth. Similar to the previous variant groups, the first ten days of exposure demonstrate the most detrimental effect on bonded joints. The recorded trend of B3 > C1 > D1 > D2 > C2 > D3 > C3 suggests the susceptibility of these variants to environmental degradation, with B3 exhibiting the most favourable performance among the low crack growth variants. The present study designates the group demonstrating a relatively low increase in crack growth as the “low increase variant.” Unlike the high and moderate-increase groups, the trend of lower crack growth after ten days of exposure was not consistent among the low-increase variants. The final crack length for this group ranged from 48.4mm for C3 to around 71mm for D1, which coincides with the final crack length of the moderate-increase group. Notably, most of the variants in group D exhibited a high increase in growth after ten days of exposure time, as observed in Figures 78 and 79.

In conclusion, it can be inferred that the most effective method for improving the durability of the PUR aluminium-to-aluminium adhesively bonded joints is the combination of surface roughening by #120 sandpaper prior to NaOH treatment and

dipodal silane (C3). This approach demonstrated the lowest crack length and growth compared to the other variants, indicating a strong interface interaction that prevented quick crack initiation and propagation under controlled environmental conditions. Based on the findings of the study, it can be inferred that the aluminium surfaces without a coupling agent (group A) are more vulnerable to moisture attack. However, the presence of a coupling agent, regardless of its molecular structure, can enhance the water-resistance of PUR adhesive bonding, provided there is an effective interaction. This improvement is particularly noticeable in the case of dipodal silane. However, it can be suggested that the degree of improvement in water-resistance of PUR adhesive bonding can vary depending on the molecular structure of the coupling agents. In other words, different types of coupling agents may lead to varying degrees of improvement in the durability of the adhesively bonded joints. The findings indicate that dipodal silane applied on the aluminium surface provides the most significant improvement, followed by zirconate and silane coupling agents. Moreover, it can be asserted that the positive impact of NaOH treatment on the deposition of coupling agents is evident in the enhanced durability of the adhesively bonded joints. As per the findings discussed in this chapter, it can be suggested that the reason behind this improvement may be the greater concentration of hydroxide groups on the aluminium surface resulting from the NaOH treatment. It is likely that the improved deposition of coupling agents on the aluminium surface is due to the reaction between the NaOH treatment and the coupling agents. (Hu et al., 2019; Saleema et al., 2012). Based on the results obtained from this study, it can be inferred that the effect of NaOH treatment on the durability of adhesively bonded joints is dependent on the presence or absence of coupling agents. Specifically, it was found that NaOH treatment alone may decrease the durability of bonded joints, while the combination of NaOH treatment and coupling agents can lead to improved durability. Therefore, it can be concluded that NaOH treatment plays an indirect role in improving the durability of adhesively bonded joints.

According to the results obtained in this study, it can be concluded that surface roughening prior to NaOH treatment and the deposition of coupling agents can enhance the durability of the adhesively bonded joints. The use of sandpaper with different mesh sizes has been shown to improve the effectiveness of NaOH treatment before the deposition of silane, dipodal silane, and zirconate Similarly to Chapter 4, it is observed that excessive surface roughening has a negative impact on the durability of the adhesively bonded joint. Upon comparison of the exposed and initial performance results, it can be inferred that the adhesively bonded joints' strength and toughness can be significantly enhanced by an optimal surface roughening process prior to the NaOH treatment and coupling agent application. As stated in the study by Rider and Arnott

(Rider, 2006), surface roughening can play an essential role in forming durable adhesive-bonded joints.

It was noted that surface roughening has the potential to impact the shear components of loading conditions and may enhance the surface's ability to dissipate stresses at the crack tip, thereby reducing the diffusion rate of moisture. However, it should be emphasised that while surface roughness was not the primary focus of this study in evaluating the durability of the adhesively bonded joints, it is important to acknowledge that it can indeed have an impact on the overall durability.

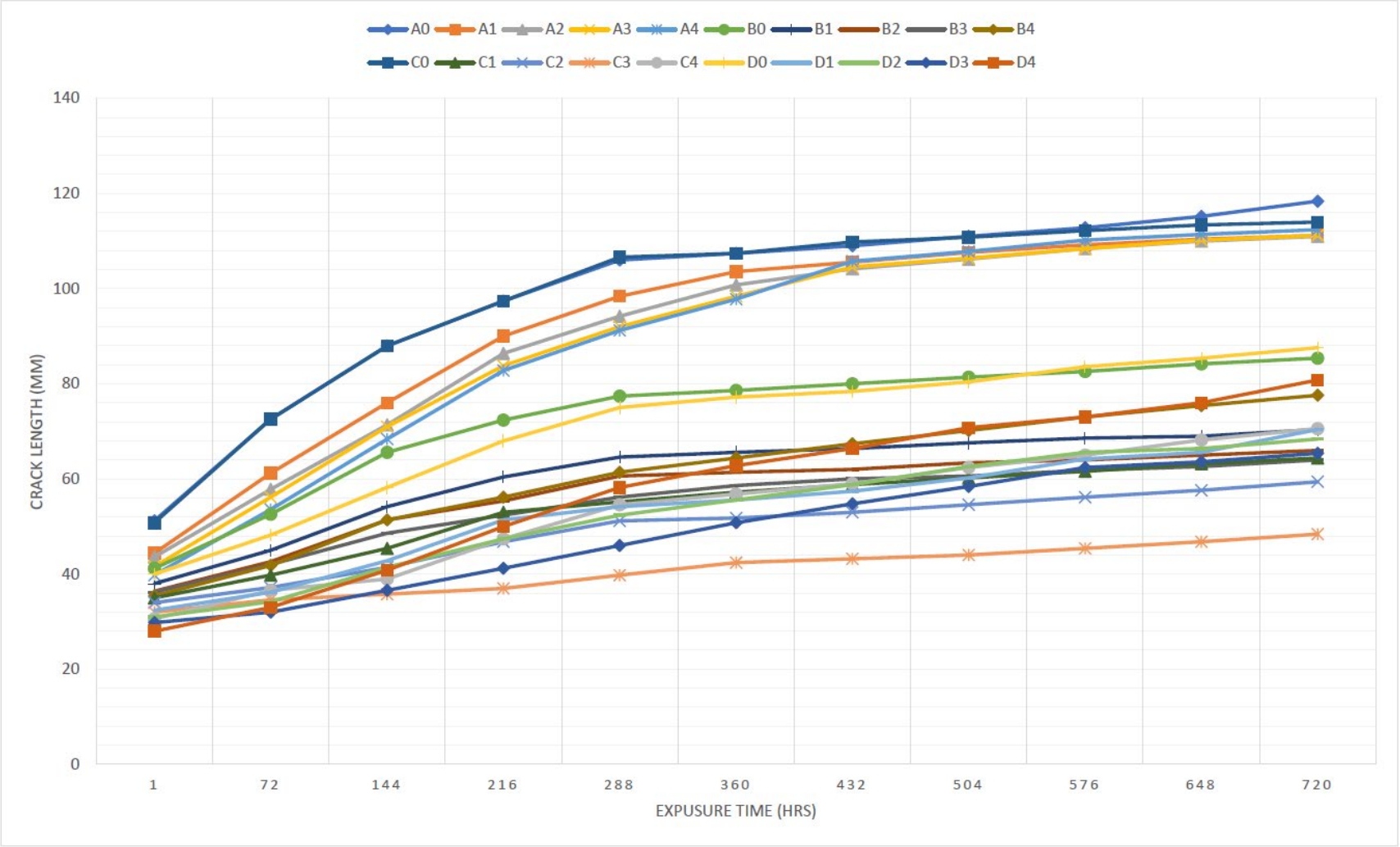

Figure 78: Average crack length of different wedge specimens in terms of selected surface treatment over the exposure period

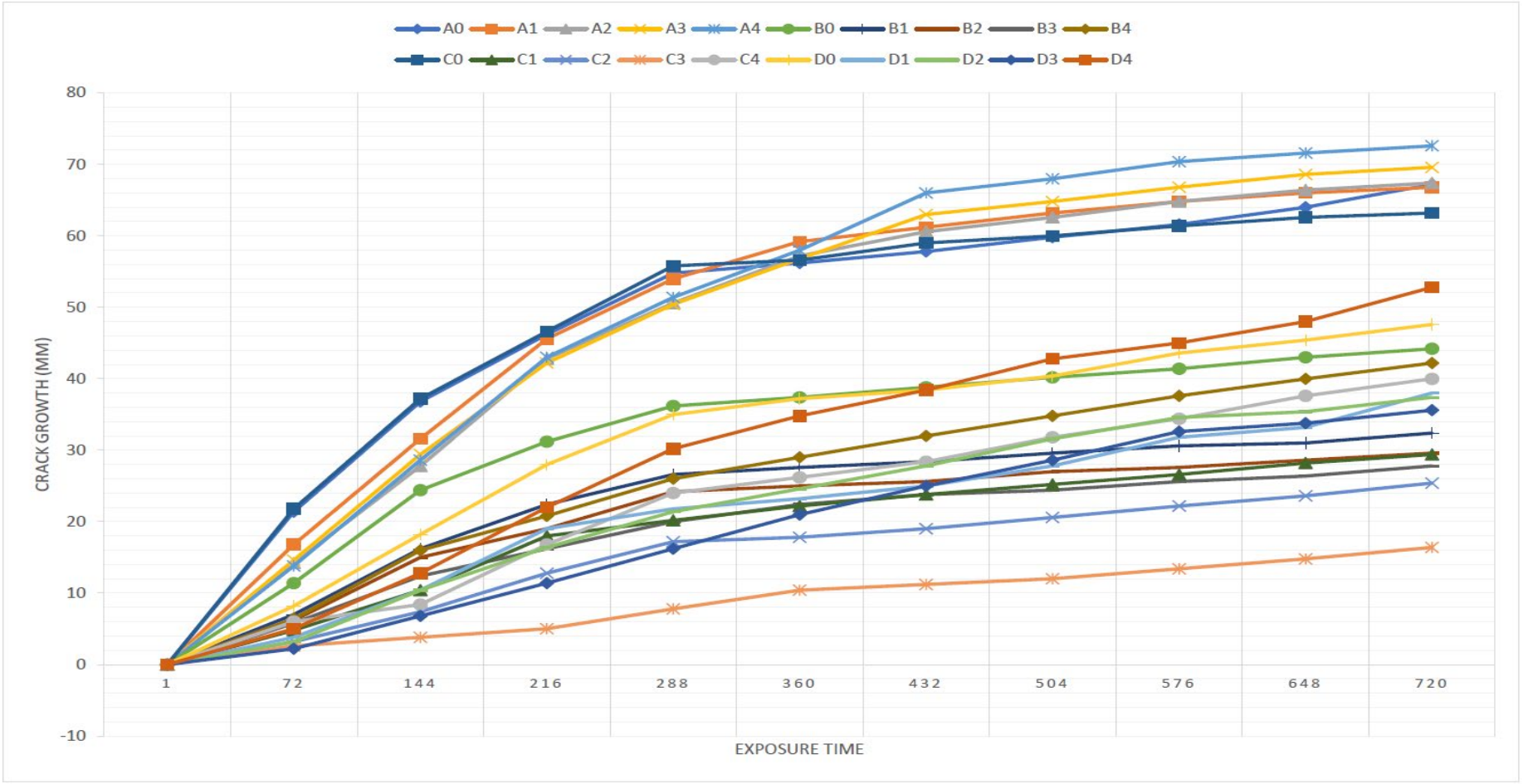

Figure 79: Average crack growth of different wedge specimens in terms of selected surface treatment over the exposure period

Based on the information presented in Figure 80, it can be observed that the initial crack length of the polished sample is considerably high compared to other surface treatments. Additionally, when comparing the results of group A, it can be inferred that the NaOH treatment has the potential to reduce the initial crack length, resulting in an improvement in the initial fracture toughness of the adhesively bonded joints. Moreover, it can be observed from Figure 80 that surface roughening before the NaOH treatment can further decrease the initial crack length. Among the samples in group A, the lowest initial crack length is measured for A4, which underwent surface roughening with a 120 grit sandpaper before the NaOH treatment. However, comparing the result in Figure 80 for group A, it can be concluded that while NaOH treatment and surface roughening may improve the initial crack length and fracture toughness of adhesively bonded joints, they are not effective in improving the exposed performance of the joints in a humid environment. Furthermore, the lack of improvement observed in sample C0, which is identical to A0, supports the finding in Chapter 3 that dipodal silane may not effectively interact with a polished aluminium surface.

Moreover, it is apparent that the initial crack length of the PUR adhesively bonded joint is significantly affected by the type of coupling agent used. The data in Figure 77 indicates that all samples treated with a coupling agent, or those with coupling agent deposition as part of their surface treatment process, display an improvement in initial crack length compared to those without any coupling agents. Furthermore, the use of zirconate as a coupling agent is shown to decrease the initial crack length of the PUR adhesively bonded joint, resulting in a stronger bond in dry conditions when compared to silane and dipodal silane. This finding is consistent with the results obtained in the single-lap joint experiments conducted in the previous chapter. The trend observed in Figure 77 also highlights the impact of NaOH treatment and surface roughening before the alkaline etching of the aluminium surface on the initial crack length of the PUR-bonded joints.

To sum up, the findings suggest that NaOH treatment can enhance the strength of the adhesively bonded joint in dry conditions indirectly by creating a fresh and larger underlying surface for better coupling agent interaction. Additionally, surface roughening prior to NaOH treatment can increase the surface area available for the NaOH solution to react with the aluminium surface, leading to decreased initial crack length.

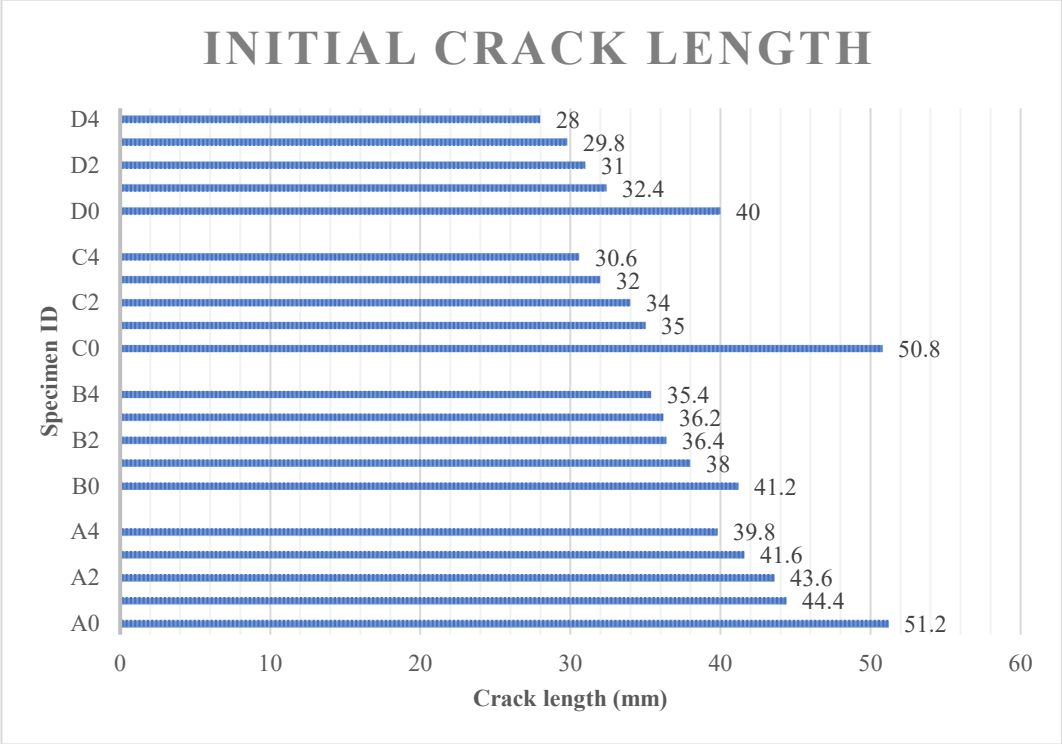

Figure 80: Initial crack length of the adhesive wedge bonded specimen as a function of different surface treatment variants

Figure 81 displays the fracture toughness of the PUR adhesively bonded joints for various surface treatments over different exposure time intervals. The given mode I fracture toughness is calculated using the simple beam theory expression Equation (4) from the measured crack length. During the first three days of exposure, it is seen that all the samples show a similar trend with different scales of reduction.

Samples with no coupling agent in their surface treatment procedure experience a rapid decrease in the mode I fracture toughness value within the first three days of exposure. Following this initial drop, all the samples in group A demonstrate a gradual decrease in mode I fracture toughness, ultimately reaching values of 22.1, 28.4, 28.6, 28.4, and 27.2 J/m^2 for A0, A1, A2, A3, and A4, respectively, as well as 81.6, 25.7, and 73.7 J/m^2 for the polished samples with silane (B0), dipodal silane (C0), and zirconate (D0), respectively. The fracture toughness of the samples treated with different coupling agents are significantly higher than that of sample A0. Specifically, the fracture toughness values for samples B0, C0, and D0 treated with silane, dipodal silane, and zirconate, respectively, are 272%, 13%, and 231% higher than the fracture toughness of A0. It is important to note once again that the lower fracture toughness value of the C0 samples suggests that dipodal silane was not effectively deposited onto the polished aluminium surface. This highlights the benefits of using coupling agents to enhance the interatomic bond strength at the adhesive-adherend interface. These results are in agreement with the literature (Abel et al., 2006; X.-X. Wang et al., 2019).

The sample that performed the best, as anticipated, is the one that underwent surface roughening with #120 sandpaper, NaOH treatment, and dipodal silane deposition. This sample exhibited a gradual decrease in fracture toughness, indicating crack propagation within the adhesive zone, which was supported by optical examination. After six days of exposure, a more abrupt drop was observed for this sample, indicating a slow crack transition from the adhesive to the interface between the adhesive and aluminium.

Based on Figure 81, it can be observed that the adhesively bonded joint of sample D4 exhibits the highest dry fracture toughness of 7062J/m^2. This highlights not only the impact of the surface treatment on the fracture toughness of the adhesively bonded joints in dry conditions, but also the significance of selecting a compatible coupling agent for the adhesive and the surface treatment. To summarise, Chapter 3 demonstrated that the deposition of zirconate increases the polar component of the surface, which leads to an increase in the free energy of the aluminium surface. This surface modification was found to enhance the lap shear strength, and consequently, the highest lap shear strength was observed for the samples in group D. The results presented here show a similar trend to that observed in Chapter 3, where it was found that the deposition of zirconate increased the polar component of the surface, resulting in higher lap shear strength for group D. However, in the current study, it is observed that while the polar nature of the zirconate and PUR adhesive promotes high fracture toughness in dry conditions, the sharp drop in fracture toughness for group D indicates their inability to withstand humid environments where crack transition to the interface is faster than other groups. It is believed that water diffusion plays a critical role in the degradation of the adhesively bonded joints due to the polar nature of the zirconate and PUR adhesive.

The graph in Figure 81 shows the effectiveness of dipodal silane and silane coupling agents in improving the exposed performance of adhesively bonded joints. Although these groups exhibit lower fracture toughness in dry conditions, the graph demonstrates their ability to maintain strength over an extended period, in contrast to zirconate. For example, the gradual reduction in fracture toughness of C3 indicates a slower crack transition to the interface, thereby enhancing the durability of the PUR-bonded joint.

Finally, it is noteworthy that sample A1 outperforms B1, C1, and D1, indicating that further improvement can be achieved by using NaOH treatment before coupling agent deposition. This improvement is mainly due to the presence of a higher number of active sites in the interaction zone, which enhances the interaction between the adhesive and adherend (Saleema et al., 2012). The comparison between the variants with NaOH treatment + coupling agent and the variants with surface roughening + NaOH treatment +

coupling agent, such as B2, C3, and D3, demonstrates that the former exhibits more than just initial qualities. This is likely due to the stronger interatomic bonding between the adhesive and adherend resulting from the NaOH treatment, which enhances the effectiveness of the coupling agent in improving the exposed performance of the adhesively bonded joint. The influence of surface roughness on adhesion performance extends beyond its impact solely on exposed performance. It is evident that the optimal combination of surface treatments varies depending on the specific coupling agent utilized. Furthermore, while higher surface roughness values may enhance fracture toughness in dry conditions, the correlation between surface roughness and the exposed performance of adhesively bonded joints is intricate and multifaceted.

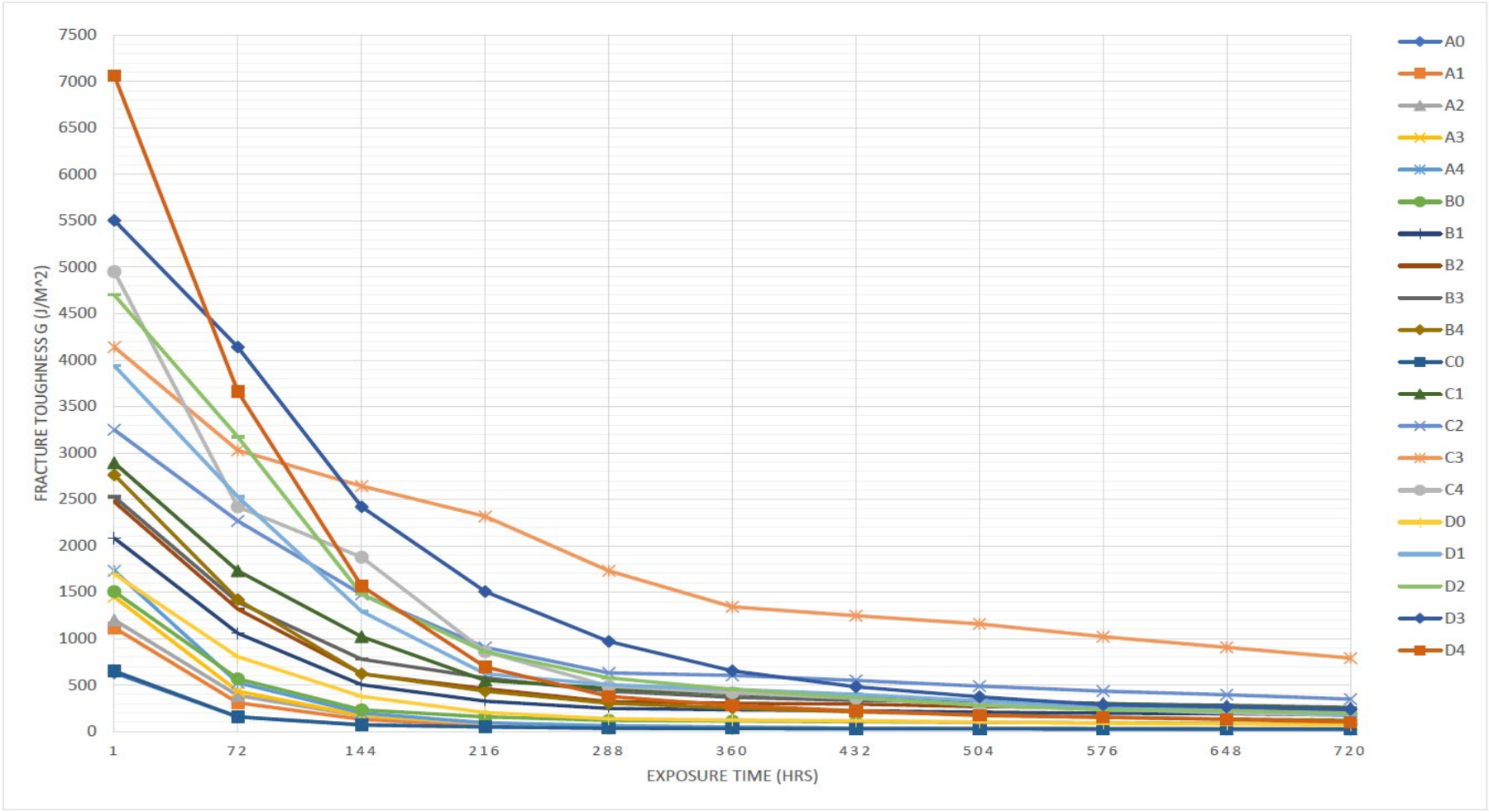

Figure 81: Average relative fracture toughness of different wedge specimens in terms of selected surface treatment over the exposure period

5.4.2 Wedge test failure modes

After the 30-day exposure period, the wedge specimens were manually pried open. The surface of the aluminium substrates on both sides of the beam coupons was thoroughly examined to determine the failure mode resulting from different surface treatments used during the study.

The observation of predominant adhesion failure in the polished sample, even in dry conditions, may be attributed to the weaker interfacial strength between the oxide layer and PUR adhesive in an aluminium-to-aluminium bonded joint. The data shows that there was a significant reduction in the fracture toughness of group A, with approximately 70-75% of the initial toughness of the bonded joint being lost within the first three days of the exposure period. Despite the initial improvement in initial toughness in dry conditions provided by NaOH treatment, it may not be sufficient to achieve an acceptable level of durability for PUR adhesively bonded joints. Moreover, it is contended that the introduction of surface roughening preceding NaOH treatment in variants A2, A3, and A4 did not yield a statistically significant enhancement in the enduring performance of the adhesively bonded joints. This determination is predicated on the observation of pronounced cohesion failures on the aluminuim surface subsequent to exposure to the specified humidity and temperature conditions. Upon visual inspection of the failure surface of variant A1, it was observed that the crack propagated quickly from the adhesive to the interface within the first three days of exposure. Similar results were observed for variants A2, A3, and A4. However, for these variants, the fracture surface revealed that the crack started to propagate diagonally to the direction of the applied force.

The results of this study show a clear trend among groups B, C, and D, with the exception of variant C0. When comparing variants B0 and D0 with A0, the fracture surfaces of these variants exhibit a higher amount of residual PUR on the aluminium surface. This suggests that coupling agents, such as silane and zirconate, can enhance the resistance of adhesively bonded joints to water diffusion. Furthermore, upon comparing variant B1, C1, and D1 with A1, it is discernible that these variants exhibit nearly twice the lengthwise residual polyurethane (PUR) on the aluminuim surface. This phenomenon, wherein a higher percentage of the surface area is covered with adhesive, serves as an indication of adhesion failure. Notably, this suggests a prospect for potential enhancements in the strength of the aluminuim bonded joints. Additionally, the comparison between the remaining specimens indicates the impact of surface roughening before NaOH treatment and coupling agent deposition. The fracture surface of variants B3 and C3 showed mostly cohesive failure, while a mixed-mode surface was observed

for D3. The transition to more adhesion failure than cohesion failure for variants B4, C4, and D4 suggests the negative effect of excessive surface roughening before adhesively bonded joints. The fractured surface of group D shows a larger area of adhesion failure compared to groups B and C, which may be due to the difference in surface polarity as discussed in the previous chapter. However, it should be noted that according to Mittal (Packham, 2006) the failure mode in the wedge test should not be the only indicator for evaluating the quality of a joint. In some cases, adhesive-substrate combinations may fail cohesively but still have weaker strength than a similar joint bonded with a stronger adhesive that fails adhesively. Therefore, depending on the selected adhesive, the ultimate strength of the joint may be more important than the mode of failure (Rider, 2006).

To sum up, the failure mode trend in the single lap joint is similar to that of the wedge test. However, group D, despite its good initial performance after surface treatment, showed weaker exposed performance under humid conditions, possibly due to the polar nature of zirconate. In contrast, groups B and C demonstrated strong and durable adhesion performance due to the presence of silane and dipodal coupling agents at the interface. Moreover, optimal surface roughening before NaOH treatment and coupling agent deposition improved the exposed performance of the joint by increasing the available surface area for higher interactions between the adhesive and the treated aluminium surface.

5.4.3 The correlation between different surface roughness parameters and exposed performance bonded joints

Chapter 4 provides an analysis of the influence of three distinct surface roughness parameters on the strength of single lap joints formed through the adhesion of aluminium and PUR. Furthermore, the chapter also explores the association between surface roughness and initial performance concerning the chosen surface treatments. The current section aims to extend this analysis and evaluate the effect of surface roughness parameters on the exposed performance of the adhesively bonded joint formed between aluminium and PUR.

The Pearson correlation coefficient revealed a significant relationship between surface roughness parameters and the exposed performance of the aluminium-PUR adhesively bonded joint. Tables 15 and 16 show the recorded fracture toughness of group A with respect to the three different surface roughness parameters over the intervals of three days for 30 days.

As per the findings presented in Table 15 a comparison between variant A0 and A1 suggests a strong positive correlation between the selected surface roughness parameters

and fracture toughness of the adhesively bonded joints. The Pearson correlation coefficient of the S_a, S_p and S_q are 0.75, 0.28 and 0.79, respectively. This implies that an enhancement in fracture toughness of the adhesively bonded joints can be observed with an increase in surface roughness resulting from NaOH treatment. On the other hand, Table 16, indicates that the correlation coefficient obtained for the variants A1 to A4 demonstrates a weak relationship between the surface roughness parameters and fracture toughness of the adhesively bonded joints. Hence, it can be inferred that surface roughening of the aluminium surface prior to NaOH treatment may not necessarily be linked to exposed performance.

Table 15: Correlation of surface roughness parameters and fracture toughness of variant A0 and A1

	1 hr	**72 hrs**	**144 hrs**	**216 hrs**	**288 hrs**	**360 hrs**	**432 hrs**	**504 hrs**	**576 hrs**	**648 hrs**	**720 hrs**		S_a	S_p	S_q
A0	631.71	156.26	72.38	48.23	34.38	32.62	30.75	28.59	26.59	26.81	24.64		0.154	1.488	0.218
A1	1117.04	309.45	130.12	66.16	46.60	37.68	34.91	32.38	30.52	29.22	28.39		2.294	7.581	3.245
ρ_{Sa}	0.65	0.87	0.85	0.83	0.88	0.55	0.58	0.63	0.74	0.83	0.81		0.75		
ρ_{Sp}	0.21	0.46	0.39	0.44	0.40	0.05	0.06	0.09	0.18	0.33	0.44			0.28	
ρ_{Sq}	0.71	0.89	0.88	0.88	0.91	0.60	0.63	0.66	0.77	0.86	0.85				0.79

Table 16: Correlation of surface roughness parameters and fracture toughness of variant A1 to A4

	1 hr	**72 hrs**	**144 hrs**	**216 hrs**	**288 hrs**	**360 hrs**	**432 hrs**	**504 hrs**	**576 hrs**	**648 hrs**	**720 hrs**		S_a	S_p	S_q
A1	1117.04	309.45	130.12	66.17	46.30	37.68	34.91	32.39	30.53	29.22	28.39		2.294	7.581	3.245
A2	1201.31	388.95	167.03	77.90	55.13	42.05	36.82	34.13	31.44	29.65	28.60		2.901	8.552	3.799
A3	1449.53	435.17	170.83	88.03	60.60	46.30	36.26	33.87	31.44	29.44	28.39		2.994	9.611	3.994
A4	1730.09	525.95	198.32	92.36	62.75	47.45	34.65	32.15	29.44	28.19	27.20		3.049	15.48	4.765
ρ_{Sa}	0.16	0.35	0.39	0.52	0.47	0.36	-0.10	-0.28	-0.09	-0.08	-0.27		0.13		
ρ_{Sp}	0.63	0.70	0.76	0.78	0.82	0.67	-0.02	-0.15	-0.18	-0.23	-0.29			0.32	
ρ_{Sq}	0.11	0.18	0.27	0.41	0.33	0.19	-0.12	-0.40	-0.19	-0.10	-0.28				0.04

Tables 17 and 18 display the fracture toughness values of Group B for the three surface roughness parameters over time intervals of three to 30 days. As demonstrated in Table 17, a comparison between variants B0 and B1 indicates a significant positive relationship between the selected surface roughness parameters and fracture toughness of the adhesively bonded joints in which the Pearson correlation coefficient of S_a, S_p and S_q are 0.87, 0.76 and 0.93, respectively. Based on the Pearson correlation coefficient values between variant A0 and A1 and the results obtained for variants B0 and B1, it can be inferred that the significant correlation observed is primarily due to the surface modification induced by NaOH treatment, and not the deposition of the silane coupling agent. In contrast, Table 18, shows that there was only a negligible correlation between the surface roughening prior to the NaOH treatment and silane deposition for the variant B1 to B4. This suggests that surface roughness and NaOH treatment may not be the primary factors contributing to the improvement of fracture toughness in the adhesively bonded joints. Moreover, it can be inferred that the alteration of surface roughness may only have a moderate positive impact on the initial fracture toughness of the bonded joint under dry conditions.

Based on the results presented in Tables 19 and 20, a similar Pearson correlation coefficient was recorded for groups C and B. Comparing the results provided for variants C0 and C1 in Table 19, it can be seen that surface roughness parameters S_a, S_p and S_q have a strong positive correlation with the fracture toughness of the bonded joints, where values are 0.93, 0.98 and 0.96, respectively. As in group B, it can be concluded that the main driving factor for these correlations is the surface alternation resulting from NaOH treatments. Furthermore, as shown in Table 20, the Pearson values between the variant C1 to C4 also confirm the weak positive correlation between the surface roughness parameters and fracture toughness of the bonded joint in the one-month exposure time. Similarly to group B, the results for the initial fracture roughness of group C indicate a strong positive correlation between surface roughness parameters resulting from the roughening of the aluminium surface prior to NaOH treatment and dipodal silane deposition.

Table 17: Correlation of surface roughness parameters and fracture toughness of variant B0 and B1

	1 hr	**72 hrs**	**144 hrs**	**216 hrs**	**288 hrs**	**360 hrs**	**432 hrs**	**504 hrs**	**576 hrs**	**648 hrs**	**720 hrs**		**S_a**	**S_p**	**S_q**
B0	1506.65	567.10	234.41	158.00	120.96	113.74	105.98	98.88	93.26	86.37	81.61		0.232	2.0808	0.3278
B1	2081.93	1058.64	503.04	326.18	249.27	234.41	223.32	207.88	196.02	191.52	176.73		1.8006	6.4804	2.8122
ρ_{Sa}	0.90	0.89	0.86	0.80	0.86	0.86	0.87	0.87	0.86	0.88	0.88		0.87		
ρ_{Sp}	0.81	0.83	0.70	0.65	0.76	0.76	0.77	0.76	0.76	0.81	0.80			0.76	
ρ_{Sq}	0.79	0.95	0.97	0.63	0.98	0.98	0.98	0.98	0.98	0.98	0.98				0.93

Table 18: Correlation of surface roughness parameters and fracture toughness of variant B1 to B4

	1 hr	**72 hrs**	**144 hrs**	**216 hrs**	**288 hrs**	**360 hrs**	**432 hrs**	**504 hrs**	**576 hrs**	**648 hrs**	**720 hrs**		**S_a**	**S_p**	**S_q**
B1	2081.93	1058.64	503.04	326.18	249.27	234.41	223.32	207.88	196.02	191.52	176.73		1.8006	6.4804	2.8122
B2	2472.83	1318.14	621.94	460.85	321.89	305.44	293.79	268.68	258.75	243.19	228.78		2.3326	8.8858	3.2568
B3	2527.94	1395.09	778.14	575.80	435.17	368.14	334.96	321.89	297.61	282.69	258.75		2.5064	9.3814	3.2672
B4	2764.31	1421.99	621.94	435.17	305.44	252.38	210.36	178.75	152.87	134.31	119.72		2.9662	17.657	3.703
ρ_{Sa}	0.50	0.26	0.09	0.01	0.11	-0.06	-0.10	-0.19	-0.17	-0.19	-0.24		0.00		
ρ_{Sp}	0.50	0.42	0.14	0.17	0.01	-0.12	-0.26	-0.39	-0.48	-0.52	-0.51			-0.09	
ρ_{Sq}	0.44	0.37	0.26	0.22	0.25	0.06	0.01	-0.11	-0.11	-0.14	-0.20				0.10

Table 19: Correlation of surface roughness parameters and fracture toughness of variant C0 and C1

	1 hr	72 hrs	144 hrs	216 hrs	288 hrs	360 hrs	432 hrs	504 hrs	576 hrs	648 hrs	720 hrs		S_a	S_p	S_q
C0	651.85	156.26	72.39	48.24	33.62	32.63	29.87	28.80	27.39	26.25	25.70		0.186	1.3624	0.2712
C1	2892.86	1730.09	1021.83	550.17	467.57	405.52	363.15	330.53	301.49	272.10	252.38		1.3368	9.4878	2.4358
ρ_{Sa}	0.96	0.89	0.93	0.95	0.93	0.93	0.94	0.93	0.93	0.95	0.94		0.93		
ρ_{Sp}	0.98	0.97	0.98	1.00	0.99	0.99	0.99	0.99	0.98	0.98	0.98			0.98	
ρ_{Sq}	0.97	0.92	0.95	0.97	0.95	0.95	0.97	0.95	0.96	0.97	0.96				0.96

Table 20: Correlation of surface roughness parameters and fracture toughness of variant C1 to C4

	1 hr	72 hrs	144 hrs	216 hrs	288 hrs	360 hrs	432 hrs	504 hrs	576 hrs	648 hrs	720 hrs		S_a	S_p	S_q
C1	2892.86	1730.09	1021.83	550.17	467.57	405.52	363.15	330.53	301.49	272.10	252.38		1.33	9.48	2.43
C2	3248.51	2266.88	1477.74	904.93	631.71	602.95	550.17	488.46	435.17	394.38	348.70		2.1322	8.8886	2.9216
C3	4140.00	3028.98	2642.82	2316.29	1730.09	1343.19	1246.42	1158.22	1021.83	904.93	791.08		2.495	12.049	3.539
C4	4951.25	2419.22	1876.47	859.98	488.46	417.07	358.25	286.33	243.19	200.66	174.74		2.8244	16.1634	3.7718
ρ_{Sa}	0.63	0.56	0.44	0.31	0.20	0.20	0.18	0.16	0.15	0.15	0.13		0.28		
ρ_{Sp}	0.59	0.27	0.39	0.14	0.05	-0.08	-0.07	-0.09	-0.04	-0.07	-0.06			0.09	
ρ_{Sq}	0.63	0.49	0.46	0.29	0.23	0.24	0.22	0.21	0.20	0.21	0.19				0.31

Based on the results presented in Tables 21 and 22, it can be concluded that the correlation between the surface roughness parameters and the fracture toughness of the adhesively bonded joints in group D is similar to groups B and C, despite the different molecular structures of zirconate. The Pearson correlation coefficient revealed a strong positive correlation for all surface roughness parameters with the fracture toughness of the bonded joints. For variants D0 and D1, as stated in Table 21, the Pearson correlation coefficient of S_a, S_p and S_q are 0.90, 0.82 and 0.95, respectively. This indicates that, similar to groups B and C, an increase in surface roughness can result in an increase in fracture toughness of the bonded joints, which can be attributed to the NaOH treatment and zirconate deposition. For the variant D1 to D4, as presented in Table 22, the Pearson correlation coefficient values suggest that changes in surface roughness parameters as a result of different surface roughness conditions prior to NaOH treatment and zirconate depositions, do not have any correlation with the recorded fracture toughness of the bonded joints. The findings of group D similarly indicate that there is a positive correlation between increasing surface roughness parameters and the initial fracture toughness of the PUR adhesively bonded joints in dry environmental conditions. In conclusion, the results suggest that NaOH treatment plays a significant role in the increase of surface roughness parameters, which consequently enhances the fracture toughness of the polished aluminium adhesively bonded joints. The findings highlight the importance of surface treatment in improving the exposed performance of adhesively bonded joints. Further research is warranted to investigate the effects of other surface treatments and deposition techniques on the mechanical properties of adhesively bonded joints.

Table 21: Correlation of surface roughness parameters and fracture toughness of variant D0 and D1

	1 hrs	72 hrs	144 hrs	216 hrs	288 hrs	360 hrs	432 hrs	504 hrs	576 hrs	648 hrs	720 hrs		S_a	S_p	S_q
D0	1695.74	804.29	378.36	203.03	137.20	122.22	114.90	103.89	88.87	81.61	73.72		0.1716	1.349	0.2376
D1	3939.31	2527.94	1293.67	621.94	503.04	454.26	399.90	330.53	255.54	234.41	176.73		1.2154	5.082	2.1092
ρ_{Sa}	0.89	0.94	0.89	0.92	0.87	0.87	0.89	0.92	0.90	0.87	0.91		0.90		
ρ_{Sp}	0.83	0.80	0.84	0.79	0.81	0.81	0.80	0.81	0.85	0.87	0.84			0.82	
ρ_{Sq}	0.93	0.94	0.94	0.97	0.94	0.94	0.95	0.97	0.95	0.92	0.95				0.95

Table 22: Correlation of surface roughness parameters and fracture toughness of variant D1 to D4

	1 hr	72 hrs	144 hrs	216 hrs	288 hrs	360 hrs	432 hrs	504 hrs	576 hrs	648 hrs	720 hrs		S_a	S_p	S_q
D1	3939.31	2527.94	1293.67	621.94	503.04	454.26	399.90	330.53	255.54	234.41	176.73		1.2154	5.082	2.1092
D2	4700.60	3173.19	1477.74	859.98	575.80	454.26	363.15	282.69	234.41	223.32	198.32		2.1038	7.8006	2.9416
D3	5504.72	4140.00	2419.22	1506.65	969.55	651.85	481.37	373.21	286.33	265.32	237.30		2.427	11.208	3.2736
D4	7062.66	3660.53	1566.61	694.58	378.36	279.10	223.32	172.77	152.87	130.12	101.85		2.794	14.3328	3.4322
ρ_{Sa}	0.55	0.51	0.15	0.19	0.00	-0.19	-0.34	-0.36	-0.32	-0.36	-0.21		-0.03		
ρ_{Sp}	0.66	0.63	0.37	0.21	0.03	-0.17	-0.29	-0.39	-0.36	-0.37	-0.27			0.00	
ρ_{Sq}	0.48	0.53	0.22	0.27	0.07	-0.08	-0.23	-0.27	-0.24	-0.28	-0.11				0.03

A comprehensive multivariate analysis of variance (MANOVA) method was employed in order to investigate the impact of selected surface treatments on the exposed performance of adhesively bonded joints, as a function of measured surface roughness parameters. Multivariate Analysis of Variance (MANOVA) constitutes a statistical extension of Analysis of Variance (ANOVA), designed to address scenarios involving multiple dependent variables. As for this study the different surface treatments and the measured mechanical characteristics of the adhesively bonded joints. Unlike ANOVA, which implemented in the previous chapter for assessing difference in means among groups (i.e. measured surface characteristics of the treated specimens) with respect to single dependent variable (i.e. selected surface treatment), MANOVA accommodates the analysis of correlated dependent variables simultaneously. Its primary purpose is to discern whether alterations in an independent variable, often categorised in nature, engender statistically significant effect on a set of interconnected dependent variables (i.e. selected surface treatment vs. measured surface characteristics vs. mechanical performance of the adhesively bonded joints). The inclusion of multiple dependent variables in MANOVA acknowledges their inherent interrelationships, thus providing a more nuanced understanding of the overall impact of the independent variable. The analytical framework of MANOVA incorporates a covariance matrix, which captures the covariance structure between dependent variables, offering insights into their collective variations. The method assumes multivariate normality and homogeneity of covariance matrices across groups. By considering the joint variance of multiple dependent variables, MANOVA proves advantageous in situations where traditional ANOVA might be limiting, especially when investigating complex phenomena wherein changes in one variable are anticipated to correlate with changes in others (Ogrodniczek, 2022). A significant MANOVA result implies overall differences among groups in the combination of dependent variables, necessitating subsequent analyses, such as univariate ANOVA or pairwise comparisons, to discern the specific variables contributing to the observed multivariate distinctions. In summary, MANOVA stands as a robust statistical tool for researchers seeking a comprehensive understanding of how changes in an independent variable reverberate across multiple correlated dependent variables (Pituch & Stevens, 2015). In this chapter, statistical analysis was conducted between different variants, namely A0 and A1, A1 to A4, B0 and B1, B1 to B4, C0 and C1, C1 to C4, D0 and D1, and D1 to D4. This analysis was based on the different fracture toughness values recorded over a 30-day exposure period, with measurements taken at intervals of three days.

The results from the MANOVA analysis show a significant difference between A0 and A1 when considered jointly on the variables' fracture toughness of the bonded joints and S_a, Wilks' Λ= 0.001, $F(8,1)$=166.728, partial η^2=0.999. In the context of Multivariate

Analysis of Variance (MANOVA), several critical statistical metrics are employed to assess the overall multivariate effect and elucidate the specific nuances of group differences. Foremost among these is Wilks' Lambda (Λ), a canonical statistic that quantifies the proportion of unexplained variance in the dependent variables (i.e. surface characteristics) relative to the total variance (Todorov & Filzmoser, 2010). A smaller Wilks' Lambda signifies a more robust effect, and its statistical significance, as denoted by the associated p-value, serves as a diagnostic criterion for detecting differences among groups on at least one dependent variable (Patel & Bhavsar, 2013). An individual ANOVA was performed for each response variable, with a significance level of 0.05 for all analyses. A significant difference was noted between A0 and A1 on fracture toughness values over all three-day intervals, as listed in Table 23. There was also a significant difference between A0 and A1 on the surface roughness parameter S_a value, $F(1,8) = 79.518$, $p < 0.01$, partial $\eta^2=0.909$. The Approximate F-Statistic, a ratio of between-group variance to within-group variance, mirrors the role of the F-ratio in univariate ANOVA. Its statistical significance, determined through comparison to the F-distribution, is pivotal in assessing the overall significance of group differences. The associated p-value is a crucial indicator, serving as the probability of observing the obtained results under the null hypothesis of no genuine group distinctions. For the S_p, the MANOVA shows no significant difference between A0 and A1, $F(1,8) = 4.899$, $p = 0.058$, partial $\eta^2=0.380$. Lastly, the result suggests a significant difference between the A0 and A1 on the value of S_q, $F(1,8) = 83.607$, $p < 0.01$, partial $\eta^2=0.913$.

Based on the conducted statistical analysis between specimens A1, A2, A3, and A4, it was aimed to investigate the effect of surface roughening on the aluminium surface prior to NaOH treatment on the selected parameters and exposed performance of the adhesively bonded joint. The MANOVA analysis revealed a significant difference among the specimens A1 to A4 when considering both fracture toughness and recorded value for S_a as dependent variable, Wilks' $\Lambda= 0.052$, $F(42,9)= 4.535$, partial $\eta^2=0.950$. The result reveals that the influence of the surface roughening prior to NaOH treatment on fracture toughness is significant only for the first 15 days of the exposure, as shown in Table 24.

Table 23: Manova results for the tests between-subjects effects of fracture toughness and surface roughness parameters for variant A0 and A1

	F Value	P value	Partial Eta Squared
Fracture toughness at day 1	39.526	<.001	.832
Fracture toughness at day 3	129.686	<.001	.942
Fracture toughness at day 6	485.463	<.001	.984
Fracture toughness at day 9	60.784	<.001	.884
Fracture toughness at day 12	258.908	<.001	.971
Fracture toughness at day 15	21.108	.002	.725
Fracture toughness at day 18	16.914	.003	.679
Fracture toughness at day 12	24.259	.001	.752
Fracture toughness at day 24	45.644	<.001	.851
Fracture toughness at day 27	122.537	<.001	.939
Fracture toughness at day 30	136.256	<.001	.945

Table 24: MANOVA results for the tests between-subjects effects of fracture toughness and surface roughness parameters for variant A1 to A4

	F Value	P value	Partial Eta Squared
Fracture toughness at day 1	13.946	<.001	.723
Fracture toughness at day 3	37.335	<.001	.875
Fracture toughness at day 6	61.437	<.001	.920
Fracture toughness at day 9	46.192	<.001	.896
Fracture toughness at day 12	78.124	<.001	.936
Fracture toughness at day 15	31.647	<.001	.856
Fracture toughness at day 18	1.162	.355	.179
Fracture toughness at day 12	2.221	.125	.294
Fracture toughness at day 24	2.781	.075	.343
Fracture toughness at day 27	1.338	.297	.201
Fracture toughness at day 30	1.315	.304	.198

The study revealed that the selected surface roughness did not exhibit a statistically significant effect on the exposed performance of the adhesively bonded joint during the latter half of the exposure period, potentially indicating the complete transition of the crack to the interface. However, due to the inclusion of more than two groups in the analysis, the precise location of the significant difference could not be ascertained. As a result, the LSD and Bonferroni methods were employed to determine the exact location of the significant differences. Referring to Appendix 1, it can be seen that significant differences were identified between the following variables: (1) fracture toughness at day 1; all the variables expect A1 and A2, (2) fracture toughness at day 3; all the variables, (3) fracture toughness at day 6; all the variables except A2 and A3, (4) fracture toughness at day 9; all the variables except A3 and A4, (5) fracture toughness at day 12; same as day 9, (6) fracture toughness at day 15; same as day 9 and 12. Furthermore, there was no significant difference between the identical specimens on S_a of the treated aluminium surface, in which $F(3,16) = 1.651$, $p = 0.217$, partial $\eta^2=0.236$. For the S_p, the MANOVA shows a significant difference between selected specimens, $F(3,16) =13.452$, $p = 0.001$, partial $\eta^2=0.716$. In the aforementioned comparison among samples A1-A4, a discernible correlation emerges, particularly in relation to the impact of surface roughness induced prior to the NaOH treatment. Notably, a substantial influence becomes apparent between samples A1 and A2. The discerned substantial impact of the NaOH treatment, particularly when comparing A1 and A2, establishes the pivotal role of NaOH in enhancing the fracture toughness of the bonded joints. It becomes evident that beyond this critical comparison, a subsequent escalation in surface roughness preceding NaOH etching does not exert a statistically significant influence on the exposed performance of the bonded joints. The findings thus suggest that the NaOH treatment, rather than variations in surface roughness, stands as the primary determinant in improving the fracture toughness of the bonded joints, emphasizing the critical role of chemical treatment in enhancing adhesive bond strength. The deduced outcome aligns notably well with extant literature in the field (van Dam et al., 2020). The consensus between the findings of the present study and prior research underscores the robustness and reliability of the observed trends. Such concurrence with established knowledge lends credence to the validity of the current investigation and strengthens the overall understanding of the influence of surface roughness and NaOH treatment on the fracture toughness of bonded joints. This harmonization with existing literature not only reinforces the reliability of the study but also contributes to the cumulative knowledge base in the domain, fostering a more comprehensive and nuanced comprehension of the subject matter. Referring to Appendix 2, it is manifest that significant differences were identified between the following variables: (1) A2, A3 and A4 in comparison to A1, (2) A1 and A4 in comparison to A2,

(3) A1 and A2 in comparison to A3, (4) A1, A2 and A3 in comparison to A4. Meanwhile, the agreement between the Bonferroni and LSD values confirmed satisfactory results for our analysis. Lastly, according to the MANOVA analysis of surface roughness parameter S_q, it can be concluded that there was no significant difference between selected specimens on total surface free energy, $F(3,16) = 0.730$, $p = 0.549$, partial η^2=0.120.

The results from the MANOVA analysis show a significant difference between B0 and B1 when considered jointly on the variables' fracture toughness of the bonded joints and S_a, Wilks' Λ= 0.03, $F(8,1)$= 45.798, partial η^2=0.997. Each dependent variable (i.e. surface characteristics) was subjected to a distinct ANOVA, with a significance level of 0.05. The results revealed a significant difference in the fracture toughness values between B0 and B1 for all three-day intervals, as listed in Table 25. There was also a significant difference between B0 and B1 on the surface roughness parameter S_a value, $F(1,8) = 28.649$, $p < 0.01$, partial η^2=0.782. For the S_p, the MANOVA shows a significant difference between B0 and B1, $F(1,8) = 15.343$, $p = 0.004$, partial η^2=0.657. Lastly, the result suggests a significant difference between the B0 and B1 on the value of S_q, $F(1,8) = 258.950$, $p < 0.01$, partial η^2=0.970.

A comparable statistical analysis was performed among samples B1, B2, B3, and B4 to examine the effect of surface roughening of aluminium prior to NaOH treatment and silane deposition on the selected surface roughness parameters and exposed performance of the adhesively bonded joint. Referring to the results from MANOVA analysis as shown in Table 26, it can be noted that there is a significant difference between specimen B1 to B4 when considered jointly on the variables' fracture toughness and recorded value for S_a, Wilks' Λ= 0.048, $F(42,9)$= 23.856, partial η^2=0.990. The results indicate that the effect of surface roughening prior to NaOH treatment and silane deposition on fracture toughness is significant throughout the entire exposure period. However, there was no significant effect of the selected surface roughness on the exposed performance of the adhesively bonded joints, indicating that there was no direct effect of surface roughening on fracture toughness. It is worth noting that, similar to the results observed for variants A1 to A4, the precise location of the significant difference could not be determined. Referring to Appendix 3, it can be seen that significant differences were identified between the following variables: (1) fracture toughness at day 1; all the variables expect B2-B3/B2-B4/B3-B4, (2) fracture toughness at day 3; same as day 1, (3) fracture toughness at days 6, 9 and 12; all the variables except B2-B4, (4) fracture toughness at days 15, 18; all the variables except B1-B4, (5) fracture toughness at days 21, 24, 27 and 30; for all the variables. The findings suggest that the application of a silane coupling agent has a discernible impact on the initial fracture toughness of bonded

joints. However, despite the rationale behind grouping the surface treatment of silane deposition with an augmentation in the surface roughness of the aluminum substrate—predicated on the expectation that such grouping would elevate the presence of hydroxide groups on the treated aluminum surface—it does not necessarily result in a concomitant increase in the fracture toughness of the bonded joints. The observed dissociation between the concurrent surface treatments implies a nuanced relationship, highlighting that while silane coupling agents may influence initial fracture toughness, their interaction with increased surface roughness does not unequivocally translate to heightened fracture toughness in the bonded joints. This underscores the importance of considering the intricate interplay of surface treatments in determining the mechanical properties of adhesive bonds, providing valuable insights for optimizing the efficacy of such treatments in practical applications. Furthermore, there was no significant difference between the identical specimens on S_a of the treated aluminium surface, in which $F(3,16) = 0.831$, $p = 0.496$, partial $\eta^2=0.712$. For the S_p, the MANOVA shows that there was a significant difference between selected specimens, $F(3,16) =13.206$, $p = 0.001$, partial $\eta^2=0.712$. Referring to Appendix 4, it is evident that significant differences were identified between B1, B2 and B3 compared to B4. Lastly, referring to the MANOVA analysis of surface roughness parameter S_q, it can be concluded that there was no significant difference between selected specimens on total surface free energy, $F(3,16) = 1.940$, $p = 0.164$, partial $\eta^2=0.267$.

Table 25: MANOVA results for the tests between-subjects effects of fracture toughness and surface roughness parameters for variant B0 and B1

	F Value	P value	Partial Eta Squared
Fracture toughness at day 1	14.315	.005	.641
Fracture toughness at day 3	241.883	<.001	.968
Fracture toughness at day 6	150.783	<.001	.950
Fracture toughness at day 9	215.836	<.001	.964
Fracture toughness at day 12	669.942	<.001	.988
Fracture toughness at day 15	680.919	<.001	.988
Fracture toughness at day 18	697.915	<.001	.989
Fracture toughness at day 12	902.689	<.001	.991
Fracture toughness at day 24	789.373	<.001	.990
Fracture toughness at day 27	4606.795	<.001	.998
Fracture toughness at day 30	1077.394	<.001	.993

Table 26: MANOVA results for the tests between-subjects effects of fracture toughness and surface roughness parameters for variant B1 to B4

	F Value	P value	Partial Eta Squared
Fracture toughness at day 1	5.676	.008	.516
Fracture toughness at day 3	18.074	<.001	.772
Fracture toughness at day 6	23.218	<.001	.813
Fracture toughness at day 9	31.617	<.001	.856
Fracture toughness at day 12	86.876	<.001	.942
Fracture toughness at day 15	38.522	<.001	.878
Fracture toughness at day 18	34.601	<.001	.866
Fracture toughness at day 12	75.957	<.001	.934
Fracture toughness at day 24	84.061	<.001	.940
Fracture toughness at day 27	152.266	<.001	.966
Fracture toughness at day 30	79.892	<.001	.937

The results from the MANOVA analysis show a significant difference between C0 and C1 when considered jointly on the variables' fracture toughness of the bonded joints and S_a, Wilks' Λ= 0.05, $F(8,1)$= 139.228, partial η^2=0.970. Each dependent variable (i.e. surface characteristics) was subjected to a separate ANOVA analysis, with a significance level of 0.05. The results of the analysis showed a significant difference between C0 and C1 regarding the values of fracture toughness over the entire 30-day exposure period, across all intervals, as listed in Table 27. There was also a significant difference between C0 and C1 on the surface roughness parameter S_a value, $F(1,8) = 65.473$, $p < 0.001$, partial η^2=0.891. For the S_p, the MANOVA shows a significant difference between C0 and C1, $F(1,8) = 189.708$, $p = 0.001$, partial η^2=0.960. Lastly, the result suggests a significant difference between the C0 and C1 on the value of S_q, $F(1,8) = 109.036$, $p < 0.01$, partial η^2=0.932.

Similar statistical analysis occurred between specimens C1, C2, C3 and C4 to identify the influence of roughening on the aluminium surface prior to NaOH treatment and dipodal silane deposition on selected roughness parameters and exposed performance of the adhesively bonded joint. Referring to the results from MANOVA analysis, it can be noted that there is a significant difference between specimen C1 to C4 when considered jointly on the variables' fracture toughness and recorded value for S_a, Wilks' Λ= 0.052, $F(42,9)$= 13.319, partial η^2=0.982. The result reveals that the influence of the surface roughening prior to NaOH treatment and dipodal silane deposition on fracture toughness is significant for the whole exposure period, as shown in Table 28. Nevertheless, to identify the location of these significant differences, the post-hoc test was performed. Referring to Appendix 5, it can be seen that significant differences were identified between the following variables: (1) fracture toughness at day 1; all the variables expect C1-C2, (2) fracture toughness at day 3; all the variables except C2-C4, (3) fracture toughness at day 6; all the variables, (4) fracture toughness at day 9; same as day 3, (5) fracture toughness at day 12; all the variables except C1-C4/C2-C4, (6) fracture toughness at days 15, 18, 21 and 27; all variables except C1-C4, (7) fracture toughness at days 24 and 30; all variables except C1-C2/C1-C4. Furthermore, there was a significant difference between the identical specimens on S_a of the treated aluminium surface, in which $F(3,16) = 9.263$, $p = 0.001$, partial η^2=0. Referring to Appendix 6, it is apparent that significant differences were identified between C3 and C4 compared to C1. For the S_p, the MANOVA shows that there was a significant difference between selected specimens, $F(3,16)$ =5.107, $p = 0.011$, partial η^2=0.489. Referring to Appendix 7, it is evident that significant differences were identified between C1 and C2 compared to C4. Lastly, referring to the MANOVA analysis of surface roughness parameter S_q, it can be concluded that there was a significant difference between selected specimens, $F(3,16)$ =

5.955, p = 0.006, partial η^2=0.528. Referring to Appendix 8, significant differences were identified between C3 and C4 compared to C1.

Table 27: MANOVA results for the tests between-subjects effects of fracture roughness and surface toughness parameters for variant C0 and C1

	F Value	P value	Partial Eta Squared
Fracture toughness at day 1	227.484	<.001	.966
Fracture toughness at day 3	225.919	<.001	.966
Fracture toughness at day 6	439.420	<.001	.982
Fracture toughness at day 9	531.032	<.001	.985
Fracture toughness at day 12	1141.492	<.001	.993
Fracture toughness at day 15	1199.750	<.001	.993
Fracture toughness at day 18	1325.987	<.001	.994
Fracture toughness at day 12	1316.631	<.001	.994
Fracture toughness at day 24	3198.229	<.001	.998
Fracture toughness at day 27	5319.045	<.001	.998
Fracture toughness at day 30	3522.102	<.001	.998

Table 28: MANOVA results for the tests between-subjects effects of fracture toughness and surface roughness parameters for variant C1 to C4

	F Value	P value	Partial Eta Squared
Fracture toughness at day 1	25.897	<.001	.829
Fracture toughness at day 3	44.875	<.001	.894
Fracture toughness at day 6	27.338	<.001	.837
Fracture toughness at day 9	72.983	<.001	.932
Fracture toughness at day 12	121.324	<.001	.958
Fracture toughness at day 15	112.639	<.001	.955
Fracture toughness at day 18	109.364	<.001	.954
Fracture toughness at day 12	107.722	<.001	.953
Fracture toughness at day 24	56.008	<.001	.913
Fracture toughness at day 27	76.995	<.001	.935
Fracture toughness at day 30	57.334	<.001	.915

The results from the MANOVA analysis show a significant difference between D0 and D1 when considered jointly on the variables' fracture toughness of the bonded joints and S_a, Wilks' Λ= 0.054, $F(8,1)$= 929.816, partial η^2=0.998. Individual ANOVAs were performed for each dependent variable (i.e. surface characteristics), with a significance level of 0.05. There was a significant difference between D0 and D1 on fracture toughness values over all three-day intervals, as listed in Table 29. There was also a significant difference between D0 and D1 on the surface roughness parameter S_a value, $F(1,8) = 28.827$, $p < 0.01$, partial η^2=0.783. For the S_p, the MANOVA shows a significant difference between D0 and D1, $F(1,8) = 14.256$, $p = 0.005$, partial η^2=0.641. Lastly, the result suggests a significant difference between the D0 and D1 on the value of S_q, $F(1,8) = 76.968$, $p < 0.01$, partial η^2=0.906.

Similar statistical analysis occurred between specimens D1, D2, D3 and D4 to identify the influence of surface roughening on the aluminium surface prior to NaOH treatment and zirconate deposition on selected surface roughness parameters exposed performance of the adhesively bonded joint. Referring to the results from MANOVA analysis, it can be noted that there is a significant difference between specimen D1 to D4 when considered jointly on the variables' fracture toughness and recorded value for S_a, Wilks' Λ= 0.082, $F(42,9)$=13.032, partial η^2=0.982. The result reveals that the influence of the surface roughening prior to NaOH treatment and zirconate deposition on fracture toughness is significant for the whole exposure period, as shown in Table 30.

Referring to Appendix 9, it can be seen that significant differences were identified between the following variables: (1) fracture toughness at day 1; all the variables expect D1-D2/D2-D3, (2) fracture toughness at day 3; all the variables except D1-D2/D2-D4/D3-D4, (3) fracture toughness at day 6; D1-D2/D1-D4/D2-D4, (4) fracture toughness at day 9; all variables except D1-D4/D2-D4, (5) fracture toughness at days 12, 15, 18 and 27; all the variables except D1-D2, (6) fracture toughness at days 21, 24 and 30; all variables. Furthermore, there was a significant difference between the identical specimens on S_a of the treated aluminium surface, in which $F(3,16) = 0.7292$, $p = 0.003$, partial η^2=0.578. Referring to Appendix 10, it is evident that significant differences were identified between D2, D3 and D4 compared to D1. For the S_p, the MANOVA shows that there was a significant difference between selected specimens, $F(3,16) = 5.448$, $p = 0.009$, partial η^2=0.505. Referring to Appendix 11, it is apparent that significant differences were identified between D3 and D4 compared to D1. Lastly, referring to the MANOVA analysis of surface roughness parameter S_q, it can be concluded that there was a significant difference between selected specimens, $F(3,16) = 5.889$, $p = 0.007$, partial η^2=0.525. Referring to Appendix 12, it is evident that significant differences, same as S_a,

existed. It is noteworthy to highlight that there exists a scarcity of information and available data concerning the influence of zirconate as a selected coupling agent on the mechanical performance of adhesively bonded joints. Despite these limitations, the present study's results demonstrate considerable alignment with the investigation conducted by van Dam et al. (van Dam et al., 2020)In their study, the influence of a zirconate with a somewhat similar chemical composition was thoroughly examined on the surface of steel substrates. The observed similarities between the outcomes of the current study and the aforementioned research by van Dam et al. suggest a congruence in the effects of zirconate treatment on bonded joints, albeit within the constraints of available information. This concordance, despite the scarcity of specific data, contributes to the coherence of knowledge in this relatively unexplored domain, indicating a potential avenue for further inquiry and validation of these findings.

Table 29: MANOVA results for the tests between-subjects effects of fracture toughness and surface roughness parameters for variant D0 and D1

	F Value	P value	Partial Eta Squared
Fracture toughness at day 1	68.019	<.001	.895
Fracture toughness at day 3	32.648	<.001	.803
Fracture toughness at day 6	112.370	<.001	.934
Fracture toughness at day 9	147.795	<.001	.949
Fracture toughness at day 12	291.011	<.001	.973
Fracture toughness at day 15	242.896	<.001	.968
Fracture toughness at day 18	408.183	<.001	.981
Fracture toughness at day 12	728.459	<.001	.989
Fracture toughness at day 24	272.428	<.001	.971
Fracture toughness at day 27	166.390	<.001	.954
Fracture toughness at day 30	173.345	<.001	.956

Table 30: MANOVA results for the tests between-subjects effects of fracture toughness and surface roughness parameters for variant D1 to D4

	F Value	P value	Partial Eta Squared
Fracture toughness at day 1	14.142	<.001	.726
Fracture toughness at day 3	8.403	.001	.612
Fracture toughness at day 6	12.18	<.001	.700
Fracture toughness at day 9	45.585	<.001	.895
Fracture toughness at day 12	38.548	<.001	.875
Fracture toughness at day 15	62.618	<.001	.922
Fracture toughness at day 18	64.325	<.001	.923
Fracture toughness at day 12	140.422	<.001	.963
.Fracture toughness at day 24	87.844	<.001	.943
Fracture toughness at day 27	74.273	<.001	.933
Fracture toughness at day 30	145.971	<.001	.965

5.4.4 The correlation between surface energy and its components and the exposed performance of bonded joints

This section aims to explore the possible relationship between the surface energy and its constituents with the exposed performance of adhesively bonded joints under different surface treatment conditions. The polished sample (A0) was selected as the primary reference point, while variant B0, C0, and D0 were used as the secondary references for comparison purposes. The treated specimens were analysed to identify the key factor that may enhance the exposed performance of the aluminium-to-aluminium PUR adhesively bonded joints.

The investigation revealed that the surface free energy and its components had varying correlations with the exposed performance of the aluminium-to-aluminium PUR adhesively bonded joints. Tables 31 and 32 present the exposed performance of the adhesively bonded joints in terms of different surface treatments in group A by comparing the fracture toughness in the different intervals and measured surface energy and its components. A comparison between variant A0 and A1, as shown in Table 31, indicates the strong negative correlation between the adhesively bonded joints' fracture toughness and the surface energy and its component. The Pearson correlation coefficient of the polar and dispersive components, and total surface free energy with fracture toughness were -0.88, -0.55 and -0.88, respectively. This implies that an enhancement in exposed durability can be anticipated through a reduction in surface-free energy and its constituent components. The measured correlation value corroborates the observed outcome, aligning with a similar finding in the context of sandblasting applied to aluminuim. The parallel nature of these results underscores the robustness of the association between decreased surface-free energy and improved exposed durability. This insight not only contributes to the broader understanding of surface modification effects but also emphasizes the potential applicability of such trends across diverse treatment methodologies, reinforcing the importance of surface engineering in optimizing material performance over extended durations (Rudawska et al., 2016).

On the other hand, as presented in Table 32, the correlation coefficient calculated for the variant A1 to A4 reveals a moderate positive correlation between the polar component of the treated samples and the durability of the adhesively bonded joint. Additionally, a weak positive correlation was observed between surface free energy and fracture toughness of the adhesively bonded joint. Comparing the correlation between the surface roughness parameters and surface energy with the exposed performance of the group A specimens, it can be inferred that a decrease in surface energy, particularly in the polar component, can lead to the formation of more robust bonded joints. Moreover, the

positive correlation between the polar component and fracture toughness can indicate the beneficial effect of surface roughening prior to NaOH treatment, considering the rose petal effect of NaOH treatment reported in previous literature. (Saleema et al., 2012).

Table 31: Correlation between the surface free energy and its components and fracture toughness of variant A0 and A1

	1 hr	72 hrs	144 hrs	216 hrs	288 hrs	360 hrs	432 hrs	504 hrs	576 hrs	648 hrs	720 hrs		Polar (P)	Dispersive (D)	SFE
A0	631.71	156.26	72.38	48.23	34.38	32.62	30.75	28.59	26.59	26.81	24.64		20.97	33.93	54.9
A1	1117.04	309.45	130.12	66.16	46.60	37.68	34.91	32.38	30.52	29.22	28.39		7.4	31.04	38.44
ρ_{polar}	-0.82	-0.93	-0.95	-0.86	-0.94	-0.83	-0.83	-0.85	-0.90	-0.88	-0.88		-0.88		
$\rho_{Dispersive}$	-0.70	-0.66	-0.57	-0.59	-0.52	-0.52	-0.55	-0.40	-0.41	-0.56	-0.60			-0.55	
ρ_{SFE}	-0.87	-0.95	-0.94	-0.87	-0.92	-0.83	-0.84	-0.81	-0.86	-0.88	-0.89				-0.88

Table 32: Correlation between the surface free energy and its components and fracture toughness of variant A1 to A4

	1 hr	72 hrs	144 hrs	216 hrs	288 hrs	360 hrs	432 hrs	504 hrs	576 hrs	648 hrs	720 hrs		P	D	SFE
A1	1117.04	309.45	130.12	66.17	46.30	37.68	34.91	32.39	30.53	29.22	28.39		2.294	7.581	3.245
A2	1201.31	388.95	167.03	77.90	55.13	42.05	36.82	34.13	31.44	29.65	28.60		2.901	8.552	3.799
A3	1449.53	435.17	170.83	88.03	60.60	46.30	36.26	33.87	31.44	29.44	28.39		2.994	9.611	3.994
A4	1730.09	525.95	198.32	92.36	62.75	47.45	34.65	32.15	29.44	28.19	27.20		3.049	15.48	4.765
ρ_{polar}	0.37	0.46	0.33	0.54	0.55	0.48	0.19	0.19	0.28	0.19	0.28		0.35		
$\rho_{Dispersive}$	-0.68	-0.60	-0.65	-0.55	-0.56	-0.50	-0.04	0.00	0.35	0.34	0.30			-0.24	
ρ_{SFE}	-0.13	0.00	-0.14	0.10	0.11	0.08	0.14	0.16	0.47	0.39	0.44				0.15

Referring to the result in Tables 33 and 34, it is seen that the polarity of the treated aluminium surface can be named as the primary factor influencing the exposed performance of the adhesively bonded joints. A comparison between the variant B0 and B1, as shown in Table 33, indicates the strong positive correlation between the polar, dispersive, and total surface free energy and the fracture toughness of the adhesively bonded joints where the Pearson values are -0.70, -0.74 and -0.74, respectively. In section 5.5.3, it was found that reducing the surface energy, especially the polar component, can improve the durability of the adhesively bonded joints. This is consistent with the result found for variants A0 and A1, which suggests that the surface polarity of the treated aluminium surface plays a significant role in improving the surface integrity of the PUR adhesively bonded joint and increasing its resistance to degradation under humid conditions. Therefore, it can be claimed that surface polarity is an important factor that should be considered when improving the exposed performance of adhesively bonded joints. Instead, the result for the variant B1 to B4, as stated in Table 34, a moderate negative correlation was suggested for both the polar component and surface free energy as a result of roughening the aluminium prior to NaOH treatment and silane deposition. The value for the Pearson correlation between the polar and dispersive components, total surface free energy and fracture toughness for variants B1 to B4 are -0.24, -0.06 and -0.26, respectively. Once again, based on the comparison between the results presented in section 5.5.4 and the current findings regarding the correlation between surface free energy and fracture toughness, it can be inferred that surface roughening prior to NaOH treatment has a significant impact on increasing the surface area, which enhances the interaction zone and promotes effective silane deposition. This, in turn, leads to improved fracture toughness and exposed performance of the adhesively bonded joint under humid conditions.

Table 33: Correlation between the surface free energy and its components and fracture toughness of variant B0 and B1

	1 hr	72 hrs	144 hrs	216 hrs	288 hrs	360 hrs	432 hrs	504 hrs	576 hrs	648 hrs	720 hrs		P	D	SFE
B0	1506.65	567.10	234.41	158.00	120.96	113.74	105.98	98.88	93.26	86.37	81.61		0.232	2.0808	0.3278
B1	2081.93	1058.64	503.04	326.18	249.27	234.41	223.32	207.88	196.02	191.52	176.73		1.8006	6.4804	2.8122
ρ_{polar}	-0.56	-0.70	-0.71	-0.70	-0.70	-0.69	-0.71	-0.71	-0.70	-0.74	-0.75		-0.70		
$\rho_{Dispersive}$	-0.66	-0.79	-0.84	0.04	-0.83	-0.83	-0.85	-0.84	-0.84	-0.84	-0.87			-0.74	
ρ_{SFE}	-0.66	-0.81	-0.84	0.07	-0.82	-0.82	-0.84	-0.83	-0.83	-0.85	-0.88				-0.74

Table 34: Correlation between the surface free energy and its components and fracture toughness of variant B1 to B4

	1 hr	72 hrs	144 hrs	216 hrs	288 hrs	360 hrs	432 hrs	504 hrs	576 hrs	648 hrs	720 hrs		P	D	SFE
B1	2081.93	1058.64	503.04	326.18	249.27	234.41	223.32	207.88	196.02	191.52	176.73		1.8006	6.4804	2.8122
B2	2472.83	1318.14	621.94	460.85	321.89	305.44	293.79	268.68	258.75	243.19	228.78		2.3326	8.8858	3.2568
B3	2527.94	1395.09	778.14	575.80	435.17	368.14	334.96	321.89	297.61	282.69	258.75		2.5064	9.3814	3.2672
B4	2764.31	1421.99	621.94	435.17	305.44	252.38	210.36	178.75	152.87	134.31	119.72		2.9662	17.657	3.703
ρ_{polar}	0.14	0.41	-0.03	-0.09	-0.14	-0.26	-0.43	-0.48	-0.55	-0.60	-0.66		-0.24		
$\rho_{Dispersive}$	-0.57	-0.59	-0.27	-0.31	-0.25	-0.05	0.13	0.20	0.32	0.40	0.40			-0.06	
ρ_{SFE}	-0.50	-0.30	-0.32	-0.42	-0.39	-0.27	-0.22	-0.19	-0.11	-0.07	-0.12				-0.26

As shown in Table 35 and 36, it is seen that a similar trend between group C and group B can be expected in terms of the obtained correlation between the surface free energy and the fracture toughness of the adhesively bonded joints. Herein, the surface free energy and its components (polar and dispersive, respectively) had a strong negative correlation with the exposed performance of the adhesively bonded joints with values of -0.64, -0.96 and -0.91 for variant C0 and C1, as stated in Table 35. The finding suggests that a decrease in polar component is closely associated with an increase in fracture toughness where dipodal silane was deposited on the aluminium surface, which implies that reducing the total surface free energy of the treated aluminium bond as a result of reduction in surface polarity, is strongly linked to improving the exposed performance of the adhesively bonded joint. This correlation can be interpreted as an indication of the direct influence of the coupling agents on the bonded joints' durability, considering the unipolar nature of the dipodal silane. Taking the results of variants C1 to C4 into account, as stated in Table 36, it can be noted that there is a moderate negative correlation between the surface free energy and polar component and fracture toughness of the adhesively bonded joints with values of -0.42 and -0.47 for polar component and total surface free energy, respectively. This assertion is supported by the findings in section 5.5.2, which showed that the surface roughening before NaOH treatment and silane deposition significantly increased the surface free energy and its polar component, leading to an improvement in the adhesively bonded joint's exposed performance under humid conditions. The positive correlation between fracture toughness and the polar component of surface free energy also supports this claim, indicating that increasing the surface roughness prior to surface treatment can enhance the adhesion strength between the aluminium surfaces, thereby increasing the bonded joints' durability. This can be regarded as supplementary confirmation to the initial findings elucidated by Saleema et al. (Saleema et al., 2012) in their study regarding the impact of NaOH treatment on aluminuim surfaces. The current study further aligns with and extends these earlier insights, offering additional corroboration to the effects previously discovered. Moreover, it substantiates the subsequent research conducted by Hu and his team (Hu et al., 2019). The collective body of evidence from Saleema et al., the present study, and the work by Hu et al. contributes to a progressively reinforced understanding of the implications and outcomes associated with NaOH treatment on aluminuim surfaces. This sequential validation across distinct studies not only enhances the reliability of the observed trends but also underscores the cumulative nature of scientific knowledge in advancing our comprehension of surface treatment effects on materials.

An intriguing finding was observed for group D in terms of the relationship between surface energy and its components and the fracture toughness of the adhesively

bonded joints. As stated in Table 37, the findings for group D reveal a notable result regarding the relationship between surface energy and its components and the fracture toughness of the adhesively bonded joint. Specifically, a significant positive correlation was observed between the polar and total surface-free energy of the treated aluminium surface and the exposed performance of the bonded joint. This is in contrast to the results for group B and group C, where the Pearson correlation coefficients between the polar component, dispersive component, and total surface free energy and fracture toughness were found to be 0.54, -0.06, and 0.44, respectively. The contrasting behaviour observed in group D regarding the correlation between surface energy and its components and fracture toughness of the adhesively bonded joint can be attributed to the high compatibility between the PUR adhesive and surfaces with high polarity. This is due to the moisture-curing nature of this type of adhesive. Therefore, the results found for group D emphasise the importance of altering surface chemistry not only by the application of the coupling agent but also by ensuring good compatibility between the adherend surface and selected adhesive for improved exposed performance of the bonded joints. The correlation between the surface energy and its component on fracture toughness of the adhesively bonded joint can be further expanded with results found for the variant D1 to D4, as stated in Table 38. Hence, it can be concluded that although the correlation between the polar and total surface free energy and fracture toughness of the adhesively bonded joint is only moderate, the surface roughening before NaOH treatment and zirconate coupling agent still have an indirect influence on the exposed performance of the bonded joints. This is in contrast to the direct influence observed on the initial fracture toughness of the PUR joint in a dry condition, as noted in section 5.4.4.

Table 35: Correlation between the surface free energy and its components and fracture toughness of variant C0 and C1

	1 hr	72 hrs	144 hrs	216 hrs	288 hrs	360 hrs	432 hrs	504 hrs	576 hrs	648 hrs	720 hrs		P	D	SFE
C0	651.85	156.26	72.39	48.24	33.62	32.63	29.87	28.80	27.39	26.25	25.70		0.186	1.3624	0.2712
C1	2892.86	1730.09	1021.83	550.17	467.57	405.52	363.15	330.53	301.49	272.10	252.38		1.3368	9.4878	2.4358
ρ_{polar}	-0.58	-0.67	-0.59	-0.63	-0.64	-0.65	-0.65	-0.64	-0.64	-0.67	-0.68		-0.64		
$\rho_{Dispersive}$	-0.98	-0.92	-0.97	-0.97	-0.96	-0.96	-0.97	-0.96	-0.96	-0.96	-0.96			-0.96	
ρ_{SFE}	-0.88	-0.90	-0.88	-0.90	-0.91	-0.91	-0.91	-0.91	-0.91	-0.93	-0.93				-0.91

Table 36: Correlation between the surface free energy and its components and fracture toughness of variant C1 to C4

	1 hr	72 hrs	144 hrs	216 hrs	288 hrs	360 hrs	432 hrs	504 hrs	576 hrs	648 hrs	720 hrs		P	D	SFE
C1	2892.86	1730.09	1021.83	550.17	467.57	405.52	363.15	330.53	301.49	272.10	252.38		1.33	9.48	2.43
C2	3248.51	2266.88	1477.74	904.93	631.71	602.95	550.17	488.46	435.17	394.38	348.70		2.1322	8.8886	2.9216
C3	4140.00	3028.98	2642.82	2316.29	1730.09	1343.19	1246.42	1158.22	1021.83	904.93	791.08		2.495	12.049	3.539
C4	4951.25	2419.22	1876.47	859.98	488.46	417.07	358.25	286.33	243.19	200.66	174.74		2.8244	16.1634	3.7718
ρ_{polar}	0.15	-0.36	-0.19	-0.45	-0.49	-0.53	-0.54	-0.55	-0.54	-0.56	-0.56		-0.42		
$\rho_{Dispersive}$	-0.35	-0.20	-0.38	-0.15	-0.05	-0.02	-0.03	0.00	0.01	0.02	0.03			-0.10	
ρ_{SFE}	-0.02	-0.46	-0.38	-0.52	-0.52	-0.54	-0.55	-0.55	-0.53	-0.55	-0.54				-0.47

Table 37: Correlation between the surface free energy and its components and fracture toughness of variant D0 and D1

	1 hr	72 hrs	144 hrs	216 hrs	288 hrs	360 hrs	432 hrs	504 hrs	576 hrs	648 hrs	720 hrs		P	D	SFE
D0	1695.74	804.29	378.36	203.03	137.20	122.22	114.90	103.89	88.87	81.61	73.72		0.1716	1.349	0.2376
D1	3939.31	2527.94	1293.67	621.94	503.04	454.26	399.90	330.53	255.54	234.41	176.73		1.2154	5.082	2.1092
ρ_{polar}	0.54	0.37	0.52	0.50	0.57	0.56	0.56	0.58	0.59	0.64	0.53		0.54		
$\rho_{Dispersive}$	-0.16	-0.20	-0.14	-0.13	0.10	0.06	-0.01	-0.01	-0.04	-0.02	-0.06			-0.06	
ρ_{SFE}	0.40	0.24	0.39	0.38	0.52	0.50	0.48	0.49	0.49	0.54	0.43				0.44

Table 38: Correlation between the surface free energy and its components and fracture toughness of variant D1 to D4

	1 hr	72 hrs	144 hrs	216 hrs	288 hrs	360 hrs	432 hrs	504 hrs	576 hrs	648 hrs	720 hrs		P	D	SFE
D1	3939.31	2527.94	1293.67	621.94	503.04	454.26	399.90	330.53	255.54	234.41	176.73		1.2154	5.082	2.1092
D2	4700.60	3173.19	1477.74	859.98	575.80	454.26	363.15	282.69	234.41	223.32	198.32		2.1038	7.8006	2.9416
D3	5504.72	4140.00	2419.22	1506.65	969.55	651.85	481.37	373.21	286.33	265.32	237.30		2.427	11.208	3.2736
D4	7062.66	3660.53	1566.61	694.58	378.36	279.10	223.32	172.77	152.87	130.12	101.85		2.794	14.3328	3.4322
ρ_{polar}	-0.04	0.19	0.23	0.51	0.49	0.43	0.35	0.33	0.38	0.41	0.48		0.34		
$\rho_{Dispersive}$	-0.60	-0.71	-0.55	-0.50	-0.28	0.00	0.14	0.24	0.25	0.27	0.05			-0.15	
ρ_{SFE}	-0.39	-0.21	-0.07	0.25	0.36	0.45	0.44	0.49	0.55	0.59	0.54				0.27

As in the previous section, the comprehensive multivariance analysis of variance (MANOVA) method was performed to identify the significant influence of selected surface treatments on, first, the exposed performance of the adhesively bonded joints and second on the surface free energy and its components. The statistical analysis was performed between the variant A0 and A1, A1 to A4, B0 and B1, B1 to B4, C0 and C1, C1 to C4 and D0 and D1, and D1 to D4 in terms of different recorded fracture toughness recorded for 30 days exposure with intervals of three days.

The results from the MANOVA analysis show a significant difference between A0 and A1 when considered jointly on the variables' fracture toughness of the bonded joints, and polar component, Wilks' Λ= 0.001, $F(8,1)$=166.728, partial η^2=0.995. An ANOVA analysis was performed for each dependent variable separately (i.e. surface characteristics), and each analysis was evaluated at a significance level of 0.05. The results showed a significant difference in fracture toughness values over all three-day intervals between variant A0 and A1, as listed in Table 39. There was also a significant difference between A0 and A1 on the value of the polar component, $F(1,8) = 79.518$, $p < 0.01$, partial η^2=0.909. For the dispersive component, the MANOVA shows no significant difference between A0 and A1, $F(1,8) = 4.899$, $p = 0.058$, partial η^2=0.380. Lastly, the result suggests a significant difference between the A0 and A1 on total surface free energy value, $F(1,8) = 83.607$, $p < 0.01$, partial η^2=0.913.

Similar statistical analysis occurred between specimens A1, A2, A3 and A4 to identify the influence of roughening on the aluminium surface prior to NaOH treatment on surface free energy and its components and exposed performance of the adhesively bonded joint. Referring to the results from MANOVA analysis, it can be noted that there is a significant difference between specimen A1 to A4 when considered jointly on the variables' fracture toughness and recorded value for polar component, Wilks' Λ= 0.182, $F(39,12)$= 11.063, partial η^2=0.970. Like the result in section 5.4.4, here also the result reveals that the influence of the surface roughening prior to NaOH treatment on fracture toughness is significant only for the first 15 days of the exposure as shown in Table 40.

Furthermore, there was a significant difference between the identical specimens on the polar component of the treated aluminium surface, in which $F(3,16) = 5.912$, $p = 0.006$, partial η^2=0.526. Referring to Appendix 13, it is evident that significant differences were identified between A1, A2 and A4 compared to A3. For the dispersive component, the MANOVA shows that there was also a significant difference between selected specimens, $F(3,16) = 6.549$, $p = 0.004$, partial η^2=0.551. Referring to Appendix 14, it is evident that there were significant differences which were identical between A1, A2, and A3 compared to A4. Lastly, referring to the MANOVA analysis of the total surface free

energy, it can be concluded that there was a significant difference between selected specimens, $F(3,16) = 4.654$, $p = 0.016$, partial $\eta^2=0.466$. Referring to Appendix 15, it is evident that significant differences were identified with the polar component.

Table 39: MANOVA results for the tests between-subjects effects of fracture toughness and surface free energy and its components for variant A0 to A1

	F Value	P value	Partial Eta Squared
Fracture toughness at day 1	39.526	<.001	.832
Fracture toughness at day 3	129.686	<.001	.942
Fracture toughness at day 6	485.463	<.001	.984
Fracture toughness at day 9	60.784	<.001	.884
Fracture toughness at day 12	258.908	<.001	.970
Fracture toughness at day 15	21.108	.002	.725
Fracture toughness at day 18	16.914	.003	.679
Fracture toughness at day 12	24.259	.001	.752
.Fracture toughness at day 24	45.644	<.001	.851
Fracture toughness at day 27	122.537	<.001	.939
Fracture toughness at day 30	136.256	<.001	.945

Table 40: MANOVA results for the tests between-subjects effects of fracture toughness and surface free energy and its components for variant A1 to A4

	F Value	P value	Partial Eta Squared
Fracture toughness at day 1	13.946	<.001	.723
Fracture toughness at day 3	37.335	<.001	.875
Fracture toughness at day 6	61.437	<.001	.920
Fracture toughness at day 9	46.192	<.001	.896
Fracture toughness at day 12	78.124	<.001	.936
Fracture toughness at day 15	31.647	<.001	.856
Fracture toughness at day 18	1.162	.355	.179
Fracture toughness at day 12	2.221	.125	.294
.Fracture toughness at day 24	2.781	.075	.343
Fracture toughness at day 27	1.338	.297	.201
Fracture toughness at day 30	1.315	.304	.198

The results from the MANOVA analysis show a significant difference between B0 and B1 when considered jointly on the variables' fracture toughness of the bonded joints and polar component, Wilks' Λ= 0.03, $F(8,1)$= 45.798, partial η^2=0.997. A separate ANOVA was conducted for each dependent variable, with each ANOVA evaluated at an alpha level of 0.05. There was a significant difference between B0 and B1 on fracture toughness values over all three-day intervals except for the initial fracture toughness, as listed in Table 41. There was also a significant difference between B0 and B1 on the value of the polar component, $F(1,8)$ = 10.487, p = 0.012, partial η^2=0.567. The MANOVA shows a significant difference between B0 and B1 for the dispersive, $F(1,8)$ = 19.983, p = 0.002, partial η^2=0.714. Lastly, the result suggests a significant difference between the B0 and B1 on the total surface free energy value, $F(1,8)$ = 23.618, p = 0.01, partial η^2=0.747.

Similar statistical analysis was taken between specimens B1, B2, B3 and B4 to identify the influence of roughening on the aluminium surface prior to NaOH treatment and silane deposition on surface free energy and its exposed component performance of the PUR adhesively bonded joint. Referring to the results from MANOVA analysis, it can be noted that there is a significant difference between specimen B1 to B4 when considered jointly on the variables' fracture toughness and recorded value for polar component, Wilks' Λ= 0.187, $F(39,12)$= 37.389, partial η^2=0.991. The result reveals that the influence of the surface roughening prior to NaOH treatment and silane deposition on fracture toughness is significant for the whole exposure period as listed in Table 42. It has been found that the selected surface free energy significantly affected the bonded joints' exposed performance. Furthermore, there was a significant difference between the identical specimens on the polar component of the treated aluminium surface, in which $F(3,16)$ = 6.370, p = 0.005, partial η^2=0.544. Referring to Appendix 16, it is evident that significant differences were identified between B1, B2, and B3 compared to B4. For the dispersive component, the MANOVA shows that there was a significant difference between selected specimens, $F(3,16)$ =23.363, p = 0.001, partial η^2=0.814. Referring to Appendix 17, it is evident that significant differences were identified between B3 and B4 compared to B1 and B3 compared to B2. Lastly, referring to the MANOVA analysis of total surface free energy, it was found that there was no significant difference between selected specimens, $F(3,16)$ = 3.072, p = 0.058, partial η^2=0.366 (see Appendix 18).

Table 41: MANOVA results for the tests between-subjects effects of fracture toughness and surface free energy and its components for variant B0 to B1

	F Value	P value	Partial Eta Squared
Fracture toughness at day 1	14.315	.005	.641
Fracture toughness at day 3	241.883	<.001	.968
Fracture toughness at day 6	150.783	<.001	.950
Fracture toughness at day 9	215.836	<.001	.964
Fracture toughness at day 12	669.942	<.001	.988
Fracture toughness at day 15	680.919	<.001	.988
Fracture toughness at day 18	697.915	<.001	.989
Fracture toughness at day 12	902.689	<.001	.991
.Fracture toughness at day 24	789.373	<.001	.990
Fracture toughness at day 27	4606.795	<.001	.998
Fracture toughness at day 30	1077.394	<.001	.993

Table 42: MANOVA results for the tests between-subjects effects of fracture toughness and surface free energy and its components for variant B1 to B4

	F Value	P value	Partial Eta Squared
Fracture toughness at day 1	5.676	.008	.516
Fracture toughness at day 3	18.074	<.001	.772
Fracture toughness at day 6	23.218	<.001	.813
Fracture toughness at day 9	31.617	<.001	.856
Fracture toughness at day 12	86.876	<.001	.942
Fracture toughness at day 15	38.522	<.001	.878
Fracture toughness at day 18	34.601	<.001	.866
Fracture toughness at day 12	75.957	<.001	.934
.Fracture toughness at day 24	84.061	<.001	.940
Fracture toughness at day 27	152.266	<.001	.966
Fracture toughness at day 30	79.892	<.001	.937

The results from the MANOVA analysis show a significant difference between C0 and C1 when considered jointly on the variables' fracture toughness of the bonded joints and polar component, Wilks' Λ= 0.05, $F(8,1)$= 139.228, partial η^2=0.970. A separate ANOVA was conducted for each dependent variable, with each ANOVA evaluated at an alpha level of 0.05. There was a significant difference between C0 and C1 on fracture toughness values over all three-day intervals, as listed in Table 43. There was also a significant difference between C0 and C1 on the value of the polar component, $F(1,8)$ =6.268, p = 0.037, partial η^2=0.439. For the dispersive component, the MANOVA shows a significant difference between C0 and C1, $F(1,8)$ = 109.247, p = 0.001, partial η^2=0.932. Lastly, the result suggests a significant difference between the C0 and C1 on the total surface free energy value.

Similar statistical analysis occurred between specimens C1, C2, C3 and C4 to identify the influence of surface roughening on the aluminium surface prior to NaOH treatment and dipodal silane deposition on surface-free energy and exposed performance of the adhesively bonded joint. Referring to the results from MANOVA analysis, it can be noted that there is a significant difference between specimen C1 to C4 when considered jointly on the variables' fracture toughness and recorded value for polar component, Wilks' Λ= 0.052, $F(42,9)$= 19.186, partial η^2=0.983. The result reveals that the influence of the surface roughening prior to NaOH treatment and dipodal silane deposition on fracture toughness is significant for the whole exposure period, as stated in Table 44.

Furthermore, there was a significant difference between the identical specimens on the polar component of the treated aluminium surface, in which $F(3,16)$ = 5.988, p = 0.006, partial η^2=0.529. Referring to Appendix 19, it is evident that significant differences were identified between C2 and C3 compared to C1 and C2 and C3 in comparison to C4. For the dispersive component, the MANOVA shows that there was no significant difference between selected specimens, $F(3,16)$ =1.810, p = 0.186, partial η^2=0.253 (see Appendix 20). Lastly, referring to the MANOVA analysis, it can be concluded that there was a significant difference between selected specimens on total surface free energy, $F(3,16)$ = 5.660, p = 0.008, partial η^2=0.515. Referring to Appendix 21, it is evident that the significant differences were identified as similar to the polar component.

Table 43: MANOVA results for the tests between-subjects effects of fracture toughness and surface free energy and its components for variant C0 and C1

	F Value	P value	Partial Eta Squared
Fracture toughness at day 1	227.484	<.001	.966
Fracture toughness at day 3	225.919	<.001	.966
Fracture toughness at day 6	439.420	<.001	.982
Fracture toughness at day 9	531.032	<.001	.985
Fracture toughness at day 12	1141.492	<.001	.993
Fracture toughness at day 15	1199.750	<.001	.993
Fracture toughness at day 18	1325.987	<.001	.994
Fracture toughness at day 12	1316.631	<.001	.994
.Fracture toughness at day 24	3198.229	<.001	.998
Fracture toughness at day 27	5319.045	<.001	.998
Fracture toughness at day 30	3522.102	<.001	.998

Table 44: MANOVA results for the tests between-subjects effects of fracture toughness and surface free energy and its components for variant C1 to C4

	F Value	P value	Partial Eta Squared
Fracture toughness at day 1	25.897	<.001	.829
Fracture toughness at day 3	44.875	<.001	.894
Fracture toughness at day 6	27.338	<.001	.937
Fracture toughness at day 9	72.983	<.001	.932
Fracture toughness at day 12	121.324	<.001	.958
Fracture toughness at day 15	112.639	<.001	.955
Fracture toughness at day 18	109.364	<.001	.954
Fracture toughness at day 12	107.722	<.001	.953
.Fracture toughness at day 24	56.008	<.001	.913
Fracture toughness at day 27	76.995	<.001	.935
Fracture toughness at day 30	57.334	<.001	.915

The results from the MANOVA analysis show a significant difference between D0 and D1 when considered jointly on the variables' fracture toughness of the bonded joints and polar component, Wilks' Λ= 0.152, $F(8,1)$= 929.816, partial η^2=0.995. A separate ANOVA was conducted for each dependent variable, with each ANOVA evaluated at an alpha level of 0.05. There was a significant difference between D0 and D1 on fracture toughness values over all three-day intervals, as listed in Table 45. There was also a significant difference between D0 and D1 on the value of the polar component, $F(1,8)$ = 5.073, p = 0.043, partial η^2=0.388. For the dispersive, the MANOVA shows no significant difference between D0 and D1, $F(1,8)$ = 0.008, p = 0.93, partial η^2=0.001. Lastly, the result suggests a significant difference between the D0 and D1 on the value of S_q, $F(1,8)$ = 3.343, p = 0.015, partial η^2=0.295.

Similar statistical analysis occurred between specimens D1, D2, D3 and D4 to identify the influence of roughening on the aluminium surface prior to NaOH treatment and zirconate deposition on selected roughness parameters exposed performance of the adhesively bonded joint. Referring to the results from the MANOVA analysis, it can be noted that there is a significant difference between specimen D1 to D4 when considered jointly on the variables' fracture toughness and recorded value for polar component, Wilks' Λ= 0.052, $F(39,12)$=13.521, partial η^2=0.976. The result reveals that the influence of the surface roughening prior to NaOH treatment and zirconate deposition on fracture toughness is significant for the whole exposure period, as stated in Table 46.

Furthermore, there was a significant difference between the identical specimens on the polar component of the treated aluminium surface, in which $F(3,16)$ = 6.463, p = 0.005, partial η^2=0.548. Referring to Appendix 22, it is evident that significant differences were identified between D2 and D3 compared to D1 and D2 and D3 compared to D4. For the dispersive component, the MANOVA shows that there was a significant difference between selected specimens, $F(3,16)$ =17.154, p = 0.001, partial η^2=0.763. Referring to Appendix 23, it is evident that significant differences were identified between D2, D3 and D4 compared to D1. Lastly, referring to the MANOVA analysis of total surface energy, it can be concluded that there was a significant difference between selected specimens, $F(3,16)$ = 3.289, p = 0.048, partial η^2=0.381. Referring to Appendix 24, it is evident that significant differences were identified between D2 and D3 compared to D4.

Table 45: MANOVA results for the tests between-subjects effects of fracture toughness and surface free energy and its components for variant D0 and D1

	F Value	P value	Partial Eta Squared
Fracture toughness at day 1	68.019	<.001	.895
Fracture toughness at day 3	32.648	<.001	.803
Fracture toughness at day 6	112.370	<.001	.934
Fracture toughness at day 9	147.795	<.001	.945
Fracture toughness at day 12	291.011	<.001	.973
Fracture toughness at day 15	242.896	<.001	.968
Fracture toughness at day 18	408.183	<.001	.981
Fracture toughness at day 12	728.459	<.001	.986
.Fracture toughness at day 24	272.428	<.001	.971
Fracture toughness at day 27	166.390	<.001	.954
Fracture toughness at day 30	173.345	<.001	.956

Table 46: MANOVA results for the tests between-subjects effects of fracture toughness and surface free energy and its components for variant D1 to D4

	F Value	P value	Partial Eta Squared
Fracture toughness at day 1	14.142	<.001	.726
Fracture toughness at day 3	8.403	<.001	.612
Fracture toughness at day 6	12.418	<.001	.700
Fracture toughness at day 9	45.585	<.001	.895
Fracture toughness at day 12	38.548	<.001	.878
Fracture toughness at day 15	62.618	<.001	.922
Fracture toughness at day 18	64.325	<.001	.923
Fracture toughness at day 12	140.422	<.001	.963
.Fracture toughness at day 24	87.844	<.001	.943
Fracture toughness at day 27	74.273	<.001	.933
Fracture toughness at day 30	145.971	<.001	.965

5.5 Conclusion

The study investigated the fracture toughness of adhesively bonded joints between aluminium substrates treated with different surface treatments under hydrothermal conditions (temperature of 50 C and humidity of 95%). It also evaluated the impact of these surface treatments on the exposed performance of the bonded joints. The correlation between various surface roughness parameters, surface energy, and its components was analysed concerning the adhesively bonded joints' exposed performance. Based on the results, several conclusions can be drawn:

- A strong correlation was observed between the recorded initial crack length and growth and the chosen surface treatments.
- In order to achieve the best exposed performance of the PUR adhesively bonded joint, it was found that the optimal surface roughness should be in the range of 2-2.5µm, which can be achieved through a combination of sandpapering prior to NaOH treatment and dipodal silane.
- It has been observed that having a high fracture toughness in dry conditions does not necessarily ensure better exposed performance of the PUR adhesively bonded joint. The fracture toughness of the PUR adhesively bonded joint decreased to 30% of its original value within the first three days of exposure time when only surface roughness was altered through manual sandpapering and NaOH treatment. This phenomenon was also observed when coupling agents were used. The study revealed that silane and dipodal silane coupling agents had better exposed performance in chamber environmental conditions compared to a zirconate coupling agent, despite having lower initial fracture toughness values.
- The exposed performance of adhesively bonded joints can be influenced by two different factors. The first group consists of factors that have a direct impact on durability, such as surface polarity and the presence of a coupling agent. The second group includes factors that can indirectly affect exposed performance, such as increasing surface roughness (i.e., surface area) or increasing the number of hydroxide groups on the aluminium surface due to NaOH treatment.
- One of the crucial factors in achieving remarkable exposed performance of adhesively bonded joints is the excellent compatibility between the adhesive and the adherend-treated surface. The effectiveness of coupling agents in improving surface stability under humid environmental conditions depends on the selected adhesive type.
- The use of coupling agents like silane and dipodal silane can slow down the decline in fracture toughness over time in humid environmental conditions.

However, the effectiveness of coupling agents in improving the performance of adhesively bonded joints depends on the type of adhesive used and the compatibility between the adhesive and the adherend treated surface. It was observed that the nature of the coupling agent can impact the improvement of adhesively bonded joints, particularly in humid conditions. Zirconate coupling agent was found to be effective in increasing the initial fracture toughness of PUR adhesively bonded joints. However, the results suggest that if good compatibility with the adhesive is achieved, silane and dipodal silane may be better options as coupling agents in humid environmental conditions than zirconate.

- The exposed performance of the aluminium adhesively bonded joint was found to depend significantly on surface roughness parameters. The study showed a strong correlation between surface roughness parameters and recorded fracture toughness, particularly for the initial fracture toughness. However, it was found that the surface roughening prior to NaOH treatment had a minimal effect on the fracture toughness of the adhesively bonded joints.
- A MANOVA was conducted at a significance level of 0.05, and the results indicate that surface treatments have a significant impact on the fracture toughness of PUR adhesive specimens. The study confirms that the primary factor contributing to a durable adhesion between PUR and aluminium substrate is the alteration of surface chemistry, with the NaOH treatment-induced surface roughness being the key driving factor in improving fracture toughness compared to polished specimens.
- The fracture surfaces of the PUR adhesively bonded joints with less polar coupling agents showed a higher ratio of cohesive failure compared to adhesion failure in wet conditions, indicating better exposed performance of the aluminium-to-aluminium joints.

CHAPTER 6

Conclusion and Future Studies

6.1 Conclusion

In this research, a thorough literature review was conducted to identify the various factors that influence the performance of adhesively bonded joints and to identify any gaps in the available literature. It is widely acknowledged that surface treatment plays a crucial role in enhancing the adhesion performance of bonded joints in both dry and wet environments. However, there is a lack of research on the specific factors that determine whether a satisfactory level of improvement in adhesion performance can be achieved. To address this, a combination of destructive methods, such as the single lap joint and Boeing wedge test, along with various surface analysis methods, were used in previous studies to evaluate the effects of different surface treatments based on their nature (i.e., mechanical, chemical). The study conducted a thorough assessment of the initial and exposed performance of the PUR aluminium-to-aluminium adhesively bonded joints, utilising a combination of different surface treatments and analysis methods. The unique approach enabled a comprehensive evaluation of the adhesion performance of the bonded joint under hydrothermal conditions. The aluminium surface properties were modified using various surface treatments. The initial and exposed performance of the adhesively bonded joint was evaluated by applying Pearson correlation coefficient to study the relationship between the joint's performance and different surface characteristics. The statistical significance of this relationship was analysed using multivariate analysis of variance (MANOVA) and post-hoc methods such as LSD and Bonferroni.

To improve the adhesion performance of the aluminium adherend, various surface treatments were applied, and the resulting surface characteristics were analysed. The contact angle of two reference liquids (DI water and diiodomethane), surface energy and its components, and five different surface roughness parameters were measured. The Pearson correlation coefficient was calculated to assess the correlation between the

surface roughness parameters (S_a, S_p, and S_q) and the polar component, dispersive component, and total surface free energy, as a function of different surface treatments. The effect of the selected treatments on the aforementioned surface characteristics was analysed through statistical analysis using MANOVA.

In order to evaluate the initial performance of the adhesively bonded joint, a single lap joint configuration was conducted according to ASTM D1002 standards. The ultimate shear strength of the adhesively bonded joints was compared with the relevant surface characteristics. The correlation between the surface roughness parameters and energy components was also investigated. Statistical analysis was carried out using MANOVA to determine the effect of the surface treatment, surface roughness parameters (S_a, S_p, and S_q), and total surface free energy and its polar and dispersive components on the initial performance of the PUR aluminium-to-aluminium adhesively bonded joints.

The exposed performance of the adhesively bonded joints was evaluated using the Boeing wedge configuration following ASTM D3672. The crack length and growth were monitored at three-day intervals for 30 days in a hydrothermal environment with 95% humidity and 50° C. Fracture toughness was determined using the simple beam theory equation to compare the different surface treatments. A comparison was made between different surface treatments in terms of the initial fracture toughness and durability over various exposure times. Like initial performance analysis, the influence of (1) the surface treatment, (2) surface roughness parameter S_a, S_p, and S_q, and (3) total surface free energy and its polar and dispersive components on the exposed performance of the PUR aluminium-to-aluminium adhesively bonded joints were assessed with the aid of Pearson correlation coefficient and MANOVA statistical method.

Based on the evaluation of the different surface treatments and surface characteristics, the following conclusions can be drawn regarding their influence on the initial and exposed performance of the PUR adhesively bonded joints:

- ✓ The deposition of coupling agents can be significantly affected by the underlying conditions of the adherend surface. Research has shown that NaOH treatment enhances the stage of coupling agent deposition. It has been suggested that the presence of a higher concentration of hydroxyl groups on the NaOH-treated aluminium surface may be the primary reason for this improvement.
- ✓ The deposition of dipodal silane requires a high concentration of hydroxyl groups as no silanol was formed on the polished aluminium surface after dipodal silane deposition.

- ✓ Surface roughening prior to NaOH treatment and different coupling agents can potentially enhance the performance of NaOH treatment by increasing the available surface area for the reaction between the etching solution and aluminium surface. This, in turn, can improve the coupling agent deposition.
- ✓ The study found that different coupling agents resulted in different surface thermodynamic characteristics. Silane and dipodal silane formed a hydrophobic surface, while zirconate formed a hydrophilic surface.
- ✓ The study found that the compatibility of the surface chemistry and polarity with the adhesive used for bonding aluminium is crucial for achieving better performance in both initial and exposed adhesively bonded joints. Therefore, it is important to carefully select the adhesive based on the polar and dispersive components of the treated surface. The results of this study indicate that the PUR adhesive has the highest compatibility with the zirconate coupling agent, which has the highest polar component.
- ✓ Surface roughening of aluminium with #120 prior to NaOH treatment and using coupling agents can promote better initial adhesion performance compared to polished specimens. The study found that the highest improvement was recorded to be 22.33% for the combination of surface roughening of aluminium with #120 prior to NaOH treatment, followed by zirconate deposition.
- ✓ The use of multiple surface treatments can lead to cohesive failure in the initial performance of adhesively bonded joints, which is not observed with polished aluminium surfaces and PUR adhesive. However, the presence of coupling agents was found to have a direct impact on the exposed performance of adhesively bonded joints.
- ✓ The combination of surface roughening using sandpaper and NaOH treatment resulted in a more significant improvement in the initial performance of the adhesively bonded joints, likely due to the complex morphology of the treated surface. Meanwhile, using different coupling agents to alter the surface chemistry showed a significant increase in both initial and exposed performance of the joints.
- ✓ The study revealed that a high fracture toughness in dry conditions did not necessarily indicate better exposed performance of the PUR adhesively bonded joint. When subjected to surface roughness alteration due to manual sandpapering and NaOH treatment, the fracture toughness of the

joint decreased to 30% of its initial value within the first three days of exposure time. This trend was also observed when coupling agents were used. It was found that silane and dipodal silane exhibited better exposed performance in harsh environmental conditions compared to the zirconate coupling agent, despite having a lower initial fracture toughness.

- ✓ The ability of coupling agents to enhance surface stability under humid environmental conditions is dependent on the type of adhesive used. Achieving excellent compatibility between the adhesive and the treated surface of the adherend is considered to be one of the essential factors in achieving remarkable exposed performance of adhesively bonded joints.
- ✓ MANOVA at 0.05 level of significance shows that the surface treatments significantly affect the fracture toughness of the specimens manufactured with PUR adhesive. It was confirmed that surface roughness due to the NaOH treatment is the driving factor in improving the fracture toughness of the adhesively bonded joint compared to polished specimens. It confirms that the alternation in surface chemistry is the primary factor contributing to a durable adhesion between the PUR and aluminium substrate.

6.2 Future studies

Recommendations for future research:

- Study the performance of the adhesively bonded joints for a specific application and examine the true strength of the bonded joint using PUR adhesively bonded joints.
- Investigating the influence of the surface treatment and bonding procedure system in this study with the aid of more advanced statistical methods such as structural equation modelling (SEM).
- Optimising the identified best-case scenario in this study by using different adherend and adhesive.
- Investigation of the influence of bondline thickness for the selected surface treatment (ideally the best-case scenario) on the exposed performance of the adhesively bonded joints.
- Damage identification and in-depth analysis of the failure surface with the aid of advanced surface analysing.
- Identifying the locus of the failure for the specimens with surfaces treated with selected coupling agents.

REFERENCES

Abel, M. L., Allington, R. D., Digby, R. P., Porritt, N., Shaw, S. J., & Watts, J. F. (2006, 2006/02/01/). Understanding the relationship between silane application conditions, bond durability and locus of failure. *International Journal of Adhesion and Adhesives, 26*(1), 2-15. https://doi.org/https://doi.org/10.1016/j.ijadhadh.2005.03.009

Abrahami, S. T., de Kok, J. M. M., Gudla, V. C., Ambat, R., Terryn, H., & Mol, J. M. C. (2017, 2017/08/21). Interface strength and degradation of adhesively bonded porous aluminum oxides. *npj Materials Degradation, 1*(1), 8. https://doi.org/10.1038/s41529-017-0007-0

Adams, D. O., DeVries, K., & Child, C. (2012). Durability of adhesively bonded joints for aircraft structures. *FAA Jt Adv Mater Struct Cent Excell Tech Rev Meet, 22*.

Adams, R., Cowap, J., Farquharson, G., Margary, G., & Vaughn, D. (2009). The relative merits of the Boeing wedge test and the double cantilever beam test for assessing the durability of adhesively bonded joints, with particular reference to the use of fracture mechanics. *International Journal of Adhesion and Adhesives, 29*(6), 609-620.

Adams, R. D. (2005). *Adhesive bonding: science, technology and applications*. Elsevier.

Adams, R. D., Adams, R. D., Comyn, J., Wake, W. C., & Wake, W. (1997). *Structural adhesive joints in engineering*. Springer Science & Business Media.

Ahmad Kamal, S. A., Ritikos, R., & Abdul Rahman, S. (2021, 2021/03/15/). Enhancement of self-cleaning properties and durability of super-hydrophobic carbon nitride nanostructures by post-annealing treatment. *Surface and Coatings Technology, 409*, 126912. https://doi.org/https://doi.org/10.1016/j.surfcoat.2021.126912

Allen, K. (1993). Current theories of adhesion and their relevance to adhesive technology. *Le Journal de Physique IV, 3*(C7), C7-1511-C1517-1516.

Anyfantis, K. N., & Tsouvalis, N. G. (2013). Loading and fracture response of CFRP-to-steel adhesively bonded joints with thick adherents–Part I: experiments. *Composite Structures, 96*, 850-857.

Arenas, J. M., Alía, C., Narbón, J. J., Ocaña, R., & González, C. (2013, 2013/01/01/). Considerations for the industrial application of structural adhesive joints in the aluminium–composite material bonding. *Composites Part B: Engineering, 44*(1), 417-423. https://doi.org/https://doi.org/10.1016/j.compositesb.2012.04.026

Arenas, J. M., Narbón, J. J., & Alía, C. (2010). Optimum adhesive thickness in structural adhesives joints using statistical techniques based on Weibull distribution. *International Journal of Adhesion and Adhesives, 30*(3), 160-165.

Arkles, B., Pan, Y., Larson, G. L., & Singh, M. (2014). Enhanced hydrolytic stability of siliceous surfaces modified with pendant dipodal silanes. *Chemistry (Weinheim an der Bergstrasse, Germany), 20*(30), 9442-9450. https://doi.org/10.1002/chem.201402757

Armstrong, K. (1997). Long-term durability in water of aluminium alloy adhesive joints bonded with epoxy adhesives. *International Journal of Adhesion and Adhesives, 17*(2), 89-105.

ASTM, D. (2005). 907-05. Standard Terminology of Adhesives. *Annu. Book ASTM Stand*.

Awaja, F., Gilbert, M., Kelly, G., Fox, B., & Pigram, P. J. (2009, 2009/09/01/). Adhesion of polymers. *Progress in Polymer Science, 34*(9), 948-968. https://doi.org/https://doi.org/10.1016/j.progpolymsci.2009.04.007

Bai, Y., Nguyen, T. C., Zhao, X. L., & Al-Mahaidi, R. (2014). Environment-assisted degradation of the bond between steel and carbon-fiber-reinforced polymer. *Journal of materials in civil engineering, 26*(9), 04014054.

Baldan, A. (2004, 2004/01/01). Adhesively-bonded joints and repairs in metallic alloys, polymers and composite materials: Adhesives, adhesion theories and surface pretreatment. *Journal of Materials Science, 39*(1), 1-49. https://doi.org/10.1023/B:JMSC.0000007726.58758.e4

Baldan, A. (2012, 2012/10/01/). Adhesion phenomena in bonded joints. *International Journal of Adhesion and Adhesives, 38*, 95-116. https://doi.org/https://doi.org/10.1016/j.ijadhadh.2012.04.007

Banea, M., & da Silva, L. F. (2009). Adhesively bonded joints in composite materials: an overview. *Proceedings of the Institution of Mechanical Engineers, Part L: Journal of Materials: Design and Applications, 223*(1), 1-18.

Banea, M. D. (2019, 2019/08/01). Influence of adherend properties on the strength of adhesively bonded joints. *MRS Bulletin, 44*(8), 625-629. https://doi.org/10.1557/mrs.2019.180

Banea, M. D., da Silva, L. F. M., & Campilho, R. D. S. G. (2015, 2015/01/01). The Effect of Adhesive Thickness on the Mechanical Behavior of a Structural Polyurethane Adhesive. *The Journal of Adhesion, 91*(5), 331-346. https://doi.org/10.1080/00218464.2014.903802

Banea, M. D., Rosioara, M., Carbas, R. J. C., & da Silva, L. F. M. (2018, 2018/10/15/). Multi-material adhesive joints for automotive industry. *Composites Part B: Engineering, 151*, 71-77. https://doi.org/https://doi.org/10.1016/j.compositesb.2018.06.009

Barnes, T., & Pashby, I. (2000). Joining techniques for aluminium spaceframes used in automobiles: Part II—adhesive bonding and mechanical fasteners. *Journal of Materials Processing Technology, 99*(1-3), 72-79.

Belingardi, G., Beyene, A. T., Koricho, E. G., & Martorana, B. (2015, 2015/02/01/). Alternative lightweight materials and component manufacturing technologies for vehicle frontal bumper beam. *Composite Structures, 120*, 483-495. https://doi.org/https://doi.org/10.1016/j.compstruct.2014.10.007

Belyaeva, L. A., van Deursen, P. M., Barbetsea, K. I., & Schneider, G. F. (2018). Hydrophilicity of graphene in water through transparency to polar and dispersive interactions. *Advanced materials, 30*(6), 1703274.

Benard, Q., Fois, M., Grisel, M., Laurens, P., & Joubert, F. (2009). Influence of the polymer surface layer on the adhesion of polymer matrix composites. *Journal of Thermoplastic Composite Materials, 22*(1), 51-61.

Bertho, J., Stolojan, V., Abel, M. L., & Watts, J. F. (2010, 2010/02/01/). The effect of silane incorporation on a metal adhesive interface: A study by electron energy loss spectroscopy. *Micron, 41*(2), 130-134. https://doi.org/https://doi.org/10.1016/j.micron.2009.10.001

Bhushan, B., & Her, E. K. (2010). Fabrication of superhydrophobic surfaces with high and low adhesion inspired from rose petal. *Langmuir, 26*(11), 8207-8217.

Boinovich, L., Emelyanenko, A., Emelyanenko, K., Domantovsky, A., & Shiryaev, A. (2016). Comment on "nanosecond laser textured superhydrophobic metallic surfaces and their chemical sensing applications" by duong v. Ta, andrew dunn, thomas j. Wasley, robert w. Kay, jonathan stringer, patrick j. Smith, colm connaughton, jonathan d. Shephard (Appl. Surf. Sci. 357 (2015) 248–254). *Applied Surface Science, 379*, 111-113.

Bouazaoui, L., & Li, A. (2008). Analysis of steel/concrete interfacial shear stress by means of pull out test. *International Journal of Adhesion and Adhesives, 28*(3), 101-108.

Boutar, Y., Naïmi, S., Mezlini, S., & Ali, M. B. S. (2016). Effect of surface treatment on the shear strength of aluminium adhesive single-lap joints for automotive applications. *International Journal of Adhesion and Adhesives, 67*, 38-43.

Boutar, Y., Naïmi, S., Mezlini, S., Carbas, R. J. C., da Silva, L. F. M., & Ben Sik Ali, M. (2018, 2018/06/01/). Fatigue resistance of an aluminium one-component polyurethane adhesive joint for the automotive industry: Effect of surface roughness and adhesive thickness. *International Journal of Adhesion and Adhesives, 83*, 143-152. https://doi.org/https://doi.org/10.1016/j.ijadhadh.2018.02.012

Bresson, G., Jumel, J., Shanahan, M. E., & Serin, P. (2012). Strength of adhesively bonded joints under mixed axial and shear loading. *International Journal of Adhesion and Adhesives, 35*, 27-35.

Budhe, S., Banea, M. D., de Barros, S., & da Silva, L. F. M. (2017, 2017/01/01/). An updated review of adhesively bonded joints in composite materials. *International Journal of Adhesion and Adhesives, 72*, 30-42. https://doi.org/https://doi.org/10.1016/j.ijadhadh.2016.10.010

Budhe, S., Ghumatkar, A., Birajdar, N., & Banea, M. D. (2015, 2015/12/14). Effect of surface roughness using different adherend materials on the adhesive bond strength. *Applied Adhesion Science, 3*(1), 20. https://doi.org/10.1186/s40563-015-0050-4

Butt, M. A., Chughtai, A., Ahmad, J., Ahmad, R., Majeed, U., & Khan, I. (2008). Theory of adhesion and its practical implications. *Journal of Faculty of Engineering & Technology, 2007*, 21-45.

Cadien, K. C., & Nolan, L. (2012). 7-CMP Method and Practice. *Handbook of Thin Film Deposition*, 179-219.

Castanie, B., Bouvet, C., & Ginot, M. (2020, 2020/08/01/). Review of composite sandwich structure in aeronautic applications. *Composites Part C: Open Access, 1*, 100004. https://doi.org/https://doi.org/10.1016/j.jcomc.2020.100004

Cavezza, F., Boehm, M., Terryn, H., & Hauffman, T. (2020). A review on adhesively bonded aluminium joints in the automotive industry. *Metals, 10*(6), 730.

Choi, M., Xiangde, L., Park, J., Choi, D., Heo, J., Chang, M., Lee, C., & Hong, J. (2017). Superhydrophilic coatings with intricate nanostructure based on biotic materials for antifogging and antibiofouling applications. *Chemical Engineering Journal, 309*, 463-470.

Correia, S., Anes, V., & Reis, L. (2018). Effect of surface treatment on adhesively bonded aluminium-aluminium joints regarding aeronautical structures. *Engineering Failure Analysis, 84*, 34-45.

Costa, M., Viana, G., Da Silva, L., & Campilho, R. (2017). Environmental effect on the fatigue degradation of adhesive joints: a review. *The Journal of Adhesion, 93*(1-2), 127-146.

Critchlow, G., & Brewis, D. (1995). Influence of surface macroroughness on the durability of epoxide-aluminium joints. *International Journal of Adhesion and Adhesives, 15*(3), 173-176.

Critchlow, G., & Brewis, D. (1996). Review of surface pretreatments for aluminium alloys. *International Journal of Adhesion and Adhesives, 16*(4), 255-275.

Croll, S. (2020). Surface roughness profile and its effect on coating adhesion and corrosion protection: A review. *Progress in Organic Coatings, 148*, 105847.

Croll, S. G., & Payne, S. A. (2020). Quantifying abrasive-blasted surface roughness profiles using scanning electron microscopy. *Journal of Coatings Technology and Research*, 1-12.

Da Silva, L. F., Ferreira, N., Richter-Trummer, V., & Marques, E. (2010). Effect of grooves on the strength of adhesively bonded joints. *International Journal of Adhesion and Adhesives, 30*(8), 735-743.

Da Silva, L. F., Öchsner, A., & Adams, R. D. (2011). *Handbook of adhesion technology*. Springer Science & Business Media.

Da Silva, L. F., Öchsner, A., & Adams, R. D. (2018). Introduction to adhesive bonding technology. *Handbook of adhesion technology*, 1-7.

Davies, P., Sohier, L., Cognard, J.-Y., Bourmaud, A., Choqueuse, D., Rinnert, E., & Créac'hcadec, R. (2009). Influence of adhesive bond line thickness on joint strength. *International Journal of Adhesion and Adhesives, 29*(7), 724-736.

Davis, M., & Bond, D. (1999). Principles and practices of adhesive bonded structural joints and repairs. *International Journal of Adhesion and Adhesives, 19*(2-3), 91-105.

Davis, M., Simpson, R., & Force, R. A. A. (2007). A comparison of adhesive bonding processes and training standards in defence and civil aviation industry. Boeing Aging Aircraft Users Forum. Brisbane, Australia,

De Chiffre, L., Lonardo, P., Trumpold, H., Lucca, D., Goch, G., Brown, C., Raja, J., & Hansen, H. N. (2000). Quantitative characterisation of surface texture. *CIRP Annals, 49*(2), 635-652.

dos Santos, R. G., Carvalho, R., Silva, E. R., Bordado, J. C., Cardoso, A. C., do Rosário Costa, M., & Mateus, M. M. (2016). Natural polymeric water-based adhesive from cork liquefaction. *Industrial Crops and Products, 84*, 314-319.

Ebnesajjad, S., & Ebnesajjad, C. (2013). *Surface treatment of materials for adhesive bonding*. William Andrew.

Emelyanenko, A., Boinovich, L., & Emelyanenko, K. (2020). Spreading of biologically relevant liquids over the laser textured surfaces. *Journal of colloid and interface science, 567*, 224-234.

Engelkemeier, K., Mücke, C., Hoyer, K. P., & Schaper, M. (2019). Anodizing of electrolytically galvanized steel surfaces for improved interface properties in fiber metal laminates. *Advanced Composites and Hybrid Materials, 2*, 189-199.

Etzler, F. M. (2018). Determination of the surface free energy of solid surfaces: Statistical considerations. *Advances in Contact Angle, Wettability and Adhesion, 3*, 301-330.

Feoktistov, D. V., Glushkov, D. O., Kuznetsov, G. V., & Orlova, E. G. (2021). Gel fuels based on oil-filled cryogels: Corrosion of tank material and spontaneous ignition. *Chemical Engineering Journal, 421*, 127765.

Fevery, S., Latré, S. K., Vandepitte, D., Debruyne, S., & Hallez, H. (2021, 2021/12/01/). Combination and interaction of ageing parameters on single lap shear adhesive joints. *International Journal of Adhesion and Adhesives, 111*, 102978. https://doi.org/https://doi.org/10.1016/j.ijadhadh.2021.102978

Foadi, F., ten Brink, G. H., Mohammadizadeh, M. R., & Palasantzas, G. (2019). Roughness dependent wettability of sputtered copper thin films: The effect of the local surface slope. *Journal of Applied Physics, 125*(24).

Fürstner, R., Barthlott, W., Neinhuis, C., & Walzel, P. (2005, 2005/02/01). Wetting and Self-Cleaning Properties of Artificial Superhydrophobic Surfaces. *Langmuir, 21*(3), 956-961. https://doi.org/10.1021/la0401011

Gadelmawla, E., Koura, M. M., Maksoud, T. M., Elewa, I. M., & Soliman, H. (2002). Roughness parameters. *Journal of Materials Processing Technology, 123*(1), 133-145.

Galvez, P., Abenojar, J., & Martinez, M. A. (2019, 2019/05/15/). Durability of steel-CFRP structural adhesive joints with polyurethane adhesives. *Composites Part B: Engineering, 165*, 1-9. https://doi.org/https://doi.org/10.1016/j.compositesb.2018.11.097

Ghumatkar, A., Budhe, S., Sekhar, R., Banea, M., & Barros, S. d. (2016). Influence of adherend surface roughness on the adhesive bond strength. *Latin American Journal of Solids and Structures, 13*(13), 2356-2370.

Golaz, B., Michaud, V., Lavanchy, S., & Månson, J.-A. (2013). Design and durability of titanium adhesive joints for marine applications. *International Journal of Adhesion and Adhesives, 45*, 150-157.

Gonzalez-Canche, N., Flores-Johnson, E., Cortes, P., & Carrillo, J. (2018). Evaluation of surface treatments on 5052-H32 aluminum alloy for enhancing the interfacial adhesion of thermoplastic-based fiber metal laminates. *International Journal of Adhesion and Adhesives, 82*, 90-99.

Grant, L., Adams, R. D., & da Silva, L. F. (2009). Experimental and numerical analysis of single-lap joints for the automotive industry. *International Journal of Adhesion and Adhesives, 29*(4), 405-413.

Groche, P., Wohletz, S., Brenneis, M., Pabst, C., & Resch, F. (2014). Joining by forming—A review on joint mechanisms, applications and future trends. *Journal of Materials Processing Technology, 214*(10), 1972-1994. https://doi.org/10.1016/j.jmatprotec.2013.12.022

Gude, M., Prolongo, S., & Ureña, A. (2012). Adhesive bonding of carbon fibre/epoxy laminates: correlation between surface and mechanical properties. *Surface and Coatings Technology, 207*, 602-607.

Guo, Y., Li, Y., Wang, S., Liu, Z.-X., Cai, B., & Wang, P.-C. (2019, 2019/06/01/). Effect of silane treatment on adhesion of adhesive-bonded carbon fiber reinforced nylon 6 composite. *International Journal of Adhesion and Adhesives, 91*, 102-115. https://doi.org/https://doi.org/10.1016/j.ijadhadh.2019.03.008

Haghpanah, B., Chiu, S., & Vaziri, A. (2014). Adhesively bonded lap joints with extreme interface geometry. *International Journal of Adhesion and Adhesives, 48*, 130-138.

Harcarik, M., & Jankovych, R. (2016). Relationship between values of profile and areal surface texture parameters. *MM Sci. J, 5*, 1659-1662.

Harikrishnan, A., Das, S. K., Agnihotri, P. K., & Dhar, P. (2017). Particle and surfactant interactions effected polar and dispersive components of interfacial energy in nanocolloids. *Journal of Applied Physics, 122*(5).

Harris, A. F., & Beevers, A. (1999). The effects of grit-blasting on surface properties for adhesion. *International Journal of Adhesion and Adhesives, 19*(6), 445-452.

Hart-Smith, L. (1999). A peel-type durability test coupon to assess interfaces in bonded, co-bonded, and co-cured composite structures. *International Journal of Adhesion and Adhesives, 19*(2-3), 181-191.

Heshmati, M., Haghani, R., & Al-Emrani, M. (2015). Environmental durability of adhesively bonded FRP/steel joints in civil engineering applications: state of the art. *Composites Part B: Engineering, 81*, 259-275.

Hirsch, J. (2014). Recent development in aluminium for automotive applications. *Transactions of Nonferrous Metals Society of China, 24*(7), 1995-2002.

Hu, Y., Yuan, B., Cheng, F., & Hu, X. (2019). NaOH etching and resin pre-coating treatments for stronger adhesive bonding between CFRP and aluminium alloy. *Composites Part B: Engineering, 178*, 107478.

Imanaka, M., Motohashi, S., Nishi, K., Nakamura, Y., & Kimoto, M. (2009). Crack-growth behavior of epoxy adhesives modified with liquid rubber and cross-linked rubber particles under mode I loading. *International Journal of Adhesion and Adhesives, 29*(1), 45-55.

Islam, M., Tong, L., & Falzon, P. (2014). Influence of metal surface preparation on its surface profile, contact angle, surface energy and adhesion with glass fibre prepreg. *International Journal of Adhesion and Adhesives, 51*, 32-41.

Issa, A. A., & Luyt, A. S. (2019). Kinetics of Alkoxysilanes and Organoalkoxysilanes Polymerization: A Review. *Polymers, 11*(3), 537.

Jaganathan, S., Balaji, A., Ismail, A., & Rathanasamy, R. (2016, 09/01). Fabrication and hemocompatibility assessment of novel polyurethane-based bio-nanofibrous dressing loaded with honey and Carica papaya extract for the management of burn injuries. *International Journal of Nanomedicine, Volume 11*, 4339-4355. https://doi.org/10.2147/IJN.S112265

Jahn, J., Weeber, M., Boehner, J., & Steinhilper, R. (2016). Assessment strategies for composite-metal joining technologies–a review. *Procedia CIRP, 50*, 689-694.

Jang, C. J., Kim, W. S., Kim, H. C., Lee, J. J., & Jeong, J. W. (2011). Study on the Nano and Micro Surface Morphology Effects on Interfacial Strength of Adhesively Bonded Bimaterials. *Procedia Engineering, 10*, 2585-2590.

Jen, Y.-M., & Ko, C.-W. (2010). Evaluation of fatigue life of adhesively bonded aluminum single-lap joints using interfacial parameters. *International Journal of Fatigue, 32*(2), 330-340.

Jiannotti, C., & Ji, H.-F. (2020). Antifogging properties brought upon from nanopillars. *Journal of Nanotechnology Research, 2*(3), 51-59.

Jurf, R. A., & Vinson, J. R. (1985). Effect of moisture on the static and viscoelastic shear properties of epoxy adhesives. *Journal of Materials Science, 20*(8), 2979-2989.

Kanerva, M., & Saarela, O. (2013). The peel ply surface treatment for adhesive bonding of composites: a review. *International Journal of Adhesion and Adhesives, 43*, 60-69.

Kemona, A., & Piotrowska, M. (2020). Polyurethane Recycling and Disposal: Methods and Prospects. *Polymers, 12*(8), 1752. https://www.mdpi.com/2073-4360/12/8/1752

Khan, M., Gali, O., Edrisy, A., & Riahi, A. R. (2016, 12/01). Effect of oxidation and surface roughness on the shear strength of single-lap-joint adhesively bonded metal specimens by tension loading. *Applied Adhesion Science, 4*. https://doi.org/10.1186/s40563-016-0077-1

Khodaei, M., & Shadmani, S. (2019). Superhydrophobicity on aluminum through reactive-etching and TEOS/GPTMS/nano-Al2O3 silane-based nanocomposite coating. *Surface and Coatings Technology, 374*, 1078-1090.

Kim, G., & Ajersch, F. (1994, 1994/02/01). Surface energy and chemical characteristics of interfaces of adhesively bonded aluminium joints. *Journal of Materials Science, 29*(3), 676-681. https://doi.org/10.1007/BF00445978

Kim, J. G., Park, S. W., Yoon, S. H., & Lee, D. G. (2010). Optimum silane treatment for the adhesively bonded aluminum adherends at the cryogenic temperature. *Journal of adhesion science and technology, 24*(4), 775-787.

Kim, W.-S., Yun, I.-H., Lee, J.-J., & Jung, H.-T. (2010, 2010/09/01/). Evaluation of mechanical interlock effect on adhesion strength of polymer–metal interfaces using micro-patterned surface topography. *International Journal of Adhesion and Adhesives, 30*(6), 408-417. https://doi.org/https://doi.org/10.1016/j.ijadhadh.2010.05.004

King, R. (2014). *Surface treatment & finishing of aluminium*. Elsevier.

Kinloch, A. J., & Kinloch, A. J. (1987). *Adhesion and adhesives: science and technology*. Springer Science & Business Media.

Kono, M., Sun, X., Li, R., Wong, K., Mitchell, K., & Foster, T. (2001). Characterization of aluminum surfaces after different pretreatments and exposure to silane coupling agents. *Surface Review and Letters, 8*(01n02), 43-50.

Kostin, V., Nasonov, F., & Zinin, A. (2021). Influence of adhesive bond line thickness on joint strength of composite aircraft structures. Journal of Physics: Conference Series,

Kuznetsov, G., Feoktistov, D., Orlova, E., Zykov, I., & Islamova, A. (2019). Droplet state and mechanism of contact line movement on laser-textured aluminum alloy surfaces. *Journal of colloid and interface science, 553*, 557-566.

Kuznetsov, G., Orlova, E., Feoktistov, D., Islamova, A., & Zhuikov, A. (2020). Droplet spreading and wettability of abrasive processed aluminum alloy surfaces. *Metals and Materials International, 26*, 46-55.

Kwon, D.-J., Kim, J.-H., Kim, Y.-J., Kim, J.-J., Park, S.-M., Kwon, I.-J., Shin, P.-S., DeVries, L. K., & Park, J.-M. (2019, 2019/08/01/). Comparison of interfacial adhesion of hybrid materials of aluminum/carbon fiber reinforced epoxy composites with different surface roughness. *Composites Part B: Engineering, 170*, 11-18. https://doi.org/https://doi.org/10.1016/j.compositesb.2019.04.022

Leach, R. (2013). *Characterisation of areal surface texture*. Springer.

Leach, R., Evans, C., He, L., Davies, A., Duparré, A., Henning, A., Jones, C. W., & O'Connor, D. (2015). Open questions in surface topography measurement: a roadmap. *Surface Topography: Metrology and Properties, 3*(1), 013001.

Leena, K., Athira, K. K., Bhuvaneswari, S., Suraj, S., & Rao, V. L. (2016, 2016/10/01/). Effect of surface pre-treatment on surface characteristics and adhesive bond strength of aluminium alloy. *International Journal of Adhesion and Adhesives, 70*, 265-270. https://doi.org/https://doi.org/10.1016/j.ijadhadh.2016.07.012

Li, J., Li, Y., Huang, M., Xiang, Y., & Liao, Y. (2018). Improvement of aluminum lithium alloy adhesion performance based on sandblasting techniques. *International Journal of Adhesion and Adhesives, 84*, 307-316.

Li, J., Yan, Y., Zhang, T., & Liang, Z. (2015). Experimental study of adhesively bonded CFRP joints subjected to tensile loads. *International Journal of Adhesion and Adhesives, 57*, 95-104.

Li, W., & Li, D. (2006). Influence of surface morphology on corrosion and electronic behavior. *Acta materialia, 54*(2), 445-452.

Li, Y., Li, J., Huang, M., Xiang, Y., & Yang, Y. (2019, 2019/08/18). Effect of combined surface treatment on the adhesion performance of aluminium-lithium alloy. *Journal of adhesion science and technology, 33*(16), 1821-1835. https://doi.org/10.1080/01694243.2019.1613947

Liao, L., Huang, C., & Sawa, T. (2013). Effect of adhesive thickness, adhesive type and scarf angle on the mechanical properties of scarf adhesive joints. *International Journal of Solids and Structures, 50*(25-26), 4333-4340.

Lunder, O., Olsen, B., & Nisancioglu, K. (2002, 2002/01/01/). Pre-treatment of AA6060 aluminium alloy for adhesive bonding. *International Journal of Adhesion and Adhesives, 22*(2), 143-150. https://doi.org/https://doi.org/10.1016/S0143-7496(01)00049-5

Malijevský, A. (2014). Does surface roughness amplify wetting? *The Journal of chemical physics, 141*(18).

Marceau, J., Moji, Y., & McMillian, J. (1977). Wedge test for evaluating adhesive-bonded surface durability. *Adhesives age, 20*(10), 28-34.

Marques, A. C., Mocanu, A., Tomić, N. Z., Balos, S., Stammen, E., Lundevall, A., Abrahami, S. T., Günther, R., de Kok, J. M. M., & Teixeira de Freitas, S. (2020). Review on Adhesives and Surface Treatments for Structural Applications: Recent Developments on Sustainability and Implementation for Metal and Composite Substrates. *Materials, 13*(24), 5590. https://www.mdpi.com/1996-1944/13/24/5590

Martínez-Landeros, V., Vargas-Islas, S., Cruz-González, C. E., Barrera, S., Mourtazov, K., & Ramírez-Bon, R. (2019). Studies on the influence of surface treatment type, in the effectiveness of structural adhesive bonding, for carbon fiber reinforced composites. *Journal of Manufacturing Processes, 39*, 160-166.

McDevitt, J. E., & Grigsby, W. J. (2014). Life cycle assessment of bio-and petro-chemical adhesives used in fiberboard production. *Journal of Polymers and the Environment, 22*(4), 537-544.

Mittal, K. L., & Pizzi, A. (1999). *Adhesion promotion techniques: technological applications*. CRC press.

Mohan, J., Ivanković, A., & Murphy, N. (2014). Mode I fracture toughness of co-cured and secondary bonded composite joints. *International Journal of Adhesion and Adhesives, 51*, 13-22.

Mohseni, M., Mirabedini, M., Hashemi, M., & Thompson, G. E. (2006, 2006/12/01/). Adhesion performance of an epoxy clear coat on aluminum alloy in the presence of vinyl and amino-silane primers. *Progress in Organic Coatings, 57*(4), 307-313. https://doi.org/https://doi.org/10.1016/j.porgcoat.2006.09.007

Monte, S. J. (1982). Why titanates and zirconates are different than silanes. Symposium on June,

Monte, S. J. (2002). Neoalkoxy Titanate and Zirconate Coupling Agent Additives in Thermoplastics. *Polymers and Polymer Composites, 10*(2), 121-172. https://doi.org/10.1177/096739110201000202

Monteiro, J., Campilho, R., Marques, E., & Da Silva, L. (2015). Experimental estimation of the mechanical and fracture properties of a new epoxy adhesive. *Applied Adhesion Science, 3*(1), 1-17.

Mühlhan, C., Weidner, S., Friedrich, J., & Nowack, H. (1999, 1999/09/01/). Improvement of bonding properties of polypropylene by low-pressure plasma treatment. *Surface and Coatings Technology, 116-119*, 783-787. https://doi.org/https://doi.org/10.1016/S0257-8972(99)00203-0

Multigner, M., Frutos, E., González-Carrasco, J. L., Jiménez, J. A., Marín, P., & Ibáñez, J. (2009). Influence of the sandblasting on the subsurface microstructure of 316LVM stainless steel: Implications on the magnetic and mechanical properties. *Materials Science and Engineering: C, 29*(4), 1357-1360.

Narbon, J. J., Moreno-Díaz, C., & Arenas, J. M. (2019, 2019/01/05/). Influence of surface treatment on the surface energy of an aluminium substrate. *Colloids and Surfaces A: Physicochemical and Engineering Aspects, 560*, 323-329. https://doi.org/https://doi.org/10.1016/j.colsurfa.2018.09.010

Nasreen, A., Shaker, K., & Nawab, Y. (2021). Effect of surface treatments on metal–composite adhesive bonding for high-performance structures: an overview. *Composite Interfaces, 28*(12), 1221-1256.

Neto, J. A. B. P., Campilho, R. D. S. G., & da Silva, L. F. M. (2012, 2012/09/01/). Parametric study of adhesive joints with composites. *International Journal of Adhesion and Adhesives, 37*, 96-101. https://doi.org/https://doi.org/10.1016/j.ijadhadh.2012.01.019

Nettikaden, V. C. (2008). *Formation of Anodic Films on Al-Ti Alloys*. The University of Manchester (United Kingdom).

Njuguna, J. (2016). *Lightweight composite structures in transport: design, manufacturing, analysis and performance*. Woodhead publishing.

Ogrodniczek, J. (2022). COMPARATIVE ANALYSIS OF THE ENDURANCE OF UV-CURED ADHESIVE JOINTS. *Journal of Technology and Exploitation in Mechanical Engineering, 8*(1), 26-31.

Okada, M., Taketa, H., Torii, Y., Irie, M., & Matsumoto, T. (2019). Optimal sandblasting conditions for conventional-type yttria-stabilized tetragonal zirconia polycrystals. *Dental Materials, 35*(1), 169-175.

Osouli-Bostanabad, K., Tutunchi, A., & Eskandarzade, M. (2017). The influence of pre-bond surface treatment over the reliability of steel epoxy/glass composites bonded joints. *International Journal of Adhesion and Adhesives, 75*, 145-154.

Ozel, A., Yazici, B., Akpinar, S., Aydin, M. D., & Temiz, Ş. (2014). A study on the strength of adhesively bonded joints with different adherends. *Composites Part B: Engineering, 62*, 167-174.

Packham, D. E. (2003). Surface energy, surface topography and adhesion. *International journal of adhesion and adhesives, 23*(6), 437-448.

Packham, D. E. (2006). *Handbook of adhesion*. John Wiley & Sons.

Park, S. Y., Choi, W. J., & Choi, H. S. (2018). A review of the recent developments in surface treatment techniques for bonded repair of aluminum airframe structures. *International Journal of Adhesion and Adhesives, 80*, 16-29.

Park, Y.-B., Song, M.-G., Kim, J.-J., Kweon, J.-H., & Choi, J.-H. (2010). Strength of carbon/epoxy composite single-lap bonded joints in various environmental conditions. *Composite Structures, 92*(9), 2173-2180.

Patel, S., & Bhavsar, C. (2013). Analysis of pharmacokinetic data by wilk's lambda (An important tool of manova). *International Journal of Pharmaceutical Science Invention, 2*(1), 36-44.

Paz, E., Narbón, J. J., Abenojar, J., Cledera, M., & del Real, J. C. (2016, 2016/11/01). Influence of Acrylic Adhesive Viscosity and Surface Roughness on the Properties of Adhesive Joint. *The Journal of Adhesion, 92*(11), 877-891. https://doi.org/10.1080/00218464.2015.1051221

Pereira, A., Ferreira, J., Antunes, F., & Bártolo, P. (2009). Study on the fatigue strength of AA 6082-T6 adhesive lap joints. *International Journal of Adhesion and Adhesives, 29*(6), 633-638.

Pituch, K. A., & Stevens, J. P. (2015). Assumptions in MANOVA. In *Applied multivariate statistics for the social sciences* (pp. 219-264). Routledge.

Pletincx, S., Fockaert, L. L. I., Mol, J. M. C., Hauffman, T., & Terryn, H. (2019, 2019/06/06). Probing the formation and degradation of chemical interactions from model molecule/metal oxide to buried polymer/metal oxide interfaces. *npj Materials Degradation, 3*(1), 23. https://doi.org/10.1038/s41529-019-0085-2

Plueddemann, E. P. (1982). Nature of adhesion through silane coupling agents. In *Silane coupling agents* (pp. 111-139). Springer.

Pohl, K., Ozcan, O., Voigt, M., & Grundmeier, G. (2016). Adhesion and corrosive delamination of epoxy films on chemically etched ZnMgAl-alloy coatings. *Materials and Corrosion, 67*(10), 1020-1026.

Possart, W., & Brede, M. (2019). *Adhesive Joints: Ageing and Durability of Epoxies and Polyurethanes*. John Wiley & Sons.

Pramanik, A., Basak, A. K., Dong, Y., Sarker, P. K., Uddin, M. S., Littlefair, G., Dixit, A. R., & Chattopadhyaya, S. (2017, 2017/10/01/). Joining of carbon fibre reinforced polymer (CFRP) composites and aluminium alloys – A review. *Composites Part A: Applied Science and Manufacturing, 101*, 1-29. https://doi.org/https://doi.org/10.1016/j.compositesa.2017.06.007

Prolongo, S. G., del Rosario, G., & Ureña, A. (2006, 2006/06/01/). Comparative study on the adhesive properties of different epoxy resins. *International Journal of Adhesion and Adhesives, 26*(3), 125-132. https://doi.org/https://doi.org/10.1016/j.ijadhadh.2005.02.004

Reddy, N. S., Jinaga, U. K., Charuku, B. R., Penumakala, P. K., & Prasad, A. V. S. S. (2019, 2019/04/01/). Failure analysis of AA8011-pultruded GFRP adhesively bonded similar and dissimilar joints. *International Journal of Adhesion and Adhesives, 90*, 97-105. https://doi.org/https://doi.org/10.1016/j.ijadhadh.2019.02.004

Reina, J. M. A., Prìeto, J. J. N., & García, C. A. (2009, 2009/05/26). Influence of the Surface Finish on the Shear Strength of Structural Adhesive Joints and Application Criteria in Manufacturing Processes. *The Journal of Adhesion, 85*(6), 324-340. https://doi.org/10.1080/00218460902880164

Reis, P. N., Ferreira, J., & Antunes, F. (2011). Effect of adherend's rigidity on the shear strength of single lap adhesive joints. *International Journal of Adhesion and Adhesives, 31*(4), 193-201.

Rhee, K., Lee, S., Choi, N., & Park, S. (2003). Treatment of CFRP by IAR method and its effect on the fracture behavior of adhesive bonded CFRP/aluminum composites. *Materials Science and Engineering: A, 357*(1-2), 270-276.

Ribbens, W., Heisler, H., Blundell, M., Harty, D., Brown, J., Serpento, S., Robertson, A., Garrett, T., Fenton, J., & Davies, G. (2009). *Automotive Engineering e-Mega Reference*. Butterworth-Heinemann.

Rider, A. N. (2006, 2006/02/01/). Factors influencing the durability of epoxy adhesion to silane pretreated aluminium. *International Journal of Adhesion and Adhesives, 26*(1), 67-78. https://doi.org/https://doi.org/10.1016/j.ijadhadh.2005.03.005

Rider, A. N., & Arnott, D. R. (2000, 2000/01/01/). Boiling water and silane pre-treatment of aluminium alloys for durable adhesive bonding. *International Journal of Adhesion and Adhesives, 20*(3), 209-220. https://doi.org/https://doi.org/10.1016/S0143-7496(99)00046-9

Rodgers, J. L., & Nicewander, W. A. (1988). Thirteen ways to look at the correlation coefficient. *American statistician*, 59-66.

Rudawska, A. (2010, 2010/10/01/). Adhesive joint strength of hybrid assemblies: Titanium sheet-composites and aluminium sheet-composites—Experimental and numerical verification. *International Journal of Adhesion and Adhesives, 30*(7), 574-582. https://doi.org/https://doi.org/10.1016/j.ijadhadh.2010.05.006

Rudawska, A. (2012). Adhesive properties. In *Scanning electron microscopy*. IntechOpen.

Rudawska, A., Danczak, I., Müller, M., & Valasek, P. (2016, 2016/10/01/). The effect of sandblasting on surface properties for adhesion. *International Journal of Adhesion and Adhesives, 70*, 176-190. https://doi.org/https://doi.org/10.1016/j.ijadhadh.2016.06.010

Sababi, M., Terryn, H., & Mol, J. (2017). The influence of a Zr-based conversion treatment on interfacial bonding strength and stability of epoxy coated carbon steel. *Progress in Organic Coatings, 105*, 29-36.

Safari, A., Farahani, M., & Ghabezi, P. (2020). Experimental study on the influences of different surface treatment processes and adhesive type on the aluminum adhesive-bonded joint strength. *Mechanics Based Design of Structures and Machines*, 1-14. https://doi.org/10.1080/15397734.2020.1777876

Sakundarini, N., Taha, Z., Abdul-Rashid, S. H., & Ghazila, R. A. R. (2013). Optimal multi-material selection for lightweight design of automotive body assembly incorporating recyclability. *Materials & Design, 50*, 846-857.

Saldanha, D., Canto, C., Da Silva, L., Carbas, R., Chaves, F., Nomura, K., & Ueda, T. (2013). Mechanical characterization of a high elongation and high toughness epoxy adhesive. *International Journal of Adhesion and Adhesives, 47*, 91-98.

Saleema, N., Sarkar, D. K., Paynter, R. W., Gallant, D., & Eskandarian, M. (2012, 2012/11/15/). A simple surface treatment and characterization of AA 6061 aluminum alloy surface for adhesive bonding applications. *Applied Surface Science, 261*, 742-748. https://doi.org/https://doi.org/10.1016/j.apsusc.2012.08.091

Sargent, J. (2005). Durability studies for aerospace applications using peel and wedge tests. *International Journal of Adhesion and Adhesives, 25*(3), 247-256.

Şekercíoğlu, T., Rende, H., Gülsöz, A., & Meran, C. (2003). The effects of surface roughness on the strength of adhesively bonded cylindrical components. *Journal of Materials Processing Technology, 142*(1), 82-86.

Shahid, M., & Hashim, S. A. (2002, 2002/01/01/). Effect of surface roughness on the strength of cleavage joints. *International Journal of Adhesion and Adhesives, 22*(3), 235-244. https://doi.org/https://doi.org/10.1016/S0143-7496(01)00059-8

Sheasby, P., & Pinner, R. (2001). Introduction: Aluminium, its properties, alloys and finishes. *Met. Finish*, 435-450.

Shrivastava, P. (1995). Environmental technologies and competitive advantage. *Strategic Management Journal, 16*(S1), 183-200. https://doi.org/10.1002/smj.4250160923

Singh, M., Keister, H., Matisons, J., Pan, Y., Zazyczny, J., & Arkles, B. (2014, 11/17). Dipodal Silanes: Important Tool for Surface Modification to Improve Durability. *MRS Online Proceeding Library, 1648*. https://doi.org/10.1557/opl.2014.257

[Record #287 is using a reference type undefined in this output style.]

Sun, L., Yuan, G., Gao, L., Yang, J., Chhowalla, M., Gharahcheshmeh, M. H., Gleason, K. K., Choi, Y. S., Hong, B. H., & Liu, Z. (2021). Chemical vapour deposition. *Nature Reviews Methods Primers, 1*(1), 5.

Sun, L., Zhang, W., Xue, W., & Zeng, Z. (2022). Reactive polyurethane hot melt adhesives based on polycarbonate and sebacic acid-based polyester polyols. *Journal of adhesion science and technology*, 1-20.

Svoboda, M., Malijevský, A., & Lísal, M. (2015). Wetting properties of molecularly rough surfaces. *The Journal of chemical physics, 143*(10).

Sykes, J. (1982). Surface treatments for steel. *Surface Analysis and Pretreatment of Plastics and Metals*, 153-174.

Tao, R., Alfano, M., & Lubineau, G. (2019). In situ analysis of interfacial damage in adhesively bonded composite joints subjected to various surface pretreatments. *Composites Part A: Applied Science and Manufacturing, 116*, 216-223.

Tatar, J., Torrence, C. E., Mecholsky Jr, J. J., Taylor, C. R., & Hamilton, H. (2018). Effects of silane surface functionalization on interfacial fracture energy and durability of adhesive bond between cement paste and epoxy. *International Journal of Adhesion and Adhesives, 84*, 132-142.

Teisala, H., Tuominen, M., & Kuusipalo, J. (2011). Adhesion mechanism of water droplets on hierarchically rough superhydrophobic rose petal surface. *Journal of Nanomaterials, 2011*, 1-6.

Todorov, V., & Filzmoser, P. (2010). Robust Statistic for the One-way MANOVA. *Computational Statistics & Data Analysis, 54*(1), 37-48.

Ungureanu, D., Taranu, N., Lupasteanu, V., Rosu, A.-R., & Mihai, P. (2016). The adhesion theories applied to adhesively bonded joints of fiber reinforced polymer composite elements. *Buletinul Institutului Politehnic din lasi. Sectia Constructii, Arhitectura, 62*(2), 37.

van Dam, J. P. B., Abrahami, S. T., Yilmaz, A., Gonzalez-Garcia, Y., Terryn, H., & Mol, J. M. C. (2020, 2020/01/01/). Effect of surface roughness and chemistry on the adhesion and durability of a steel-epoxy adhesive interface. *International Journal of Adhesion and Adhesives, 96*, 102450. https://doi.org/https://doi.org/10.1016/j.ijadhadh.2019.102450

Viswanadham, P. (2000). Role of adhesion and its reliability implications in electronic assemblies. 4th International Conference on Adhesive Joining and Coating Technology in Electronics Manufacturing. Proceedings. Presented at Adhesives in Electronics 2000 (Cat. No. 00EX431),

Volpe, A., Gaudiuso, C., & Ancona, A. (2020). Laser Fabrication of Anti-Icing Surfaces: A Review. *Materials, 13*(24), 5692. https://www.mdpi.com/1996-1944/13/24/5692

Wake, W. C. (1982). *Adhesion and the Formulation of Adhesives*.

Wang, B., Hu, X., & Lu, P. (2017, 2017/03/01/). Improvement of adhesive bonding of grit-blasted steel substrates by using diluted resin as a primer. *International Journal of Adhesion and Adhesives, 73*, 92-99. https://doi.org/https://doi.org/10.1016/j.ijadhadh.2016.11.012

Wang, H.-Y., Zhu, R.-F., Lu, Y.-P., Xiao, G.-Y., He, K., Yuan, Y., Ma, X.-N., & Li, Y. (2014). Effect of sandblasting intensity on microstructures and properties of pure titanium micro-arc oxidation coatings in an optimized composite technique. *Applied Surface Science, 292*, 204-212.

Wang, S., Liu, Z., Zhang, L., Guo, Y., Song, J., Lou, J., Guan, Q., He, C., & You, Z. (2019). Strong, detachable, and self-healing dynamic crosslinked hot melt polyurethane adhesive [10.1039/C9QM00233B]. *Materials Chemistry Frontiers, 3*(9), 1833-1839. https://doi.org/10.1039/C9QM00233B

Wang, X.-X., Fu, H.-L., Jiang, M.-Y., Liu, Y.-C., & Hu, J.-M. (2019, 04/02). Understanding the role of silane pretreatments in an organic coating system. Part 2: a study of molecular dynamics simulation. *Journal of Coatings Technology and Research, 16*. https://doi.org/10.1007/s11998-019-00183-9

Wang, X., Qu, Z., Lai, T., Ren, G., & Wang, W. (2022). Enhancing water transport performance of gas diffusion layers through coupling manipulation of pore structure and hydrophobicity. *Journal of Power Sources, 525*, 231121.

Wang, X., & Zhang, Q. (2020). Role of surface roughness in the wettability, surface energy and flotation kinetics of calcite. *Powder technology, 371*, 55-63.

Wenzel, R. N. (1936). Resistance of solid surfaces to wetting by water. *Industrial & Engineering Chemistry, 28*(8), 988-994.

Werner, O., Wågberg, L., & Lindström, T. (2005). Wetting of structured hydrophobic surfaces by water droplets. *Langmuir, 21*(26), 12235-12243.

Wielant, J., Posner, R., Hausbrand, R., Grundmeier, G., & Terryn, H. (2010). SKP as a tool to study the physicochemical interaction at buried metal–coating interfaces. *Surface and Interface Analysis, 42*(6-7), 1005-1009.

Wu, C., Yu, Y.-Z., Tam, L.-h., Orr, J., & He, L. (2021). Effect of glass fiber sheet in adhesive on the bond and galvanic corrosion behaviours of CFRP-Steel bonded system. *Composite Structures, 259*, 113218.

Xu, Y., Li, H., Shen, Y., Liu, S., Wang, W., & Tao, J. (2016). Improvement of adhesion performance between aluminum alloy sheet and epoxy based on anodizing technique. *International Journal of Adhesion and Adhesives, 70*, 74-80.

Yang, G., Yang, T., Yuan, W., & Du, Y. (2019, 2019/03/01/). The influence of surface treatment on the tensile properties of carbon fiber-reinforced epoxy composites-bonded joints. *Composites Part B: Engineering, 160*, 446-456. https://doi.org/https://doi.org/10.1016/j.compositesb.2018.12.095

Yu, S., Oh, K. H., Hwang, J. Y., & Hong, S. H. (2019, 2019/04/15/). The effect of amino-silane coupling agents having different molecular structures on the mechanical properties of basalt fiber-reinforced polyamide 6,6 composites. *Composites Part B: Engineering, 163*, 511-521. https://doi.org/https://doi.org/10.1016/j.compositesb.2018.12.148

Zain, N. M., Ahmad, S. H., & Ali, E. S. (2014, 2014/12/01/). Effect of surface treatments on the durability of green polyurethane adhesive bonded aluminium alloy. *International Journal of Adhesion and Adhesives, 55*, 43-55. https://doi.org/https://doi.org/10.1016/j.ijadhadh.2014.07.007

Zhang, J., Zhao, X., Zuo, Y., Xiong, J., & Zhang, X. (2008). Effect of surface pretreatment on adhesive properties of aluminum alloys. *Journal of Materials Science & Technology, 24*(2), 236-240.

Zhang, S., Wang, Z., Wang, Z., Xu, Y., & Chen, K. (2004). Some new features in the development of metal forming technology. *Journal of Materials Processing Technology, 151*(1-3), 39-47.

Zhou, J., Liu, F., Dai, X., Jiao, L., Yao, H., Du, Z., Wang, H., & Qiu, X. (2019). Surface modification of high-performance polyimide fibres by using a silane coupling agent. *Composite Interfaces, 26*(8), 687-698.

Zhu, W., Li, W., Mu, S., Yang, Y., & Zuo, X. (2016, 2016/10/30/). The adhesion performance of epoxy coating on AA6063 treated in Ti/Zr/V based solution. *Applied Surface Science, 384*, 333-340. https://doi.org/https://doi.org/10.1016/j.apsusc.2016.05.083

Zielecfei, W., Pawlus, P., Perłowski, R., & Dzierwa, A. (2013). Surface topography effect on strength of lap adhesive joints after mechanical pre-treatment. *Archives of Civil and Mechanical Engineering, 13*(2), 175-185.

APPENDIX

Appendix 1a

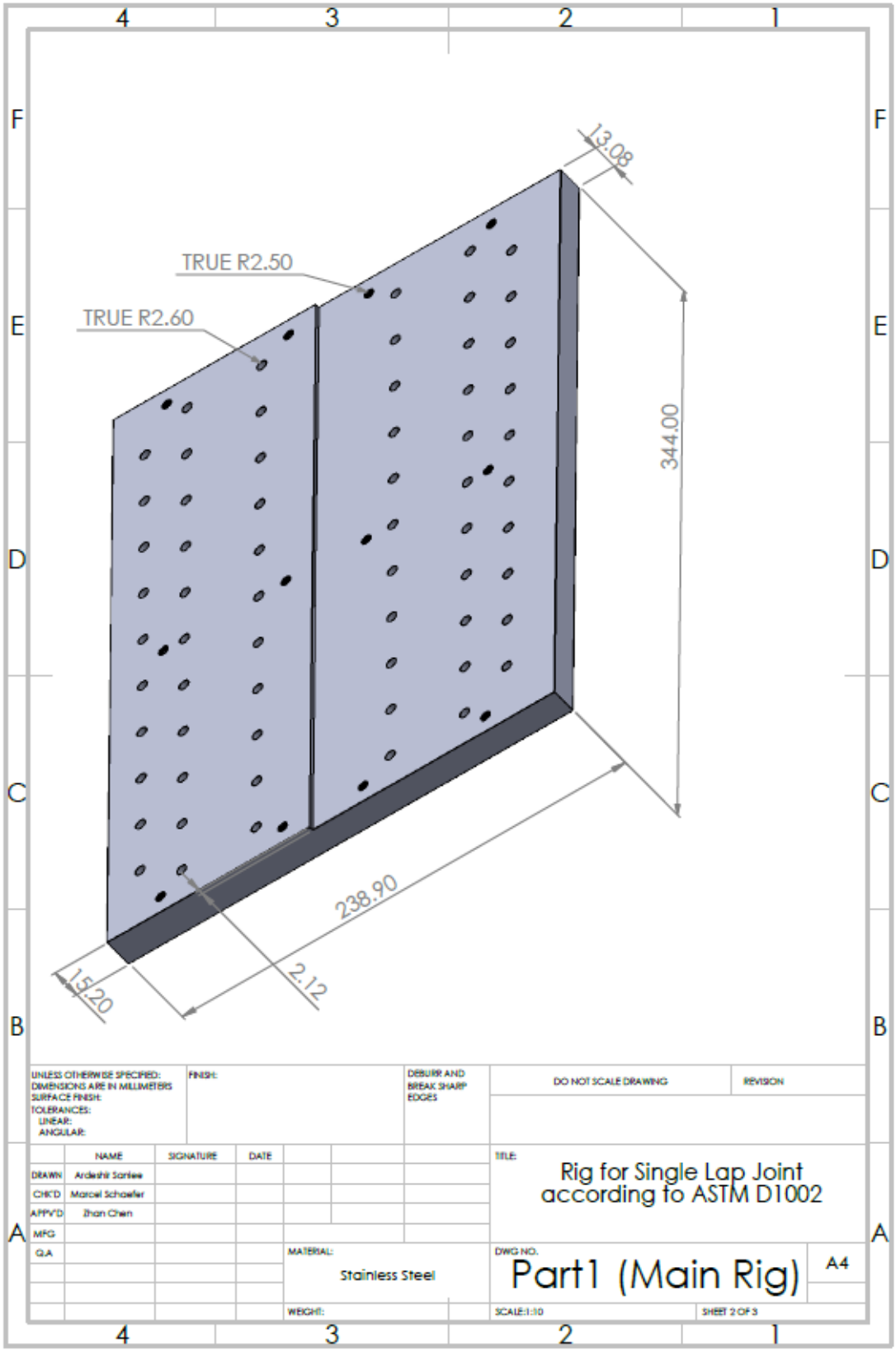

Appendix 1b

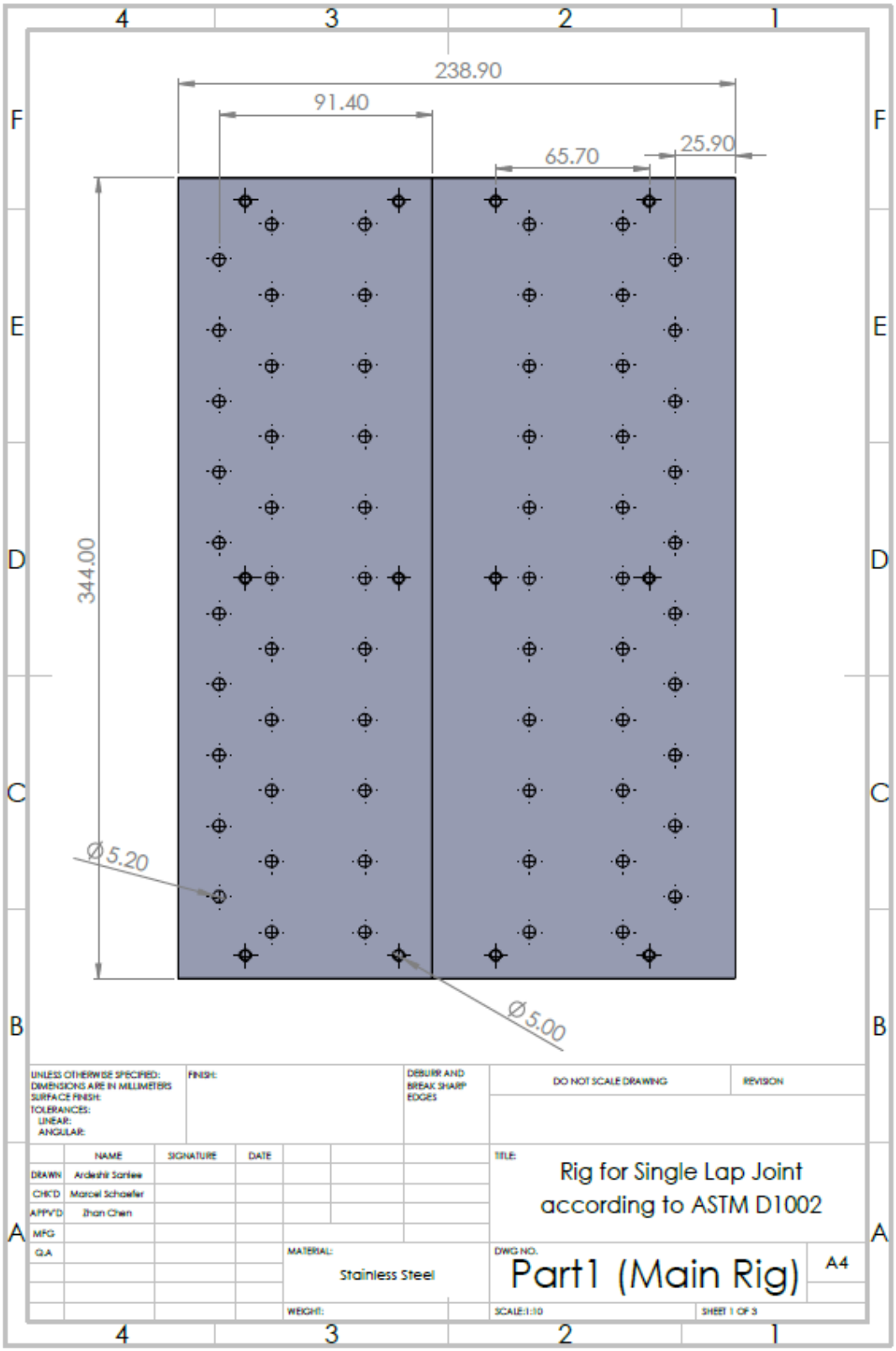
238.90
91.40
65.70
25.90
344.00
Ø5.20
Ø5.00
UNLESS OTHERWISE SPECIFIED:
DIMENSIONS ARE IN MILLIMETERS
SURFACE FINISH:
TOLERANCES:
LINEAR:
ANGULAR:
FINISH:
DEBURR AND BREAK SHARP EDGES
DO NOT SCALE DRAWING
REVISION
NAME
SIGNATURE
DATE
DRAWN
Ardeshir Sarlee
CHK'D
Marcel Schaefer
APPV'D
Zhan Chen
MFG
Q.A
MATERIAL:
Stainless Steel
WEIGHT:
TITLE:
Rig for Single Lap Joint
according to ASTM D1002
DWG NO.
Part1 (Main Rig)
A4
SCALE:1:10
SHEET 1 OF 3

Appendix 1c

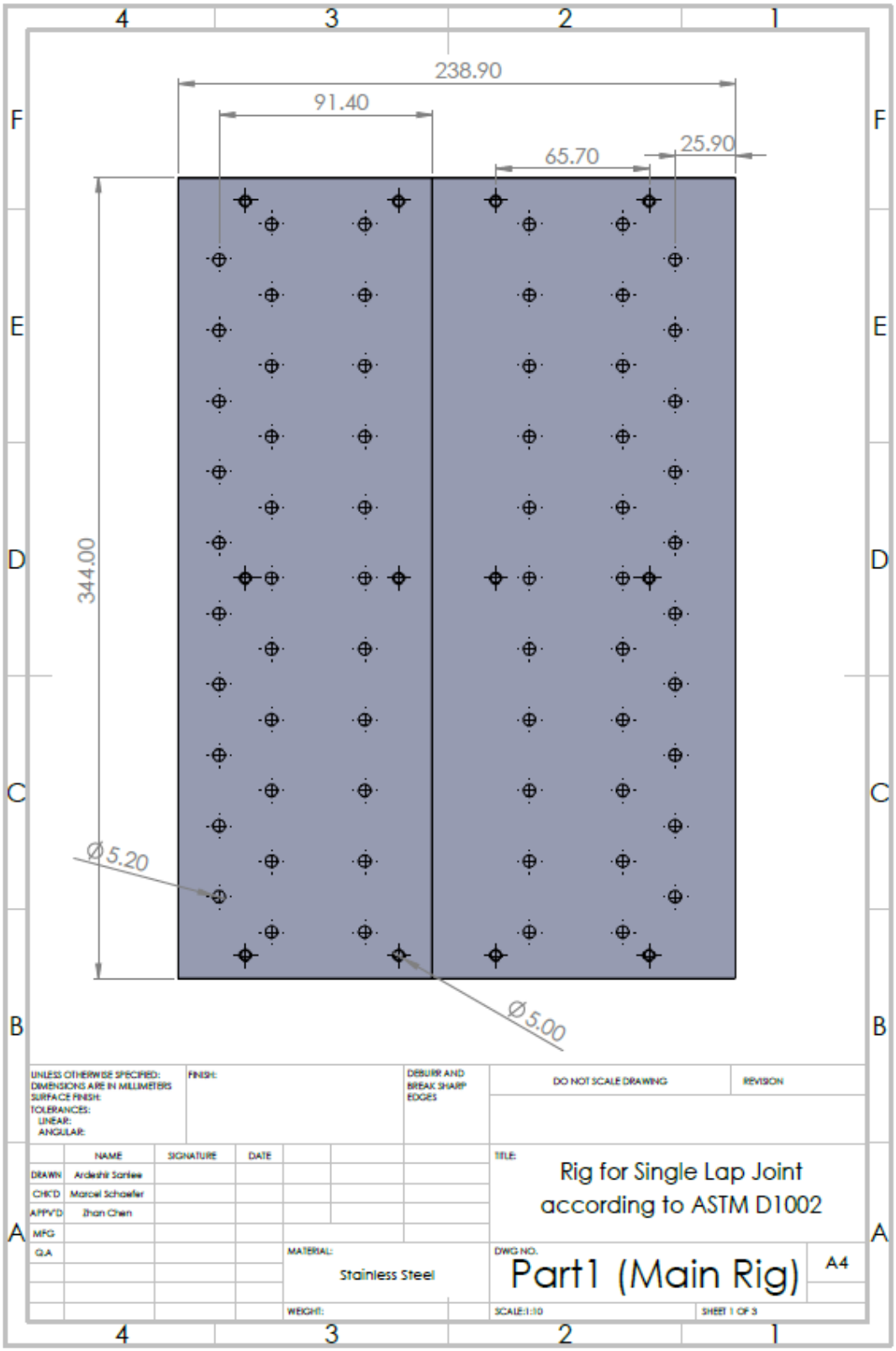
238.90
91.40
65.70
25.90
344.00
Ø5.20
Ø5.00
UNLESS OTHERWISE SPECIFIED:
DIMENSIONS ARE IN MILLIMETERS
SURFACE FINISH:
TOLERANCES:
LINEAR:
ANGULAR:
FINISH:
DEBURR AND BREAK SHARP EDGES
DO NOT SCALE DRAWING
REVISION
NAME
SIGNATURE
DATE
DRAWN
Ardeshir Sarlee
CHK'D
Marcel Schaefer
APPV'D
Zhan Chen
MFG
Q.A
MATERIAL:
Stainless Steel
WEIGHT:
TITLE:
Rig for Single Lap Joint
according to ASTM D1002
DWG NO.
Part1 (Main Rig)
A4
SCALE:1:10
SHEET 1 OF 3

Appendix 1

Multiple Comparisons

Dependent Variable		(I) Surface Treatment Method	(J) Surface Treatment Method	Mean Difference (I-J)	Std. Error	Sig.	95% Confidence Interval	
							Lower Bound	Upper Bound
Fracture toughness @1	LSD	A1	A2	-74.81000	105.863037	.490	-299.22961	149.60961
			A3	-330.36360*	105.863037	.007	-554.78321	-105.94399
			A4	-617.30360*	105.863037	<.001	-841.72321	-392.88399
		A2	A1	74.81000	105.863037	.490	-149.60961	299.22961
			A3	-255.55360*	105.863037	.028	-479.97321	-31.13399
			A4	-542.49360*	105.863037	<.001	-766.91321	-318.07399
		A3	A1	330.36360*	105.863037	.007	105.94399	554.78321
			A2	255.55360*	105.863037	.028	31.13399	479.97321
			A4	-286.94000*	105.863037	.015	-511.35961	-62.52039
		A4	A1	617.30360*	105.863037	<.001	392.88399	841.72321
			A2	542.49360*	105.863037	<.001	318.07399	766.91321
			A3	286.94000*	105.863037	.015	62.52039	511.35961
	Bonferroni	A1	A2	-74.81000	105.863037	1.000	-393.28136	243.66136
			A3	-330.36360*	105.863037	.040	-648.83496	-11.89224
			A4	-617.30360*	105.863037	<.001	-935.77496	-298.83224
		A2	A1	74.81000	105.863037	1.000	-243.66136	393.28136
			A3	-255.55360	105.863037	.169	-574.02496	62.91776
			A4	-542.49360*	105.863037	<.001	-860.96496	-224.02224
		A3	A1	330.36360*	105.863037	.040	11.89224	648.83496
			A2	255.55360	105.863037	.169	-62.91776	574.02496
			A4	-286.94000	105.863037	.093	-605.41136	31.53136
		A4	A1	617.30360*	105.863037	<.001	298.83224	935.77496
			A2	542.49360*	105.863037	<.001	224.02224	860.96496
			A3	286.94000	105.863037	.093	-31.53136	605.41136
Fracture toughness @3	LSD	A1	A2	-79.67260*	21.089452	.002	-124.38024	-34.96496
			A3	-127.09600*	21.089452	<.001	-171.80364	-82.38836
			A4	-217.95440*	21.089452	<.001	-262.66204	-173.24676
		A2	A1	79.67260*	21.089452	.002	34.96496	124.38024
			A3	-47.42340*	21.089452	.039	-92.13104	-2.71576
			A4	-138.28180*	21.089452	<.001	-182.98944	-93.57416
		A3	A1	127.09600*	21.089452	<.001	82.38836	171.80364
			A2	47.42340*	21.089452	.039	2.71576	92.13104
			A4	-90.85840*	21.089452	<.001	-135.56604	-46.15076
		A4	A1	217.95440*	21.089452	<.001	173.24676	262.66204
			A2	138.28180*	21.089452	<.001	93.57416	182.98944
			A3	90.85840*	21.089452	<.001	46.15076	135.56604
	Bonferroni	A1	A2	-79.67260*	21.089452	.010	-143.11671	-16.22849
			A3	-127.09600*	21.089452	<.001	-190.54011	-63.65189
			A4	-217.95440*	21.089452	<.001	-281.39851	-154.51029
		A2	A1	79.67260*	21.089452	.010	16.22849	143.11671
			A3	-47.42340	21.089452	.234	-110.86751	16.02071
			A4	-138.28180*	21.089452	<.001	-201.72591	-74.83769
		A3	A1	127.09600*	21.089452	<.001	63.65189	190.54011
			A2	47.42340	21.089452	.234	-16.02071	110.86751
			A4	-90.85840*	21.089452	.003	-154.30251	-27.41429
		A4	A1	217.95440*	21.089452	<.001	154.51029	281.39851
			A2	138.28180*	21.089452	<.001	74.83769	201.72591
			A3	90.85840*	21.089452	.003	27.41429	154.30251

Fracture toughness @6	LSD	A1	A2	-37.03760*	5.068647	<.001	-47.78265	-26.29255
			A3	-40.75560*	5.068647	<.001	-51.50065	-30.01055
			A4	-68.38980*	5.068647	<.001	-79.13485	-57.64475
		A2	A1	37.03760*	5.068647	<.001	26.29255	47.78265
			A3	-3.71800	5.068647	.474	-14.46305	7.02705
			A4	-31.35220*	5.068647	<.001	-42.09725	-20.60715
		A3	A1	40.75560*	5.068647	<.001	30.01055	51.50065
			A2	3.71800	5.068647	.474	-7.02705	14.46305
			A4	-27.63420*	5.068647	<.001	-38.37925	-16.88915
		A4	A1	68.38980*	5.068647	<.001	57.64475	79.13485
			A2	31.35220*	5.068647	<.001	20.60715	42.09725
			A3	27.63420*	5.068647	<.001	16.88915	38.37925
	Bonferroni	A1	A2	-37.03760*	5.068647	<.001	-52.28578	-21.78942
			A3	-40.75560*	5.068647	<.001	-56.00378	-25.50742
			A4	-68.38980*	5.068647	<.001	-83.63798	-53.14162
		A2	A1	37.03760*	5.068647	<.001	21.78942	52.28578
			A3	-3.71800	5.068647	1.000	-18.96618	11.53018
			A4	-31.35220*	5.068647	<.001	-46.60038	-16.10402
		A3	A1	40.75560*	5.068647	<.001	25.50742	56.00378
			A2	3.71800	5.068647	1.000	-11.53018	18.96618
			A4	-27.63420*	5.068647	<.001	-42.88238	-12.38602
		A4	A1	68.38980*	5.068647	<.001	53.14162	83.63798
			A2	31.35220*	5.068647	<.001	16.10402	46.60038
			A3	27.63420*	5.068647	<.001	12.38602	42.88238

Fracture toughness @9	LSD	A1	A2	-11.64060*	2.418782	<.001	-16.76819	-6.51301
			A3	-21.76940*	2.418782	<.001	-26.89699	-16.64181
			A4	-26.10480*	2.418782	<.001	-31.23239	-20.97721
		A2	A1	11.64060*	2.418782	<.001	6.51301	16.76819
			A3	-10.12880*	2.418782	<.001	-15.25639	-5.00121
			A4	-14.46420*	2.418782	<.001	-19.59179	-9.33661
		A3	A1	21.76940*	2.418782	<.001	16.64181	26.89699
			A2	10.12880*	2.418782	<.001	5.00121	15.25639
			A4	-4.33540	2.418782	.092	-9.46299	.79219
		A4	A1	26.10480*	2.418782	<.001	20.97721	31.23239
			A2	14.46420*	2.418782	<.001	9.33661	19.59179
			A3	4.33540	2.418782	.092	-.79219	9.46299
	Bonferroni	A1	A2	-11.64060*	2.418782	.001	-18.91710	-4.36410
			A3	-21.76940*	2.418782	<.001	-29.04590	-14.49290
			A4	-26.10480*	2.418782	<.001	-33.38130	-18.82830
		A2	A1	11.64060*	2.418782	.001	4.36410	18.91710
			A3	-10.12880*	2.418782	.004	-17.40530	-2.85230
			A4	-14.46420*	2.418782	<.001	-21.74070	-7.18770
		A3	A1	21.76940*	2.418782	<.001	14.49290	29.04590
			A2	10.12880*	2.418782	.004	2.85230	17.40530
			A4	-4.33540	2.418782	.552	-11.61190	2.94110
		A4	A1	26.10480*	2.418782	<.001	18.82830	33.38130
			A2	14.46420*	2.418782	<.001	7.18770	21.74070
			A3	4.33540	2.418782	.552	-2.94110	11.61190

Fracture toughness @12	LSD	A1	A2	-8.8502*	1.17514	<.001	-11.3414	-6.3590
			A3	-14.3098*	1.17514	<.001	-16.8010	-11.8186
			A4	-16.4780*	1.17514	<.001	-18.9692	-13.9868
		A2	A1	8.8502*	1.17514	<.001	6.3590	11.3414
			A3	-5.4596*	1.17514	<.001	-7.9508	-2.9684
			A4	-7.6278*	1.17514	<.001	-10.1190	-5.1366
		A3	A1	14.3098*	1.17514	<.001	11.8186	16.8010
			A2	5.4596*	1.17514	<.001	2.9684	7.9508
			A4	-2.1682	1.17514	.084	-4.6594	.3230
		A4	A1	16.4780*	1.17514	<.001	13.9868	18.9692
			A2	7.6278*	1.17514	<.001	5.1366	10.1190
			A3	2.1682	1.17514	.084	-.3230	4.6594
	Bonferroni	A1	A2	-8.8502*	1.17514	<.001	-12.3854	-5.3150
			A3	-14.3098*	1.17514	<.001	-17.8450	-10.7746
			A4	-16.4780*	1.17514	<.001	-20.0132	-12.9428
		A2	A1	8.8502*	1.17514	<.001	5.3150	12.3854
			A3	-5.4596*	1.17514	.002	-8.9948	-1.9244
			A4	-7.6278*	1.17514	<.001	-11.1630	-4.0926
		A3	A1	14.3098*	1.17514	<.001	10.7746	17.8450
			A2	5.4596*	1.17514	.002	1.9244	8.9948
			A4	-2.1682	1.17514	.502	-5.7034	1.3670
		A4	A1	16.4780*	1.17514	<.001	12.9428	20.0132
			A2	7.6278*	1.17514	<.001	4.0926	11.1630
			A3	2.1682	1.17514	.502	-1.3670	5.7034
Fracture toughness @15	LSD	A1	A2	-4.3230*	1.11435	.001	-6.6853	-1.9607
			A3	-8.5862*	1.11435	<.001	-10.9485	-6.2239
			A4	-9.7296*	1.11435	<.001	-12.0919	-7.3673
		A2	A1	4.3230*	1.11435	.001	1.9607	6.6853
			A3	-4.2632*	1.11435	.001	-6.6255	-1.9009
			A4	-5.4066*	1.11435	<.001	-7.7689	-3.0443
		A3	A1	8.5862*	1.11435	<.001	6.2239	10.9485
			A2	4.2632*	1.11435	.001	1.9009	6.6255
			A4	-1.1434	1.11435	.320	-3.5057	1.2189
		A4	A1	9.7296*	1.11435	<.001	7.3673	12.0919
			A2	5.4066*	1.11435	<.001	3.0443	7.7689
			A3	1.1434	1.11435	.320	-1.2189	3.5057
	Bonferroni	A1	A2	-4.3230*	1.11435	.008	-7.6753	-.9707
			A3	-8.5862*	1.11435	<.001	-11.9385	-5.2339
			A4	-9.7296*	1.11435	<.001	-13.0819	-6.3773
		A2	A1	4.3230*	1.11435	.008	.9707	7.6753
			A3	-4.2632*	1.11435	.009	-7.6155	-.9109
			A4	-5.4066*	1.11435	.001	-8.7589	-2.0543
		A3	A1	8.5862*	1.11435	<.001	5.2339	11.9385
			A2	4.2632*	1.11435	.009	.9109	7.6155
			A4	-1.1434	1.11435	1.000	-4.4957	2.2089
		A4	A1	9.7296*	1.11435	<.001	6.3773	13.0819
			A2	5.4066*	1.11435	.001	2.0543	8.7589
			A3	1.1434	1.11435	1.000	-2.2089	4.4957
Fracture toughness @18	LSD	A1	A2	-1.9566	1.40561	.183	-4.9364	1.0232
			A3	-1.3974	1.40561	.335	-4.3772	1.5824
			A4	.2540	1.40561	.859	-2.7258	3.2338
		A2	A1	1.9566	1.40561	.183	-1.0232	4.9364
			A3	.5592	1.40561	.696	-2.4206	3.5390
			A4	2.2106	1.40561	.135	-.7692	5.1904
		A3	A1	1.3974	1.40561	.335	-1.5824	4.3772
			A2	-.5592	1.40561	.696	-3.5390	2.4206
			A4	1.6514	1.40561	.257	-1.3284	4.6312
		A4	A1	-.2540	1.40561	.859	-3.2338	2.7258
			A2	-2.2106	1.40561	.135	-5.1904	.7692
			A3	-1.6514	1.40561	.257	-4.6312	1.3284
	Bonferroni	A1	A2	-1.9566	1.40561	1.000	-6.1851	2.2719
			A3	-1.3974	1.40561	1.000	-5.6259	2.8311
			A4	.2540	1.40561	1.000	-3.9745	4.4825
		A2	A1	1.9566	1.40561	1.000	-2.2719	6.1851
			A3	.5592	1.40561	1.000	-3.6693	4.7877
			A4	2.2106	1.40561	.812	-2.0179	6.4391
		A3	A1	1.3974	1.40561	1.000	-2.8311	5.6259
			A2	-.5592	1.40561	1.000	-4.7877	3.6693
			A4	1.6514	1.40561	1.000	-2.5771	5.8799
		A4	A1	-.2540	1.40561	1.000	-4.4825	3.9745
			A2	-2.2106	1.40561	.812	-6.4391	2.0179
			A3	-1.6514	1.40561	1.000	-5.8799	2.5771

Fracture toughness @21	LSD	A1	A2	-1.7534	.96084	.087	-3.7903	.2835
			A3	-1.4878	.96084	.141	-3.5247	.5491
			A4	.2310	.96084	.813	-1.8059	2.2679
		A2	A1	1.7534	.96084	.087	-.2835	3.7903
			A3	.2656	.96084	.786	-1.7713	2.3025
			A4	1.9844	.96084	.055	-.0525	4.0213
		A3	A1	1.4878	.96084	.141	-.5491	3.5247
			A2	-.2656	.96084	.786	-2.3025	1.7713
			A4	1.7188	.96084	.093	-.3181	3.7557
		A4	A1	-.2310	.96084	.813	-2.2679	1.8059
			A2	-1.9844	.96084	.055	-4.0213	.0525
			A3	-1.7188	.96084	.093	-3.7557	.3181
	Bonferroni	A1	A2	-1.7534	.96084	.520	-4.6439	1.1371
			A3	-1.4878	.96084	.846	-4.3783	1.4027
			A4	.2310	.96084	1.000	-2.6595	3.1215
		A2	A1	1.7534	.96084	.520	-1.1371	4.6439
			A3	.2656	.96084	1.000	-2.6249	3.1561
			A4	1.9844	.96084	.333	-.9061	4.8749
		A3	A1	1.4878	.96084	.846	-1.4027	4.3783
			A2	-.2656	.96084	1.000	-3.1561	2.6249
			A4	1.7188	.96084	.556	-1.1717	4.6093
		A4	A1	-.2310	.96084	1.000	-3.1215	2.6595
			A2	-1.9844	.96084	.333	-4.8749	.9061
			A3	-1.7188	.96084	.556	-4.6093	1.1717
Fracture toughness @24	LSD	A1	A2	-.9142	.82513	.284	-2.6634	.8350
			A3	-.9686	.82513	.258	-2.7178	.7806
			A4	1.1036	.82513	.200	-.6456	2.8528
		A2	A1	.9142	.82513	.284	-.8350	2.6634
			A3	-.0544	.82513	.948	-1.8036	1.6948
			A4	2.0178*	.82513	.026	.2686	3.7670
		A3	A1	.9686	.82513	.258	-.7806	2.7178
			A2	.0544	.82513	.948	-1.6948	1.8036
			A4	2.0722*	.82513	.023	.3230	3.8214
		A4	A1	-1.1036	.82513	.200	-2.8528	.6456
			A2	-2.0178*	.82513	.026	-3.7670	-.2686
			A3	-2.0722*	.82513	.023	-3.8214	-.3230
	Bonferroni	A1	A2	-.9142	.82513	1.000	-3.3965	1.5681
			A3	-.9686	.82513	1.000	-3.4509	1.5137
			A4	1.1036	.82513	1.000	-1.3787	3.5859
		A2	A1	.9142	.82513	1.000	-1.5681	3.3965
			A3	-.0544	.82513	1.000	-2.5367	2.4279
			A4	2.0178	.82513	.158	-.4645	4.5001
		A3	A1	.9686	.82513	1.000	-1.5137	3.4509
			A2	.0544	.82513	1.000	-2.4279	2.5367
			A4	2.0722	.82513	.139	-.4101	4.5545
		A4	A1	-1.1036	.82513	1.000	-3.5859	1.3787
			A2	-2.0178	.82513	.158	-4.5001	.4645
			A3	-2.0722	.82513	.139	-4.5545	.4101
Fracture toughness @27	LSD	A1	A2	-.4314	.81195	.602	-2.1527	1.2899
			A3	-.2982	.81195	.718	-2.0195	1.4231
			A4	1.0352	.81195	.221	-.6861	2.7565
		A2	A1	.4314	.81195	.602	-1.2899	2.1527
			A3	.1332	.81195	.872	-1.5881	1.8545
			A4	1.4666	.81195	.090	-.2547	3.1879
		A3	A1	.2982	.81195	.718	-1.4231	2.0195
			A2	-.1332	.81195	.872	-1.8545	1.5881
			A4	1.3334	.81195	.120	-.3879	3.0547
		A4	A1	-1.0352	.81195	.221	-2.7565	.6861
			A2	-1.4666	.81195	.090	-3.1879	.2547
			A3	-1.3334	.81195	.120	-3.0547	.3879
	Bonferroni	A1	A2	-.4314	.81195	1.000	-2.8740	2.0112
			A3	-.2982	.81195	1.000	-2.7408	2.1444
			A4	1.0352	.81195	1.000	-1.4074	3.4778
		A2	A1	.4314	.81195	1.000	-2.0112	2.8740
			A3	.1332	.81195	1.000	-2.3094	2.5758
			A4	1.4666	.81195	.538	-.9760	3.9092
		A3	A1	.2982	.81195	1.000	-2.1444	2.7408
			A2	-.1332	.81195	1.000	-2.5758	2.3094
			A4	1.3334	.81195	.720	-1.1092	3.7760
		A4	A1	-1.0352	.81195	1.000	-3.4778	1.4074
			A2	-1.4666	.81195	.538	-3.9092	.9760
			A3	-1.3334	.81195	.720	-3.7760	1.1092

Fracture toughness @30	LSD	A1	A2	-.2014	.80354	.805	-1.9048	1.5020
			A3	-.0734	.80354	.928	-1.7768	1.6300
			A4	1.2006	.80354	.155	-.5028	2.9040
		A2	A1	.2014	.80354	.805	-1.5020	1.9048
			A3	.1280	.80354	.875	-1.5754	1.8314
			A4	1.4020	.80354	.100	-.3014	3.1054
		A3	A1	.0734	.80354	.928	-1.6300	1.7768
			A2	-.1280	.80354	.875	-1.8314	1.5754
			A4	1.2740	.80354	.132	-.4294	2.9774
		A4	A1	-1.2006	.80354	.155	-2.9040	.5028
			A2	-1.4020	.80354	.100	-3.1054	.3014
			A3	-1.2740	.80354	.132	-2.9774	.4294
	Bonferroni	A1	A2	-.2014	.80354	1.000	-2.6187	2.2159
			A3	-.0734	.80354	1.000	-2.4907	2.3439
			A4	1.2006	.80354	.928	-1.2167	3.6179
		A2	A1	.2014	.80354	1.000	-2.2159	2.6187
			A3	.1280	.80354	1.000	-2.2893	2.5453
			A4	1.4020	.80354	.601	-1.0153	3.8193
		A3	A1	.0734	.80354	1.000	-2.3439	2.4907
			A2	-.1280	.80354	1.000	-2.5453	2.2893
			A4	1.2740	.80354	.795	-1.1433	3.6913
		A4	A1	-1.2006	.80354	.928	-3.6179	1.2167
			A2	-1.4020	.80354	.601	-3.8193	1.0153
			A3	-1.2740	.80354	.795	-3.6913	1.1433

Appendix 2

Sp	LSD	A1	A2	-8.4430*	2.09523	<.001	-12.8847	-4.0013
			A3	-7.3174*	2.09523	.003	-11.7591	-2.8757
			A4	-13.1316*	2.09523	<.001	-17.5733	-8.6899
		A2	A1	8.4430*	2.09523	<.001	4.0013	12.8847
			A3	1.1256	2.09523	.599	-3.3161	5.5673
			A4	-4.6886*	2.09523	.040	-9.1303	-.2469
		A3	A1	7.3174*	2.09523	.003	2.8757	11.7591
			A2	-1.1256	2.09523	.599	-5.5673	3.3161
			A4	-5.8142*	2.09523	.014	-10.2559	-1.3725
		A4	A1	13.1316*	2.09523	<.001	8.6899	17.5733
			A2	4.6886*	2.09523	.040	.2469	9.1303
			A3	5.8142*	2.09523	.014	1.3725	10.2559
	Bonferroni	A1	A2	-8.4430*	2.09523	.006	-14.7462	-2.1398
			A3	-7.3174*	2.09523	.018	-13.6206	-1.0142
			A4	-13.1316*	2.09523	<.001	-19.4348	-6.8284
		A2	A1	8.4430*	2.09523	.006	2.1398	14.7462
			A3	1.1256	2.09523	1.000	-5.1776	7.4288
			A4	-4.6886	2.09523	.239	-10.9918	1.6146
		A3	A1	7.3174*	2.09523	.018	1.0142	13.6206
			A2	-1.1256	2.09523	1.000	-7.4288	5.1776
			A4	-5.8142	2.09523	.081	-12.1174	.4890
		A4	A1	13.1316*	2.09523	<.001	6.8284	19.4348
			A2	4.6886	2.09523	.239	-1.6146	10.9918
			A3	5.8142	2.09523	.081	-.4890	12.1174

Appendix 3

Dependent Variable		(I) Surface Treatment Method	(J) Surface Treatment Method	Mean Difference (I-J)	Std. Error	Sig.	95% Confidence Interval	
							Lower Bound	Upper Bound
Fracture toughness @1	LSD	B1	B2	-371.21000*	165.307559	.039	-721.64637	-20.77363
			B3	-432.86640*	165.307559	.019	-783.30277	-82.43003
			B4	-672.96860*	165.307559	<.001	-1023.40497	-322.53223
		B2	B1	371.21000*	165.307559	.039	20.77363	721.64637
			B3	-61.65640	165.307559	.714	-412.09277	288.77997
			B4	-301.75860	165.307559	.087	-652.19497	48.67777
		B3	B1	432.86640*	165.307559	.019	82.43003	783.30277
			B2	61.65640	165.307559	.714	-288.77997	412.09277
			B4	-240.10220	165.307559	.166	-590.53857	110.33417
		B4	B1	672.96860*	165.307559	<.001	322.53223	1023.40497
			B2	301.75860	165.307559	.087	-48.67777	652.19497
			B3	240.10220	165.307559	.166	-110.33417	590.53857
	Bonferroni	B1	B2	-371.21000	165.307559	.235	-868.51033	126.09033
			B3	-432.86640	165.307559	.112	-930.16673	64.43393
			B4	-672.96860*	165.307559	.005	-1170.26893	-175.66827
		B2	B1	371.21000	165.307559	.235	-126.09033	868.51033
			B3	-61.65640	165.307559	1.000	-558.95673	435.64393
			B4	-301.75860	165.307559	.520	-799.05893	195.54173
		B3	B1	432.86640	165.307559	.112	-64.43393	930.16673
			B2	61.65640	165.307559	1.000	-435.64393	558.95673
			B4	-240.10220	165.307559	.994	-737.40253	257.19813
		B4	B1	672.96860*	165.307559	.005	175.66827	1170.26893
			B2	301.75860	165.307559	.520	-195.54173	799.05893
			B3	240.10220	165.307559	.994	-257.19813	737.40253
Fracture toughness @3	LSD	B1	B2	-259.16360*	55.427907	<.001	-376.66551	-141.66169
			B3	-337.52460*	55.427907	<.001	-455.02651	-220.02269
			B4	-365.75800*	55.427907	<.001	-483.25991	-248.25609
		B2	B1	259.16360*	55.427907	<.001	141.66169	376.66551
			B3	-78.36100	55.427907	.177	-195.86291	39.14091
			B4	-106.59440	55.427907	.072	-224.09631	10.90751
		B3	B1	337.52460*	55.427907	<.001	220.02269	455.02651
			B2	78.36100	55.427907	.177	-39.14091	195.86291
			B4	-28.23340	55.427907	.617	-145.73531	89.26851
		B4	B1	365.75800*	55.427907	<.001	248.25609	483.25991
			B2	106.59440	55.427907	.072	-10.90751	224.09631
			B3	28.23340	55.427907	.617	-89.26851	145.73531
	Bonferroni	B1	B2	-259.16360*	55.427907	.002	-425.90925	-92.41795
			B3	-337.52460*	55.427907	<.001	-504.27025	-170.77895
			B4	-365.75800*	55.427907	<.001	-532.50365	-199.01235
		B2	B1	259.16360*	55.427907	.002	92.41795	425.90925
			B3	-78.36100	55.427907	1.000	-245.10665	88.38465
			B4	-106.59440	55.427907	.435	-273.34005	60.15125
		B3	B1	337.52460*	55.427907	<.001	170.77895	504.27025
			B2	78.36100	55.427907	1.000	-88.38465	245.10665
			B4	-28.23340	55.427907	1.000	-194.97905	138.51225
		B4	B1	365.75800*	55.427907	<.001	199.01235	532.50365
			B2	106.59440	55.427907	.435	-60.15125	273.34005
			B3	28.23340	55.427907	1.000	-138.51225	194.97905

Fracture toughness @6	LSD	B1	B2	-120.01560*	32.912209	.002	-189.78637	-50.24483
			B3	-273.59280*	32.912209	<.001	-343.36357	-203.82203
			B4	-119.02760*	32.912209	.002	-188.79837	-49.25683
		B2	B1	120.01560*	32.912209	.002	50.24483	189.78637
			B3	-153.57720*	32.912209	<.001	-223.34797	-83.80643
			B4	.98800	32.912209	.976	-68.78277	70.75877
		B3	B1	273.59280*	32.912209	<.001	203.82203	343.36357
			B2	153.57720*	32.912209	<.001	83.80643	223.34797
			B4	154.56520*	32.912209	<.001	84.79443	224.33597
		B4	B1	119.02760*	32.912209	.002	49.25683	188.79837
			B2	-.98800	32.912209	.976	-70.75877	68.78277
			B3	-154.56520*	32.912209	<.001	-224.33597	-84.79443
	Bonferroni	B1	B2	-120.01560*	32.912209	.013	-219.02651	-21.00469
			B3	-273.59280*	32.912209	<.001	-372.60371	-174.58189
			B4	-119.02760*	32.912209	.014	-218.03851	-20.01669
		B2	B1	120.01560*	32.912209	.013	21.00469	219.02651
			B3	-153.57720*	32.912209	.002	-252.58811	-54.56629
			B4	.98800	32.912209	1.000	-98.02291	99.99891
		B3	B1	273.59280*	32.912209	<.001	174.58189	372.60371
			B2	153.57720*	32.912209	.002	54.56629	252.58811
			B4	154.56520*	32.912209	.001	55.55429	253.57611
		B4	B1	119.02760*	32.912209	.014	20.01669	218.03851
			B2	-.98800	32.912209	1.000	-99.99891	98.02291
			B3	-154.56520*	32.912209	.001	-253.57611	-55.55429
Fracture toughness @9	LSD	B1	B2	-136.63240*	25.825634	<.001	-191.38030	-81.88450
			B3	-250.08580*	25.825634	<.001	-304.83370	-195.33790
			B4	-109.91800*	25.825634	<.001	-164.66590	-55.17010
		B2	B1	136.63240*	25.825634	<.001	81.88450	191.38030
			B3	-113.45340*	25.825634	<.001	-168.20130	-58.70550
			B4	26.71440	25.825634	.316	-28.03350	81.46230
		B3	B1	250.08580*	25.825634	<.001	195.33790	304.83370
			B2	113.45340*	25.825634	<.001	58.70550	168.20130
			B4	140.16780*	25.825634	<.001	85.41990	194.91570
		B4	B1	109.91800*	25.825634	<.001	55.17010	164.66590
			B2	-26.71440	25.825634	.316	-81.46230	28.03350
			B3	-140.16780*	25.825634	<.001	-194.91570	-85.41990
	Bonferroni	B1	B2	-136.63240*	25.825634	<.001	-214.32453	-58.94027
			B3	-250.08580*	25.825634	<.001	-327.77793	-172.39367
			B4	-109.91800*	25.825634	.004	-187.61013	-32.22587
		B2	B1	136.63240*	25.825634	<.001	58.94027	214.32453
			B3	-113.45340*	25.825634	.003	-191.14553	-35.76127
			B4	26.71440	25.825634	1.000	-50.97773	104.40653
		B3	B1	250.08580*	25.825634	<.001	172.39367	327.77793
			B2	113.45340*	25.825634	.003	35.76127	191.14553
			B4	140.16780*	25.825634	<.001	62.47567	217.85993
		B4	B1	109.91800*	25.825634	.004	32.22587	187.61013
			B2	-26.71440	25.825634	1.000	-104.40653	50.97773
			B3	-140.16780*	25.825634	<.001	-217.85993	-62.47567
Fracture toughness @12	LSD	B1	B2	-72.6894*	11.86130	<.001	-97.8342	-47.5446
			B3	-186.5314*	11.86130	<.001	-211.6762	-161.3866
			B4	-56.8632*	11.86130	<.001	-82.0080	-31.7184
		B2	B1	72.6894*	11.86130	<.001	47.5446	97.8342
			B3	-113.8420*	11.86130	<.001	-138.9868	-88.6972
			B4	15.8262	11.86130	.201	-9.3186	40.9710
		B3	B1	186.5314*	11.86130	<.001	161.3866	211.6762
			B2	113.8420*	11.86130	<.001	88.6972	138.9868
			B4	129.6682*	11.86130	<.001	104.5234	154.8130
		B4	B1	56.8632*	11.86130	<.001	31.7184	82.0080
			B2	-15.8262	11.86130	.201	-40.9710	9.3186
			B3	-129.6682*	11.86130	<.001	-154.8130	-104.5234
	Bonferroni	B1	B2	-72.6894*	11.86130	<.001	-108.3721	-37.0067
			B3	-186.5314*	11.86130	<.001	-222.2141	-150.8487
			B4	-56.8632*	11.86130	.001	-92.5459	-21.1805
		B2	B1	72.6894*	11.86130	<.001	37.0067	108.3721
			B3	-113.8420*	11.86130	<.001	-149.5247	-78.1593
			B4	15.8262	11.86130	1.000	-19.8565	51.5089
		B3	B1	186.5314*	11.86130	<.001	150.8487	222.2141
			B2	113.8420*	11.86130	<.001	78.1593	149.5247
			B4	129.6682*	11.86130	<.001	93.9855	165.3509
		B4	B1	56.8632*	11.86130	.001	21.1805	92.5459
			B2	-15.8262	11.86130	1.000	-51.5089	19.8565
			B3	-129.6682*	11.86130	<.001	-165.3509	-93.9855

Fracture toughness @15	LSD	B1	B2	-71.0898*	13.73069	<.001	-100.1976	-41.9820
			B3	-134.7212*	13.73069	<.001	-163.8290	-105.6134
			B4	-19.4798	13.73069	.175	-48.5876	9.6280
		B2	B1	71.0898*	13.73069	<.001	41.9820	100.1976
			B3	-63.6314*	13.73069	<.001	-92.7392	-34.5236
			B4	51.6100*	13.73069	.002	22.5022	80.7178
		B3	B1	134.7212*	13.73069	<.001	105.6134	163.8290
			B2	63.6314*	13.73069	<.001	34.5236	92.7392
			B4	115.2414*	13.73069	<.001	86.1336	144.3492
		B4	B1	19.4798	13.73069	.175	-9.6280	48.5876
			B2	-51.6100*	13.73069	.002	-80.7178	-22.5022
			B3	-115.2414*	13.73069	<.001	-144.3492	-86.1336
	Bonferroni	B1	B2	-71.0898*	13.73069	<.001	-112.3963	-29.7833
			B3	-134.7212*	13.73069	<.001	-176.0277	-93.4147
			B4	-19.4798	13.73069	1.000	-60.7863	21.8267
		B2	B1	71.0898*	13.73069	<.001	29.7833	112.3963
			B3	-63.6314*	13.73069	.002	-104.9379	-22.3249
			B4	51.6100*	13.73069	.010	10.3035	92.9165
		B3	B1	134.7212*	13.73069	<.001	93.4147	176.0277
			B2	63.6314*	13.73069	.002	22.3249	104.9379
			B4	115.2414*	13.73069	<.001	73.9349	156.5479
		B4	B1	19.4798	13.73069	1.000	-21.8267	60.7863
			B2	-51.6100*	13.73069	.010	-92.9165	-10.3035
			B3	-115.2414*	13.73069	<.001	-156.5479	-73.9349
Fracture toughness @18	LSD	B1	B2	-70.6538*	14.05356	<.001	-100.4460	-40.8616
			B3	-112.2668*	14.05356	<.001	-142.0590	-82.4746
			B4	10.2850	14.05356	.475	-19.5072	40.0772
		B2	B1	70.6538*	14.05356	<.001	40.8616	100.4460
			B3	-41.6130*	14.05356	.009	-71.4052	-11.8208
			B4	80.9388*	14.05356	<.001	51.1466	110.7310
		B3	B1	112.2668*	14.05356	<.001	82.4746	142.0590
			B2	41.6130*	14.05356	.009	11.8208	71.4052
			B4	122.5518*	14.05356	<.001	92.7596	152.3440
		B4	B1	-10.2850	14.05356	.475	-40.0772	19.5072
			B2	-80.9388*	14.05356	<.001	-110.7310	-51.1466
			B3	-122.5518*	14.05356	<.001	-152.3440	-92.7596
	Bonferroni	B1	B2	-70.6538*	14.05356	<.001	-112.9316	-28.3760
			B3	-112.2668*	14.05356	<.001	-154.5446	-69.9890
			B4	10.2850	14.05356	1.000	-31.9928	52.5628
		B2	B1	70.6538*	14.05356	<.001	28.3760	112.9316
			B3	-41.6130	14.05356	.055	-83.8908	.6648
			B4	80.9388*	14.05356	<.001	38.6610	123.2166
		B3	B1	112.2668*	14.05356	<.001	69.9890	154.5446
			B2	41.6130	14.05356	.055	-.6648	83.8908
			B4	122.5518*	14.05356	<.001	80.2740	164.8296
		B4	B1	-10.2850	14.05356	1.000	-52.5628	31.9928
			B2	-80.9388*	14.05356	<.001	-123.2166	-38.6610
			B3	-122.5518*	14.05356	<.001	-164.8296	-80.2740
Fracture toughness @21	LSD	B1	B2	-60.8544*	10.27036	<.001	-82.6266	-39.0822
			B3	-114.1134*	10.27036	<.001	-135.8856	-92.3412
			B4	27.2920*	10.27036	.017	5.5198	49.0642
		B2	B1	60.8544*	10.27036	<.001	39.0822	82.6266
			B3	-53.2590*	10.27036	<.001	-75.0312	-31.4868
			B4	88.1464*	10.27036	<.001	66.3742	109.9186
		B3	B1	114.1134*	10.27036	<.001	92.3412	135.8856
			B2	53.2590*	10.27036	<.001	31.4868	75.0312
			B4	141.4054*	10.27036	<.001	119.6332	163.1776
		B4	B1	-27.2920*	10.27036	.017	-49.0642	-5.5198
			B2	-88.1464*	10.27036	<.001	-109.9186	-66.3742
			B3	-141.4054*	10.27036	<.001	-163.1776	-119.6332
	Bonferroni	B1	B2	-60.8544*	10.27036	<.001	-91.7511	-29.9577
			B3	-114.1134*	10.27036	<.001	-145.0101	-83.2167
			B4	27.2920	10.27036	.103	-3.6047	58.1887
		B2	B1	60.8544*	10.27036	<.001	29.9577	91.7511
			B3	-53.2590*	10.27036	<.001	-84.1557	-22.3623
			B4	88.1464*	10.27036	<.001	57.2497	119.0431
		B3	B1	114.1134*	10.27036	<.001	83.2167	145.0101
			B2	53.2590*	10.27036	<.001	22.3623	84.1557
			B4	141.4054*	10.27036	<.001	110.5087	172.3021
		B4	B1	-27.2920	10.27036	.103	-58.1887	3.6047
			B2	-88.1464*	10.27036	<.001	-119.0431	-57.2497
			B3	-141.4054*	10.27036	<.001	-172.3021	-110.5087

Fracture toughness @24	LSD	B1	B2	-63.1320*	9.89062	<.001	-84.0992	-42.1648
			B3	-101.9184*	9.89062	<.001	-122.8856	-80.9512
			B4	41.8846*	9.89062	<.001	20.9174	62.8518
		B2	B1	63.1320*	9.89062	<.001	42.1648	84.0992
			B3	-38.7864*	9.89062	.001	-59.7536	-17.8192
			B4	105.0166*	9.89062	<.001	84.0494	125.9838
		B3	B1	101.9184*	9.89062	<.001	80.9512	122.8856
			B2	38.7864*	9.89062	.001	17.8192	59.7536
			B4	143.8030*	9.89062	<.001	122.8358	164.7702
		B4	B1	-41.8846*	9.89062	<.001	-62.8518	-20.9174
			B2	-105.0166*	9.89062	<.001	-125.9838	-84.0494
			B3	-143.8030*	9.89062	<.001	-164.7702	-122.8358
	Bonferroni	B1	B2	-63.1320*	9.89062	<.001	-92.8863	-33.3777
			B3	-101.9184*	9.89062	<.001	-131.6727	-72.1641
			B4	41.8846*	9.89062	.004	12.1303	71.6389
		B2	B1	63.1320*	9.89062	<.001	33.3777	92.8863
			B3	-38.7864*	9.89062	.007	-68.5407	-9.0321
			B4	105.0166*	9.89062	<.001	75.2623	134.7709
		B3	B1	101.9184*	9.89062	<.001	72.1641	131.6727
			B2	38.7864*	9.89062	.007	9.0321	68.5407
			B4	143.8030*	9.89062	<.001	114.0487	173.5573
		B4	B1	-41.8846*	9.89062	.004	-71.6389	-12.1303
			B2	-105.0166*	9.89062	<.001	-134.7709	-75.2623
			B3	-143.8030*	9.89062	<.001	-173.5573	-114.0487
Fracture toughness @27	LSD	B1	B2	-52.1314*	7.35220	<.001	-67.7174	-36.5454
			B3	-91.3396*	7.35220	<.001	-106.9256	-75.7536
			B4	56.3992*	7.35220	<.001	40.8132	71.9852
		B2	B1	52.1314*	7.35220	<.001	36.5454	67.7174
			B3	-39.2082*	7.35220	<.001	-54.7942	-23.6222
			B4	108.5306*	7.35220	<.001	92.9446	124.1166
		B3	B1	91.3396*	7.35220	<.001	75.7536	106.9256
			B2	39.2082*	7.35220	<.001	23.6222	54.7942
			B4	147.7388*	7.35220	<.001	132.1528	163.3248
		B4	B1	-56.3992*	7.35220	<.001	-71.9852	-40.8132
			B2	-108.5306*	7.35220	<.001	-124.1166	-92.9446
			B3	-147.7388*	7.35220	<.001	-163.3248	-132.1528
	Bonferroni	B1	B2	-52.1314*	7.35220	<.001	-74.2493	-30.0135
			B3	-91.3396*	7.35220	<.001	-113.4575	-69.2217
			B4	56.3992*	7.35220	<.001	34.2813	78.5171
		B2	B1	52.1314*	7.35220	<.001	30.0135	74.2493
			B3	-39.2082*	7.35220	<.001	-61.3261	-17.0903
			B4	108.5306*	7.35220	<.001	86.4127	130.6485
		B3	B1	91.3396*	7.35220	<.001	69.2217	113.4575
			B2	39.2082*	7.35220	<.001	17.0903	61.3261
			B4	147.7388*	7.35220	<.001	125.6209	169.8567
		B4	B1	-56.3992*	7.35220	<.001	-78.5171	-34.2813
			B2	-108.5306*	7.35220	<.001	-130.6485	-86.4127
			B3	-147.7388*	7.35220	<.001	-169.8567	-125.6209

Fracture toughness @30	LSD	B1	B2	-52.1814*	9.70139	<.001	-72.7474	-31.6154
			B3	-83.2052*	9.70139	<.001	-103.7712	-62.6392
			B4	56.4760*	9.70139	<.001	35.9100	77.0420
		B2	B1	52.1814*	9.70139	<.001	31.6154	72.7474
			B3	-31.0238*	9.70139	.006	-51.5898	-10.4578
			B4	108.6574*	9.70139	<.001	88.0914	129.2234
		B3	B1	83.2052*	9.70139	<.001	62.6392	103.7712
			B2	31.0238*	9.70139	.006	10.4578	51.5898
			B4	139.6812*	9.70139	<.001	119.1152	160.2472
		B4	B1	-56.4760*	9.70139	<.001	-77.0420	-35.9100
			B2	-108.6574*	9.70139	<.001	-129.2234	-88.0914
			B3	-139.6812*	9.70139	<.001	-160.2472	-119.1152
	Bonferroni	B1	B2	-52.1814*	9.70139	<.001	-81.3664	-22.9964
			B3	-83.2052*	9.70139	<.001	-112.3902	-54.0202
			B4	56.4760*	9.70139	<.001	27.2910	85.6610
		B2	B1	52.1814*	9.70139	<.001	22.9964	81.3664
			B3	-31.0238*	9.70139	.034	-60.2088	-1.8388
			B4	108.6574*	9.70139	<.001	79.4724	137.8424
		B3	B1	83.2052*	9.70139	<.001	54.0202	112.3902
			B2	31.0238*	9.70139	.034	1.8388	60.2088
			B4	139.6812*	9.70139	<.001	110.4962	168.8662
		B4	B1	-56.4760*	9.70139	<.001	-85.6610	-27.2910
			B2	-108.6574*	9.70139	<.001	-137.8424	-79.4724
			B3	-139.6812*	9.70139	<.001	-168.8662	-110.4962

Appendix 4

Sp	LSD	B1	B2	-2.4038	1.89565	.223	-6.4224	1.6148
			B3	-2.8988	1.89565	.146	-6.9174	1.1198
			B4	-11.1750*	1.89565	<.001	-15.1936	-7.1564
		B2	B1	2.4038	1.89565	.223	-1.6148	6.4224
			B3	-.4950	1.89565	.797	-4.5136	3.5236
			B4	-8.7712*	1.89565	<.001	-12.7898	-4.7526
		B3	B1	2.8988	1.89565	.146	-1.1198	6.9174
			B2	.4950	1.89565	.797	-3.5236	4.5136
			B4	-8.2762*	1.89565	<.001	-12.2948	-4.2576
		B4	B1	11.1750*	1.89565	<.001	7.1564	15.1936
			B2	8.7712*	1.89565	<.001	4.7526	12.7898
			B3	8.2762*	1.89565	<.001	4.2576	12.2948
	Bonferroni	B1	B2	-2.4038	1.89565	1.000	-8.1066	3.2990
			B3	-2.8988	1.89565	.874	-8.6016	2.8040
			B4	-11.1750*	1.89565	<.001	-16.8778	-5.4722
		B2	B1	2.4038	1.89565	1.000	-3.2990	8.1066
			B3	-.4950	1.89565	1.000	-6.1978	5.2078
			B4	-8.7712*	1.89565	.002	-14.4740	-3.0684
		B3	B1	2.8988	1.89565	.874	-2.8040	8.6016
			B2	.4950	1.89565	1.000	-5.2078	6.1978
			B4	-8.2762*	1.89565	.003	-13.9790	-2.5734
		B4	B1	11.1750*	1.89565	<.001	5.4722	16.8778
			B2	8.7712*	1.89565	.002	3.0684	14.4740
			B3	8.2762*	1.89565	.003	2.5734	13.9790

Appendix 5

Dependent Variable		(I) Surface Treatment Method	(J) Surface Treatment Method	Mean Difference (I-J)	Std. Error	Sig.	95% Confidence Interval	
							Lower Bound	Upper Bound
Fracture toughness @1	LSD	C1	C2	-359.25100	256.664311	.181	-903.35503	184.85303
			C3	-1260.64360*	256.664311	<.001	-1804.74763	-716.53957
			C4	-2052.30560*	256.664311	<.001	-2596.40963	-1508.20157
		C2	C1	359.25100	256.664311	.181	-184.85303	903.35503
			C3	-901.39260*	256.664311	.003	-1445.49663	-357.28857
			C4	-1693.05460*	256.664311	<.001	-2237.15863	-1148.95057
		C3	C1	1260.64360*	256.664311	<.001	716.53957	1804.74763
			C2	901.39260*	256.664311	.003	357.28857	1445.49663
			C4	-791.66200*	256.664311	.007	-1335.76603	-247.55797
		C4	C1	2052.30560*	256.664311	<.001	1508.20157	2596.40963
			C2	1693.05460*	256.664311	<.001	1148.95057	2237.15863
			C3	791.66200*	256.664311	.007	247.55797	1335.76603
	Bonferroni	C1	C2	-359.25100	256.664311	1.000	-1131.38293	412.88093
			C3	-1260.64360*	256.664311	<.001	-2032.77553	-488.51167
			C4	-2052.30560*	256.664311	<.001	-2824.43753	-1280.17367
		C2	C1	359.25100	256.664311	1.000	-412.88093	1131.38293
			C3	-901.39260*	256.664311	.017	-1673.52453	-129.26067
			C4	-1693.05460*	256.664311	<.001	-2465.18653	-920.92267
		C3	C1	1260.64360*	256.664311	<.001	488.51167	2032.77553
			C2	901.39260*	256.664311	.017	129.26067	1673.52453
			C4	-791.66200*	256.664311	.043	-1563.79393	-19.53007
		C4	C1	2052.30560*	256.664311	<.001	1280.17367	2824.43753
			C2	1693.05460*	256.664311	<.001	920.92267	2465.18653
			C3	791.66200*	256.664311	.043	19.53007	1563.79393
Fracture toughness @3	LSD	C1	C2	-524.08660*	112.079865	<.001	-761.68530	-286.48790
			C3	-1289.79080*	112.079865	<.001	-1527.38950	-1052.19210
			C4	-678.27520*	112.079865	<.001	-915.87390	-440.67650
		C2	C1	524.08660*	112.079865	<.001	286.48790	761.68530
			C3	-765.70420*	112.079865	<.001	-1003.30290	-528.10550
			C4	-154.18860	112.079865	.188	-391.78730	83.41010
		C3	C1	1289.79080*	112.079865	<.001	1052.19210	1527.38950
			C2	765.70420*	112.079865	<.001	528.10550	1003.30290
			C4	611.51560*	112.079865	<.001	373.91690	849.11430
		C4	C1	678.27520*	112.079865	<.001	440.67650	915.87390
			C2	154.18860	112.079865	.188	-83.41010	391.78730
			C3	-611.51560*	112.079865	<.001	-849.11430	-373.91690
	Bonferroni	C1	C2	-524.08660*	112.079865	.002	-861.26025	-186.91295
			C3	-1289.79080*	112.079865	<.001	-1626.96445	-952.61715
			C4	-678.27520*	112.079865	<.001	-1015.44885	-341.10155
		C2	C1	524.08660*	112.079865	.002	186.91295	861.26025
			C3	-765.70420*	112.079865	<.001	-1102.87785	-428.53055
			C4	-154.18860	112.079865	1.000	-491.36225	182.98505
		C3	C1	1289.79080*	112.079865	<.001	952.61715	1626.96445
			C2	765.70420*	112.079865	<.001	428.53055	1102.87785
			C4	611.51560*	112.079865	<.001	274.34195	948.68925
		C4	C1	678.27520*	112.079865	<.001	341.10155	1015.44885
			C2	154.18860	112.079865	1.000	-182.98505	491.36225
			C3	-611.51560*	112.079865	<.001	-948.68925	-274.34195

Fracture toughness @6	LSD	C1	C2	-459.68980*	189.084555	.027	-860.53115	-58.84845
			C3	-1644.77220*	189.084555	<.001	-2045.61355	-1243.93085
			C4	-886.96920*	189.084555	<.001	-1287.81055	-486.12785
		C2	C1	459.68980*	189.084555	.027	58.84845	860.53115
			C3	-1185.08240*	189.084555	<.001	-1585.92375	-784.24105
			C4	-427.27940*	189.084555	.038	-828.12075	-26.43805
		C3	C1	1644.77220*	189.084555	<.001	1243.93085	2045.61355
			C2	1185.08240*	189.084555	<.001	784.24105	1585.92375
			C4	757.80300*	189.084555	.001	356.96165	1158.64435
		C4	C1	886.96920*	189.084555	<.001	486.12785	1287.81055
			C2	427.27940*	189.084555	.038	26.43805	828.12075
			C3	-757.80300*	189.084555	.001	-1158.64435	-356.96165
	Bonferroni	C1	C2	-459.68980	189.084555	.163	-1028.51927	109.13967
			C3	-1644.77220*	189.084555	<.001	-2213.60167	-1075.94273
			C4	-886.96920*	189.084555	.001	-1455.79867	-318.13973
		C2	C1	459.68980	189.084555	.163	-109.13967	1028.51927
			C3	-1185.08240*	189.084555	<.001	-1753.91187	-616.25293
			C4	-427.27940	189.084555	.229	-996.10887	141.55007
		C3	C1	1644.77220*	189.084555	<.001	1075.94273	2213.60167
			C2	1185.08240*	189.084555	<.001	616.25293	1753.91187
			C4	757.80300*	189.084555	.006	188.97353	1326.63247
		C4	C1	886.96920*	189.084555	.001	318.13973	1455.79867
			C2	427.27940	189.084555	.229	-141.55007	996.10887
			C3	-757.80300*	189.084555	.006	-1326.63247	-188.97353
Fracture toughness @9	LSD	C1	C2	-361.27080*	132.349361	.015	-641.83891	-80.70269
			C3	-1792.20680*	132.349361	<.001	-2072.77491	-1511.63869
			C4	-316.35520*	132.349361	.029	-596.92331	-35.78709
		C2	C1	361.27080*	132.349361	.015	80.70269	641.83891
			C3	-1430.93600*	132.349361	<.001	-1711.50411	-1150.36789
			C4	44.91560	132.349361	.739	-235.65251	325.48371
		C3	C1	1792.20680*	132.349361	<.001	1511.63869	2072.77491
			C2	1430.93600*	132.349361	<.001	1150.36789	1711.50411
			C4	1475.85160*	132.349361	<.001	1195.28349	1756.41971
		C4	C1	316.35520*	132.349361	.029	35.78709	596.92331
			C2	-44.91560	132.349361	.739	-325.48371	235.65251
			C3	-1475.85160*	132.349361	<.001	-1756.41971	-1195.28349
	Bonferroni	C1	C2	-361.27080	132.349361	.089	-759.42186	36.88026
			C3	-1792.20680*	132.349361	<.001	-2190.35786	-1394.05574
			C4	-316.35520	132.349361	.177	-714.50626	81.79586
		C2	C1	361.27080	132.349361	.089	-36.88026	759.42186
			C3	-1430.93600*	132.349361	<.001	-1829.08706	-1032.78494
			C4	44.91560	132.349361	1.000	-353.23546	443.06666
		C3	C1	1792.20680*	132.349361	<.001	1394.05574	2190.35786
			C2	1430.93600*	132.349361	<.001	1032.78494	1829.08706
			C4	1475.85160*	132.349361	<.001	1077.70054	1874.00266
		C4	C1	316.35520	132.349361	.177	-81.79586	714.50626
			C2	-44.91560	132.349361	1.000	-443.06666	353.23546
			C3	-1475.85160*	132.349361	<.001	-1874.00266	-1077.70054
Fracture toughness @12	LSD	C1	C2	-166.5112*	78.51938	.050	-332.9648	-.0576
			C3	-1276.8974*	78.51938	<.001	-1443.3510	-1110.4438
			C4	-21.7508	78.51938	.785	-188.2044	144.7028
		C2	C1	166.5112*	78.51938	.050	.0576	332.9648
			C3	-1110.3862*	78.51938	<.001	-1276.8398	-943.9326
			C4	144.7604	78.51938	.084	-21.6932	311.2140
		C3	C1	1276.8974*	78.51938	<.001	1110.4438	1443.3510
			C2	1110.3862*	78.51938	<.001	943.9326	1276.8398
			C4	1255.1466*	78.51938	<.001	1088.6930	1421.6002
		C4	C1	21.7508	78.51938	.785	-144.7028	188.2044
			C2	-144.7604	78.51938	.084	-311.2140	21.6932
			C3	-1255.1466*	78.51938	<.001	-1421.6002	-1088.6930
	Bonferroni	C1	C2	-166.5112	78.51938	.300	-402.7237	69.7013
			C3	-1276.8974*	78.51938	<.001	-1513.1099	-1040.6849
			C4	-21.7508	78.51938	1.000	-257.9633	214.4617
		C2	C1	166.5112	78.51938	.300	-69.7013	402.7237
			C3	-1110.3862*	78.51938	<.001	-1346.5987	-874.1737
			C4	144.7604	78.51938	.503	-91.4521	380.9729
		C3	C1	1276.8974*	78.51938	<.001	1040.6849	1513.1099
			C2	1110.3862*	78.51938	<.001	874.1737	1346.5987
			C4	1255.1466*	78.51938	<.001	1018.9341	1491.3591
		C4	C1	21.7508	78.51938	1.000	-214.4617	257.9633
			C2	-144.7604	78.51938	.503	-380.9729	91.4521
			C3	-1255.1466*	78.51938	<.001	-1491.3591	-1018.9341

Fracture toughness @15	LSD	C1	C2	-199.6368*	59.84654	.004	-326.5058	-72.7678
			C3	-949.8120*	59.84654	<.001	-1076.6810	-822.9430
			C4	-11.5614	59.84654	.849	-138.4304	115.3076
		C2	C1	199.6368*	59.84654	.004	72.7678	326.5058
			C3	-750.1752*	59.84654	<.001	-877.0442	-623.3062
			C4	188.0754*	59.84654	.006	61.2064	314.9444
		C3	C1	949.8120*	59.84654	<.001	822.9430	1076.6810
			C2	750.1752*	59.84654	<.001	623.3062	877.0442
			C4	938.2506*	59.84654	<.001	811.3816	1065.1196
		C4	C1	11.5614	59.84654	.849	-115.3076	138.4304
			C2	-188.0754*	59.84654	.006	-314.9444	-61.2064
			C3	-938.2506*	59.84654	<.001	-1065.1196	-811.3816
	Bonferroni	C1	C2	-199.6368*	59.84654	.025	-379.6752	-19.5984
			C3	-949.8120*	59.84654	<.001	-1129.8504	-769.7736
			C4	-11.5614	59.84654	1.000	-191.5998	168.4770
		C2	C1	199.6368*	59.84654	.025	19.5984	379.6752
			C3	-750.1752*	59.84654	<.001	-930.2136	-570.1368
			C4	188.0754*	59.84654	.038	8.0370	368.1138
		C3	C1	949.8120*	59.84654	<.001	769.7736	1129.8504
			C2	750.1752*	59.84654	<.001	570.1368	930.2136
			C4	938.2506*	59.84654	<.001	758.2122	1118.2890
		C4	C1	11.5614	59.84654	1.000	-168.4770	191.5998
			C2	-188.0754*	59.84654	.038	-368.1138	-8.0370
			C3	-938.2506*	59.84654	<.001	-1118.2890	-758.2122

Fracture toughness @18	LSD	C1	C2	-188.7018*	57.75500	.005	-311.1369	-66.2667
			C3	-896.1182*	57.75500	<.001	-1018.5533	-773.6831
			C4	5.0708	57.75500	.931	-117.3643	127.5059
		C2	C1	188.7018*	57.75500	.005	66.2667	311.1369
			C3	-707.4164*	57.75500	<.001	-829.8515	-584.9813
			C4	193.7726*	57.75500	.004	71.3375	316.2077
		C3	C1	896.1182*	57.75500	<.001	773.6831	1018.5533
			C2	707.4164*	57.75500	<.001	584.9813	829.8515
			C4	901.1890*	57.75500	<.001	778.7539	1023.6241
		C4	C1	-5.0708	57.75500	.931	-127.5059	117.3643
			C2	-193.7726*	57.75500	.004	-316.2077	-71.3375
			C3	-901.1890*	57.75500	<.001	-1023.6241	-778.7539
	Bonferroni	C1	C2	-188.7018*	57.75500	.029	-362.4481	-14.9555
			C3	-896.1182*	57.75500	<.001	-1069.8645	-722.3719
			C4	5.0708	57.75500	1.000	-168.6755	178.8171
		C2	C1	188.7018*	57.75500	.029	14.9555	362.4481
			C3	-707.4164*	57.75500	<.001	-881.1627	-533.6701
			C4	193.7726*	57.75500	.024	20.0263	367.5189
		C3	C1	896.1182*	57.75500	<.001	722.3719	1069.8645
			C2	707.4164*	57.75500	<.001	533.6701	881.1627
			C4	901.1890*	57.75500	<.001	727.4427	1074.9353
		C4	C1	-5.0708	57.75500	1.000	-178.8171	168.6755
			C2	-193.7726*	57.75500	.024	-367.5189	-20.0263
			C3	-901.1890*	57.75500	<.001	-1074.9353	-727.4427

Fracture toughness @21	LSD	C1	C2	-161.0308*	55.90953	.011	-279.5537	-42.5079
			C3	-840.3852*	55.90953	<.001	-958.9081	-721.8623
			C4	44.2400	55.90953	.440	-74.2829	162.7629
		C2	C1	161.0308*	55.90953	.011	42.5079	279.5537
			C3	-679.3544*	55.90953	<.001	-797.8773	-560.8315
			C4	205.2708*	55.90953	.002	86.7479	323.7937
		C3	C1	840.3852*	55.90953	<.001	721.8623	958.9081
			C2	679.3544*	55.90953	<.001	560.8315	797.8773
			C4	884.6252*	55.90953	<.001	766.1023	1003.1481
		C4	C1	-44.2400	55.90953	.440	-162.7629	74.2829
			C2	-205.2708*	55.90953	.002	-323.7937	-86.7479
			C3	-884.6252*	55.90953	<.001	-1003.1481	-766.1023
	Bonferroni	C1	C2	-161.0308	55.90953	.065	-329.2253	7.1637
			C3	-840.3852*	55.90953	<.001	-1008.5797	-672.1907
			C4	44.2400	55.90953	1.000	-123.9545	212.4345
		C2	C1	161.0308	55.90953	.065	-7.1637	329.2253
			C3	-679.3544*	55.90953	<.001	-847.5489	-511.1599
			C4	205.2708*	55.90953	.012	37.0763	373.4653
		C3	C1	840.3852*	55.90953	<.001	672.1907	1008.5797
			C2	679.3544*	55.90953	<.001	511.1599	847.5489
			C4	884.6252*	55.90953	<.001	716.4307	1052.8197
		C4	C1	-44.2400	55.90953	1.000	-212.4345	123.9545
			C2	-205.2708*	55.90953	.012	-373.4653	-37.0763
			C3	-884.6252*	55.90953	<.001	-1052.8197	-716.4307

Fracture toughness @24	LSD	C1	C2	-137.0296	69.43456	.066	-284.2243	10.1651
			C3	-742.6672*	69.43456	<.001	-889.8619	-595.4725
			C4	58.2640	69.43456	.414	-88.9307	205.4587
		C2	C1	137.0296	69.43456	.066	-10.1651	284.2243
			C3	-605.6376*	69.43456	<.001	-752.8323	-458.4429
			C4	195.2936*	69.43456	.013	48.0989	342.4883
		C3	C1	742.6672*	69.43456	<.001	595.4725	889.8619
			C2	605.6376*	69.43456	<.001	458.4429	752.8323
			C4	800.9312*	69.43456	<.001	653.7365	948.1259
		C4	C1	-58.2640	69.43456	.414	-205.4587	88.9307
			C2	-195.2936*	69.43456	.013	-342.4883	-48.0989
			C3	-800.9312*	69.43456	<.001	-948.1259	-653.7365
	Bonferroni	C1	C2	-137.0296	69.43456	.396	-345.9119	71.8527
			C3	-742.6672*	69.43456	<.001	-951.5495	-533.7849
			C4	58.2640	69.43456	1.000	-150.6183	267.1463
		C2	C1	137.0296	69.43456	.396	-71.8527	345.9119
			C3	-605.6376*	69.43456	<.001	-814.5199	-396.7553
			C4	195.2936	69.43456	.075	-13.5887	404.1759
		C3	C1	742.6672*	69.43456	<.001	533.7849	951.5495
			C2	605.6376*	69.43456	<.001	396.7553	814.5199
			C4	800.9312*	69.43456	<.001	592.0489	1009.8135
		C4	C1	-58.2640	69.43456	1.000	-267.1463	150.6183
			C2	-195.2936	69.43456	.075	-404.1759	13.5887
			C3	-800.9312*	69.43456	<.001	-1009.8135	-592.0489

Fracture toughness @27	LSD	C1	C2	-125.9080*	52.30627	.029	-236.7923	-15.0237
			C3	-646.3726*	52.30627	<.001	-757.2569	-535.4883
			C4	71.4806	52.30627	.191	-39.4037	182.3649
		C2	C1	125.9080*	52.30627	.029	15.0237	236.7923
			C3	-520.4646*	52.30627	<.001	-631.3489	-409.5803
			C4	197.3886*	52.30627	.002	86.5043	308.2729
		C3	C1	646.3726*	52.30627	<.001	535.4883	757.2569
			C2	520.4646*	52.30627	<.001	409.5803	631.3489
			C4	717.8532*	52.30627	<.001	606.9689	828.7375
		C4	C1	-71.4806	52.30627	.191	-182.3649	39.4037
			C2	-197.3886*	52.30627	.002	-308.2729	-86.5043
			C3	-717.8532*	52.30627	<.001	-828.7375	-606.9689
	Bonferroni	C1	C2	-125.9080	52.30627	.171	-283.2627	31.4467
			C3	-646.3726*	52.30627	<.001	-803.7273	-489.0179
			C4	71.4806	52.30627	1.000	-85.8741	228.8353
		C2	C1	125.9080	52.30627	.171	-31.4467	283.2627
			C3	-520.4646*	52.30627	<.001	-677.8193	-363.1099
			C4	197.3886*	52.30627	.010	40.0339	354.7433
		C3	C1	646.3726*	52.30627	<.001	489.0179	803.7273
			C2	520.4646*	52.30627	<.001	363.1099	677.8193
			C4	717.8532*	52.30627	<.001	560.4985	875.2079
		C4	C1	-71.4806	52.30627	1.000	-228.8353	85.8741
			C2	-197.3886*	52.30627	.010	-354.7433	-40.0339
			C3	-717.8532*	52.30627	<.001	-875.2079	-560.4985

Fracture toughness @30	LSD	C1	C2	-97.6082	52.97295	.084	-209.9058	14.6894
			C3	-555.5208*	52.97295	<.001	-667.8184	-443.2232
			C4	77.5706	52.97295	.162	-34.7270	189.8682
		C2	C1	97.6082	52.97295	.084	-14.6894	209.9058
			C3	-457.9126*	52.97295	<.001	-570.2102	-345.6150
			C4	175.1788*	52.97295	.004	62.8812	287.4764
		C3	C1	555.5208*	52.97295	<.001	443.2232	667.8184
			C2	457.9126*	52.97295	<.001	345.6150	570.2102
			C4	633.0914*	52.97295	<.001	520.7938	745.3890
		C4	C1	-77.5706	52.97295	.162	-189.8682	34.7270
			C2	-175.1788*	52.97295	.004	-287.4764	-62.8812
			C3	-633.0914*	52.97295	<.001	-745.3890	-520.7938
	Bonferroni	C1	C2	-97.6082	52.97295	.504	-256.9685	61.7521
			C3	-555.5208*	52.97295	<.001	-714.8811	-396.1605
			C4	77.5706	52.97295	.975	-81.7897	236.9309
		C2	C1	97.6082	52.97295	.504	-61.7521	256.9685
			C3	-457.9126*	52.97295	<.001	-617.2729	-298.5523
			C4	175.1788*	52.97295	.027	15.8185	334.5391
		C3	C1	555.5208*	52.97295	<.001	396.1605	714.8811
			C2	457.9126*	52.97295	<.001	298.5523	617.2729
			C4	633.0914*	52.97295	<.001	473.7311	792.4517
		C4	C1	-77.5706	52.97295	.975	-236.9309	81.7897
			C2	-175.1788*	52.97295	.027	-334.5391	-15.8185
			C3	-633.0914*	52.97295	<.001	-792.4517	-473.7311

Appendix 6

Sa	LSD	C1	C2	-.7993*	.29740	.016	-1.4297	-.1688
			C3	-1.1547*	.29740	.001	-1.7851	-.5242
			C4	-1.4915*	.29740	<.001	-2.1219	-.8610
		C2	C1	.7993*	.29740	.016	.1688	1.4297
			C3	-.3554	.29740	.249	-.9859	.2751
			C4	-.6922*	.29740	.033	-1.3227	-.0617
		C3	C1	1.1547*	.29740	.001	.5242	1.7851
			C2	.3554	.29740	.249	-.2751	.9859
			C4	-.3368	.29740	.274	-.9673	.2937
		C4	C1	1.4915*	.29740	<.001	.8610	2.1219
			C2	.6922*	.29740	.033	.0617	1.3227
			C3	.3368	.29740	.274	-.2937	.9673
	Bonferroni	C1	C2	-.7993	.29740	.097	-1.6940	.0954
			C3	-1.1547*	.29740	.008	-2.0494	-.2600
			C4	-1.4915*	.29740	<.001	-2.3862	-.5968
		C2	C1	.7993	.29740	.097	-.0954	1.6940
			C3	-.3554	.29740	1.000	-1.2501	.5393
			C4	-.6922	.29740	.200	-1.5869	.2025
		C3	C1	1.1547*	.29740	.008	.2600	2.0494
			C2	.3554	.29740	1.000	-.5393	1.2501
			C4	-.3368	.29740	1.000	-1.2315	.5579
		C4	C1	1.4915*	.29740	<.001	.5968	2.3862
			C2	.6922	.29740	.200	-.2025	1.5869
			C3	.3368	.29740	1.000	-.5579	1.2315

Appendix 7

Sp	LSD	C1	C2	.5992	2.07010	.776	-3.7892	4.9876
			C3	-2.5612	2.07010	.234	-6.9496	1.8272
			C4	-6.6756*	2.07010	.005	-11.0640	-2.2872
		C2	C1	-.5992	2.07010	.776	-4.9876	3.7892
			C3	-3.1604	2.07010	.146	-7.5488	1.2280
			C4	-7.2748*	2.07010	.003	-11.6632	-2.8864
		C3	C1	2.5612	2.07010	.234	-1.8272	6.9496
			C2	3.1604	2.07010	.146	-1.2280	7.5488
			C4	-4.1144	2.07010	.064	-8.5028	.2740
		C4	C1	6.6756*	2.07010	.005	2.2872	11.0640
			C2	7.2748*	2.07010	.003	2.8864	11.6632
			C3	4.1144	2.07010	.064	-.2740	8.5028
	Bonferroni	C1	C2	.5992	2.07010	1.000	-5.6284	6.8268
			C3	-2.5612	2.07010	1.000	-8.7888	3.6664
			C4	-6.6756*	2.07010	.032	-12.9032	-.4480
		C2	C1	-.5992	2.07010	1.000	-6.8268	5.6284
			C3	-3.1604	2.07010	.878	-9.3880	3.0672
			C4	-7.2748*	2.07010	.017	-13.5024	-1.0472
		C3	C1	2.5612	2.07010	1.000	-3.6664	8.7888
			C2	3.1604	2.07010	.878	-3.0672	9.3880
			C4	-4.1144	2.07010	.386	-10.3420	2.1132
		C4	C1	6.6756*	2.07010	.032	.4480	12.9032
			C2	7.2748*	2.07010	.017	1.0472	13.5024
			C3	4.1144	2.07010	.386	-2.1132	10.3420

Appendix 8

Sq	LSD	C1	C2	-.4858	.34225	.175	-1.2113	.2397
			C3	-1.1032*	.34225	.005	-1.8287	-.3777
			C4	-1.2912*	.34225	.002	-2.0167	-.5657
		C2	C1	.4858	.34225	.175	-.2397	1.2113
			C3	-.6174	.34225	.090	-1.3429	.1081
			C4	-.8054*	.34225	.032	-1.5309	-.0799
		C3	C1	1.1032*	.34225	.005	.3777	1.8287
			C2	.6174	.34225	.090	-.1081	1.3429
			C4	-.1880	.34225	.590	-.9135	.5375
		C4	C1	1.2912*	.34225	.002	.5657	2.0167
			C2	.8054*	.34225	.032	.0799	1.5309
			C3	.1880	.34225	.590	-.5375	.9135
	Bonferroni	C1	C2	-.4858	.34225	1.000	-1.5154	.5438
			C3	-1.1032*	.34225	.032	-2.1328	-.0736
			C4	-1.2912*	.34225	.010	-2.3208	-.2616
		C2	C1	.4858	.34225	1.000	-.5438	1.5154
			C3	-.6174	.34225	.541	-1.6470	.4122
			C4	-.8054	.34225	.190	-1.8350	.2242
		C3	C1	1.1032*	.34225	.032	.0736	2.1328
			C2	.6174	.34225	.541	-.4122	1.6470
			C4	-.1880	.34225	1.000	-1.2176	.8416
		C4	C1	1.2912*	.34225	.010	.2616	2.3208
			C2	.8054	.34225	.190	-.2242	1.8350
			C3	.1880	.34225	1.000	-.8416	1.2176

Appendix 9

Dependent Variable		(I) Surface Treatment Method	(J) Surface Treatment Method	Mean Difference (I-J)	Std. Error	Sig.	95% Confidence Interval	
							Lower Bound	Upper Bound
Fracture toughness @1	LSD	D1	D2	-805.49520	505.732921	.131	-1877.60110	266.61070
			D3	-1561.04060*	505.732921	.007	-2633.14650	-488.93470
			D4	-3157.11800*	505.732921	<.001	-4229.22390	-2085.01210
		D2	D1	805.49520	505.732921	.131	-266.61070	1877.60110
			D3	-755.54540	505.732921	.155	-1827.65130	316.56050
			D4	-2351.62280*	505.732921	<.001	-3423.72870	-1279.51690
		D3	D1	1561.04060*	505.732921	.007	488.93470	2633.14650
			D2	755.54540	505.732921	.155	-316.56050	1827.65130
			D4	-1596.07740*	505.732921	.006	-2668.18330	-523.97150
		D4	D1	3157.11800*	505.732921	<.001	2085.01210	4229.22390
			D2	2351.62280*	505.732921	<.001	1279.51690	3423.72870
			D3	1596.07740*	505.732921	.006	523.97150	2668.18330
	Bonferroni	D1	D2	-805.49520	505.732921	.785	-2326.90866	715.91826
			D3	-1561.04060*	505.732921	.042	-3082.45406	-39.62714
			D4	-3157.11800*	505.732921	<.001	-4678.53146	-1635.70454
		D2	D1	805.49520	505.732921	.785	-715.91826	2326.90866
			D3	-755.54540	505.732921	.928	-2276.95886	765.86806
			D4	-2351.62280*	505.732921	.002	-3873.03626	-830.20934
		D3	D1	1561.04060*	505.732921	.042	39.62714	3082.45406
			D2	755.54540	505.732921	.928	-765.86806	2276.95886
			D4	-1596.07740*	505.732921	.037	-3117.49086	-74.66394
		D4	D1	3157.11800*	505.732921	<.001	1635.70454	4678.53146
			D2	2351.62280*	505.732921	.002	830.20934	3873.03626
			D3	1596.07740*	505.732921	.037	74.66394	3117.49086
Fracture toughness @3	LSD	D1	D2	-580.65600	323.641440	.092	-1266.74520	105.43320
			D3	-1553.17840*	323.641440	<.001	-2239.26760	-867.08920
			D4	-1054.74700*	323.641440	.005	-1740.83620	-368.65780
		D2	D1	580.65600	323.641440	.092	-105.43320	1266.74520
			D3	-972.52240*	323.641440	.008	-1658.61160	-286.43320
			D4	-474.09100	323.641440	.162	-1160.18020	211.99820
		D3	D1	1553.17840*	323.641440	<.001	867.08920	2239.26760
			D2	972.52240*	323.641440	.008	286.43320	1658.61160
			D4	498.43140	323.641440	.143	-187.65780	1184.52060
		D4	D1	1054.74700*	323.641440	.005	368.65780	1740.83620
			D2	474.09100	323.641440	.162	-211.99820	1160.18020
			D3	-498.43140	323.641440	.143	-1184.52060	187.65780
	Bonferroni	D1	D2	-580.65600	323.641440	.550	-1554.27750	392.96550
			D3	-1553.17840*	323.641440	.001	-2526.79990	-579.55690
			D4	-1054.74700*	323.641440	.030	-2028.36850	-81.12550
		D2	D1	580.65600	323.641440	.550	-392.96550	1554.27750
			D3	-972.52240	323.641440	.050	-1946.14390	1.09910
			D4	-474.09100	323.641440	.974	-1447.71250	499.53050
		D3	D1	1553.17840*	323.641440	.001	579.55690	2526.79990
			D2	972.52240	323.641440	.050	-1.09910	1946.14390
			D4	498.43140	323.641440	.859	-475.19010	1472.05290
		D4	D1	1054.74700*	323.641440	.030	81.12550	2028.36850
			D2	474.09100	323.641440	.974	-499.53050	1447.71250
			D3	-498.43140	323.641440	.859	-1472.05290	475.19010

Fracture toughness @6	LSD	D1	D2	-177.96480	213.288302	.416	-630.11580	274.18620
			D3	-1187.11880*	213.288302	<.001	-1639.26980	-734.96780
			D4	-263.15880	213.288302	.235	-715.30980	188.99220
		D2	D1	177.96480	213.288302	.416	-274.18620	630.11580
			D3	-1009.15400*	213.288302	<.001	-1461.30500	-557.00300
			D4	-85.19400	213.288302	.695	-537.34500	366.95700
		D3	D1	1187.11880*	213.288302	<.001	734.96780	1639.26980
			D2	1009.15400*	213.288302	<.001	557.00300	1461.30500
			D4	923.96000*	213.288302	<.001	471.80900	1376.11100
		D4	D1	263.15880	213.288302	.235	-188.99220	715.30980
			D2	85.19400	213.288302	.695	-366.95700	537.34500
			D3	-923.96000*	213.288302	<.001	-1376.11100	-471.80900
	Bonferroni	D1	D2	-177.96480	213.288302	1.000	-819.60722	463.67762
			D3	-1187.11880*	213.288302	<.001	-1828.76122	-545.47638
			D4	-263.15880	213.288302	1.000	-904.80122	378.48362
		D2	D1	177.96480	213.288302	1.000	-463.67762	819.60722
			D3	-1009.15400*	213.288302	.001	-1650.79642	-367.51158
			D4	-85.19400	213.288302	1.000	-726.83642	556.44842
		D3	D1	1187.11880*	213.288302	<.001	545.47638	1828.76122
			D2	1009.15400*	213.288302	.001	367.51158	1650.79642
			D4	923.96000*	213.288302	.003	282.31758	1565.60242
		D4	D1	263.15880	213.288302	1.000	-378.48362	904.80122
			D2	85.19400	213.288302	1.000	-556.44842	726.83642
			D3	-923.96000*	213.288302	.003	-1565.60242	-282.31758
Fracture toughness @9	LSD	D1	D2	-239.93940*	85.948989	.013	-422.14312	-57.73568
			D3	-898.33640*	85.948989	<.001	-1080.54012	-716.13268
			D4	-68.67020	85.948989	.436	-250.87392	113.53352
		D2	D1	239.93940*	85.948989	.013	57.73568	422.14312
			D3	-658.39700*	85.948989	<.001	-840.60072	-476.19328
			D4	171.26920	85.948989	.064	-10.93452	353.47292
		D3	D1	898.33640*	85.948989	<.001	716.13268	1080.54012
			D2	658.39700*	85.948989	<.001	476.19328	840.60072
			D4	829.66620*	85.948989	<.001	647.46248	1011.86992
		D4	D1	68.67020	85.948989	.436	-113.53352	250.87392
			D2	-171.26920	85.948989	.064	-353.47292	10.93452
			D3	-829.66620*	85.948989	<.001	-1011.86992	-647.46248
	Bonferroni	D1	D2	-239.93940	85.948989	.078	-498.50265	18.62385
			D3	-898.33640*	85.948989	<.001	-1156.89965	-639.77315
			D4	-68.67020	85.948989	1.000	-327.23345	189.89305
		D2	D1	239.93940	85.948989	.078	-18.62385	498.50265
			D3	-658.39700*	85.948989	<.001	-916.96025	-399.83375
			D4	171.26920	85.948989	.382	-87.29405	429.83245
		D3	D1	898.33640*	85.948989	<.001	639.77315	1156.89965
			D2	658.39700*	85.948989	<.001	399.83375	916.96025
			D4	829.66620*	85.948989	<.001	571.10295	1088.22945
		D4	D1	68.67020	85.948989	1.000	-189.89305	327.23345
			D2	-171.26920	85.948989	.382	-429.83245	87.29405
			D3	-829.66620*	85.948989	<.001	-1088.22945	-571.10295
Fracture toughness @12	LSD	D1	D2	-77.6460	59.33449	.209	-203.4295	48.1375
			D3	-476.8732*	59.33449	<.001	-602.6567	-351.0897
			D4	126.3446*	59.33449	.049	.5611	252.1281
		D2	D1	77.6460	59.33449	.209	-48.1375	203.4295
			D3	-399.2272*	59.33449	<.001	-525.0107	-273.4437
			D4	203.9906*	59.33449	.003	78.2071	329.7741
		D3	D1	476.8732*	59.33449	<.001	351.0897	602.6567
			D2	399.2272*	59.33449	<.001	273.4437	525.0107
			D4	603.2178*	59.33449	<.001	477.4343	729.0013
		D4	D1	-126.3446*	59.33449	.049	-252.1281	-.5611
			D2	-203.9906*	59.33449	.003	-329.7741	-78.2071
			D3	-603.2178*	59.33449	<.001	-729.0013	-477.4343
	Bonferroni	D1	D2	-77.6460	59.33449	1.000	-256.1439	100.8519
			D3	-476.8732*	59.33449	<.001	-655.3711	-298.3753
			D4	126.3446	59.33449	.295	-52.1533	304.8425
		D2	D1	77.6460	59.33449	1.000	-100.8519	256.1439
			D3	-399.2272*	59.33449	<.001	-577.7251	-220.7293
			D4	203.9906*	59.33449	.020	25.4927	382.4885
		D3	D1	476.8732*	59.33449	<.001	298.3753	655.3711
			D2	399.2272*	59.33449	<.001	220.7293	577.7251
			D4	603.2178*	59.33449	<.001	424.7199	781.7157
		D4	D1	-126.3446	59.33449	.295	-304.8425	52.1533
			D2	-203.9906*	59.33449	.020	-382.4885	-25.4927
			D3	-603.2178*	59.33449	<.001	-781.7157	-424.7199

Fracture toughness @15	LSD	D1	D2	2.2624	27.44969	.935	-55.9283	60.4531
			D3	-198.4758*	27.44969	<.001	-256.6665	-140.2851
			D4	177.3792*	27.44969	<.001	119.1885	235.5699
		D2	D1	-2.2624	27.44969	.935	-60.4531	55.9283
			D3	-200.7382*	27.44969	<.001	-258.9289	-142.5475
			D4	175.1168*	27.44969	<.001	116.9261	233.3075
		D3	D1	198.4758*	27.44969	<.001	140.2851	256.6665
			D2	200.7382*	27.44969	<.001	142.5475	258.9289
			D4	375.8550*	27.44969	<.001	317.6643	434.0457
		D4	D1	-177.3792*	27.44969	<.001	-235.5699	-119.1885
			D2	-175.1168*	27.44969	<.001	-233.3075	-116.9261
			D3	-375.8550*	27.44969	<.001	-434.0457	-317.6643
	Bonferroni	D1	D2	2.2624	27.44969	1.000	-80.3154	84.8402
			D3	-198.4758*	27.44969	<.001	-281.0536	-115.8980
			D4	177.3792*	27.44969	<.001	94.8014	259.9570
		D2	D1	-2.2624	27.44969	1.000	-84.8402	80.3154
			D3	-200.7382*	27.44969	<.001	-283.3160	-118.1604
			D4	175.1168*	27.44969	<.001	92.5390	257.6946
		D3	D1	198.4758*	27.44969	<.001	115.8980	281.0536
			D2	200.7382*	27.44969	<.001	118.1604	283.3160
			D4	375.8550*	27.44969	<.001	293.2772	458.4328
		D4	D1	-177.3792*	27.44969	<.001	-259.9570	-94.8014
			D2	-175.1168*	27.44969	<.001	-257.6946	-92.5390
			D3	-375.8550*	27.44969	<.001	-458.4328	-293.2772
Fracture toughness @18	LSD	D1	D2	37.4160	19.14770	.068	-3.1753	78.0073
			D3	-82.4344*	19.14770	<.001	-123.0257	-41.8431
			D4	177.7134*	19.14770	<.001	137.1221	218.3047
		D2	D1	-37.4160	19.14770	.068	-78.0073	3.1753
			D3	-119.8504*	19.14770	<.001	-160.4417	-79.2591
			D4	140.2974*	19.14770	<.001	99.7061	180.8887
		D3	D1	82.4344*	19.14770	<.001	41.8431	123.0257
			D2	119.8504*	19.14770	<.001	79.2591	160.4417
			D4	260.1478*	19.14770	<.001	219.5565	300.7391
		D4	D1	-177.7134*	19.14770	<.001	-218.3047	-137.1221
			D2	-140.2974*	19.14770	<.001	-180.8887	-99.7061
			D3	-260.1478*	19.14770	<.001	-300.7391	-219.5565
	Bonferroni	D1	D2	37.4160	19.14770	.410	-20.1867	95.0187
			D3	-82.4344*	19.14770	.003	-140.0371	-24.8317
			D4	177.7134*	19.14770	<.001	120.1107	235.3161
		D2	D1	-37.4160	19.14770	.410	-95.0187	20.1867
			D3	-119.8504*	19.14770	<.001	-177.4531	-62.2477
			D4	140.2974*	19.14770	<.001	82.6947	197.9001
		D3	D1	82.4344*	19.14770	.003	24.8317	140.0371
			D2	119.8504*	19.14770	<.001	62.2477	177.4531
			D4	260.1478*	19.14770	<.001	202.5451	317.7505
		D4	D1	-177.7134*	19.14770	<.001	-235.3161	-120.1107
			D2	-140.2974*	19.14770	<.001	-197.9001	-82.6947
			D3	-260.1478*	19.14770	<.001	-317.7505	-202.5451

Fracture toughness @21	LSD	D1	D2	48.1886*	10.33016	<.001	26.2896	70.0876
			D3	-42.8756*	10.33016	<.001	-64.7746	-20.9766
			D4	158.0870*	10.33016	<.001	136.1880	179.9860
		D2	D1	-48.1886*	10.33016	<.001	-70.0876	-26.2896
			D3	-91.0642*	10.33016	<.001	-112.9632	-69.1652
			D4	109.8984*	10.33016	<.001	87.9994	131.7974
		D3	D1	42.8756*	10.33016	<.001	20.9766	64.7746
			D2	91.0642*	10.33016	<.001	69.1652	112.9632
			D4	200.9626*	10.33016	<.001	179.0636	222.8616
		D4	D1	-158.0870*	10.33016	<.001	-179.9860	-136.1880
			D2	-109.8984*	10.33016	<.001	-131.7974	-87.9994
			D3	-200.9626*	10.33016	<.001	-222.8616	-179.0636
	Bonferroni	D1	D2	48.1886*	10.33016	.002	17.1120	79.2652
			D3	-42.8756*	10.33016	.005	-73.9522	-11.7990
			D4	158.0870*	10.33016	<.001	127.0104	189.1636
		D2	D1	-48.1886*	10.33016	.002	-79.2652	-17.1120
			D3	-91.0642*	10.33016	<.001	-122.1408	-59.9876
			D4	109.8984*	10.33016	<.001	78.8218	140.9750
		D3	D1	42.8756*	10.33016	.005	11.7990	73.9522
			D2	91.0642*	10.33016	<.001	59.9876	122.1408
			D4	200.9626*	10.33016	<.001	169.8860	232.0392
		D4	D1	-158.0870*	10.33016	<.001	-189.1636	-127.0104
			D2	-109.8984*	10.33016	<.001	-140.9750	-78.8218
			D3	-200.9626*	10.33016	<.001	-232.0392	-169.8860

Fracture toughness @24	LSD	D1	D2	21.8760*	8.61572	.022	3.6115	40.1405
			D3	-30.0802*	8.61572	.003	-48.3447	-11.8157
			D4	103.2218*	8.61572	<.001	84.9573	121.4863
		D2	D1	-21.8760*	8.61572	.022	-40.1405	-3.6115
			D3	-51.9562*	8.61572	<.001	-70.2207	-33.6917
			D4	81.3458*	8.61572	<.001	63.0813	99.6103
		D3	D1	30.0802*	8.61572	.003	11.8157	48.3447
			D2	51.9562*	8.61572	<.001	33.6917	70.2207
			D4	133.3020*	8.61572	<.001	115.0375	151.5665
		D4	D1	-103.2218*	8.61572	<.001	-121.4863	-84.9573
			D2	-81.3458*	8.61572	<.001	-99.6103	-63.0813
			D3	-133.3020*	8.61572	<.001	-151.5665	-115.0375
	Bonferroni	D1	D2	21.8760	8.61572	.131	-4.0430	47.7950
			D3	-30.0802*	8.61572	.018	-55.9992	-4.1612
			D4	103.2218*	8.61572	<.001	77.3028	129.1408
		D2	D1	-21.8760	8.61572	.131	-47.7950	4.0430
			D3	-51.9562*	8.61572	<.001	-77.8752	-26.0372
			D4	81.3458*	8.61572	<.001	55.4268	107.2648
		D3	D1	30.0802*	8.61572	.018	4.1612	55.9992
			D2	51.9562*	8.61572	<.001	26.0372	77.8752
			D4	133.3020*	8.61572	<.001	107.3830	159.2210
		D4	D1	-103.2218*	8.61572	<.001	-129.1408	-77.3028
			D2	-81.3458*	8.61572	<.001	-107.2648	-55.4268
			D3	-133.3020*	8.61572	<.001	-159.2210	-107.3830

Fracture toughness @27	LSD	D1	D2	12.4320	9.57150	.212	-7.8587	32.7227
			D3	-29.6070*	9.57150	.007	-49.8977	-9.3163
			D4	105.4738*	9.57150	<.001	85.1831	125.7645
		D2	D1	-12.4320	9.57150	.212	-32.7227	7.8587
			D3	-42.0390*	9.57150	<.001	-62.3297	-21.7483
			D4	93.0418*	9.57150	<.001	72.7511	113.3325
		D3	D1	29.6070*	9.57150	.007	9.3163	49.8977
			D2	42.0390*	9.57150	<.001	21.7483	62.3297
			D4	135.0808*	9.57150	<.001	114.7901	155.3715
		D4	D1	-105.4738*	9.57150	<.001	-125.7645	-85.1831
			D2	-93.0418*	9.57150	<.001	-113.3325	-72.7511
			D3	-135.0808*	9.57150	<.001	-155.3715	-114.7901
	Bonferroni	D1	D2	12.4320	9.57150	1.000	-16.3623	41.2263
			D3	-29.6070*	9.57150	.042	-58.4013	-.8127
			D4	105.4738*	9.57150	<.001	76.6795	134.2681
		D2	D1	-12.4320	9.57150	1.000	-41.2263	16.3623
			D3	-42.0390*	9.57150	.003	-70.8333	-13.2447
			D4	93.0418*	9.57150	<.001	64.2475	121.8361
		D3	D1	29.6070*	9.57150	.042	.8127	58.4013
			D2	42.0390*	9.57150	.003	13.2447	70.8333
			D4	135.0808*	9.57150	<.001	106.2865	163.8751
		D4	D1	-105.4738*	9.57150	<.001	-134.2681	-76.6795
			D2	-93.0418*	9.57150	<.001	-121.8361	-64.2475
			D3	-135.0808*	9.57150	<.001	-163.8751	-106.2865
Fracture toughness @30	LSD	D1	D2	-21.1940*	6.66941	.006	-35.3325	-7.0555
			D3	-60.0210*	6.66941	<.001	-74.1595	-45.8825
			D4	75.4716*	6.66941	<.001	61.3331	89.6101
		D2	D1	21.1940*	6.66941	.006	7.0555	35.3325
			D3	-38.8270*	6.66941	<.001	-52.9655	-24.6885
			D4	96.6656*	6.66941	<.001	82.5271	110.8041
		D3	D1	60.0210*	6.66941	<.001	45.8825	74.1595
			D2	38.8270*	6.66941	<.001	24.6885	52.9655
			D4	135.4926*	6.66941	<.001	121.3541	149.6311
		D4	D1	-75.4716*	6.66941	<.001	-89.6101	-61.3331
			D2	-96.6656*	6.66941	<.001	-110.8041	-82.5271
			D3	-135.4926*	6.66941	<.001	-149.6311	-121.3541
	Bonferroni	D1	D2	-21.1940*	6.66941	.035	-41.2578	-1.1302
			D3	-60.0210*	6.66941	<.001	-80.0848	-39.9572
			D4	75.4716*	6.66941	<.001	55.4078	95.5354
		D2	D1	21.1940*	6.66941	.035	1.1302	41.2578
			D3	-38.8270*	6.66941	<.001	-58.8908	-18.7632
			D4	96.6656*	6.66941	<.001	76.6018	116.7294
		D3	D1	60.0210*	6.66941	<.001	39.9572	80.0848
			D2	38.8270*	6.66941	<.001	18.7632	58.8908
			D4	135.4926*	6.66941	<.001	115.4288	155.5564
		D4	D1	-75.4716*	6.66941	<.001	-95.5354	-55.4078
			D2	-96.6656*	6.66941	<.001	-116.7294	-76.6018
			D3	-135.4926*	6.66941	<.001	-155.5564	-115.4288

Appendix 10

Sa	LSD	D1	D2	-.8884*	.35342	.023	-1.6376	-.1392
			D3	-1.2116*	.35342	.003	-1.9608	-.4624
			D4	-1.5786*	.35342	<.001	-2.3278	-.8294
		D2	D1	.8884*	.35342	.023	.1392	1.6376
			D3	-.3232	.35342	.374	-1.0724	.4260
			D4	-.6902	.35342	.069	-1.4394	.0590
		D3	D1	1.2116*	.35342	.003	.4624	1.9608
			D2	.3232	.35342	.374	-.4260	1.0724
			D4	-.3670	.35342	.315	-1.1162	.3822
		D4	D1	1.5786*	.35342	<.001	.8294	2.3278
			D2	.6902	.35342	.069	-.0590	1.4394
			D3	.3670	.35342	.315	-.3822	1.1162
	Bonferroni	D1	D2	-.8884	.35342	.138	-1.9516	.1748
			D3	-1.2116*	.35342	.021	-2.2748	-.1484
			D4	-1.5786*	.35342	.002	-2.6418	-.5154
		D2	D1	.8884	.35342	.138	-.1748	1.9516
			D3	-.3232	.35342	1.000	-1.3864	.7400
			D4	-.6902	.35342	.411	-1.7534	.3730
		D3	D1	1.2116*	.35342	.021	.1484	2.2748
			D2	.3232	.35342	1.000	-.7400	1.3864
			D4	-.3670	.35342	1.000	-1.4302	.6962
		D4	D1	1.5786*	.35342	.002	.5154	2.6418
			D2	.6902	.35342	.411	-.3730	1.7534
			D3	.3670	.35342	1.000	-.6962	1.4302

Appendix 11

Sp	LSD	D1	D2	-2.7186	2.43966	.282	-7.8905	2.4533
			D3	-6.1260*	2.43966	.023	-11.2979	-.9541
			D4	-9.2508*	2.43966	.002	-14.4227	-4.0789
		D2	D1	2.7186	2.43966	.282	-2.4533	7.8905
			D3	-3.4074	2.43966	.182	-8.5793	1.7645
			D4	-6.5322*	2.43966	.017	-11.7041	-1.3603
		D3	D1	6.1260*	2.43966	.023	.9541	11.2979
			D2	3.4074	2.43966	.182	-1.7645	8.5793
			D4	-3.1248	2.43966	.219	-8.2967	2.0471
		D4	D1	9.2508*	2.43966	.002	4.0789	14.4227
			D2	6.5322*	2.43966	.017	1.3603	11.7041
			D3	3.1248	2.43966	.219	-2.0471	8.2967
	Bonferroni	D1	D2	-2.7186	2.43966	1.000	-10.0579	4.6207
			D3	-6.1260	2.43966	.139	-13.4653	1.2133
			D4	-9.2508*	2.43966	.010	-16.5901	-1.9115
		D2	D1	2.7186	2.43966	1.000	-4.6207	10.0579
			D3	-3.4074	2.43966	1.000	-10.7467	3.9319
			D4	-6.5322	2.43966	.099	-13.8715	.8071
		D3	D1	6.1260	2.43966	.139	-1.2133	13.4653
			D2	3.4074	2.43966	1.000	-3.9319	10.7467
			D4	-3.1248	2.43966	1.000	-10.4641	4.2145
		D4	D1	9.2508*	2.43966	.010	1.9115	16.5901
			D2	6.5322	2.43966	.099	-.8071	13.8715
			D3	3.1248	2.43966	1.000	-4.2145	10.4641

Appendix 12

Sq	LSD	D1	D2	-.8324*	.34374	.028	-1.5611	-.1037
			D3	-1.1644*	.34374	.004	-1.8931	-.4357
			D4	-1.3230*	.34374	.001	-2.0517	-.5943
		D2	D1	.8324*	.34374	.028	.1037	1.5611
			D3	-.3320	.34374	.348	-1.0607	.3967
			D4	-.4906	.34374	.173	-1.2193	.2381
		D3	D1	1.1644*	.34374	.004	.4357	1.8931
			D2	.3320	.34374	.348	-.3967	1.0607
			D4	-.1586	.34374	.651	-.8873	.5701
		D4	D1	1.3230*	.34374	.001	.5943	2.0517
			D2	.4906	.34374	.173	-.2381	1.2193
			D3	.1586	.34374	.651	-.5701	.8873
	Bonferroni	D1	D2	-.8324	.34374	.166	-1.8665	.2017
			D3	-1.1644*	.34374	.023	-2.1985	-.1303
			D4	-1.3230*	.34374	.009	-2.3571	-.2889
		D2	D1	.8324	.34374	.166	-.2017	1.8665
			D3	-.3320	.34374	1.000	-1.3661	.7021
			D4	-.4906	.34374	1.000	-1.5247	.5435
		D3	D1	1.1644*	.34374	.023	.1303	2.1985
			D2	.3320	.34374	1.000	-.7021	1.3661
			D4	-.1586	.34374	1.000	-1.1927	.8755
		D4	D1	1.3230*	.34374	.009	.2889	2.3571
			D2	.4906	.34374	1.000	-.5435	1.5247
			D3	.1586	.34374	1.000	-.8755	1.1927

Appendix 13

Polar	LSD	A1	A2	-2.1400	2.32748	.372	-7.0740	2.7940
			A3	-9.3314*	2.32748	.001	-14.2654	-4.3974
			A4	-4.4008	2.32748	.077	-9.3348	.5332
		A2	A1	2.1400	2.32748	.372	-2.7940	7.0740
			A3	-7.1914*	2.32748	.007	-12.1254	-2.2574
			A4	-2.2608	2.32748	.346	-7.1948	2.6732
		A3	A1	9.3314*	2.32748	.001	4.3974	14.2654
			A2	7.1914*	2.32748	.007	2.2574	12.1254
			A4	4.9306	2.32748	.050	-.0034	9.8646
		A4	A1	4.4008	2.32748	.077	-.5332	9.3348
			A2	2.2608	2.32748	.346	-2.6732	7.1948
			A3	-4.9306	2.32748	.050	-9.8646	.0034
	Bonferroni	A1	A2	-2.1400	2.32748	1.000	-9.1418	4.8618
			A3	-9.3314*	2.32748	.006	-16.3332	-2.3296
			A4	-4.4008	2.32748	.461	-11.4026	2.6010
		A2	A1	2.1400	2.32748	1.000	-4.8618	9.1418
			A3	-7.1914*	2.32748	.042	-14.1932	-.1896
			A4	-2.2608	2.32748	1.000	-9.2626	4.7410
		A3	A1	9.3314*	2.32748	.006	2.3296	16.3332
			A2	7.1914*	2.32748	.042	.1896	14.1932
			A4	4.9306	2.32748	.301	-2.0712	11.9324
		A4	A1	4.4008	2.32748	.461	-2.6010	11.4026
			A2	2.2608	2.32748	1.000	-4.7410	9.2626
			A3	-4.9306	2.32748	.301	-11.9324	2.0712

Appendix 14

Dispersive	LSD	A1	A2	.8152	1.73548	.645	-2.8638	4.4942
			A3	1.6066	1.73548	.368	-2.0724	5.2856
			A4	6.9498*	1.73548	.001	3.2708	10.6288
		A2	A1	-.8152	1.73548	.645	-4.4942	2.8638
			A3	.7914	1.73548	.655	-2.8876	4.4704
			A4	6.1346*	1.73548	.003	2.4556	9.8136
		A3	A1	-1.6066	1.73548	.368	-5.2856	2.0724
			A2	-.7914	1.73548	.655	-4.4704	2.8876
			A4	5.3432*	1.73548	.007	1.6642	9.0222
		A4	A1	-6.9498*	1.73548	.001	-10.6288	-3.2708
			A2	-6.1346*	1.73548	.003	-9.8136	-2.4556
			A3	-5.3432*	1.73548	.007	-9.0222	-1.6642
	Bonferroni	A1	A2	.8152	1.73548	1.000	-4.4057	6.0361
			A3	1.6066	1.73548	1.000	-3.6143	6.8275
			A4	6.9498*	1.73548	.006	1.7289	12.1707
		A2	A1	-.8152	1.73548	1.000	-6.0361	4.4057
			A3	.7914	1.73548	1.000	-4.4295	6.0123
			A4	6.1346*	1.73548	.017	.9137	11.3555
		A3	A1	-1.6066	1.73548	1.000	-6.8275	3.6143
			A2	-.7914	1.73548	1.000	-6.0123	4.4295
			A4	5.3432*	1.73548	.043	.1223	10.5641
		A4	A1	-6.9498*	1.73548	.006	-12.1707	-1.7289
			A2	-6.1346*	1.73548	.017	-11.3555	-.9137
			A3	-5.3432*	1.73548	.043	-10.5641	-.1223

Appendix 15

SFE	LSD	A1	A2	-1.3248	2.86646	.650	-7.4014	4.7518
			A3	-7.7248*	2.86646	.016	-13.8014	-1.6482
			A4	2.5490	2.86646	.387	-3.5276	8.6256
		A2	A1	1.3248	2.86646	.650	-4.7518	7.4014
			A3	-6.4000*	2.86646	.040	-12.4766	-.3234
			A4	3.8738	2.86646	.195	-2.2028	9.9504
		A3	A1	7.7248*	2.86646	.016	1.6482	13.8014
			A2	6.4000*	2.86646	.040	.3234	12.4766
			A4	10.2738*	2.86646	.002	4.1972	16.3504
		A4	A1	-2.5490	2.86646	.387	-8.6256	3.5276
			A2	-3.8738	2.86646	.195	-9.9504	2.2028
			A3	-10.2738*	2.86646	.002	-16.3504	-4.1972
	Bonferroni	A1	A2	-1.3248	2.86646	1.000	-9.9481	7.2985
			A3	-7.7248	2.86646	.096	-16.3481	.8985
			A4	2.5490	2.86646	1.000	-6.0743	11.1723
		A2	A1	1.3248	2.86646	1.000	-7.2985	9.9481
			A3	-6.4000	2.86646	.241	-15.0233	2.2233
			A4	3.8738	2.86646	1.000	-4.7495	12.4971
		A3	A1	7.7248	2.86646	.096	-.8985	16.3481
			A2	6.4000	2.86646	.241	-2.2233	15.0233
			A4	10.2738*	2.86646	.015	1.6505	18.8971
		A4	A1	-2.5490	2.86646	1.000	-11.1723	6.0743
			A2	-3.8738	2.86646	1.000	-12.4971	4.7495
			A3	-10.2738*	2.86646	.015	-18.8971	-1.6505

Appendix 16

Polar	LSD	B1	B2	-.4888	1.35548	.723	-3.3623	2.3847
			B3	.6310	1.35548	.648	-2.2425	3.5045
			B4	-4.7032*	1.35548	.003	-7.5767	-1.8297
		B2	B1	.4888	1.35548	.723	-2.3847	3.3623
			B3	1.1198	1.35548	.421	-1.7537	3.9933
			B4	-4.2144*	1.35548	.007	-7.0879	-1.3409
		B3	B1	-.6310	1.35548	.648	-3.5045	2.2425
			B2	-1.1198	1.35548	.421	-3.9933	1.7537
			B4	-5.3342*	1.35548	.001	-8.2077	-2.4607
		B4	B1	4.7032*	1.35548	.003	1.8297	7.5767
			B2	4.2144*	1.35548	.007	1.3409	7.0879
			B3	5.3342*	1.35548	.001	2.4607	8.2077
	Bonferroni	B1	B2	-.4888	1.35548	1.000	-4.5665	3.5889
			B3	.6310	1.35548	1.000	-3.4467	4.7087
			B4	-4.7032*	1.35548	.019	-8.7809	-.6255
		B2	B1	.4888	1.35548	1.000	-3.5889	4.5665
			B3	1.1198	1.35548	1.000	-2.9579	5.1975
			B4	-4.2144*	1.35548	.040	-8.2921	-.1367
		B3	B1	-.6310	1.35548	1.000	-4.7087	3.4467
			B2	-1.1198	1.35548	1.000	-5.1975	2.9579
			B4	-5.3342*	1.35548	.007	-9.4119	-1.2565
		B4	B1	4.7032*	1.35548	.019	.6255	8.7809
			B2	4.2144*	1.35548	.040	.1367	8.2921
			B3	5.3342*	1.35548	.007	1.2565	9.4119

Appendix 17

Dispersive	LSD	B1	B2	1.6994	1.12298	.150	-.6812	4.0800
			B3	4.4008*	1.12298	.001	2.0202	6.7814
			B4	8.8002*	1.12298	<.001	6.4196	11.1808
		B2	B1	-1.6994	1.12298	.150	-4.0800	.6812
			B3	2.7014*	1.12298	.029	.3208	5.0820
			B4	7.1008*	1.12298	<.001	4.7202	9.4814
		B3	B1	-4.4008*	1.12298	.001	-6.7814	-2.0202
			B2	-2.7014*	1.12298	.029	-5.0820	-.3208
			B4	4.3994*	1.12298	.001	2.0188	6.7800
		B4	B1	-8.8002*	1.12298	<.001	-11.1808	-6.4196
			B2	-7.1008*	1.12298	<.001	-9.4814	-4.7202
			B3	-4.3994*	1.12298	.001	-6.7800	-2.0188
	Bonferroni	B1	B2	1.6994	1.12298	.898	-1.6789	5.0777
			B3	4.4008*	1.12298	.007	1.0225	7.7791
			B4	8.8002*	1.12298	<.001	5.4219	12.1785
		B2	B1	-1.6994	1.12298	.898	-5.0777	1.6789
			B3	2.7014	1.12298	.172	-.6769	6.0797
			B4	7.1008*	1.12298	<.001	3.7225	10.4791
		B3	B1	-4.4008*	1.12298	.007	-7.7791	-1.0225
			B2	-2.7014	1.12298	.172	-6.0797	.6769
			B4	4.3994*	1.12298	.007	1.0211	7.7777
		B4	B1	-8.8002*	1.12298	<.001	-12.1785	-5.4219
			B2	-7.1008*	1.12298	<.001	-10.4791	-3.7225
			B3	-4.3994*	1.12298	.007	-7.7777	-1.0211

Appendix 18

SFE	LSD	B1	B2	1.2106	1.91179	.536	-2.8422	5.2634
			B3	5.0318*	1.91179	.018	.9790	9.0846
			B4	4.0970*	1.91179	.048	.0442	8.1498
		B2	B1	-1.2106	1.91179	.536	-5.2634	2.8422
			B3	3.8212	1.91179	.063	-.2316	7.8740
			B4	2.8864	1.91179	.151	-1.1664	6.9392
		B3	B1	-5.0318*	1.91179	.018	-9.0846	-.9790
			B2	-3.8212	1.91179	.063	-7.8740	.2316
			B4	-.9348	1.91179	.632	-4.9876	3.1180
		B4	B1	-4.0970*	1.91179	.048	-8.1498	-.0442
			B2	-2.8864	1.91179	.151	-6.9392	1.1664
			B3	.9348	1.91179	.632	-3.1180	4.9876
	Bonferroni	B1	B2	1.2106	1.91179	1.000	-4.5407	6.9619
			B3	5.0318	1.91179	.109	-.7195	10.7831
			B4	4.0970	1.91179	.287	-1.6543	9.8483
		B2	B1	-1.2106	1.91179	1.000	-6.9619	4.5407
			B3	3.8212	1.91179	.378	-1.9301	9.5725
			B4	2.8864	1.91179	.904	-2.8649	8.6377
		B3	B1	-5.0318	1.91179	.109	-10.7831	.7195
			B2	-3.8212	1.91179	.378	-9.5725	1.9301
			B4	-.9348	1.91179	1.000	-6.6861	4.8165
		B4	B1	-4.0970	1.91179	.287	-9.8483	1.6543
			B2	-2.8864	1.91179	.904	-8.6377	2.8649
			B3	.9348	1.91179	1.000	-4.8165	6.6861

Appendix 19

Polar	LSD	C1	C2	5.6360*	2.47975	.037	.3792	10.8928
			C3	6.6288*	2.47975	.017	1.3719	11.8856
			C4	-2.2014	2.47975	.388	-7.4582	3.0554
		C2	C1	-5.6360*	2.47975	.037	-10.8928	-.3792
			C3	.9928	2.47975	.694	-4.2641	6.2496
			C4	-7.8374*	2.47975	.006	-13.0942	-2.5806
		C3	C1	-6.6288*	2.47975	.017	-11.8856	-1.3719
			C2	-.9928	2.47975	.694	-6.2496	4.2641
			C4	-8.8302*	2.47975	.003	-14.0870	-3.5733
		C4	C1	2.2014	2.47975	.388	-3.0554	7.4582
			C2	7.8374*	2.47975	.006	2.5806	13.0942
			C3	8.8302*	2.47975	.003	3.5733	14.0870
	Bonferroni	C1	C2	5.6360	2.47975	.223	-1.8239	13.0959
			C3	6.6288	2.47975	.100	-.8311	14.0887
			C4	-2.2014	2.47975	1.000	-9.6613	5.2585
		C2	C1	-5.6360	2.47975	.223	-13.0959	1.8239
			C3	.9928	2.47975	1.000	-6.4671	8.4527
			C4	-7.8374*	2.47975	.036	-15.2973	-.3775
		C3	C1	-6.6288	2.47975	.100	-14.0887	.8311
			C2	-.9928	2.47975	1.000	-8.4527	6.4671
			C4	-8.8302*	2.47975	.016	-16.2901	-1.3703
		C4	C1	2.2014	2.47975	1.000	-5.2585	9.6613
			C2	7.8374*	2.47975	.036	.3775	15.2973
			C3	8.8302*	2.47975	.016	1.3703	16.2901

Appendix 20

Dispersive	LSD	C1	C2	1.1346	1.56251	.478	-2.1778	4.4470
			C3	2.2446	1.56251	.170	-1.0678	5.5570
			C4	3.4672*	1.56251	.041	.1548	6.7796
		C2	C1	-1.1346	1.56251	.478	-4.4470	2.1778
			C3	1.1100	1.56251	.488	-2.2024	4.4224
			C4	2.3326	1.56251	.155	-.9798	5.6450
		C3	C1	-2.2446	1.56251	.170	-5.5570	1.0678
			C2	-1.1100	1.56251	.488	-4.4224	2.2024
			C4	1.2226	1.56251	.445	-2.0898	4.5350
		C4	C1	-3.4672*	1.56251	.041	-6.7796	-.1548
			C2	-2.3326	1.56251	.155	-5.6450	.9798
			C3	-1.2226	1.56251	.445	-4.5350	2.0898
	Bonferroni	C1	C2	1.1346	1.56251	1.000	-3.5660	5.8352
			C3	2.2446	1.56251	1.000	-2.4560	6.9452
			C4	3.4672	1.56251	.248	-1.2334	8.1678
		C2	C1	-1.1346	1.56251	1.000	-5.8352	3.5660
			C3	1.1100	1.56251	1.000	-3.5906	5.8106
			C4	2.3326	1.56251	.930	-2.3680	7.0332
		C3	C1	-2.2446	1.56251	1.000	-6.9452	2.4560
			C2	-1.1100	1.56251	1.000	-5.8106	3.5906
			C4	1.2226	1.56251	1.000	-3.4780	5.9232
		C4	C1	-3.4672	1.56251	.248	-8.1678	1.2334
			C2	-2.3326	1.56251	.930	-7.0332	2.3680
			C3	-1.2226	1.56251	1.000	-5.9232	3.4780

Appendix 21

SFE	LSD	C1	C2	6.7706*	2.53813	.017	1.3900	12.1512
			C3	8.8734*	2.53813	.003	3.4928	14.2539
			C4	1.2658	2.53813	.625	-4.1148	6.6464
		C2	C1	-6.7706*	2.53813	.017	-12.1512	-1.3900
			C3	2.1028	2.53813	.420	-3.2778	7.4833
			C4	-5.5048*	2.53813	.046	-10.8854	-.1242
		C3	C1	-8.8734*	2.53813	.003	-14.2539	-3.4928
			C2	-2.1028	2.53813	.420	-7.4833	3.2778
			C4	-7.6076*	2.53813	.009	-12.9881	-2.2270
		C4	C1	-1.2658	2.53813	.625	-6.6464	4.1148
			C2	5.5048*	2.53813	.046	.1242	10.8854
			C3	7.6076*	2.53813	.009	2.2270	12.9881
	Bonferroni	C1	C2	6.7706	2.53813	.101	-.8649	14.4061
			C3	8.8734*	2.53813	.018	1.2378	16.5089
			C4	1.2658	2.53813	1.000	-6.3697	8.9013
		C2	C1	-6.7706	2.53813	.101	-14.4061	.8649
			C3	2.1028	2.53813	1.000	-5.5328	9.7383
			C4	-5.5048	2.53813	.273	-13.1403	2.1307
		C3	C1	-8.8734*	2.53813	.018	-16.5089	-1.2378
			C2	-2.1028	2.53813	1.000	-9.7383	5.5328
			C4	-7.6076	2.53813	.051	-15.2431	.0280
		C4	C1	-1.2658	2.53813	1.000	-8.9013	6.3697
			C2	5.5048	2.53813	.273	-2.1307	13.1403
			C3	7.6076	2.53813	.051	-.0280	15.2431

Appendix 22

Polar	LSD	D1	D2	-10.6390*	3.74697	.012	-18.5822	-2.6958
			D3	-14.6542*	3.74697	.001	-22.5974	-6.7110
			D4	-3.0858	3.74697	.422	-11.0290	4.8574
		D2	D1	10.6390*	3.74697	.012	2.6958	18.5822
			D3	-4.0152	3.74697	.300	-11.9584	3.9280
			D4	7.5532	3.74697	.061	-.3900	15.4964
		D3	D1	14.6542*	3.74697	.001	6.7110	22.5974
			D2	4.0152	3.74697	.300	-3.9280	11.9584
			D4	11.5684*	3.74697	.007	3.6252	19.5116
		D4	D1	3.0858	3.74697	.422	-4.8574	11.0290
			D2	-7.5532	3.74697	.061	-15.4964	.3900
			D3	-11.5684*	3.74697	.007	-19.5116	-3.6252
	Bonferroni	D1	D2	-10.6390	3.74697	.071	-21.9111	.6331
			D3	-14.6542*	3.74697	.007	-25.9263	-3.3821
			D4	-3.0858	3.74697	1.000	-14.3579	8.1863
		D2	D1	10.6390	3.74697	.071	-.6331	21.9111
			D3	-4.0152	3.74697	1.000	-15.2873	7.2569
			D4	7.5532	3.74697	.366	-3.7189	18.8253
		D3	D1	14.6542*	3.74697	.007	3.3821	25.9263
			D2	4.0152	3.74697	1.000	-7.2569	15.2873
			D4	11.5684*	3.74697	.042	.2963	22.8405
		D4	D1	3.0858	3.74697	1.000	-8.1863	14.3579
			D2	-7.5532	3.74697	.366	-18.8253	3.7189
			D3	-11.5684*	3.74697	.042	-22.8405	-.2963

Appendix 23

Dispersive	LSD	D1	D2	6.3132*	1.48345	<.001	3.1684	9.4580
			D3	9.1098*	1.48345	<.001	5.9650	12.2546
			D4	9.3156*	1.48345	<.001	6.1708	12.4604
		D2	D1	-6.3132*	1.48345	<.001	-9.4580	-3.1684
			D3	2.7966	1.48345	.078	-.3482	5.9414
			D4	3.0024	1.48345	.060	-.1424	6.1472
		D3	D1	-9.1098*	1.48345	<.001	-12.2546	-5.9650
			D2	-2.7966	1.48345	.078	-5.9414	.3482
			D4	.2058	1.48345	.891	-2.9390	3.3506
		D4	D1	-9.3156*	1.48345	<.001	-12.4604	-6.1708
			D2	-3.0024	1.48345	.060	-6.1472	.1424
			D3	-.2058	1.48345	.891	-3.3506	2.9390
	Bonferroni	D1	D2	6.3132*	1.48345	.004	1.8505	10.7759
			D3	9.1098*	1.48345	<.001	4.6471	13.5725
			D4	9.3156*	1.48345	<.001	4.8529	13.7783
		D2	D1	-6.3132*	1.48345	.004	-10.7759	-1.8505
			D3	2.7966	1.48345	.466	-1.6661	7.2593
			D4	3.0024	1.48345	.360	-1.4603	7.4651
		D3	D1	-9.1098*	1.48345	<.001	-13.5725	-4.6471
			D2	-2.7966	1.48345	.466	-7.2593	1.6661
			D4	.2058	1.48345	1.000	-4.2569	4.6685
		D4	D1	-9.3156*	1.48345	<.001	-13.7783	-4.8529
			D2	-3.0024	1.48345	.360	-7.4651	1.4603
			D3	-.2058	1.48345	1.000	-4.6685	4.2569

Appendix 24

SFE	LSD	D1	D2	-4.3258	4.14981	.313	-13.1230	4.4714
			D3	-5.5444	4.14981	.200	-14.3416	3.2528
			D4	6.2298	4.14981	.153	-2.5674	15.0270
		D2	D1	4.3258	4.14981	.313	-4.4714	13.1230
			D3	-1.2186	4.14981	.773	-10.0158	7.5786
			D4	10.5556*	4.14981	.022	1.7584	19.3528
		D3	D1	5.5444	4.14981	.200	-3.2528	14.3416
			D2	1.2186	4.14981	.773	-7.5786	10.0158
			D4	11.7742*	4.14981	.012	2.9770	20.5714
		D4	D1	-6.2298	4.14981	.153	-15.0270	2.5674
			D2	-10.5556*	4.14981	.022	-19.3528	-1.7584
			D3	-11.7742*	4.14981	.012	-20.5714	-2.9770
	Bonferroni	D1	D2	-4.3258	4.14981	1.000	-16.8098	8.1582
			D3	-5.5444	4.14981	1.000	-18.0284	6.9396
			D4	6.2298	4.14981	.917	-6.2542	18.7138
		D2	D1	4.3258	4.14981	1.000	-8.1582	16.8098
			D3	-1.2186	4.14981	1.000	-13.7026	11.2654
			D4	10.5556	4.14981	.130	-1.9284	23.0396
		D3	D1	5.5444	4.14981	1.000	-6.9396	18.0284
			D2	1.2186	4.14981	1.000	-11.2654	13.7026
			D4	11.7742	4.14981	.071	-.7098	24.2582
		D4	D1	-6.2298	4.14981	.917	-18.7138	6.2542
			D2	-10.5556	4.14981	.130	-23.0396	1.9284
			D3	-11.7742	4.14981	.071	-24.2582	.7098